

Synthesis of curcuminoids as non-steroidal anti-inflammatory drugs.

MOIN, Mahera.

Available from the Sheffield Hallam University Research Archive (SHURA) at:

<http://shura.shu.ac.uk/20760/>

A Sheffield Hallam University thesis

This thesis is protected by copyright which belongs to the author.

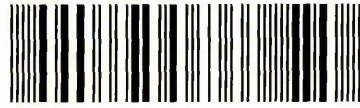
The content must not be changed in any way or sold commercially in any format or medium without the formal permission of the author.

When referring to this work, full bibliographic details including the author, title, awarding institution and date of the thesis must be given.

Please visit <http://shura.shu.ac.uk/20760/> and <http://shura.shu.ac.uk/information.html> for further details about copyright and re-use permissions.

COLLEGIATE CRESCENT
SHEFFIELD S10 2BP

101 963 648 3



REFERENCE

ProQuest Number: 10702859

All rights reserved

INFORMATION TO ALL USERS

The quality of this reproduction is dependent upon the quality of the copy submitted.

In the unlikely event that the author did not send a complete manuscript and there are missing pages, these will be noted. Also, if material had to be removed, a note will indicate the deletion.



ProQuest 10702859

Published by ProQuest LLC (2017). Copyright of the Dissertation is held by the Author.

All rights reserved.

This work is protected against unauthorized copying under Title 17, United States Code
Microform Edition © ProQuest LLC.

ProQuest LLC.
789 East Eisenhower Parkway
P.O. Box 1346
Ann Arbor, MI 48106 – 1346

Synthesis of Curcuminoids as Non-Steroidal Anti-inflammatory Drugs

Mahera Moin

A thesis submitted in partial fulfilment of the requirements of
Sheffield Hallam University
for the degree of Doctor of Philosophy

May 2009

Dedicated to My

Beloved

Parents, Uncle and Aunt

Acknowledgement

Firstly, thanks be to God Almighty for giving me the courage to take on and complete this task successfully.

I am very grateful to my supervisors Dr. Akram Khan, Prof. Nicola Woodroofe and Prof. Kim Rainsford for their guidance throughout.

I would like to express my gratitude to Dr. Roger Jackson and Dr. Christine LeMatire for accommodating me whenever I needed their invaluable time. Special thanks to Kevin Osbourne and Daniel Kinsman for all the technical support during my lab work.

I am truly indebted to my uncle and aunt Dr. and Mrs. Mukhtaruddin Ahmed for making it possible in every respect. I am thankful to my parents Mr & Mrs. Moinuddin Ahmed for their love and support that kept me going during the toughest times.

I thank my colleagues at BMRC and friends Yon Ju Nam and Susan Boyce for their time and support when it was most needed.

Finally, I would like to thank my sisters Fakhira, Bushra, Rabia and brother Amin for being ever so encouraging.

Abstract

Nonsteroidal anti-inflammatory drugs (NSAIDs) are the most widely prescribed therapeutic agents used worldwide, to treat various inflammatory diseases. However, these drugs do not solve the underlying problem of inflammation and their long-term administration is associated with serious gastrointestinal complications, such as gastric ulcers and bleeding. Curcumin 1, (figure A) the diferuloylmethane, a yellow pigment found in the rhizomes of turmeric (*Curcuma longa*) possesses a well established role as an anti-inflammatory agent since ancient times to treat various inflammatory diseases. Thiophene features in many natural products and possesses anti-inflammatory properties. Similarly, nitric oxide donating NSAIDs are emerging as a novel class of NSAIDs which offers better efficacy and possesses lesser side-effects associated with the conventional NSAIDs. In search of better NSAIDs, we have successfully synthesised and spectroscopically characterised four thiophene curcuminoids **47a-d** and novel nitric oxide donating derivatives of curcumin **51a-d**, (figure A) using Pabon's method. The cytotoxic effects of these drugs along with the lead compound curcumin 1 and their effect on the production of reactive oxygen species i.e. nitric oxide and pro-inflammatory cytokines IL-1 β , TNF- α and CXCL-8 were evaluated using THP-1 and CACO-2 cancer cells. The thiophene curcuminoids **47a** at 10, 50 and 100 μ M and **47d** at 10 and 50 μ M, appeared to be non-cytotoxic to THP-1 cells, whereas, **47b** and **47c** were non-cytotoxic at 10 μ M only. When compared with curcumin 1, at 10 μ M, **47a** and **47d** were as non-cytotoxic as curcumin 1, however, **47b** and **47c** were more toxic than curcumin 1. In CACO-2 cells, **47b** and **47d** appeared to be non-toxic at 10 to 100 μ M, whereas, **47a** was non-toxic at 10 and 100 μ M and **47c** was non-cytotoxic at 10 μ M only. In THP-1 cells, drugs **47a-d** significantly decreased the IL-1- β production at their non-cytotoxic concentrations, whereas, did not decrease the TNF- α production. For the effects on CXCL-8 in CACO-2 cells, **47a** at 100 μ M and **47b** and **47d** at 50 and 100 μ M showed significant decrease in CXCL-8 production. In comparison to curcumin 1 at 10 μ M only drug **47c** significantly reduced CXCL-8 production. All of the nitric oxide donating curcuminoids **51a-d** are non-cytotoxic to THP-1 cells at a concentration range of 10-100 μ M and in comparison with curcumin 1, all drugs at 10 μ M were as non-toxic as curcumin 1, whereas at 50 and 100 μ M were significantly more non-toxic to the cells. All of them except **51c** enhanced the production of nitric oxide in unstimulated THP-1 cells, whereas in LPS stimulated cells drugs **51a** and **51d** showed similar effects to unstimulated cells, however drug **51b** equally produced NO at 10, 50 and 100 μ M and **51c** was effective at 100 μ M only. In comparison with curcumin 1 drug **51b** at 10 μ M enhanced the NO production both in LPS stimulated and unstimulated cells. These results clearly indicate that the replacement of both of the phenyl rings of the curcumin 1 with unsubstituted thiophenes and the introduction of a nitroxybutyl moiety to curcumin 1 reduce the cytotoxic effect of the parent curcumin 1, whereas, methyl substituted thiophenes increase its cytotoxic effects in THP-1 cells. The synthesis of fused-ring aromatic heterocyclic curcuminoids **57b** and **61** (figure A) was carried out via two different routes however both methods resulted in poor yields. On the other hand in case of nitrogen derived curcuminoids **63**, **65** and **69** (figure A) no product was obtained at all. New method for the synthesis of curcuminoids using Claisen condensation reaction was tried but complete evidence of curcumin formation was not achieved.

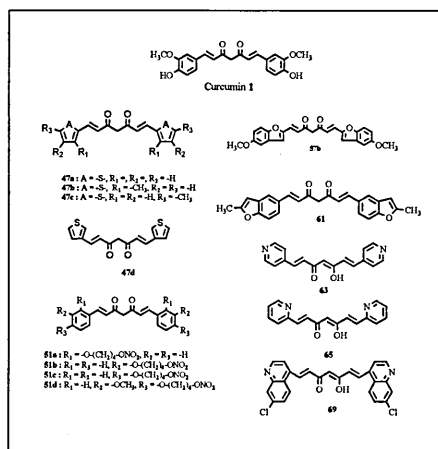


Figure A : Chemical structures of curcumin 1, thiophene curcuminoids **47a-d**, nitric oxide donating curcuminoids **51a-d**, fused ring aromatic heterocyclic curcuminoids **57b**, **61** and nitrogen containing curcuminoids **63**, **65** and **69**.

Abbreviations

Ar	Aromatic
AP	Alternative pathway
BB	Blocking buffer
Bcl-2	B-cell lymphoma-2
BID	Beta-interaction domain
br	Broad
BSA	Bovine serum albumin
CACO-2	Human caucasian colon adenocarcinoma-2 cell line
CEM	Human caucasian acute lymphoblastic leukaemia cell line
cIAP1	Caspase- inhibitor of apoptosis protein
CP	Classical pathway
CR1, CR2, CR3	Complement receptors 1, 2 and 3
cGMP	Cyclic guanosine monophosphate
DAF-DA	4-amino-5-methylamino-2',7'-difluorescein diacetate
DED	Death effect domain
DETA-NO	(z)-1-[2-(2-aminoethyl)-N-(2- aminoethyl)amino] diazen-1-ium-1,2 diolate
DISC	Death inducing signalling complex
DMSO	Dimethylsulfoxide
DPBS or PBS	Dulbecco's phosphate buffer saline
DR	Death receptor
EDTA	Ethylene-diaminetetraacetate
EIMS	Electron ionization mass spectrometry
ELISA	Enzyme-linked immunosorbant assay
ESMS	Electrospray mass spectrometry

EtOAc	Ethyl acetate
FADD	Fas-associated death domain
FBS	Foetal bovine serum
FCM	Flow-cytometry
FITC	Fluorescein isothiocyanate
FOXO	Transcription factor
GI	Gastrointestinal
GSK3	Glycogen synthase kinase 3
HE	Hydroethidine
HO-1	Heme-oxygenase-1
HP-γ-CD	Hydroxypropyl- gamma- cyclodextrin
HSB2	Human acute T lymphoblastic leukaemia cell
HTLV-1	Human T cell lymphotropic/leukaemia virus type 1
HUVEC	Human umbilical vein endothelial cells
IBD	Inflammatory bowel disease
IL-1β	Interleukin 1-beta
IR	Infra-red
JAK	Janus associated family of kinase
JC-1	5,5',6,6'-tetrachloro-1,1',3,3'- tetraethylbenzimidazolcarbocyanine iodide
LP	Lectin pathway
LPS	Lipopolysaccharide
m.p.	Melting point
mAb	Monoclonal antibody
MALDI	Matrix assisted laser desorption ionization
MEM	Minimum essential medium
MS	L-methionine sulfoximine

MTS	3-(4,5-dimethylthiazol-2yl)-5-(3-carboxymethoxyphenyl)-2-(4-sulfophenyl)-2H-tetrazolium, inner salt
NEAA	Non-essential amino acid
NED	<i>N</i> -1-(naphthyl)ethylenediamine
NMR	Nuclear magnetic resonance
NO-ASA	Nitric oxide donating acetylsalicylic acid
NO-CUR	Nitric oxide donating curcuminoids
NO-NSAIDs	Nitric oxide donating nonsteroidal anti-inflammatory drugs
NO-SAIDs	Nitric oxide donating steroidal anti-inflammatory drugs
PES	Phenazine ethosulfate
PGs	Prostaglandins
PMNs	Polymorphonuclear leukocytes
RA	Rheumatoid arthritis
RD	Reagent diluent
<i>R_F</i>	Retardation factor
SAA	Sulfanilamide
SEM	Standard error of the mean
Ser	Serine
siRNA	Small interfering ribonucleic acid
SnPP	Tin protoporphyrin
STAT	Signal transducers and activators of transcription protein
T-ALL	T-cell acute lymphoblastic leukaemia cells
THP-1	Human monocytic leukaemia cell line
Thr	Threonine
TLC	Thin-layer chromatography
TMB	3,3',5,5'-tetramethylbenzidine

TMS	Tetramethylsilane
TNFR	Tumor necrosis factor receptor
TNF-α	Tumor necrosis factor-alpha
WB	Wash buffer
XIAP	X-linked inhibitor of apoptosis protein

CONTENTS

Acknowledgement	I
Abstract	II
Abbreviations	III
 Chapter 1 : Introduction	 1
 Part A	
Scope of investigations	2
1.0 Definition of inflammation	4
1.1 Definition based on the signs and symptoms of inflammation	5
1.2 General aspects of inflammation	5
1.3 Mechanism of inflammation	8
1.4 Molecular mediators of inflammation	8
1.4.1 Histamine	11
1.4.1.1 Different histamine responses towards early and late inflammatory conditions	13
1.4.1.2 Mode of histamine release	13
1.4.1.3 Storage sites for histamine	14
1.4.2 Serotonin	14
1.4.3 Kinins	16
1.4.4 Complement system	16
1.4.5 Cytokines	20
1.5 Vascular events of inflammation (change in vascular flow and calibre)	21
1.6 Chemotaxis	26
1.7 Inflammatory responses	28
 Part B	
1.8 Anti-inflammatory drugs	29
1.9 The traditional therapeutic "pyramid approach"	29
1.10 Nitric oxide	30
1.11 Nitric oxide donating non-steroidal anti-inflammatory drugs (NO- NSAIDs)	33
1.11.1 Rationale behind the development of NO-NSAIDs	33
1.11.2 Mechanism of action of NO-aspirin	38
1.11.3 Pharmacokinetic properties of NO-aspirin	38

1.11.4 Pharmacodynamic properties of NO-aspirin	39
1.12 Cytoprotective and cytotoxic effects of nitric oxide	42
1.12.1 Cytoprotective effects of nitric oxide	42

Part C

1.13 Curcumin	50
1.14 Use in folk medicine	51
1.15 Morphology	52
1.16 Rhizome	52
1.17 Structural features of curcumin molecule and structural-activity relationships with regard to its anti-inflammatory properties	52
1.18 Biological activities of curcumin	57
1.19 Anti-inflammatory action of curcumin	63
1.20 Synthesis of curcumin and curcuminoids	67
1.21 Pabon's method of curcumin synthesis	68
1.22 Basic steps of Pabon synthesis	69
1.23 The aldol reaction	71
1.24 Aims and objectives	73
1.24.1 Synthetic aspects	73
1.24.2 Pharmacological aspects	74

Chapter 2 : Experimental 76

Part A : Chemistry

2.0 Materials	77
2.1 Methods	78
2.1.1 Preparation of tri- <i>sec</i> -butylborate	79
2.1.2 Preparation of acetyl-acetone boronoxide complex 31	79
2.1.3 Synthesis of bromobutoxybenzaldehyde 45a-d	80
2.1.4 Synthesis of curcuminoids	83
2.1.5 Synthesis of butoxy nitrate curcuminoids 51a-d	95
2.1.6 Synthesis of aromatic ethers 53a-c and thioether 53d	99
2.1.7 Synthesis of 2-(2-chloroallyl)phenols 54a-c and 2-methylbenzo[<i>b</i>]thiophene 55d	102
2.1.8 Synthesis of 2-methylbenzofuran 55a-c	104
2.1.9 Synthesis of benzo[<i>b</i>]furan-2-carbaldehydes 56a-c and benzo[<i>b</i>]thiophene-2-carbaldehyde 56d	106
2.1.10 Synthesis of benzo[<i>b</i>]furan curcuminoid 57b and attempted synthesis of 57c and benzo[<i>b</i>]thiophene curcuminoid 57d	108

2.1.11 Synthesis of 4-(2-bromoallyloxy)benzaldehyde 59	109
2.1.12 Synthesis of bromoallyloxy curcumin 60	110
2.1.13 Synthesis of 2-methylbenzofuran-5-ylcurcumin 61	111
2.1.14 Attempted synthesis of pyridine curcuminoids 63 and 65	112
2.1.15 Synthesis of 7-chloro-4-methylquinoline 67	113
2.1.16 Oxidation of 7-chloro-4-methylquinoline 67 with selenium dioxide	114
2.1.17 Attempted synthesis of quinoline curcuminoid 69	115
2.1.18 Synthesis of (E)-4-(phenylbut)-3-en-2-one 71a and 71b	116
2.1.19 Condensation reaction of (E)-4-(phenylbut)-3-en-2-one 71a with ethyl cinnamate 72	117
2.1.20 Condensation reaction of (E)-4-(furan-2-yl)but-3-en-2-one 71b with ethyl cinnamate 72	118
2.1.21 Synthesis of hydroxylpropyl- γ -cyclodextrin (HP- γ -CD) complexes of thiophene curcuminoids 47a-d/HP-γ-CD	119
 Part B : Pharmacology	
2.2 Materials	120
2.2.1 Chemicals	120
2.2.2 Cell lines	121
2.3 Methods	121
2.3.1 Preparation of drug treatments	121
2.3.2 Cell culture (general procedures)	122
2.3.3 THP-1 cell culture	122
2.3.4 Trypan-blue exclusion test	123
2.3.5 Plating THP-1 cells	123
2.3.6 Application of drug treatments to THP-1 cells and collection of supernatants	124
2.3.6.1 For the measurement of the MTS assay, Griess reagent assay and ELISAs (IL-1 β , TNF- α)	124
2.3.7 CACO-2 cell culture	125
2.3.8 Passaging and plating CACO-2 cells	125
2.3.9 Application of treatments to CACO-2 cells	126
2.3.9.1 Measurement of cell viability using MTS assay	126
2.3.9.2 ELISAs for CXCL-8	126
2.4 Cytotoxicity assay	127
2.4.1 MTS assay	127
2.4.2 Principle of the assay	127
2.4.3 Assay protocol	128

2.5 Nitric oxide production assay	129
2.5.1 The Griess reagent assay	129
2.5.2 Principle of the assay	129
2.5.3 Assay protocol	131
2.5.3.1 Preparation of nitrite standard curve	131
2.5.3.2 Griess reaction	131
2.6 Enzyme-linked immunosorbant assay ELISA	132
2.6.1 Sandwich ELISA, principle of the assay	132
2.6.2 Assay protocol	133
2.6.2.1 ELISA plate preparation for the detection of IL-1 β or TNF- α in cell supernatants of THP-1 cells	133
2.6.2.2 Preparation of standard curve	135
2.6.2.3 Assay procedure	135
2.6.2.4 ELISA plate preparation for the detection of CXCL-8 in CACO-2 cell supernatants	136
2.6.2.5 Preparation of standard curve	136
2.6.2.6 Assay procedure	137
2.7 Data manipulation and statistical analysis	137

Chapter 3 : Results and discussion 139

Part A : Chemistry

3.1 Results and discussion

3.1.1 Synthesis of nitric oxide donating curcuminoids 51a-d and curcumin 1	140
3.1.2 Synthesis of aromatic heterocyclic curcuminoids	147
3.1.3 Synthesis of fused ring aromatic heterocyclic curcuminoids 57b-d and 61	150
3.1.4 Attempted synthesis of pyridine and quinoline curcuminoids 63, 65 and 69	157
3.1.5 Attempted syntheses in search of new synthetic protocol for curcumin formation	160

Part B : Pharmacology

3.2 Results

3.2.1 Effect of drugs on cell viability (The MTS assay)	167
---	-----

3.2.1.1 Effects of curcumin and nitric oxide donating curcuminoids on the viability of THP-1 cells	167
3.2.1.2 Effects of curcumin and thiophene curcuminoids on the viability of THP-1 cells	170
3.2.1.3 Effects of curcumin and thiophene curcuminoids on the viability of CACO-2 cells	172
3.2.1.4 Effects of hydroxylpropyl- γ -cyclodextrin (HP- γ -CD) and 47a-d/HP- γ -CD on the viability of THP-1 cells	174
3.2.2 The nitric oxide production assay (Griess reagent system)	176
3.2.2.1 Standard curve for nitric oxide	176
3.2.2.2 Measurement of nitrite concentration in THP-1 cells treated with curcumin and nitric oxide donating curcuminoids	177
3.2.2.3 Measurement of nitrite concentration in THP-1 cells treated with curcumin and nitric oxide donating curcuminoids stimulated with LPS	179
3.2.3 Enzyme-linked immunosorbent assay (ELISA)	181
3.2.3.1 Standard curve for IL-1 β	181
3.2.3.2 Effects of curcumin and thiophene curcuminoids on the production of IL-1 β in THP-1 cells	182
3.2.3.3 Standard curve for TNF- α	184
3.2.3.4 Effects of curcumin and thiophene curcuminoids on the production of TNF- α in THP-1 cells	185
3.2.3.5 Standard curve for CXCL-8	187
3.2.3.6 Effects of curcumin and thiophene curcuminoids on the production of CXCL-8 in CACO-2 cells	188
3.3 Discussion	
3.3.1 Cytotoxic effects	192
3.3.2 The Griess reagent assay or the ELISA	192
3.3.2.1 Cytotoxic and nitric oxide donating effects of curcumin and nitric oxide donating curcuminoids in THP-1 cells	193
3.3.2.2 Effects of curcumin and thiophene curcuminoids on the viability and IL-1 β production in THP-1 cells	203
3.3.2.3 Effects of curcumin and thiophene curcuminoids on the viability and TNF- α production in THP-1 cells	209

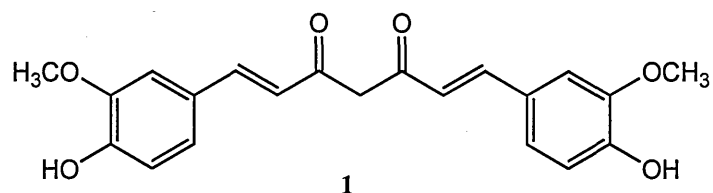
3.3.2.4 Effects of curcumin and thiophene curcuminoids on the viability and CXCL-8 production in CACO-2 cells	211
Chapter 4 : Conclusion	214
Chapter 5 : Future work	218
Part A : Chemistry	
Part B : Pharmacology	
References	223

CHAPTER 1
INTRODUCTION

Part A

Scope of investigations

Various inflammatory diseases (e.g. arthritis, inflammatory bowel disease, neurodegenerative diseases, parasitic diseases and cancer) are among the most serious and debilitating group of pathological conditions affecting humans world-wide. Current therapies, while being effective, often find limited use, either because of their inefficiency towards the effects on the disease processes or due to the occurrence of serious adverse drug reactions. In this thesis the potential for the natural product, curcumin **1** (figure 1.1), to serve as a platform for the development of novel derivatives (curcuminoids) is explored. Curcumin **1** has recently been shown to have many novel actions on molecular components of inflammatory processes which are considered as advanced and novel targets for therapeutic intervention in various inflammatory diseases. It is from this basis and the long-standing recognition that turmeric (curcumin **1**) has therapeutic benefits, albeit modest, in various chronic inflammatory diseases, that derivatives of curcumin **1** could be developed which may be more potent than curcumin **1** itself, or other anti-inflammatory drugs, as well as having the favourable safety profile of this natural product. The focus on novel derivatives of curcumin **1** was directed to preparing nitroxybutyl, thiophene and furan derivatives. These moieties have been found to have potency enhancing and novel actions when applied to other established drugs, e.g. the non-steroidal anti-inflammatory drugs (NSAIDs).



Curcumin or [1,7-bis-(4-hydroxy-3-methoxyphenyl)-1,6-heptadiene-3,5-dione]

Figure 1.1 : Chemical structure of curcumin 1.

The main focus of this chapter is to review (1) the mechanisms of inflammatory reactions showing the potential molecular and cellular targets that may be affected by curcumin **1** and its derivatives, (2) the actions of conventional anti-inflammatory drugs on these inflammatory processes, and (3) the effects of curcumin **1** (turmeric) recognised in folk medicine, as a nutraceutical and on pathways and cells involved in inflammation

1.0 Definition of inflammation

Inflammation is an active defensive reaction of multi-cellular organisms against diverse insults, designed by nature, not only to remove or inactivate noxious agents but also to inhibit and reverse their detrimental effects¹ and hence is necessary for survival. In order to achieve this ultimate goal the inflammatory reaction represents a non-specific and dynamic response that consists of a highly coordinated set of humoral and cellular events which allow tissues to respond to injury or infection by the participation of various cell types, expressing and reacting to diverse mediators.² However, the persistence of an inflammatory stimulus (due to the inadvertent activation of the inflammatory cascade) or the dysregulation of the endogenous anti-inflammatory mechanisms (due to the lack of appropriate termination signal)³ leads to chronic tissue injury associated with typical inflammatory disorders with high morbidity and mortality rates e.g. arthritis, colitis, inflammatory bowel disease, asthma and many other pathologies that have an inflammatory component associated with them, such as stroke, atherosclerosis, Alzheimer's disease.⁴

1.1 Definition based on the signs and symptoms of inflammation

Based on signs and symptoms, the term inflammation was defined in the first century as "Redness and swelling with heat, pain and disturbed function". The observation of plasma exudation and local leukocyte extravasation into the affected tissues was pioneered by Julius Conheim. Collectively, these concepts still hold true for the current definition of inflammation as the phenomenon that involves local vascular changes in diameter and blood flow, increased vascular permeability and leukocyte infiltration.⁵

1.2 General aspects of inflammation

A wide array of insults that include microbial invasion, trauma, thermal, immunological, physical/chemical injury is responsible for the tissue injury that results in the subsequent inflammatory response (figure 1.2), and regardless of the cause or anatomical site; the tissue injury initiates a series of biochemical events that result in the following three major pathophysiological components of the inflammatory response.⁶

- Increased tissue perfusion
- Increased vascular permeability
- Leukocytic exudation

In normal circumstances the inflammatory response is closely linked with the process of repair that begins during the early phase of inflammation, but completes usually after the injurious influence has been neutralized to heal and reconstitute the damaged tissue as soon as possible.⁷ This process of injury and repair usually involves a series

of events. The production of specific cytokines and chemokines initiates the processes of inflammation that is further promoted by the leukocyte recruitment to the site of damage. Attracted leukocytes exhibit new adhesion properties and produce several mediators that both increase local blood flow and activate phagocytes to eliminate dead cells and tissue debris. Damage is eventually repaired by proliferation of vascular capillary endothelial cells and fibroblasts. At this step, various molecules with anti-inflammatory properties are synthesized to resolve the process.²

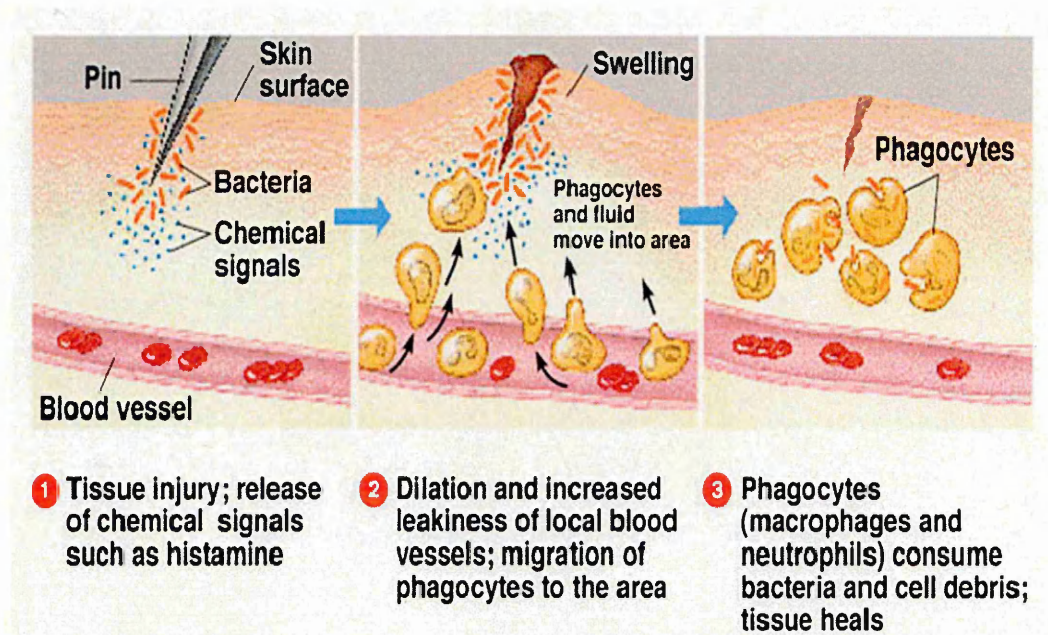


Figure 1.2 : Diagram showing the pathophysiological signs of inflammation followed by an injury.⁸

1.3 Mechanism of inflammation

In order to understand the process of inflammation, the following major aspects are taken into consideration in this thesis:

- Molecular mediators of inflammation
- Vascular events involved in inflammation
- Cellular events involved in inflammation including chemotaxis.

1.4 Molecular mediators of inflammation

Although various inflammatory diseases have different inflammatory responses, they can be characterized by the common spectrum of genes and a multitude of endogenous mediators involved. These include soluble proteins (specifically histamines, kinins, complement system), cytokines interleukin-1 β (IL-1 β), tumor necrosis factor- α (TNF- α), chemokines CXCL-8, macrophage inflammatory protein 1 α , β (MIP-1 α , β), reactive oxygen species e.g. nitric oxide and free radicals⁹ and eicosanoids (prostaglandins, leukotrienes).¹⁰ The molecular mediators of inflammation are summarised in table 1.1.

Table 1.1 : Molecular mediators of inflammation and their functions.¹¹

Functions	Mediators
Increased vascular permeability of small blood vessels	Histamine, serotonin, bradykinin, complement components (C3a, C5a), prostaglandin E ₂ (PGE ₂), leukotrienes (LTC ₄ , LTD ₄), prostacyclins, activated Hageman factor, high-molecular-weight kininogen fragments, fibrinopeptides.
Vasoconstriction	Thromboxane A ₂ (TXA ₂), leukotrienes (LTB ₄ , LTC ₄ , LTD ₄), complement component (C5a), N-formyl peptides.
Smooth muscle contraction	Complement components (C3a, C5a), histamine, leukotrienes (LTB ₄ , LTC ₄ , LTD ₄), thromboxane A ₂ (TXA ₂), serotonin, platelet aggregation factor (PAF), bradykinin.
Increased endothelial cell stickiness	Interleukin-1 (IL-1), tumor necrosis factor- α (TNF- α), chemotactic protein (MCP), endotoxin, leukotriene B ₄ (LTB ₄).
Mast cell degranulation	Complement components (C3a, C5a).
<i>Phagocytes</i>	
Stem cell proliferation	Interleukin-3 (IL-3), granulocyte colony stimulating factor (G-CSF), granulocyte macrophage colony stimulating factor (GM-CSF), macrophage colony stimulating factor (M-CSF).
Recruitment from bone marrow	Colony stimulating factors (CSFs), interleukin-1 (IL-1).

Adherence/aggregation	Proteolytically inactive product of complement cleavage factor C3b (iC3b), immunoglobulin G (IgG), fibronectin, lectins.
Chemotaxis	Complement component (C5a), leukotriene B ₄ (LTB ₄), interleukin-8 (IL-8) and other chemokines, platelet aggregation factor (PAF) PAF, histamine (for eosinophils), laminin, N-formyl peptides, collagen fragments, lymphocyte-derived chemotactic factor, fibrinopeptides.
Lysosomal granule release	Complement component (C5a), interleukin-8 IL-8, platelet aggregation factor (PAF), most chemoattractants, phagocytosis.
Production of reactive oxygen intermediates	Complement component (C5a), tumor necrosis factor- α (TNF- α), platelet aggregation factor (PAF), interleukin-8 (IL-8), phagocytic particles, interferon- γ (IFN- γ).
Phagocytosis	Complement component (C3b), proteolytically inactive product of complement cleavage factor C3b (iC3b), immunoglobulin G (IgG, Fc portion) fibronectin, interferon- γ (IFN- γ) increases Fc receptor expression.
Granuloma formation	Interferon- γ (IFN- γ), tumor necrosis factor- α (TNF- α), interleukin-1 (IL-1).
Pyrogens	Interleukin-1 (IL-1), tumor necrosis factor- α (TNF- α), prostaglandin E ₂ (PGE ₂), interleukin-6 (IL-6).
Pain	Prostaglandin E ₂ (PGE ₂), bradykinin.

1.4.1 Histamine

Histamine **2** (figure 1.3), is an important naturally occurring mediator that is not only responsible for the various physiological responses of the multi-cellular organisms¹² and functions as a neurotransmitter¹³ but is also involved in several pathological responses and has a well established role as a mediator of inflammation.¹⁴ The pleiotropic functions of histamine **2** are mediated through four distinct G-protein coupled receptors that are classified as H1, H2, H3 and H4. A fifth receptor; histamine H_{1C} located intracellularly has also been described in hematopoietic cells.¹⁵ During normal physiological conditions, histamine **2** is metabolically degraded to the biologically inactive compounds by one of the two enzymatic pathways : (i) Histaminase (found in neutrophils and eosinophils) which converts histamine **2** to N-methylhistamine **3** and (ii) imidazole-acetic acid **4** (figure 1.3); whereas its cellular release is initiated by specific antigen-IgE reactions or by C5a and is calcium ion dependent. Histamine **2** has been found to influence the release of cytokines and inflammatory mediators from a variety of inflammatory and immune cells.¹⁶ Following are the major aspects of histamine **2** reactions that are considered to contribute to both types (e.g. acute and chronic) inflammation.

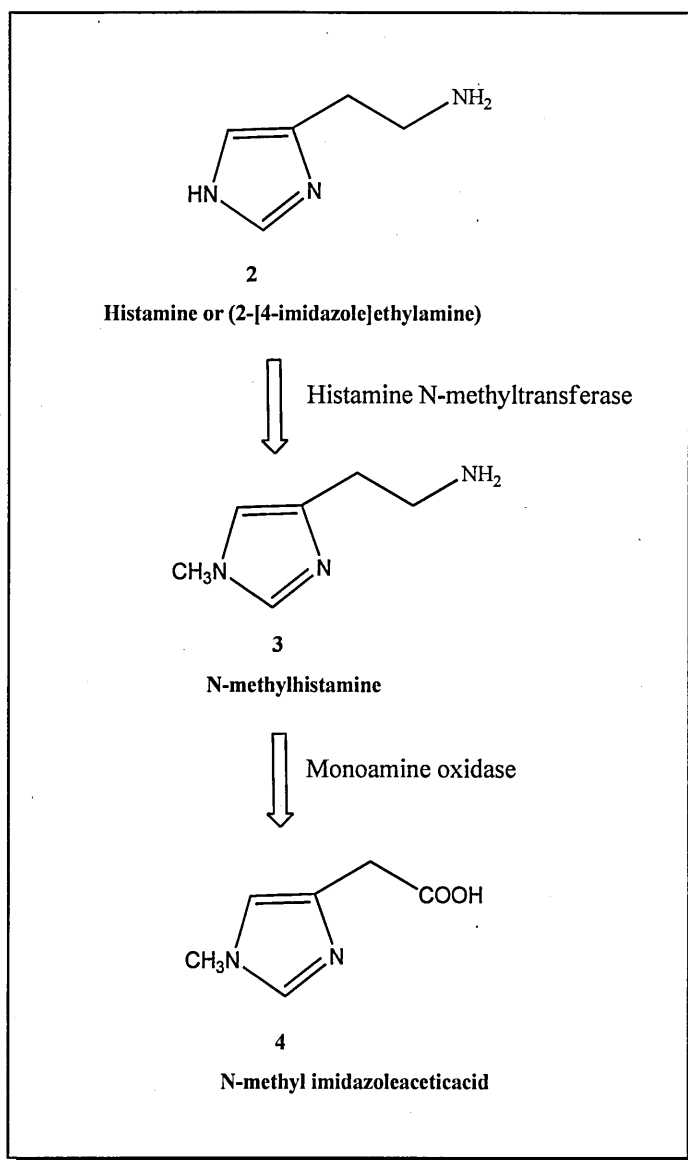


Figure 1.3 : Histamine 2 and its major metabolic pathway.¹⁹

Histamine 2 is metabolized mainly by the action of histamine N-methyltransferase and monoamine oxidase.

1.4.1.1 Different histamine responses towards early and late inflammatory conditions

In response to the early stages of acute allergy or inflammatory reactions, histamine 2 causes bronchoconstriction, vasodilation and increased vascular permeability, which are responsible for most of the symptoms of rhinitis, asthma, urticaria and phylaxis.¹⁷

On the other hand, during the progression of allergic-inflammatory responses; histamine 2 contributes towards the enhancement of the secretion of pro-inflammatory cytokines e.g. IL-1 α , IL-1 β , IL-6 and chemokines.¹⁸

1.4.1.2 Mode of histamine release

Another aspect that can also contribute to the histamine 2 dependent chronic allergy or inflammatory reactions, involves the mode of release of histamine 2. When histamine 2 is released from mast cells and basophils the interaction of antigen with IgE antibodies anchored to the cell surface triggers a rise in the cytosolic concentration of free calcium ions that results in the exocytosis of histamine 2 storage granule and then the release of histamine 2 from the granules by the process of cation exchange.¹⁹ In contrast to this, cells other than mast cells and basophils produce histamine 2 through the induction of histamine forming enzyme called histidine decarboxylase (HDC). Such histamine 2 production has been suggested to play a part in the exacerbation of collagen-induced experimental arthritis, muscle fatigue, the prolonged accumulation of gastric acid induced by lipopolysaccharide (LPS) and interleukin-1 (IL-1), and has a distinct feature of rapid formation and release

associated with it in comparison to the mast cells and basophils which can store histamine **2** before release.²⁰

1.4.1.3 Storage sites for histamine

Mast cells and basophils are the major sites of histamine **2** storage and within these cells it is stored as a granular complex with high molecular weight heparin and an acidic protein. Based on the fact that mast cell numbers are abundant in the lung, skin and gastrointestinal mucosa, the highest concentrations of histamine **2** is therefore found in these tissues, whereas in blood, histamine **2** is stored in basophils. However, there is evidence regarding the involvement of other types of cells including histaminocytes of stomach and histaminergic neurons of the hypothalamus that also supply histamine **2**.¹⁹

1.4.2 Serotonin

Serotonin **5** (figure 1.4) is another vasoactive amine which also acts as a neurotransmitter²¹ and is synthesized by the decarboxylation of tryptophan **6** (figure 1.4) in the diet and is found in the mast cell granules of rodents²², however, in mammals 95% of the serotonin **5** is produced and stored by the mucosal enterochromaffin cells of the gastrointestinal tract where as only 5% is restricted to brain.²³ Results from various studies of carrageenan-induced inflammatory models show the involvement of serotonin **5** along with histamine **2** during the early phase of inflammation.²⁴

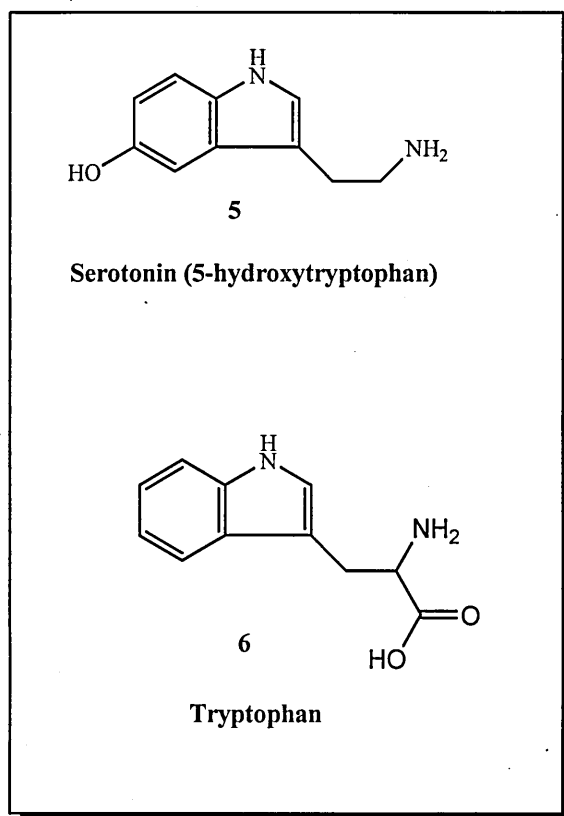


Figure 1.4 : Chemical structures of serotonin 5 and tryptophan 6.²⁵

1.4.3 Kinins

Kinins are amongst the first agents produced at the site of injury or inflammation in the periphery.²⁶ Kinins that include bradykinin (plasma kinin) and Lys-bradykinin (tissue kinin) are biologically active peptides, generated from their kinin precursor proteins, kininogens²⁷ by the action of the enzyme kallikrein from its inactive form prekallikrein, which is activated either by the Hageman factor or by tissue proteases.²⁶ Kinins are inflammatory mediators that are not only considered to be responsible for the constriction of venules, dilation of arteriole, increasing permeability of the capillary membrane and interacting with sensory nerve terminal transmitters and serve as autocoids to evoke pain and mediate oedema respectively, but are also involved in the release of substance P (known transmitters from nerve terminals), stimulate the synthesis of IL-1 and induce the formation of prostaglandins and leukotrienes by activating phospholipase A₂.²⁸ The fore mentioned inflammatory responses of kinins are exhibited by two specific types of receptors B₁ and B₂.²⁶

1.4.4 Complement system

The complement system is a part of the innate immune system that is mainly involved in defence against invading pathogens (particularly microbial) and in the acquired immune response²⁹ however the cascade is also likely to be activated during tissue injury as well as it plays a role in cellular injury associated with major trauma and burns.^{30,31} Inappropriate activation and/or inefficient regulation of the complement system can result in various inflammatory and immunologic diseases.³² Activity of the complement system is established by the interaction of 30-40 soluble plasma and

cell surface proteins, regulators, complement factors (C1q, C3a, C4a, C5a) and their receptors (CR1, CR2 and CR3).^{33,34}

The biochemical cascade of the complement system proceeds through controlled proteolysis and conformational changes of the constituent proteins via three activation pathways (table 1.2). These include the Classical Pathway (CP), the Alternative Pathway (AP) and the Lectin Pathway (LP).³⁵

Components of the Early and Late Events in the Complement Cascade		
Lectin Pathway	Classical Pathway	Alternative Pathway
Early events		
MASP-1, -2, -3	C1	factor D
C4	C4	C3b
C2	C2	factor B
Late events		
C5	C5	C5
C6, C7, C8, C9	C6, C7, C8, C9	C6, C7, C8, C9

Table 1.2 : Activation pathways of complement cascade and their early and late event components.³⁶

Deficiencies of complement components of all three pathways have been reported to be involved in distinct pathologies³⁷ including sepsis, adult respiratory distress syndrome, hyperacute rejection of transplants³³ and various neuroinflammatory diseases including multiple sclerosis, ischemia, Alzheimer's disease etc.³⁸

Describing the events that take place during the CP, Bonifati and Kishore³⁹ suggest that the CP is activated by the binding of the C1q to IgG or IgM containing immune complex which leads to the auto-activation of C1r, which in turn activates C1s, C1r and C1s together with C1q from the first component C1 of the complement system. The activation of the C1q complex (C1q+C1s-C1r-C1-r-C1s) subsequently activates the complement through the cleavage of C4 and C2 to yield C3 convertase that cleaves C3, leading to the activation of the C2-C9 components and the formation of the terminal membrane attack complex (MAC).³⁹ The MAC inserts or binds itself to the bacteria or viruses' membrane leading to death however, if the host cells are inadequately protected then MAC can contribute to their damage as well through a process called 'bystander lysis'.⁴⁰

The alternative pathway is initiated by the spontaneous hydrolysis (slow rate = 0.005% per minute) of the thioester bond of the C3, resulting in conformational changes of the protein.³⁷ This intermediate form of C3 can bind factor B and cleavage of factor B by factor D yields the C3 convertase C3 (H₂O)Bb which continues the alternative pathway by cleaving the additional C3 molecules into C3a and C3b fragments. The C3b binds to factor B resulting in the activated C3bBb complex which forms more C3 convertases and hence amplify the cascade (explosively fast reaction, rate of C3b production = 10¹⁵ molecules per minute). As the complement

cascade progresses, active C5 convertase enzymes specifically convert C5 into C5a and C5b. The newly formed C5b initiates the assembly of the terminal complement membrane attack complex C5b-C9 (also known as terminal complement complex, TCC).⁴¹

The lectin pathway of the complement system can be activated by binding of its recognition molecule mannose binding lectin (MBL) to one of its carbohydrate ligands found either on the surface of the microorganism bound IgG, or altered self-molecule. Binding of MBL, activates MBL-associated serine proteases (MASPs) which cleave C4 and C2 leading to the formation of C4b2a, cleavage of C3 and complement activation up to the formation of MAC.³⁷

1.4.5 Cytokines

Cytokines are a group of cell-derived poly-peptides which to a larger extent orchestrate the inflammatory response i.e. they are the major determinants of the make-up of the cellular infiltrate, the state of cellular activation and the systemic responses to inflammation.⁴² These are pleiotropic in their effect and elicit their effects locally or systemically in autocrine or paracrine manner.⁴² Cytokines activate many signal transduction pathways, which engage in a high level of crosstalk.⁴³ Macrophages play an important role in the production of inflammatory cytokines such as interleukin-1 β , tumour necrosis factor- α and other inflammatory mediators i.e. nitric oxide and prostaglandins.⁴⁴

1.5 Vascular events of inflammation (change in vascular flow and calibre)

1. Vasodilation

Immediately following an injury, there is frequent vasoconstriction of arterioles due to the vasomotor reflex; that lasts for few seconds and is followed by the hemodynamically more important vasodilation of capillaries and venules. Dilation is mediated by vasoactive agents and results in the increased blood flow to the injured site and consequently the area becomes red and gets warm, however over time, the rate of blood flow decreases.^{8,45}

2. Increased vascular permeability

Vasodilation and increased vessel permeability are histological events commonly observed during acute inflammation.⁴⁶ Vasodilation is usually accompanied by increased permeability of the microvasculature, which usually affects the venules and refers to the outpouring of the fluid rich proteins from the blood vessels into the extravascular tissues resulting in the slowing down of the blood circulation due to the increased viscosity.⁸

3. Leukocyte adherence and emigration

Vasodilation and exudation are accompanied by leukocyte (mainly polymorphonuclear leukocytes, PMNs) adherence, followed by their emigration, and although these events occur simultaneously these are not necessarily interdependent.⁴⁵ The adherence of neutrophils to the endothelial cells and their emigration from the blood stream into the tissues is an essential part of the host

defence against invading pathogens.³⁰ However, if the pro-inflammatory properties of these neutrophils are not properly regulated, these normally beneficial leukocytes can also contribute to the pathogenesis of infectious diseases or excessive inflammation.⁴⁷ During inflammation, the resident cells in tissues, for example macrophage, release neutrophil chemotactic factors that are mainly responsible for rolling and adhesion of neutrophils on endothelial cells, followed by their transmigration.⁴⁸ The transmigration phenomenon consists of the following overlapping steps.³⁰

a. Margination

b. Rolling

c. Adhesion

d. Diapedesis

e. Chemotaxis

Margination

Margination is a passive rheological phenomenon⁴⁹ that allows neutrophil movement from the central blood stream to the periphery of the vessel and is facilitated by the process of stasis and fluid exudation at the site of inflammation and physical interactions between erythrocytes and neutrophils.³⁰ Using Pentoxifylline (PTX), a rheologically active drug Hussain et al⁵⁰ have demonstrated that adhesion of leukocytes to endothelial cells is only possible if the cells undergo margination due to these rheological interactions.

Rolling

After margination, the endothelial cells, lining the blood vessels of the infected tissues are stimulated to express receptors belonging to the selectin family (E and /or P-selectin), that capture neutrophils from the bloodstream and support their rolling form of adhesion along the endothelium, driven by the shear force applied by the flow⁵¹ (figure 1.5).

As a result of rolling, the leukocytes are simultaneously halted in the microcirculation and exposed to chemoattractants or activators either present on the endothelial surface or released from the injured tissue.⁵²

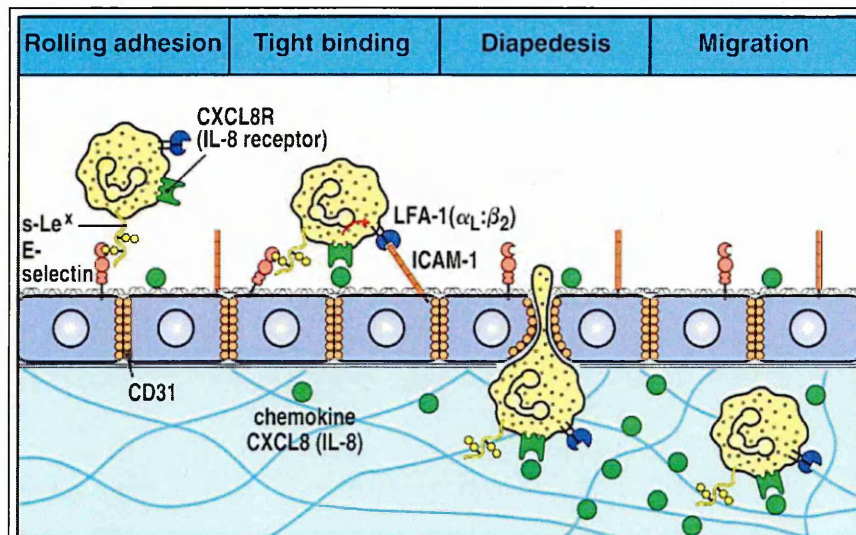


Figure 1.5 : Leukocyte rolling along the surface of endothelial cells.⁵³

E-selectin is binding reversably with carbohydrate on the leukocyte cellular membrane. P-selectin is not shown.

PECAM-1 or CD31 = Cluster of differentiation molecule, ICAM-1 = Intracellular adhesion molecule 1, LFA-1 = Lymphocyte function-associated antigen 1.

Adhesion

As rolling progresses, a high affinity adhesive interaction known as adherence develops which is necessary for subsequent neutrophil diapedesis and chemotaxis.³⁰ Binding of leukocytes to the blood vessel wall is controlled by a complex cascade of molecular interactions between the leukocyte and the endothelial cell layer mediated by cell adhesion molecules and leukocyte activating factor.⁵⁴ Cell adhesion molecules that have been characterized to date include E-selectin, P-selectin, vascular cell adhesion molecules (VCAM)-1, intercellular adhesion molecules (ICAM)-1 and platelet/endothelial cell adhesion molecule (PECAM)-1.⁵⁵

Diapedesis

Following a period of stationary adhesion, a leukocyte may leave the postcapillary venule by extending pseudopodia between endothelial cells and pulling itself into the subendothelial space and the adjacent interstitial compartment, through a complex process which is often termed as leukocyte diapedesis, extravasation or emigration. This event is dependent on an array of cellular processes including adhesion molecule expression and activation, cytoskeletal reorganisation and alteration in membrane fluidity.⁵⁶ Members of three major families of adhesion receptors that have been implicated in this cascade include selectins, integrins and the immunoglobulin superfamily.⁵⁷

1.6 Chemotaxis

Chemotaxis is a process that directs the orientation of cell motility in response to chemical gradients (chemotactic agents) and is necessary for the maintenance of normal biological functions, including the immune response of neutrophils, growth of blood vessels, embryonic development and the aggregation of the amoeboid cell.⁵⁸ However, negative consequences are also associated with the process when inflammation leads to a chronic response.⁵⁹

Cell motility is a complex process that involves the coordination of many cellular functions, including the conversion of information from the environment into a series of coordinated responses that culminate in directed cell movement.⁶⁰ The following description of the chemotactic response of the neutrophils is one of the examples (among the fore-mentioned biological functions involving chemotaxis), that illustrates the mechanism of chemotaxis involved in the immune response.

In humans, polymorphonuclear leukocytes (PMNs), bind to various chemoattractants or chemotactic chemical substances (that include host tissue derived chemokines e.g. CXCL-8, leukotrienes LTB₄, complement reaction product C3 or C5a and pathogen products e.g. bacterial N-formylated peptides) through cell surface G protein-coupled receptors, that further activate multiple downstream signalling molecules involved in the stepwise regulation of PMN migration.⁶¹ (figure 1.6). The sequence of events involved in the cellular chemotactic response is believed to occur as follows:⁴⁵

- Recognition of the chemoattractant at the cell surface
- Transduction of the initial signal into the effector mechanism.
- The effector mechanisms.

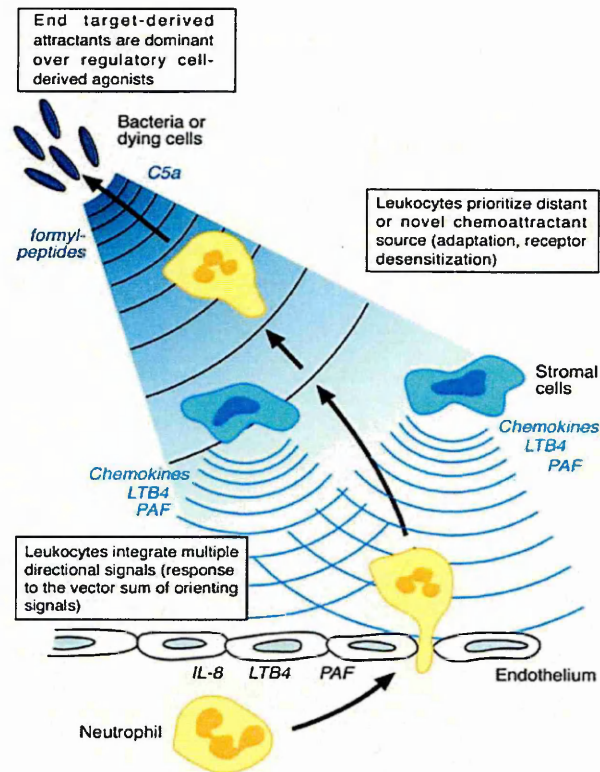


Figure 1.6 : Chemotactic response of neutrophils.⁶²

Schematic view of the chemotactic migration of leukocytes towards an inflammation site. Neutrophils move through the endothelium and within tissues by responding to successive combinations of chemoattractant gradients. Chemoattractants are released by endothelial cells, by activated stromal cells (macrophages, epithelial cells), and by the inflammatory targets, i.e, bacteria or dying cells. The direction of neutrophil movement is first guided by the steepest local chemoattractant gradient and is then regulated by successive receptor desensitization and attraction by secondary distant agonists. Finally, end-target attractants are dominant over regulatory cell-derived agonists.

1.7 Inflammatory responses

As recently reviewed by Lawrence,⁶³ inflammation involves the sequential activation of pro- and anti-inflammatory pathways (mediators). Among these two pathways relatively little is known about the anti-inflammatory mechanisms that "switch-off" or resolve inflammation because the resolution of the acute inflammatory response does not simply involve the catabolism of pro-inflammatory mediators, but is actively coordinated by its own endogenous 'proresolving and anti-inflammatory' mediators, however the activation of the transcription factor NF κ B is considered to be involved in both the events. The aim of the acute pro-inflammatory response is to neutralize the noxious or foreign agents or the injurious process and remove it before it spreads to other parts of the body.

During the pro-inflammatory pathway the activation of NF κ B is responsible for the expression of pro-inflammatory mediators such as cytokines (TNF and IL-1 β), adhesion molecules, chemokines, growth factors and inducible enzymes cyclooxygenase-2 (COX-2) and inducible nitric oxide synthase (iNOS), whereas such activation during the resolution (anti-inflammatory pathway) of inflammation is associated with the induction of apoptosis and the expression of the anti-inflammatory mediators (TGF β 1 and cyclopentenone prostaglandins).

Part B

1.8 Anti-inflammatory drugs

In general, the major therapeutic agents used for the treatment of a variety of inflammatory and autoimmune diseases (e.g. arthritis, psoriasis, atopic dermatitis, inflammatory bowel disease, multiple sclerosis, asthma etc) have been classified as: the Non-Steroidal Anti-Inflammatory Drugs (NSAIDs), the Corticosteroids, the Disease-Modifying Anti-Rheumatic Drugs (DMARDs), the antagonists of bradykinin and kallidin and the anti-histamines.^{64,65} This classification is based on the action of these drugs towards the production and propagation of the inflammatory mediators (eicosanoids, cytokines, peptides, histamine, serotonin, and platelet-activating factor).⁶⁴ Rheumatoid arthritis (RA) is a systemic inflammatory disorder of joints that affects about 1% of the world's population and leads to substantial societal effect in terms of functional loss, disability and increased mortality.⁶⁶ Drugs used for the treatment of RA are usually divided (following the pyramid approach) into first-line drugs (the NSAIDs) and the second-line drugs (the DMARDs); whereas the glucocorticoids are usually considered as a separate category and are often considered essential for the treatment of RA.⁶⁷

1.9 The traditional therapeutic “pyramid approach”

Gardner⁶⁸ describes the evolution involved in the treatment philosophy of RA based on the “pyramid approach”. In the late 1960's and early 1970's, the patients were prescribed NSAIDs along with physical therapy. In the beginning, this approach was

based on the fact that all NSAIDs readily suppress the signs of inflammation i.e. pain and stiffness; but subsequently it was realized that the NSAIDs do not prevent joint damage and disability in many patients.⁶⁹ With the phenomenal advancements made in molecular biology defining the molecular, humoral and cellular events of RA, new therapeutic opportunities were defined to inhibit specific events involved in the inflammatory process.⁷⁰ Thus the successive steps then progressed up the pyramid to second-line drugs, the DMARDs; at first with low toxic ones like anti-malarial and then to the more toxic ones like gold preparations, depending upon the severity or progression of the disease.⁶⁸ Furthermore, based on the statistical findings over 90% of arthritic patients had joint erosions by 2 years of disease, that 5-10% went on disability each year, remission was very rare and men died 4 years earlier and women 10 years earlier than normal population; the period for a patient to start DMARDs was also evolved starting from 120 months (1965) to 30 months (1975) and to only 5 months (1985).⁶⁸

1.10 Nitric oxide (NO)

Nitric oxide (figure 1.7) is a pleiotropic, short-lived free radical that participates in diverse biological processes such as regulation of blood vessel and airway tone, inflammation, neurotransmission, apoptosis and is widely utilised as a signalling molecule in cells throughout the body, carrying out numerous roles but most notably regulating local vascular tone and blood flow. In general, NO causes local vasodilatation and increases oxygen delivery.⁷¹ During normal endothelial nitric oxide pathway; NO diffuses from endothelial cells into the vessel lumen and into the neighbouring smooth muscle cells, where it activates soluble guanylate cyclase

leading to an increase in intracellular cyclic guanosine monophosphate (cGMP). In smooth muscle cells cGMP causes smooth muscle relaxation and hence dilation of the artery.⁷² On the other hand, several non-cGMP dependent actions activated by NO have also been reported, such as inhibition of the transcription factor nuclear factor- κ B, leading to the inhibition of pro-inflammatory cytokines.⁷³ In biological systems, NO is produced via two different metabolic pathways. (i) Nitric oxide synthase (NOS) dependent pathway in which the oxidation of the guanido group of L-arginine **7** to L-citrulline **8**, results in NO production and the reaction is catalyzed by NOS,⁷⁴ (figure 1.7) and (ii) by the chemical reduction of the nitrite anion (NO_2^-) to NO, a reaction that is generally accelerated in an acidic milieu.⁷⁵ There are three isoforms of NOS, namely, neuronal NOS (nNOS or type I), endothelial NOS (eNOS or type III), and inducible NOS (iNOS or type II). nNOS and eNOS are constitutively expressed in the gut under normal conditions and are primarily regulated by the levels of intracellular calcium via calmodulin and release NO in response to calcium fluxes, on the other hand, the induction of iNOS usually occurs during inflammation and immune activation and does not depend on calcium/calmodulin.⁷⁶ The NOS-independent pathway of NO generation was first described in the stomach but more recent studies show that nitrite reduction can take place also in blood and in other tissues. The substrate for intragastric NO generation (nitrite) is derived from saliva. Saliva naturally contains much nitrate as a result of an active uptake from blood by the salivary glands. By the action of nitrate reductase in commensal bacteria inhabiting the oral cavity much of this nitrate is reduced to nitrite.⁷⁵

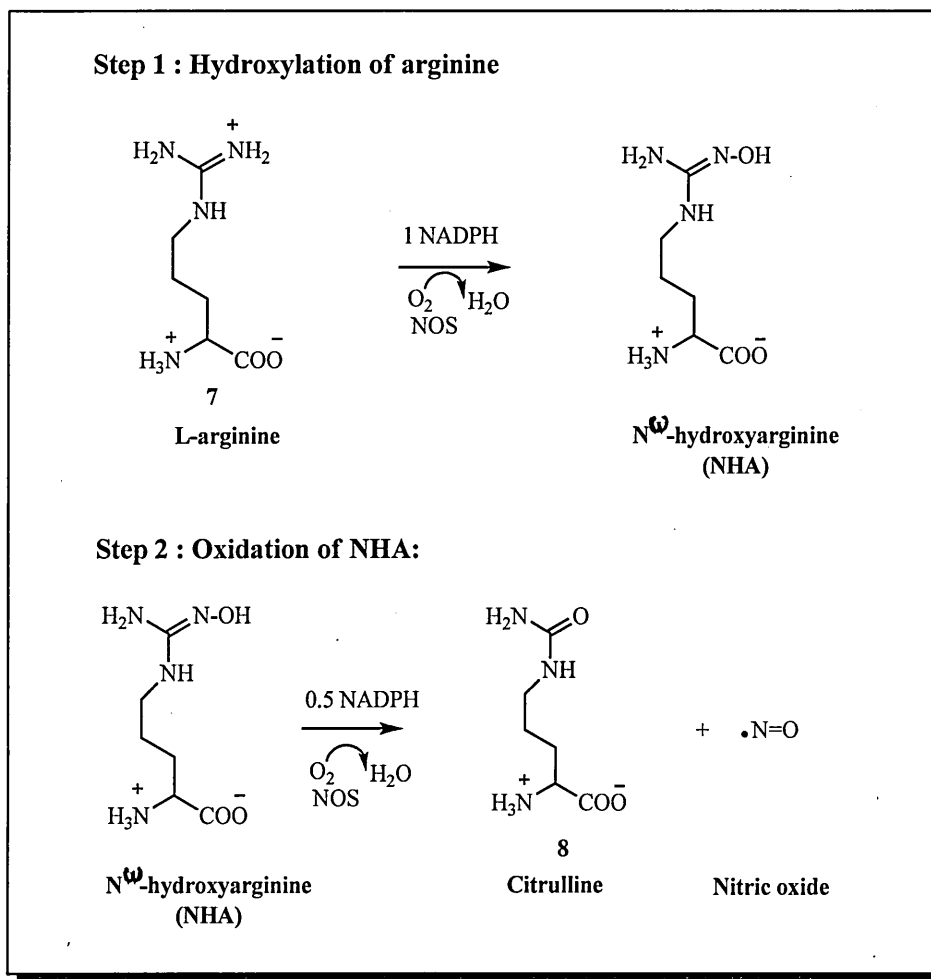


Figure 1.7 : Synthesis of nitric oxide (NO) via NOS dependent pathway.⁷⁷

In the first step, arginine 7 is hydroxylated to produce an enzyme-bound intermediate N ω -hydroxy-L-arginine (NHA), and 1 mol of NADPH and oxygen are consumed. In the second step, NHA is oxidized to citrulline 8 and nitric oxide with the consumption of 0.5 mol of NADPH and 1 mol of oxygen.

The physiological chemistry of NO is variable and complex, however, the most important and direct reaction of NO in cells are of two general types: those between NO and metal complexes of protein (as occurs in guanylate cyclase activation) and those between NO and radical intermediates of biological transformations e.g. capture of the tyrosyl radical formed during ribonucleotide reductase.⁷⁸ Hence due to its versatile nature, NO may affect diverse cellular responses and have both pro- and anti-inflammatory properties.⁷⁹

1.11 Nitric oxide donating nonsteroidal anti-inflammatory drugs (NO-NSAIDs)

1.11.1 Rationale behind the development of NO-NSAIDs

Nonsteroidal anti-inflammatory drugs (NSAIDs) have been widely used to mitigate pain and inflammation; however, their use is associated with serious gastrointestinal side effects.⁸⁰ The development of nitric oxide donating nonsteroidal anti-inflammatory drugs (NO-NSAIDs) (figure 1.8 A) or nitric oxide donating steroidal anti-inflammatory drugs (NO-SAIDs) (figure 1.8 B) is based on the strategy of introducing a NO-donating moiety (e.g. nitroxyalkyl group or other nitro linker) which is covalently bonded to a spacer molecule, into a bioactive molecule such as conventional NSAIDs⁸¹ or SAIDs.⁸² Their development is based on various findings that have shown that NO possesses some of the properties of prostaglandins (PGs) within the gastric mucosa and hence the NO-coupled NSAIDs might deliver NO to the site of NSAIDs induced damage, thereby decreasing the gastric toxicity which is often a consequence of diminished PGs level in the gastric mucosa.⁸¹ Therefore, the

development of NO-NSAIDs has been the next step forward in the search for safer NSAIDs.

To the best of our knowledge the data available on the NO-donating oxicams (the enolic acid class of NSAIDs) figure 1.9, is limited. Therefore, the NO-aspirin **9** is used in this thesis to help understand the mechanism of action of NO-NSAIDs via their pharmacokinetic and pharmacodynamic properties and their safety profile over the conventional NSAIDs.

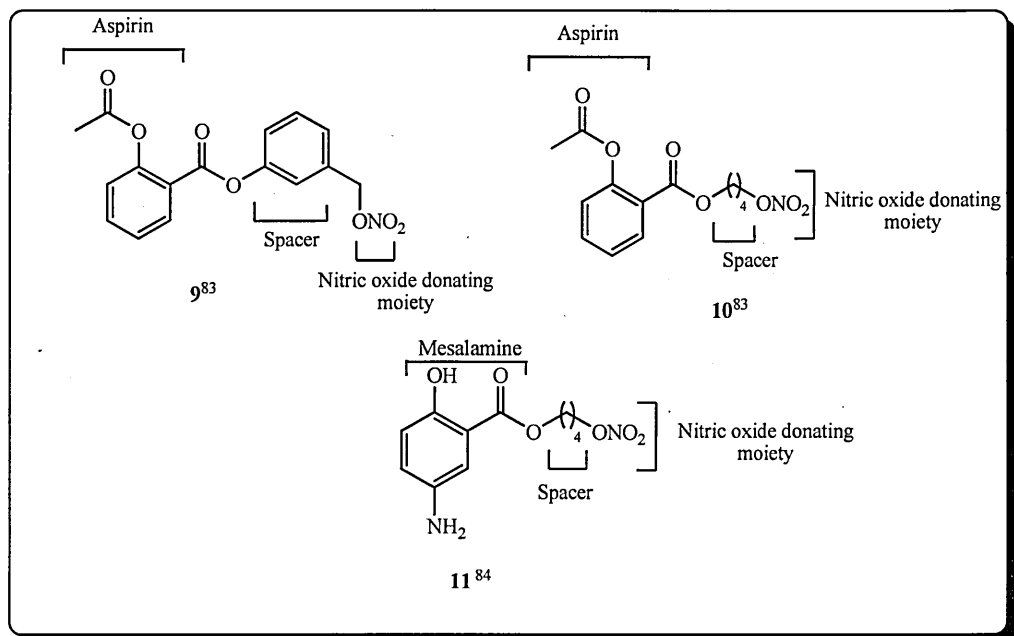


Figure 1.8 : (A) Structural features of various nitric oxide donating non-steroidal anti-inflammatory drugs (NO-NSAIDs).

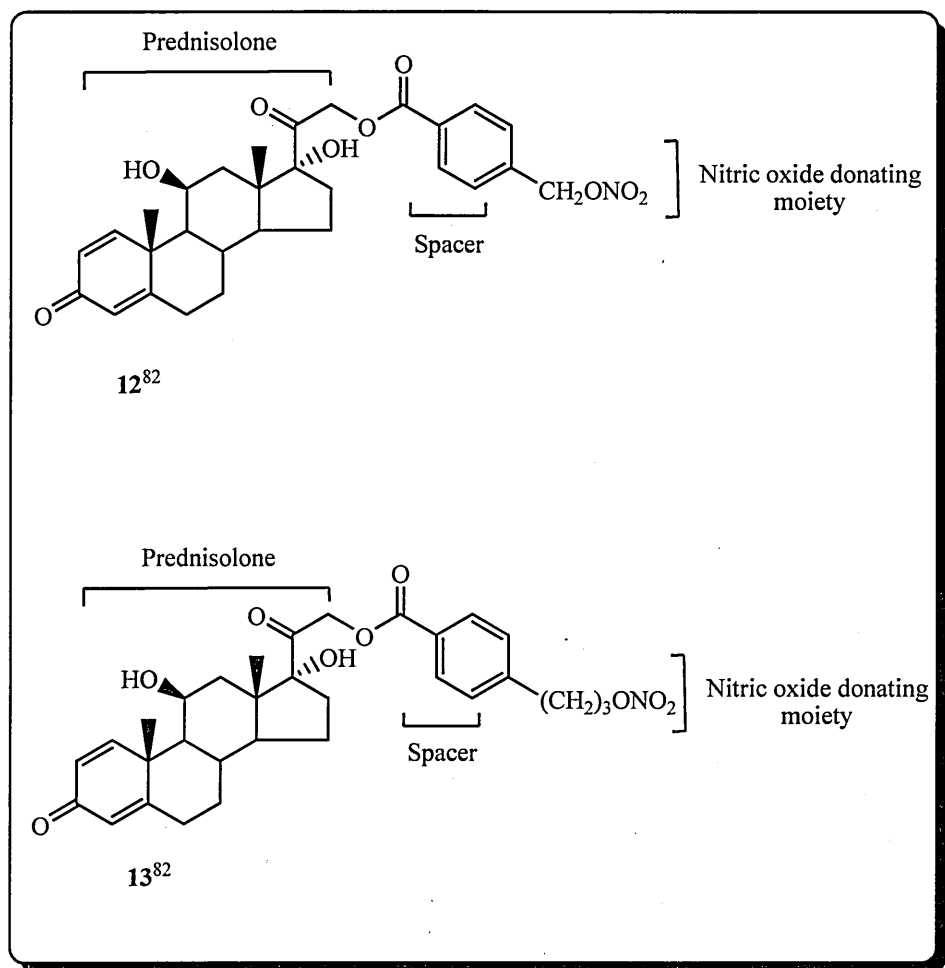


Figure 1.8 : (B) Structural features of various nitric oxide donating steroidal anti-inflammatory drugs (NO-SAIDs).

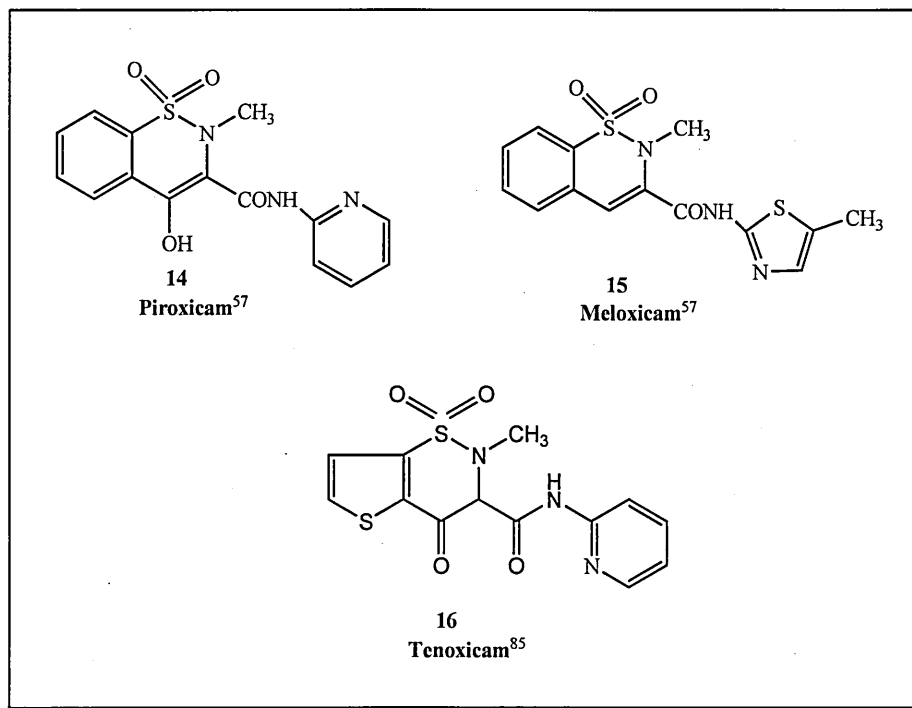


Figure 1.9 : Chemical structures of various oxicams.

1.11.2 Mechanism of action of NO-aspirin

As reviewed by Wallace⁸⁶, due to its ability to suppress platelet aggregation and thereby inflammation, while sparing the gastrointestinal (GI) tract, NO-aspirin **9** (figure 1.10) has attracted a particular interest among several other NO-aspirin candidates and therefore has been best characterized both experimentally as well as clinically. Also from structure-activity relationship, both individual bioactive moieties e.g. conventional aspirin and the NO, collectively appear to be responsible for the effectiveness of NO-aspirin **9**.

1.11.3 Pharmacokinetic properties of NO-aspirin

Regarding their pharmacokinetic properties, NO-aspirins in general, are stable in aqueous solutions in contrast to conventional NO donors, however, NO-aspirin **9** in particular; is well absorbed after oral administration.⁸⁶ As a consequence of efficient absorption after oral administration, the ester linkage of the conventional aspirin moiety in NO-aspirin **9** is rapidly cleaved by the action of esterase enzymes in the liver and in plasma, on the other hand the release of NO occurs at much slower rates over many hours after administration of NO-aspirin **9**, as shown by the peak levels in plasma as well as the increase in cyclic guanosine monophosphate (cGMP) levels in platelets was lower than the ones found using equimolar doses of traditional organic nitrates such as glyceryl trinitrate or isosorbide dinitrate. This low level of NO release provides an evidence of lack of effect of NO-aspirin **9** on systemic arterial blood pressure in contrast to other NO-donors.⁸⁶

1.11.4 Pharmacodynamic properties of NO-aspirin

Metabolism of ester linkage of NO-aspirin

In rats : Using rat liver subcellular fractions (S 9000 x g, microsomes and cytosol), Carini et al⁸⁷ have studied the metabolic fate of NO-aspirin **9** *in vitro*. The authors of the study have postulated that the drug is largely absorbed by the small intestine, reaches the liver where it is readily metabolized. HPLC, LC and LC-MS techniques were used in order to elucidate the structures of the postulated metabolites (figure 1.11) which could arise from different biotransformation pathways via single or multiple hydrolytic cleavage of the different ester moieties e.g. acetate, benzoate or nitrate ester. The presence of salicylic acid **17** (SA), 3-(nitromethyl) phenol **18** (HBN) and 3-hydroxybenzylalcohol **19** (HBA) (figure 1.10) and the absence of other postulated acetyl derivatives (acetylsalicylic acid **20**, **21** and **22**) (figure 1.11) revealed that the most labile functionality in NO-aspirin **9** is the acetate ester. Furthermore, the retention of HBN **18** and the absence of **23** (figure 1.11) show that the nitrate group of NO-aspirin **9** is more resistant to the enzymatic attack.

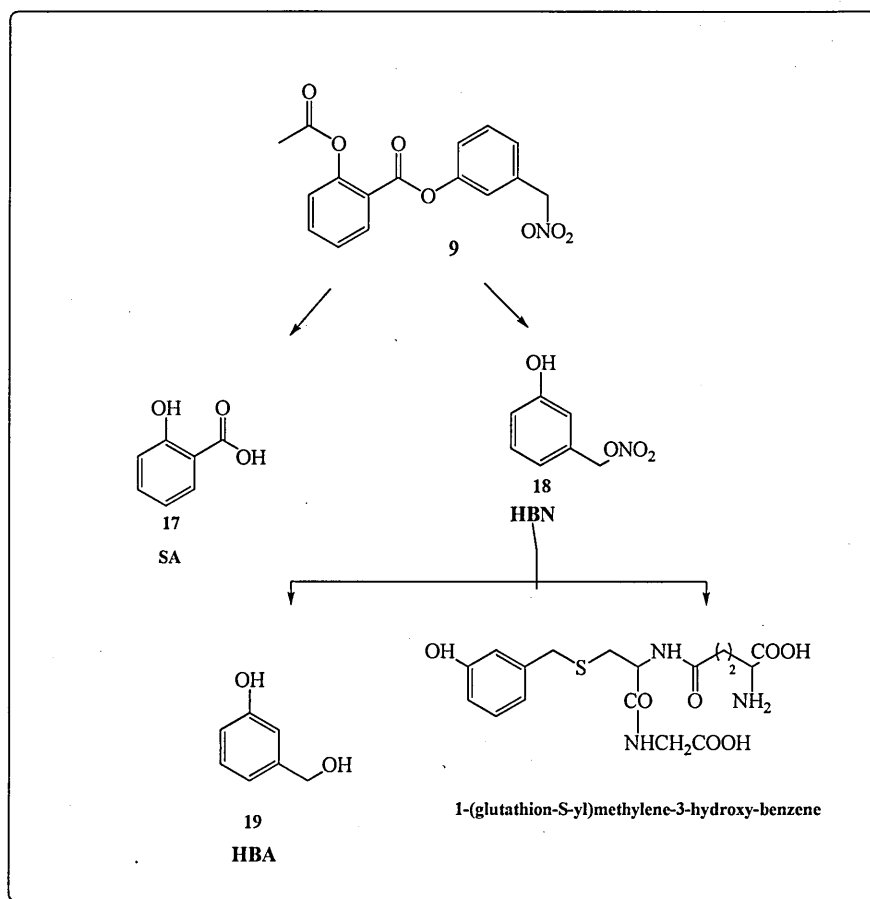


Figure 1.10 : Metabolites of NO-aspirin 9 obtained by the cleavage of acetyl ester moiety in rat liver.⁸⁷

(SA) 17 = Salicylic acid, (HBN) 18 = 3-(nitromethyl) phenol, (HBA) 19 = 3-hydroxybenzylalcohol.

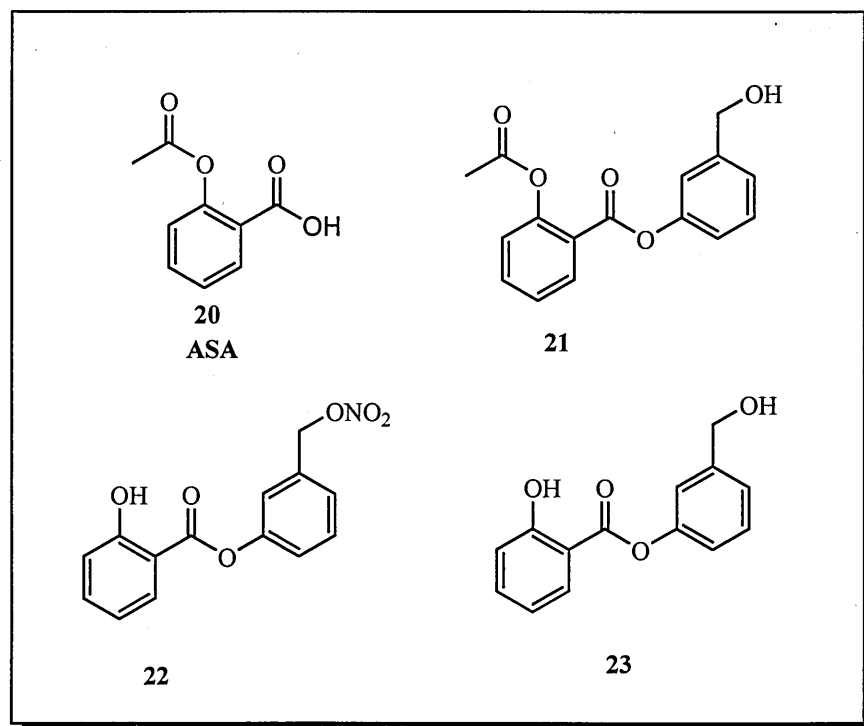


Figure 1.11: Postulated metabolites of NO-aspirin **9**.⁸⁷

(ASA) **20** = Acetylsalicylic acid.

1.12 Cytoprotective and cytotoxic effects of nitric oxide (NO)

Several studies have shown that NO-releasing agents can either cause endothelial cell death by activating intracellular mediators associated with apoptotic pathway or rescue cells from apoptosis⁸⁸ thereby confirming its dual role in cell life.

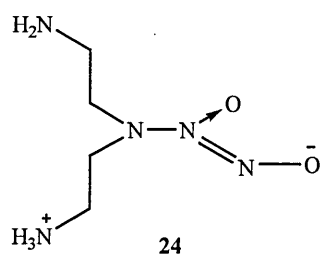
1.12.1 Cytoprotective effects of nitric oxide (NO)

In spite of the cytotoxic effects various studies have convincingly demonstrated, using different cell types of essentially every organ and tissue such as human B lymphocytes, splenocytes, eosinophils, ovarian follicles, cardiac myocytes and endothelial cells, a cytoprotective role of NO that occurs via suppression of apoptosis.⁸⁹ It has been reported that the defensive mechanism exhibited by NO (both exogenous and endogenous) against cell death induced by pro-apoptotic stimuli is triggered via two main mechanisms: (a) regulation of mitochondrial respiration and (b) regulation of cytochrome *c* release.⁸⁸

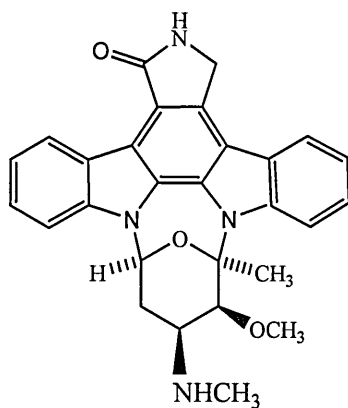
Effect of exogenous nitric oxide (NO) on cell respiration

Using human adult T cell leukemia (Jukart) cells, Beltran et al⁹⁰ have studied the effects of exogenous nitric oxide on cell respiration and investigated the effects of continuous inhibition of cell respiration by NO donor, DETA-NO, **24**, (figure 1.12) on mitochondrial energy status and cell viability in serum-deprived and staurosporin, **25**, (figure 1.12) treated cells. Using the cationic lipophilic fluorochrome, JC-1, **26**, (figure 1.12), serum-deprived cells showed a gradual decrease in mitochondrial membrane potential ($\Delta\psi_m$, an indicator of energy status of mitochondria in particular

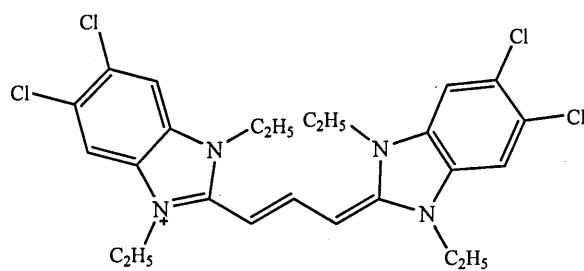
and of cellular homeostasis in general), signifying apoptotic cell-death, however there was a significant increase in $\Delta\psi_m$ after the addition of DETA-NO **24**, (0.5mM) for 3-5 h. This shows that despite the respiration being blocked the $\Delta\psi_m$ was maintained and the cells were protected from apoptosis. Similar results were obtained with staurosporin **25**. On the other hand as the exposure of serum-deprived cells to NO was continued (>5 h) the fall in $\Delta\psi_m$ was observed correlating the appearance of early apoptotic features and a decrease in cell viability.



DETA-NO⁹¹



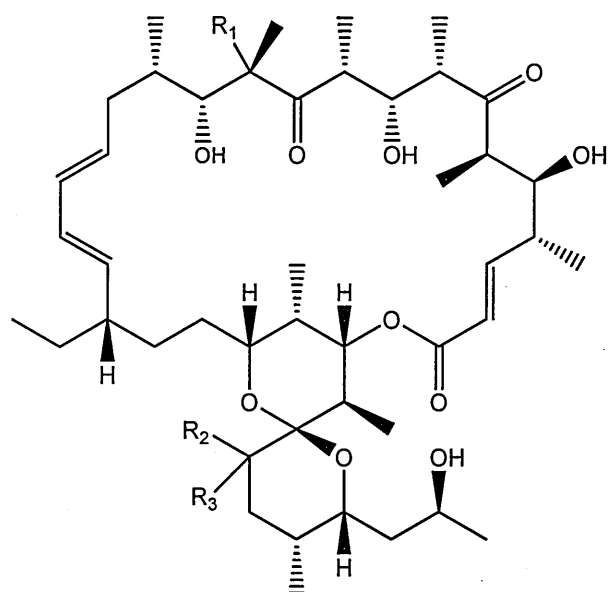
Staurosporin⁹²



JC-1⁹³

Figure 1.12 : Chemical structures of nitric oxide donor (diethylenetriamine nitric oxide DETA-NO) **24**, pro-apoptotic stimulus (staurosporin) **25** and fluorochrome (JC-1) **26**.

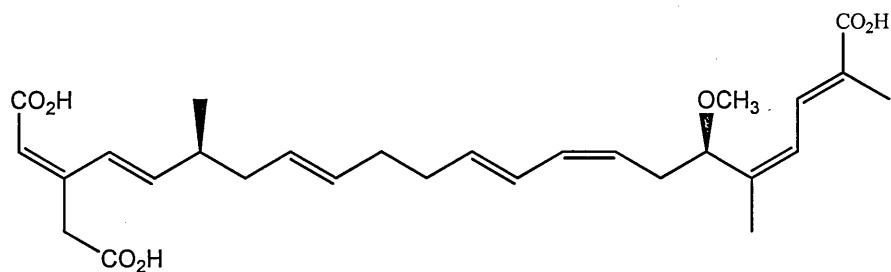
The effect of NO on energy metabolism of serum-deprived cells was also assessed, based on the fact that there is an involvement of a source of energy other than the respiratory chain as $\Delta\psi_m$ was initially maintained despite the inhibition of respiration. This was confirmed by analysing the role of glycolytic ATP in maintaining the $\Delta\psi_m$. Glucose deprivation or iodoacetate treatment of the cells in the presence of NO resulted in a collapse of $\Delta\psi_m$ demonstrating the involvement of glycolytic ATP in its maintenance. Treatment with 8 μ M of oligomycin **27** (an inhibitor of the ATP synthase) (figure 1.13) and 50 μ M of bongkreikic acid **28** (an inhibitor of adenine nucleotide translocator, ANT), (figure 1.13) in the presence of DETA-NO **24** resulted in a partial depolarization, suggesting that the maintenance of $\Delta\psi_m$ during the exposure to NO is caused by the reversal of the ATP synthase and ANT. These results demonstrate that in the presence of exogenous NO a constant inhibition of complex IV (mitochondrial enzyme cytochrome *c* oxidase) occurs that results in inhibition of mitochondrial respiration and initiates a protective action in the mitochondria to maintain $\Delta\psi_m$ through a mechanism that involves the hydrolysis of glycolytic ATP, and hence in the prevention of apoptosis.⁹⁰



27

Oligomycins⁹⁴

A : $R_1 = -OH, R_2 = R_3 = -H$
 B : $R_1 = -OH, R_2 = R_3 = -O-$
 C : $R_1 = -H, R_2 = R_3 = -H$



28

Bongkreikic acid⁹⁵

Figure 1.13 : Chemical structures of oligomycins **27** and bongkreikic acid **28**.

Effect of endogenous nitric oxide (NO) on cell respiration

Describing the role of endogenous NO in cell respiration, Beltran et al⁹⁶ have reported that the activation of human adult T cell leukemia (Jukart cells) with pro-apoptotic stimulus, anti-Fas Ab (10-100ng/mL) induced an immediate (2 minutes, the earliest reading) and concentration-dependent (that progressed for up to 1.5 h) increase in intracellular NO production that was decreased to the control levels thereafter. This NO production inhibited mitochondrial respiration, as a concentration-dependent hyperpolarization was observed after the addition of anti-Fas Ab (10-100 ng/mL). The hyperpolarization of the mitochondrial membrane was described to be the result of the inhibition of cell respiration by the endogenously released NO as confirmed by the use of 500 μ M of N^o-nitro-L-arginine methyl ester **29**, (L-NAME, an inhibitor of NO) (figure 1.14), which reverses both, the inhibition of respiration and hyperpolarization. Furthermore, in these studies also, the hyperpolarization was dependent on the reversal of F₁F_o-ATP. In addition to hyperpolarization, the generation of reactive oxygen species (ROS) was also observed. Treatment of the cells with anti-Fas Ab (10ng/mL) resulted in an increase in hydroetidine (HE) fluorescence from 30 minutes onwards reaching a maximum after 1 h and returning to control levels after 2 h. The early peak of ROS can be completely inhibited by L-NAME **29** and by rotenone confirming that the production of ROS depends on NO production and is generated in mitochondria.

After 2 h stimulation with anti-Fas Ab, a distinct second phase was detected which resulted in a concentration-dependent collapse in mitochondrial membrane potential, a second wave of free radical production and activation of caspase-8 leading to apoptosis.

In conclusion, these results demonstrate that endogenous NO generates the mitochondrial membrane hyperpolarization as well as an early release of free radicals both of which are protective events and occur before the activation of caspases in the second phase and may overcome by the pro-apoptotic mechanisms that occur in parallel.⁹⁶

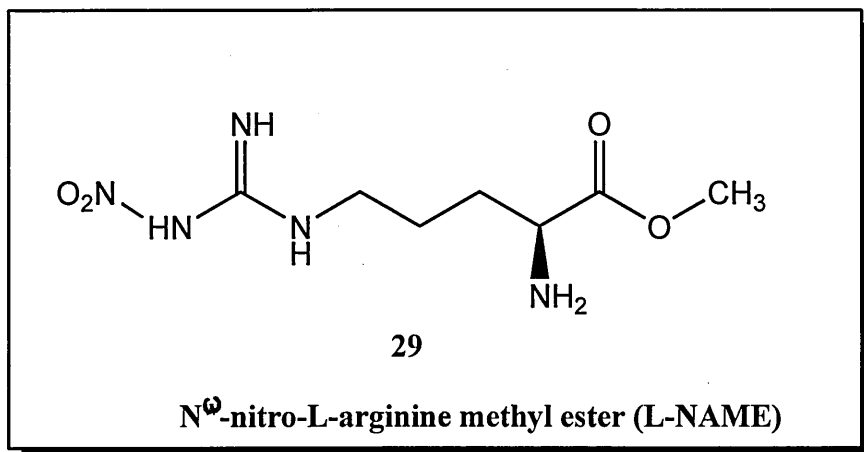


Figure 1.14 : Chemical structure of L-NAME **29**.⁹⁷

Part C

1.13 Curcumin

Modern scientific investigation has proved that the ancient use of spices and culinary herbs in food was associated not only to enhance the flavour and taste of the food but also to serve as a dietary medicine. Moreover, because most of these spices and culinary herbs are a rich source of antioxidants and phyto-nutrients they may help to improve health and reduce the risks of diseases; without the addition of calories, added salt or artificial flavour to the food.⁹⁸ The emerging renewed interest for the use of plants as pharmaceuticals or nutraceuticals relies heavily on the knowledge of their indigenous use in traditional medicine systems.⁹⁹

Curcuma longa

Turmeric, the aromatic, yellow-orange coloured spice is obtained from the dried and ground rhizomes of the plant *Curcuma longa* (figure 1.15A) which belongs to the family *Zingiberaceae* (the ginger family) and is naturally distributed or widely cultivated (as a cash crop) throughout the tropical and subtropical regions of the world¹⁰⁰ including India, China, Indonesia, Jamaica and Haiti.¹⁰¹

Curcuma is a Latin name for curcumin 1 (figure 1.15A), derived from Arabic word “Kouroum” meaning saffron. Due to its specific aroma, flavour, colour-imparting, preservative, digestive and many other medicinal properties; turmeric has a long (dating back to thousands of years) and distinguished use in Eastern civilization.¹⁰²

1.14 Use in folk medicine

Because of its apparent lack of cytotoxicity, turmeric finds a prominent place in two of the world's ancient traditional medicinal systems i.e. Traditional Chinese Medicinal System (TCM) and Indian Medicinal System (IMS) (composed of two major branches – Unani and Ayurveda).¹⁰³ It has been administered effectively via different routes for the treatment of various ailments, diseases and injuries.¹⁰⁴ In the Unani system of medicine turmeric has been reported to be used internally to remove liver obstruction dropsy and jaundice while externally it is used to treat ulcers and inflammation.¹⁰⁵ In both the Ayurveda and the traditional Chinese medicine^{100,101} the topical use of turmeric or its poultices is associated with the treatment of bruises, pains, sprains, boils, swellings, sinusitis and other skin disorders. When taken orally (as decoction) it is considered to be effective for flatulence, hepatic disorders and menstrual difficulties. In chronic rhinitis and coryza (cold) it has been used via inhalation.¹⁰⁴ Further more, in the Ayurveda medicinal system, turmeric rhizomes and flowers have long been used with other natural supplements to treat a wide variety of health disorders; e.g. rhizome with tobacco for hazy vision, inflammation of eye, night blindness; with ginger and green gram for fever, body pain, rheumatism and scabies; with *Dolichos biflorus* for sores; with mustard and roots of *Solanum surattense* for coughs. Flowers on their own are used to treat dyspepsia and cholera while with flowers of *Shorea robusta* and bark of *Ventilago calyculata* for sore throat and syphilis.¹⁰⁶ In traditional Chinese system of medicine turmeric has been reported to serve as an effective remedy to cure angina, abdominal pain, stomach-ache and gallstones.¹⁰⁷

1.15 Morphology

Curcuma longa (figure 1.15B), is a perennial herb which measures up to 60-90 cm in height. The leaves are very large 30-40 cm in length and 10-15 cm in breadth with prominent mid-rib underneath. The flowers are pale-yellow and grow in autumnal spikes.¹⁰⁸ Above the ground the stem is usually short and tapered at the base¹⁰² while underground it modifies into a rhizome.

1.16 Rhizome

Externally, the rhizome is yellowish or yellowish-brown whereas internally it is yellow or yellow-orange, bears an aromatic odour and tastes somewhat bitter. Based upon its morphology, the rhizome has been classified into the following two types:

- Primary rhizome: It is an ovate, oblong, pyriform or round denominated bulb; and is the main source of commercially available turmeric.
- Secondary rhizome: This is also named as “fingers” and is more cylindrical measuring 4-7 cm in length and 1-1.5 cm in width.¹⁰²

1.17 Structural features of curcumin molecule and structural-activity relationships with regard to its anti-inflammatory properties

In an effort to develop a robust and effective pharmacophore model of curcumin **1** analogues and to understand the basis of their biological activity, the structural features of the molecule of curcumin **1** can be divided into three regions as shown in figure 1.16. These include, two substituted aromatic moieties (A and C) joined together by a conjugated β -diketone linker (B).¹¹⁰



(A)

(B)

Figure 1.15 : (A) Whole and powdered rhizomes of *Curcuma longa*, containing the bioactive ingredient curcumin 1, (B) The plant *Curcuma longa*.¹⁰⁹

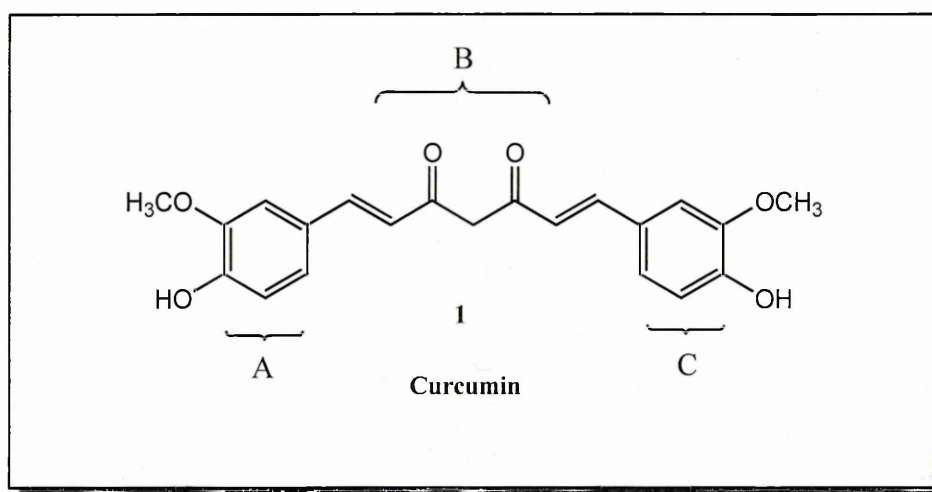


Figure 1.16 : Structural features of curcumin 1 molecule.¹¹⁰

In a recent review, Anand et al¹¹¹ describe that saturation of the alkenes and reduction of the carbonyl moiety in the 7-C linker of curcumin **1** appear to reduce its anti-inflammatory activity, and the mechanism involved behind this behaviour is the suppression of NF- κ B through inhibition of I κ B kinase activity. However, regarding the involvement of the para-hydroxyphenyl rings, there are contradictory findings in the literature, as some studies claim that 4-hydroxyphenyl rings are required for anti-inflammatory activity.¹¹¹ For example, Nurfina et al¹¹² studied the anti-inflammatory properties of several symmetrical curcuminoids on the inhibition of carragenin-induced oedema and have suggested that para-hydroxyl groups in curcumin **1** are important for its anti-inflammatory activity and this effect is enhanced when in combination with the para-hydroxyl groups, the meta-positions are also occupied with less bulky alkyl groups. On the other hand, many analogues of curcumin **1** that lack 4-hydroxyphenyl moieties such as **30a** and **30b**, (figure 1.17) have been reported to be more potent COX-1 inhibitors than curcumin.¹¹¹

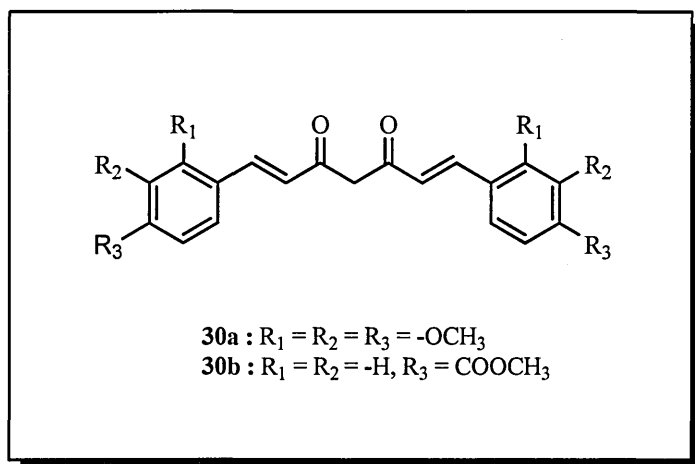


Figure 1.17 : Chemical structures of curcuminoids **30a** and **30b**.¹¹³

1.18 Biological activities of curcumin

Curcumin **1** and essential oils found in turmeric are the major secondary metabolites shown to be largely responsible for the pharmacological properties of turmeric powder.¹¹⁴ The main biological activities of curcumin **1** are summarised in table 1.3, however, its anti-inflammatory property will be dealt with detail as it is the main focus of the present study.

Table 1.3 : Biological activities of curcumin 1 (Modified from Han et al)¹¹⁵

Biological activity	Protective effects and their mechanism	Experimental model	Level	Reference
Anti-inflammatory properties.	<ul style="list-style-type: none"> - Decreased myeloperoxidase (MPO) activity and tumour necrosis factor-α (TNF-α) on chronic colitis. - Reduced nitrite levels and the activation of p38 mitogen activated protein kinase (MAPK). - Down regulation of cyclooxygenase-2 (COX-2) and inducible nitric oxide synthase (iNOS) expression. 	Rats	<i>In vivo</i>	116
	<ul style="list-style-type: none"> - Up regulation of MAPK 58hosphatase-5. 	Prostrate cells	<i>In vitro</i>	117
	<ul style="list-style-type: none"> - Suppressed induction of COX-2 and iNOS. - Inhibition of the expression of ICAM-1 and monocyte chemoattractant protein-1 (MCP-1). - Janus associated kinase-signal transducers and activators of transcription protein (JAK-STAT) suppression via activation of Src homology 2 domain containing protein tyrosine phosphatases-2 (SHP-2). 	Rat primary microglia and murine BV-2 microglial cells.	<i>In vitro</i>	118

Biological activity	Protective effects and their mechanism	Experimental model	Level	Reference
Anti-oxidant and free radical scavenging properties.	- Inhibition of cytochrome P (CYP1A2, CYP3A4, CYP2B6, CYP2D6 and CYP2C9).	Plasmids with human cytochrome P450 NADPH reductase.	<i>In vitro</i>	119
	- Inhibition of mitochondrial proton F0F1-ATPase/ATP synthase.	Rat brain and liver F0F1-ATPase.	<i>In vitro</i>	120
	- Increased expression of glutathione S-transferase P1 (GSTP1) by the activation of anti-oxidant response element (ARE) and NF-E2 related factor 2.	HepG-2 cells.	<i>In vivo</i>	121
	- Increased catalase (CAT), superoxide dismutase (SOD) activity and heat shock protein 70 expression. - Decreased iNOS activity. - Decreased malondialdehyde (MDA), $\text{NO}_2^- + \text{NO}_3^-$ and MPO levels and serum transaminase concentration.	Rat model.	<i>In vivo</i>	122
Modulation of signal transduction pathways. (cont.)	- Inhibition of homodimerization of toll-like receptor 4 (TLR4) in addition to $\text{I}_\text{k}\text{B}$ kinase ($\text{IKK}\beta$). - Inhibition of lipopolysaccharide (LPS) induced nuclear factor-kappa B ($\text{NF-}\kappa\text{B}$) and interferon	293-T cells, RAW-264.7 cells.	<i>In vitro</i>	123

Biological activity	Protective effects and their mechanism	Experimental model	Level	Reference
Modulation of signal transduction pathways. (cont.)	regulatory factor 3 (IRF3) activation through inhibition of myeloid differential factor 88 (MyD88) and TIR domain containing adapter inducing interferon- β (TRIF) dependent pathways.			
	<ul style="list-style-type: none"> - Reduction of 130kDa protein and 4.5kb, mRNA level of iNOS. - Inhibition of activation of NF-κB through prevention of I κB degradation. 	RAW-264.7 cells.	<i>In vitro</i>	124
	<ul style="list-style-type: none"> - Inhibition of interleukin-6 (IL-6) inducible STAT3 phosphorylation and nuclear translocation. 	Human multiple myeloma cells.	<i>In vitro</i>	125
	<ul style="list-style-type: none"> - Up regulation of CYP3A4 via pregnane X receptor (PXR) activation. - Activation of the electrophile responsive element (EpRE) of heme-oxygenase-1 (HO-1) and enhancing the gastrointestinal glutathione peroxidase (GI-GP_x) activity. 	HepG-2 cells.	<i>In vitro</i>	126

Biological activity	Protective effects and their mechanism	Experimental model	Level	Reference
	- Suppression of JAK-STAT inflammatory signalling through activation of SHP-2.	Rat primary microglia and murine BV-2 microglial cells.	<i>In vitro</i>	118
Anti-diabetic properties.	- Inhibition of diabetes-induced elevated levels of interleukin-1 β (IL-1 β), vascular endothelial growth factor (VEGF) and NF- κ B). - Decrease in oxidatively modified DNA and nitrotyrosine production.	Streptozotocin induced diabetic rats.	<i>In vivo</i>	127
Anti-mutagenic/anti-carcinogenic properties.	- Suppression of proliferation and angiogenesis. - Inhibition of NF- κ B regulated gene products (cyclin D1, c-myc, Bcl-2, Bcl-xL, cellular inhibition of apoptotic protein-1, COX-2, matrix metalloproteinase (MMP) and VEGF.	Various pancreatic cancer cell lines. Nude mice.	<i>In vitro</i> <i>In vivo</i>	128
	- Induction of apoptosis by sustained phosphorylation of c-jun N-terminal kinase (JNK) and p38 MAPK. - Inhibition of NF- κ B transcriptional activity. - Induction of phosphorylation of c-jun	HCT-116 cells.	<i>In vitro</i>	129

Biological activity	Protective effects and their mechanism	Experimental model	Level	Reference
	and stimulation of AP-1 transcriptional activity.			
	<ul style="list-style-type: none"> - Induction of apoptosis through activation of caspase-8, BID cleavage and cytochrome c release. - Suppression of ectopic expression of Bcl-2 and Bcl-xL. 	HL-60 cells.	<i>In vitro</i>	130
	<ul style="list-style-type: none"> - Inhibition of Akt, mammalian target of rapamycin (mTOR), p70 ribosomal protein S6 kinase (p70S6K) pathway and activation of ERK1/2 pathway. - Inhibition of tumour growth and induction of autophagy. 	U87-MG, U373-MG cells. Subcutaneous xenograft model of U87-MG cells.	<i>In vitro</i> <i>In vivo</i>	131
Neuroprotective properties.	<ul style="list-style-type: none"> - Disruption of existing plaques and distorted neuritis. - Crossing the blood brain barrier and labels senile plaques and cerebrovascular amyloid angiopathy. 	Alzheimer mouse and APPswe/PS1dE9 mice.	<i>In vivo</i>	132

1.19 Anti-inflammatory action of curcumin

The main molecular targets involved in the anti-inflammatory action of curcumin **1** are described as follows.

Nuclear factor κ -B (NF- κ B)

Figure 1.18 shows the multiple levels at which curcumin **1** interrupts the NF- κ B signalling.¹³³ NF- κ B is a dimeric protein built up from different members of the Rel family and is a ubiquitous transcription factor which is involved in the pro-inflammatory response to cytokines (such as IL-1 or TNF- α) and some particular stresses and is maintained in the cytoplasm in its inactive form.¹³⁴ However, in response to an extracellular signal such as IL-1 or TNF- α , its inhibitory subunit I κ B is phosphorylated, polyubiquitinated and targeted to the proteasome where it is degraded and results in the nuclear localization sequence of NF- κ B, which is rapidly translocated to the nucleus and binds to specific nucleotide sequences.¹³⁴ This binding recruits the RNA polymerase complex and leads to the specific transcription of several genes involved in the pro-inflammatory response.¹³⁴

Using both, the *in vitro* as well as *in vivo* models of inflammation various reports in the literature have shown that curcumin **1** inhibits NF- κ B in various tissues via different mechanisms. Describing the mechanism of NF- κ B suppression by curcumin **1** in human articular chondrocytes, Shakibaei et al¹³⁵ have shown that curcumin **1** suppressed IL-1 β induced NF- κ B activation via inhibition of I κ B α phosphorylation, I κ B α degradation, p65 phosphorylation and p65 nuclear translocation, and these events resulted in the down regulation of NF- κ B targets including COX-2 and

MMP-9.¹³⁵ In another study, Reyes-Gordillo et al¹³⁶ have shown that curcumin **1** at dose of 200mg/kg, protects against carbon tetrachloride induced acute liver damage in rats by blocking the NF- κ B-DNA binding activity. These findings suggest that curcumin **1** prevents acute liver damage by at least two mechanisms, that is, acting as an antioxidant and by inhibiting NF- κ B activation and thus production of pro-inflammatory cytokines.

Interleukin-1 β (IL-1 β)

Interleukin-1 β is one of the cytokines that is involved in the inflammatory process and exhibits its action through its ability to induce the expression of genes associated with inflammatory and autoimmune diseases.¹³⁷ When it binds to the cell-surface of its receptor, it initiates a cascade of signalling events, including activation of extracellular signal-regulated kinase, p38 MAP kinase, Junc N-terminal kinase (JNK) and NF- κ B.¹³⁷

Curcumin **1** inhibits IL-1 β production by affecting the early as well as late signalling events of the inflammatory cascade. Investigating the curcumin **1** mediated inhibition of IL-1 β , Jurrmann et al¹³⁸ have shown that in murine thymoma EL-4 cells, curcumin **1** blocks IL-1 β signalling by inhibiting the recruitment of the IL-1 receptor-associated kinase IRAK. Other studies on intracellular signalling have shown that curcumin **1** inhibits late events in the TNF- α and IL-1 β mediated signalling cascade e.g. inhibitor of I κ B, kinase activation and thus NF- κ B activation finally blocking the expression of intercellular adhesion molecule-1.

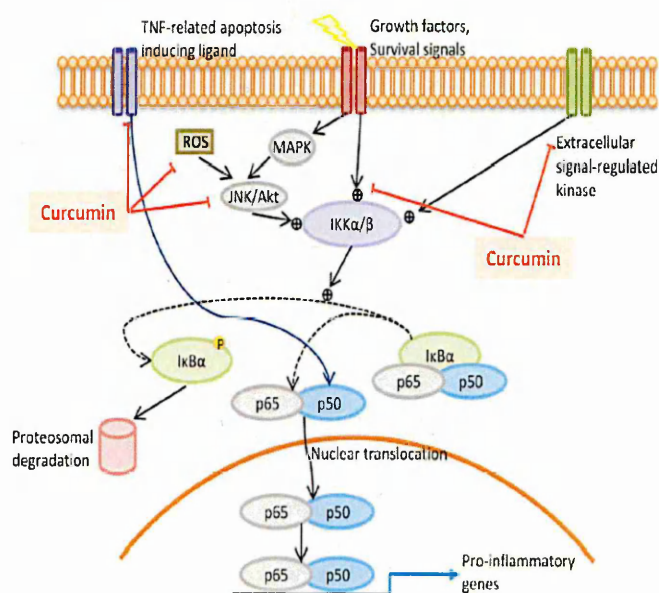


Figure 1.18 : Schematic representation of the molecular mechanisms for the anti-inflammatory activity of curcumin **1**.¹³³

Curcumin **1** is known to exert its anti-inflammatory effects significantly by interrupting NF- κ B signalling at multiple levels. For example, reactive oxygen species (ROS) mediate inflammation through the activation of stress kinases and redox-sensitive transcription factors such as NF- κ B, however, curcumin is a ROS scavenger and thus prevents the inflammatory signalling. In addition, curcumin can interfere with the functions of Akt and MAPKs, and in turn down-regulate the downstream molecule NF- κ B.

Tumour necrosis factor- α (TNF- α)

As reviewed by Menon and Sudheer,¹³⁹ TNF has been shown to mediate tumor initiation, promotion and metastasis, and the induction of pro-inflammatory genes by TNF has been linked to many diseases. The pro-inflammatory effects of TNF are primarily due to its ability to activate NF- κ B, and almost all cell types when exposed to TNF activate NF- κ B leading to the expression of inflammatory genes. Curcumin **1** has been shown to significantly affect the production of TNF. The constitutive activation of NF- κ B in mantle lymphoma cells is due to autocrine expression of TNF. TNF mRNA is constitutively expressed in mantle cell lines. Suppression of TNF by curcumin **1** led to inhibition of NF- κ B and cell proliferation.

CXCL-8

Interleukin-8 (IL-8) was first purified and molecularly cloned as a neutrophil chemotactic factor from lipopolysaccharide-stimulated human mononuclear cell supernatants, and because most of them exhibit chemotactic activity for a limited spectrum of leukocytes these are now called chemokines (chemotactic cytokines).¹⁴⁰ It is a 6-8 kDa protein, which has been detected in synovial fluid from patients with various inflammatory rheumatic diseases and elevated mucosal levels of CXCL-8 are also found in patients with ulcerative colitis.⁴² CXCL-8 mediates its broad biological activity by binding to two highly regulated receptors, CXCR1 and CXCR2, both of which are the members of the seven-transmembrane domain rhodopsin-like G protein coupled receptor superfamily, sharing 78% amino acid sequence homology.¹⁴¹ The

angiogenic effects of CXCL-8 in intestinal endothelial cells are mediated by CXCR2 receptor, while modulation of neutrophil functions like transepithelial neutrophil migration is CXCR1 dependent.¹⁴¹ Suppression of CXCL-8 production by curcumin **1** has been associated with the simultaneous increase in the expression of CXCL-8 receptors CXCR1 and CXCR2 indicating that curcumin inhibits CXCL-8 induced internalization of CXCL-8 receptors.¹⁴²

1.20 Synthesis of curcumin and curcuminoids

Due to the facts that curcumin **1**, is remarkably non-toxic to humans (at an orally administered dosage of up to 12g/day), however, it is cytotoxic to a variety of tumor cells, and exhibits multifunctional pharmacological properties including anti-inflammatory and anti-cancer activities as shown by several recent clinical trials conducted in patients with rheumatoid arthritis, inflammatory bowel disease, psoriasis, pancreatic cancer, multiple myeloma, cystic fibrosis and other disorders.¹⁴³ Its poor bioavailability and pharmacokinetic profiles (due to its instability under physiological conditions) have limited its application, and hence synthetic modifications of curcumin **1** have been sought to overcome these limitations as well as to develop molecules with enhanced bioactivities.¹⁴³

Curcumin **1** was first isolated in 1870 and its chemical structure was determined in 1910.¹⁴⁴ So far, the method devised by Pabon¹⁴⁴ is the best method used for the synthesis of curcumin **1** and most of its analogues that have an intact 7 carbon α,β -unsaturated di-enone moiety, with aromatic (substituted or unsubstituted) and heterocyclic ring systems.

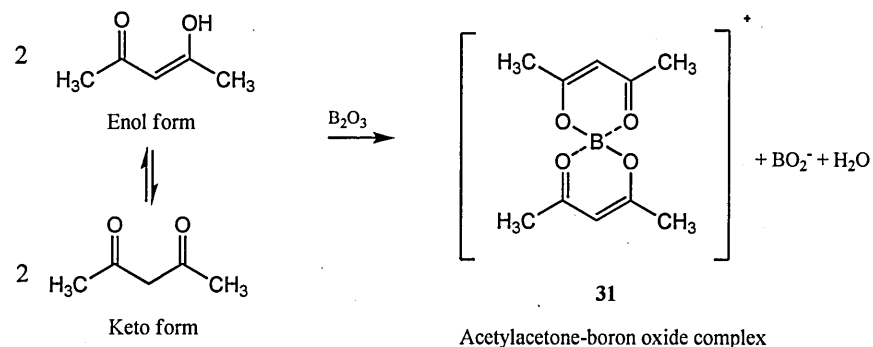
1.21 Pabon's method of curcumin synthesis

Before Pabon, various synthetic methods were reported for the synthesis of curcumin **1**, however these methods resulted in low yields. For example, Lampe for the first time in 1918 synthesized curcumin **1**, in eight steps using vanillin but this method had little practical value.¹⁴⁴ Later on, Pavolini prepared curcumin **1** in only one step by heating vanillin, acetylacetone and boric anhydride in (2:1:2) ratio over a free flame for 30 minutes, however the yield claimed from this procedure was only 10%.¹⁴⁴ Pabon then continued to follow the method of Pavolini but with amendments such as using butanol, piperidine and introduced for the first time the use of boric ester, which promotes the formation of acetylacetone boron oxide complex **31**¹⁴⁴ (figure 1.19). By this improved method, Pabon synthesized curcumin **1** at elevated temperatures (100 °C) with 45% yield, as well as at room temperature, with 73% yield and studied the effects of various factors involved. However, the procedure for synthesizing curcumin **1** at room temperature did not always yield the desired products and therefore the reaction to synthesize curcumin **1** at elevated temperature was adopted as a suitable method. The best temperature range for the condensation, proposed by Pabon was 85-110 °C. Amongst the different variety of bases that were studied, n-butylamine gave the best results. From the different alkylborates that were used in the study, tri-sec-butylborate and isopropylborate gave the best yields i.e. 78% and 80% respectively. Pabon further reported that higher yields could be obtained by using a solvent in the reaction and showed that ethyl acetate was the solvent of choice.¹⁴⁴

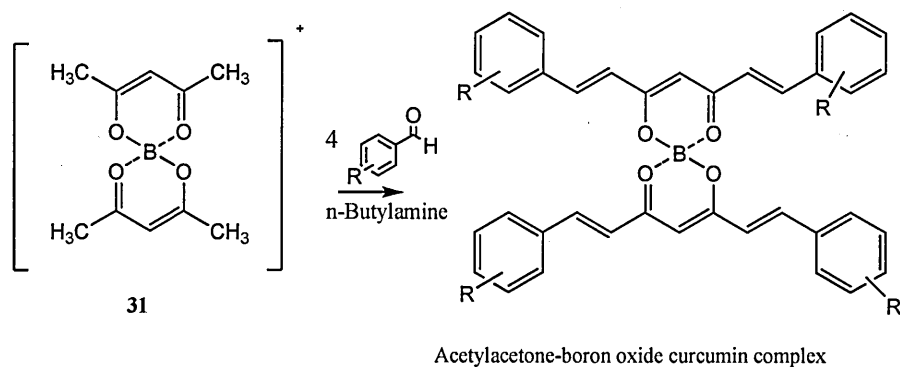
1.22 Basic steps of Pabon's synthesis

The main steps involved in the synthesis of curcumin **1** using Pabon's method are shown in figure 1.19. The first step is the reaction of acetylacetone with boron oxide to form acetylacetone-boron oxide complex **31**.¹¹³ The purpose of this strategy is to avoid Knoevenagel condensation at the active methylene group, so that the aldol condensation takes place at the terminal carbons.¹⁴⁵ In the second step, after the addition of the corresponding benzaldehyde in the presence of a base, the condensation of the acetylacetone-boron oxide complex **31** with benzaldehyde occurs, and eventually in the third step, heating with dilute acid cleaves the boron complex to give the desired curcumin **1** molecule in free form.¹¹³

Step 1: Formation of acetylacetone-boron oxide complex 31



Step 2: Condensation of acetylacetone-boron oxide complex 31 with aromatic aldehyde



Step 3: Cleavage of acetylacetone-boron oxide curcumin complex via acid hydrolysis

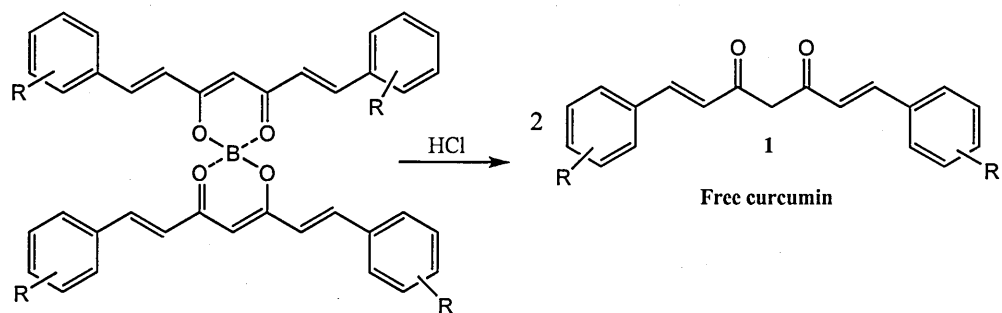


Figure 1.19 : Basic steps involved in Pabon's method of curcumin **1** synthesis.
Modified from reference¹¹³

1.23 The aldol reaction

Pabon's method of curcumin **1** synthesis follows the strategy of aldol condensation reaction as the product obtained is an α,β -unsaturated ketone or keto-enol, or strictly speaking (by excluding the type of the base which is usually employed, i.e. the *n*-butylamine), the Claisen-Schmidt condensation reaction, in which the condensation of an aromatic aldehyde with an aliphatic ketone or aldehyde in the presence of relatively stronger base (such as alkoxide ion) occurs to form the aldol product i.e. the α,β -unsaturated ketone or aldehyde. However, the basic mechanism involved in both the reactions is the same as discussed previously.

As reviewed by Mestres¹⁴⁶, aldol reaction is a carbon-carbon (C-C) bond forming reaction that results in β -hydroxy aldehydes (aldols) **36** or β -hydroxy ketones (ketols) **37** through the addition reaction (aldolization) or to the α,β -unsaturated aldehydes **40** or ketones **41** that result from a subsequent dehydration (aldol condensation). The reaction may involve two molecules of the same aldehyde **32** or ketone **33** (self-aldolization or self-condensation) or two different substances **34** and **35** (cross-aldolization or cross-condensation). However in any case one of the molecule reacts as a carbon acid that donates its lone pair of electrons to the carbonyl group of the other molecule which behaves as a lone pair acceptor (figure 1.20).

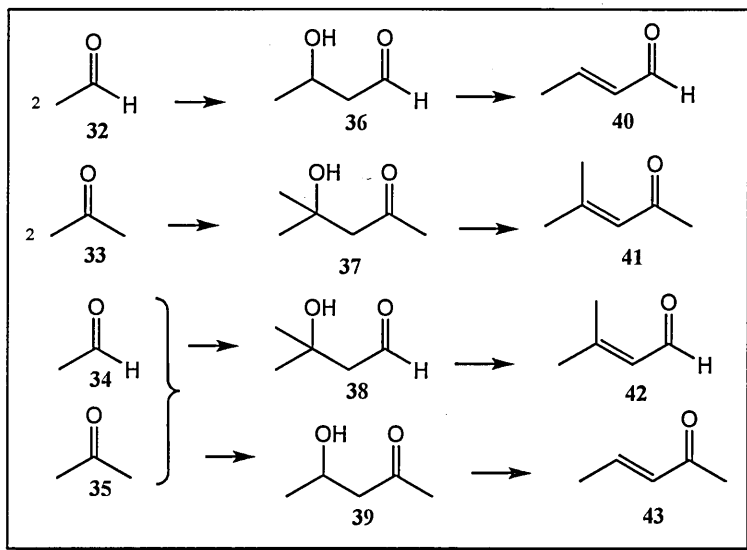


Figure 1.20 : Examples of self and cross aldol reaction.¹⁴⁶

1.24 Aims and objectives

In the light of the previous findings describing the side-effects of NSAIDs (that result in high rate of morbidity and mortality), as well as the beneficial role of curcumin **1** in inflammation and on gastrointestinal tract, using curcumin **1** as a lead compound our aim was to discover a new class of drugs which have anti-inflammatory properties without the side-effects associated with the conventional NSAIDs.

The project had the following two major aspects associated with it.

1.24.1 Synthetic aspects

Specific objectives

- To synthesise nitric oxide donating derivatives of curcumin **1**, as nitric oxide donating NSAIDs are emerging as a new interesting class of anti-inflammatory drugs without the side-effects which accompany the other NSAIDs used thus far.¹⁴⁷
- To synthesise (un)substituted thiophene and furan derivatives of curcumin **1**.
- To synthesise benzothiophene and benzofuran derivatives of curcumin **1**.
- To synthesise nitrogen containing heterocyclic curcuminoids.

Thiophene, furan and likewise benzofuran and benzothiophene feature in many natural products and possess anti-inflammatory properties, and hence it was envisaged that curcumin **1** derivatives of these would make good candidates for pharmacological activities.^{148,149,150} Few selected examples of thiophene and furan derived curcuminoids had appeared in the literature at the time this work was started,

however there was no literature precedence for benzo[b]thiophene or benzo[b]furan derived curcumins.

- To develop a new method of curcumin 1 synthesis.

1.24.2 Pharmacological aspects

Specific objectives

Using two different cancer cell lines i.e. the human monocytic leukemia or THP-1 cells and the human caucasian colon adenocarcinoma-2 or CACO-2 cells, the objective was to determine the actions of the synthesised compounds on (a) the effects *in vitro* on several novel cellular reactions involving cytokine-mediated responses that underline chronic inflammatory reactions, and, (b) to ascertain the cytotoxic effects of the synthesised curcuminoids as a guide to the concentrations used for testing, as well as a guide to their intrinsic toxicity.

- To evaluate the effects of nitric oxide donating curcuminoids on the production of nitric oxide in cell supernatants of THP-1 cells.
- Assay activities of synthesised (un)substituted thiophene curcuminoids on the production of pro-inflammatory cytokines IL-1 β , TNF- α using THP-1 cells and CXCL-8 using CACO-2 cells, as it has been reported that the accumulation of IL-1 β and TNF- α , initiates a cascade of events leading to inflammation and tissue destruction in various inflammatory diseases.¹⁵¹

Similarly, CXCL-8 has been reported to be involved in the pathogenesis of inflammatory bowel diseases.¹⁵²

- To compare the effects of the active compounds with the parent compound curcumin **1**.
- Determine structure-activity relationship of the active compounds as a guide to design future derivatives of curcumin **1** with enhanced biological potency.

CHAPTER 2
EXPERIMENTAL

Part A

Chemistry section

2.0 Materials

Chemicals

4-Hydroxy-3-methoxybenzaldehyde (vanillin), 3-hydroxybenzaldehyde, 4-hydroxybenzaldehyde, thiophene-2-carboxyaldehyde, thiophene-3-carboxyaldehyde, 3-methylthiophene-2-carboxyaldehyde, 5-methylthiophene-2-carboxyaldehyde, 2,4,6-trimethoxybenzaldehyde, 4-hydroxy-1-naphthaldehyde, furan-2-carbaldehyde, 3-methylfuran-2-carbaldehyde, 5-methylfuran-2-carbaldehyde, benzaldehyde, (+/-)-2-butanol 99%, 1,4-dibromobutane, n-butylamine, tri-n-butyl-borate, silver nitrate, phenol, 4-methoxyphenol 98%, 4-chlorophenol 99%, trans-cinnamaldehyde 98+%, selenium oxide, 2,3-dichloro-1-propene 97%, 2,3-dibromo-1-propene with copper tech. 85% stabilized, 1,2-dichlorobenzene 99%, diethyl ether (anhydrous) 99.7%, dioxane, tetrahydrofuran, methylmagnesium bromide, ethyl cinnamate were purchased from Alfa Aesar, (Lancaster, UK). Magnesium sulphate, boric acid, calcium chloride (anhydrous), potassium bromide, potassium carbonate, acetyl acetone, petroleum ether, ethyl acetate, ethanol, acetone, toluene, cyclohexane, trifluoroacetic acid were obtained from Fisher Scientific (Leicestershire, UK). 2-Hydroxybenzaldehyde (salicylaldehyde), 4,7-dichloroquinoline, sodium hydride and sodium metal in kerosene were obtained from Sigma-Aldrich Inc. (St. Louis, MO, USA). Acetonitrile 99.93%, (HPLC grade) was purchased from Sigma-Aldrich (Gillingham, England). Hydroxypropyl- γ -cyclodextrin was purchased from Sigma-

Aldrich (Ayrshire, UK). Boron oxide was obtained from Aldrich Chemical Company Inc. (Milwaukee, USA). Deuterated chloroform (CDCl_3) was purchased from Apollo Scientific Ltd. UK. Silica gel for flash chromatography was purchased from VWR International (Poole, England). Thin layer chromatography (TLC) plates 20 x 20 cm aluminium sheets silica gel 60 F₂₅₄ were from Merck (Germany).

2.1 Methods

General procedures

All apparatus were oven-dried over night prior to use. Ethanol and ethyl acetate were dried over molecular sieves, other solvents and chemicals were used as received without further purification. The progress of the chemical reactions and the purity of the synthesised compounds were confirmed by thin-layer chromatography TLC. The ultra-violet analysis of the TLC was performed at wavelengths of 254 and 365 nm using Mineral Light[®] Lamp, MultiBand UV- 254/365 nm, Model UVGL-58. Detection of the desired product was further confirmed by spraying the TLC plates with a solution of alkaline potassium permanganate solution.

¹H and ¹³C nuclear magnetic resonance (NMR) spectra were recorded on Bruker AC 250 spectrometer operating at 250 and 62.9 MHz respectively, for solutions in deuterated chloroform unless otherwise stated. Chemical shifts (δ) were recorded in parts per million (ppm) relative to the reference, tetramethylsilane (TMS) and coupling constants (J) were calculated in Hz. Electron impact mass spectra (EIMS) were recorded on a VG 7070 Analytical Mass spectrometer. Electrospray mass spectra (ESMS) were obtained on Micromass Platform single quadrupole mass

spectrometer fitted with a Harvard syringe driver. The accurate mass of the compounds was detected using an Applied Biosystems/MDS Sciex Hybrid quadrupole time-of-flight instrument (Q-Star Pulsar-i) fitted with an orthogonal MALDI ion source and an ND:VAG Laser. Infra-red spectra were recorded on ATI Mattson Genesis Series FTIR spectrophotometer using either potassium bromide pellets as a support for solid samples or sodium chloride disc for liquid samples. Data was recorded as wave number ν (cm^{-1}). Melting points ($^{\circ}\text{C}$) were recorded on Stuart SMP 3 digital electrothermal melting point apparatus and are uncorrected. The drugs/hydroxypropyl- γ -cyclodextrin complexes were freeze-dried using Thermo ModulyoD freeze-dryer.

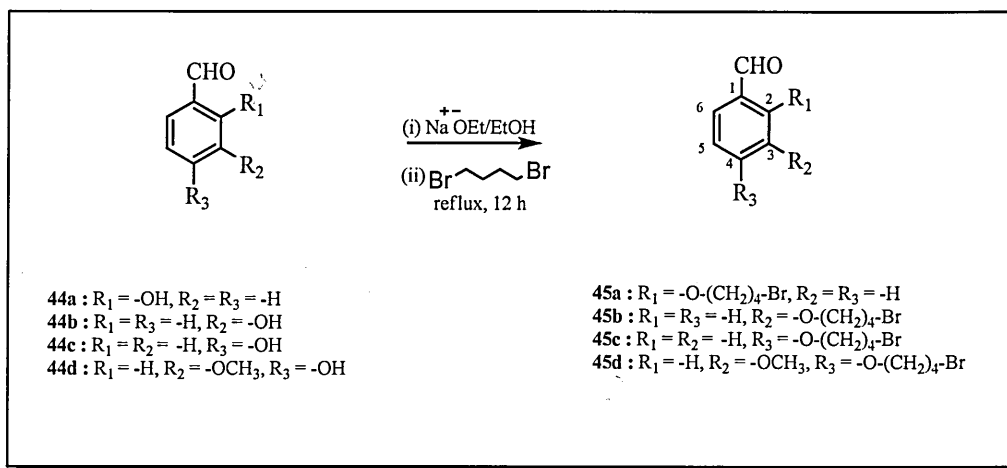
2.1.1 Preparation of tri-*sec*-butyl borate

A mixture of powdered boric acid (12.4 gm; 0.2 mol) and 2-butanol (44.4 gm; 0.6 mol) in toluene (120 ml) was refluxed with azeotropic removal of water using the Dean - Stark apparatus. The toluene was evaporated on a rotary evaporator at 60°C to give tri-*sec*-butyl borate as a clear liquid which was stored in a tightly sealed bottle.

2.1.2 Preparation of acetylacetone-boron oxide complex 31

Acetyl acetone/boron oxide complex **31** was prepared according to the method of Pabon.¹⁴⁴ In a 100 ml round-bottom flask, ground boric oxide (5 gm; 0.07 mol) was mixed with acetyl-acetone (10 gm; 0.14 mol). The reaction mixture was stirred for 1 h, and the complex obtained as a thick white paste was stored in a tightly sealed bottle.

2.1.3 Synthesis of bromobutoxybenzaldehyde **45a-d**



Scheme 2.1

General procedure

All of the four compounds **45a-d**, (scheme 2.1) were synthesised by a typical procedure which is illustrated for the formation of compound 2-(4-bromobutoxy)benzaldehyde, **45a**. A three-neck round bottom flask fitted with a dropping funnel, double surface condenser having a calcium chloride drying tube was charged with dry EtOH (60 ml). Freshly cut sodium metal (2.3 gm; 0.1 mol) pre-washed in toluene was added slowly to EtOH with gentle stirring under reflux, until all the sodium had reacted. 2-Hydroxybenzaldehyde **44a** (0.1 mol) was added and the reaction mixture was heated at 80 °C for 30 minutes. 1,4-Dibromobutane (65 gm; 0.3 mol) was added dropwise to the reaction mixture through a dropping funnel over a period of 35 minutes. The reaction mixture was refluxed for 12 h after which the mixture was allowed to settle and then filtered by suction filtration on a Buchner flask. To the filtrate was added water (60 ml) and extracted with EtOAc (2 x 60 ml).

The organic layers were combined and dried over MgSO_4 , filtered and the solvent was evaporated on a rotary evaporator. The residue was distilled under reduced pressure (boiling point $45\text{-}50^\circ\text{C}/8\text{mmHg}$) to remove the excess 1,4-dibromobutane and the crude product was purified by silica-gel flash chromatography using [petroleum ether : EtOAc, 8:1 v/v] as eluent, to yield product **45a**, (58%) as a light yellow oil, R_f 0.45 [petroleum ether : EtOAc, 5:1 v/v]. IR (ν) 3075 (aromatic C-H stretch), 2932 (aliphatic C-H stretch), 2759 (aldehyde C-H stretch), 1687 (conjugated >C=O stretch), 1598 and 1577 (aromatic C=C stretch), 1242 (asymmetric C-O-C stretch), 1042 (symmetric C-O-C stretch), 758 cm^{-1} (ortho di-substituted out of plane C - H stretch); ^1H NMR δ 1.89 - 2.17 (4H, m, $-\text{CH}_2-\text{CH}_2-$), 3.50 (2H, t, $J = 6.2$ Hz, $-\text{CH}_2-\text{Br}$), 4.11 (2H, t, $J = 5.6$ Hz, $-\text{O}-\text{CH}_2-$), 6.95 - 7.05 (2H, m, Ar H-3 and H-5), 7.53 (1H, td, $J = 6.9$ and 1.5 Hz, Ar H-4), 7.82 (1H, dd, $J = 7.7$ and 1.5 Hz, Ar H-6), 10.5 (1H, s, $-\text{CHO}$); ^{13}C NMR δ 28.0 ($-\text{O}-\text{CH}_2-\text{CH}_2-$), 29.4 ($\text{Br}-\text{CH}_2-\text{CH}_2-$), 33.4 ($\text{Br}-\text{CH}_2-$), 67.9 ($-\text{O}-\text{CH}_2-$), 112.8 (Ar C-3), 121.0 (Ar C-5), 122.5 (Ar C-1), 128.7 (Ar C-6), 136.2 (Ar C-4), 161.4 (Ar C-2), 189.9 ($-\text{CHO}$); (EIMS m/z 256 $[\text{M}^{79}\text{Br}]^+$ (12%), 258 $[\text{M}^{81}\text{Br}]^+$ (12%), 227 $[\text{M}-\text{CHO}]^+$ (3%), 135 $[\text{C}_4\text{H}_8^{79}\text{Br}]^+$ (62%), 137 $[\text{C}_4\text{H}_8^{81}\text{Br}]^+$ (59%), 121 $[\text{C}_7\text{H}_5\text{O}_2]^+$ (85%); Accurate mass found: m/z 256.0093 (Br^{79}), calculated for $\text{C}_{11}\text{H}_{13}\text{O}_2^{79}\text{Br}$: 256.0099.

3-(4-Bromobutoxy)benzaldehyde, **45b**, (79%) as a pale yellow oil, R_f 0.50 [petroleum ether : EtOAc, 5:1 v/v]. IR (ν) 3067 (aromatic C-H stretch), 2945 (aliphatic C-H stretch), 2729 (aldehyde C-H stretch), 1696 (conjugated C=O stretch), 1596 and 1585 (aromatic C=C stretch), 1262 (asymmetric C-O-C stretch), 1043 cm^{-1} (symmetric C-O-C stretch); ^1H NMR δ 1.90 - 2.16 (4H, m, $-\text{CH}_2-\text{CH}_2-$), 3.48 (2H, t, $J = 6.4$ Hz, $-\text{O}-\text{CH}_2-$), 6.95 - 7.05 (2H, m, Ar H-3 and H-5), 7.53 (1H, td, $J = 6.9$ and 1.5 Hz, Ar H-4), 7.82 (1H, dd, $J = 7.7$ and 1.5 Hz, Ar H-6), 10.5 (1H, s, $-\text{CHO}$); ^{13}C NMR δ 28.0 ($-\text{O}-\text{CH}_2-\text{CH}_2-$), 29.4 ($\text{Br}-\text{CH}_2-\text{CH}_2-$), 33.4 ($\text{Br}-\text{CH}_2-$), 67.9 ($-\text{O}-\text{CH}_2-$), 112.8 (Ar C-3), 121.0 (Ar C-5), 122.5 (Ar C-1), 128.7 (Ar C-6), 136.2 (Ar C-4), 161.4 (Ar C-2), 189.9 ($-\text{CHO}$); (EIMS m/z 256 $[\text{M}^{79}\text{Br}]^+$ (12%), 258 $[\text{M}^{81}\text{Br}]^+$ (12%), 227 $[\text{M}-\text{CHO}]^+$ (3%), 135 $[\text{C}_4\text{H}_8^{79}\text{Br}]^+$ (62%), 137 $[\text{C}_4\text{H}_8^{81}\text{Br}]^+$ (59%), 121 $[\text{C}_7\text{H}_5\text{O}_2]^+$ (85%); Accurate mass found: m/z 256.0093 (Br^{79}), calculated for $\text{C}_{11}\text{H}_{13}\text{O}_2^{79}\text{Br}$: 256.0099.

CH₂-Br), 4.04 (2H, t, J = 5.9 Hz, -O-CH₂-), 7.11 - 7.46 (4H, m, Ar H), 9.95 (1H, s, -CHO); ¹³C NMR δ 28.0 (-O-CH₂-CH₂-), 29.7 (Br-CH₂-CH₂-), 33.5 (Br-CH₂-), 67.4 (-O-CH₂-), 113.0 (Ar C-2), 122.1 (Ar C-4), 123.8 (Ar C-6), 130.3 (Ar C-5), 138.1 (Ar C-1), 159.4 (Ar C-3), 192.3 (-CHO); EIMS m/z: 256 [M ⁷⁹Br]⁺ (7%), 258 [M ⁸¹Br]⁺ (7%), 135 [C₄H₈ ⁷⁹Br]⁺ (71%), 137 [C₄H₈ ⁸¹Br]⁺ (69%), 121 [C₇H₅O₂]⁺ (69%);

Accurate mass found: m/z 256.0089, calculated for C₁₁H₁₃O₂ ⁷⁹Br : 256.0099.

4-(4-Bromobutoxy) benzaldehyde, 45c, (81%), as golden yellow oil, *R*_f 0.47

[petroleum ether: EtOAc, 5:1 v/v]. IR (ν) 3074 (aromatic C-H stretch), 2945 (aliphatic C-H stretch), 2738 (aldehyde C-H stretch), 1690 (conjugated C=O stretch), 1600 and 1577 (aromatic C=C stretch), 1255 (asymmetric C-O-C stretch), 1040 (symmetric C-O-C stretch), 832 cm⁻¹ (para di-substituted out of plane C-H stretch); ¹H NMR δ 1.85 - 2.13 (4H, m, -CH₂-CH₂-), 3.49 (2H, t, J = 6.4 Hz, -CH₂-Br), 4.08 (2H, t, J = 5.9 Hz, -O-CH₂-), 6.98 (2H, d, J = 8.5 Hz, Ar H-3 and H-3'), 7.82 (2H, d, J = 8.5 Hz, Ar H-2 and H-2'), 9.87 (1H, s, -CHO); ¹³C NMR δ 28.0 (-O-CH₂-CH₂-), 29.6 (Br-CH₂-CH₂-), 33.4 (Br-CH₂-), 67.5 (-O-CH₂-), 115.0 (Ar C-3), 130.3 (Ar C-1), 132.2 (Ar C-2), 164.3 (Ar C-4), 191.0 (-CHO) EIMS m/z 256 [M ⁷⁹Br]⁺ (6%), 258 [M ⁸¹Br]⁺ (6%), 135 [C₄H₈ ⁷⁹Br]⁺ (58%), 137 [C₄H₈ ⁸¹Br]⁺ (56%); Accurate mass found: m/z 257.0176, calculated for C₁₂H₁₄O₂ ⁷⁹Br : 257.0171.

4-(4-Bromobutoxy)-3-methoxybenzaldehyde, 45d, (50%), as a white solid, *R*_f 0.33

[petroleum ether: EtOAc, 3:1 v/v], m.p. 49.7 °C. IR (ν) 3081 (aromatic C-H stretch), 2872 and 2933 (aliphatic C-H stretch), 2756 and 2821 (aldehyde C-H stretch), 1679 (conjugated C=O stretch), 1596 and 1584 (aromatic C=C stretch), 1263 (asymmetric C-O-C stretch), 1046 cm⁻¹ (symmetric C-O-C stretch); ¹H NMR δ 2.06 - 2.08 (4H, m,

-CH₂-CH₂-), 3.51 (2H, t, J = 6.4 Hz, -CH₂-Br), 3.92 (3H, s, -O-CH₃), 4.14 (2H, t, J = 5.9 Hz, -O-CH₂-), 6.96 (1H, d, J = 7.7 Hz, Ar H-5), 7.40 - 7.46 (2H, m, Ar H-2 and H-6), 9.85 (1H, s, -CHO); ¹³C NMR δ 27.9 (-O-CH₂-CH₂-), 29.6 (Br-CH₂-CH₂-), 33.5 (Br-CH₂-), 56.3 (O-CH₃), 68.4 (-O-CH₂-), 109.7 (Ar C-2), 111.8 (Ar C-5), 126.9 (Ar C-6), 130.5 (Ar C-1), 150.2 (Ar C-3), 154.1 (Ar C-4), 191.1 (-CHO); EIMS m/z 286 [M ⁷⁹Br]⁺ (9%), 288 [M ⁸¹Br]⁺ (8%), 135 [C₄H₈ ⁷⁹Br]⁺ (54%), 151 [C₄H₈ ⁸¹Br]⁺ (54%); Accurate mass found: m/z 286.0200 (⁷⁹Br), calculated for C₁₂H₁₅O₃⁷⁹Br : 286.0205.

2.1.4 Synthesis of curcuminoids

Method A:¹⁴⁴ In this procedure the synthesis of curcuminoids was carried out according to Pabon's method¹⁴⁴ in which separately prepared acetyl acetone-boron oxide complex 31 was used.

A typical procedure for making the curcuminoids shown in scheme 2.2 is illustrated by the formation of (1E,6E)-1,7-bis(2-(4-bromobutoxy)phenyl)hepta-1,6-diene-3,5-dione, **46a**. In a round bottom flask, fitted with drying-tube, compound **45a**, (0.01 mol) was dissolved in dried EtOAc and tri-sec-butyl-borate (4.6 gm; 0.02 mol) was added to it with constant stirring. The acetyl-acetone/boron oxide complex 31 (0.9375 gm) was added and the whole reaction mixture was left to stir for 15 minutes. n-Butylamine (0.125 ml) was added dropwise over 10 minutes and the stirring was continued for 4 h at 60 °C. After that, the reaction mixture was allowed to stand overnight. Hydrochloric acid (0.4 M, 8 ml) was added and the mixture was stirred at 60 °C for an hour, and then extracted with EtOAc (3 x 30 ml). The combined organic

same method AS JAMES.

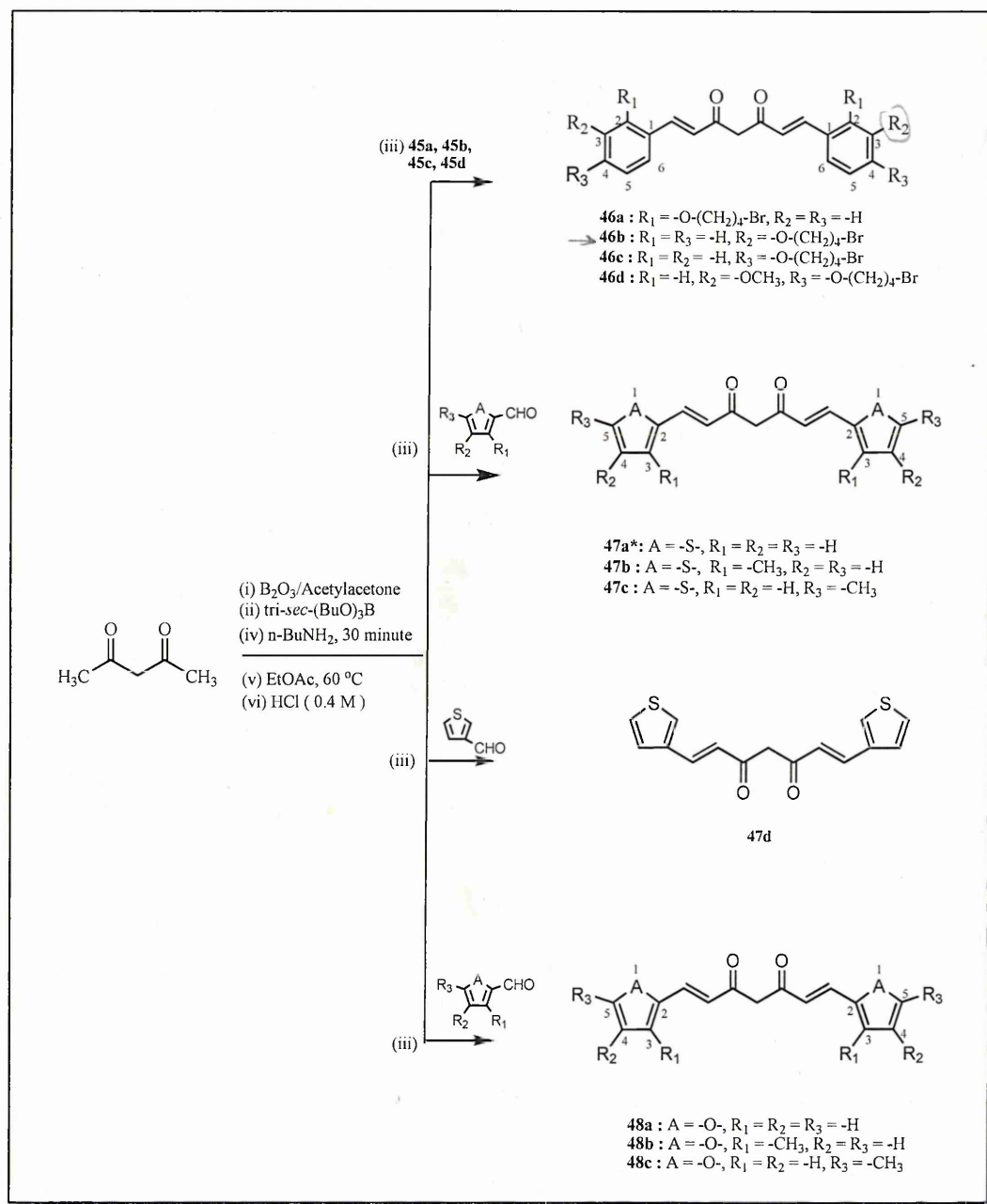
layer after drying over anhydrous MgSO_4 was filtered and evaporated on the rotary evaporator. The crude product obtained was purified by flash column chromatography using [petroleum ether: EtOAc 8:1 v/v] as eluent to give pure **46a**, (34%) dark brown gum, R_f 0.44 [petroleum ether: EtOAc, 3:1 v/v]. IR (KBr pellet) ν 3032 (aromatic C-H stretch), 2924 (aliphatic C-H stretch), 1620 (H-bonded $>\text{C}=\text{O}$ stretch), 1595 and 1570 (aromatic C=C stretch), 1244 (asymmetric C-O-C stretch), 1046 (symmetric C-O-C stretch), 750 cm^{-1} (ortho di-substituted out of plane C-H stretch); ^1H NMR δ 1.98 - 2.20, (8H, m, $-\text{CH}_2-\text{CH}_2-$), 3.55 (4H, t, $J = 5.9\text{ Hz}$, $-\text{CH}_2-\text{Br}$), 4.10 (4H, t, $J = 5.6\text{ Hz}$, $-\text{O}-\text{CH}_2-$), 5.87 (1H, s, enolic $-\text{CH}$), 6.75 (2H, d, $J = 16.0\text{ Hz}$, $\text{Ar}-\text{CH}=\text{CH}-\text{CO}-$), 6.91 (2H, d, $J = 8.0\text{ Hz}$, Ar H-3), 6.98 (2H, t, $J = 8.0\text{ Hz}$, Ar H-5), 7.33 (2H, td, $J = 8.0$ and $J = 1.6\text{ Hz}$, Ar H-4), 7.57 (2H, dd, $J = 8.0$ and $J = 1.6\text{ Hz}$, Ar H-6), 7.97 (2H, d, $J = 16.0\text{ Hz}$, $-\text{CO}-\text{CH}=\text{CH}-\text{Ar}$); ^{13}C NMR δ 28.1 ($-\text{O}-\text{CH}_2-\text{CH}_2-$), 29.8 ($\text{Br}-\text{CH}_2-\text{CH}_2-$), 33.7 ($\text{Br}-\text{CH}_2-$), 67.7 ($-\text{O}-\text{CH}_2-$), 101.9 (enolic methine C), 112.4 (Ar C-3), 121.1 (α -olefinic C adjacent to enol), 124.5 (Ar C-5), 125.5 (Ar C-1), 129.1 (Ar C-4), 131.5 (β -olefinic C adjacent to enol), 136.0 (Ar C-6), 157.9 (Ar C-2), 184.0 (enolic C); EIMS m/z 576 [M^{79}Br] $^+$ (4%), 580 [M^{81}Br] $^+$ (6%), 577 [$\text{M} + \text{H}$] $^+$, (2%), 578, [$\text{M} + 2\text{H}$] $^+$, (7%), 135 [$\text{C}_4\text{H}_8^{79}\text{Br}$] $^+$ (39%), 137 [$\text{C}_4\text{H}_8^{81}\text{Br}$] $^+$ (37%); Accurate mass found: m/z 577.0583, calculated for $\text{C}_{27}\text{H}_{31}\text{O}_4^{79}\text{Br}_2$: 577.0589.

The compound **46a** was obtained in 21% yield under the conditions of method B.

(1*E*,6*E*)-1,7-bis(3-(4-bromobutoxy)phenyl)hepta-1,6-diene-3,5-dione, **46b**, (24%) as a dark brown solid, R_f 0.41 [petroleum ether : EtOAc, 3:1 v/v], m.p. 74.6-75.9 $^\circ\text{C}$. IR (ν) 3426 (OH stretch), 3052 (aromatic C-H stretch), 2947 (aliphatic C-H stretch), 1625 (H-bonded $>\text{C}=\text{O}$ stretch), 1596 and 1579 (aromatic C=C stretch), 1508 (enol),

1243 (asymmetric C-O-C stretch), 1044 (symmetric C-O-C stretch), 885, 791, 677 cm^{-1} (meta di-substituted out of plane C-H stretch); ^1H NMR δ 1.95 - 2.18 (8H, m, -CH₂-CH₂-), 3.51 (4H, t, J = 6.45 Hz, -CH₂-Br), 4.04 (4H, t, J = 5.9 Hz, -O-CH₂-), 5.85 (1H, s, enolic -CH), 6.62 (2H, d, J = 16.0 Hz, Ar-CH=CH-CO-), 6.92 (2H, d, J = 7.7 Hz, Ar H-4), 7.07 (2H, s, Ar H-2), 7.16 (2H, d, J = 7.7 Hz, Ar H-6), 7.31 (2H, t, J = 7.7 Hz, Ar H-5), 7.63 (2H, d, J = 16.0 Hz, -CO-CH=CH-Ar); ^{13}C NMR δ 28.1 (-O-CH₂-CH₂-), 29.8 (Br-CH₂-CH₂-), 33.6 (Br-CH₂-), 67.2 (-O-CH₂-), 102.0 (enolic methine C), 113.9 (Ar C-2), 116.7 (Ar C-4), 121.2 (α -olefinic C adjacent to enol), 124.7 (Ar C-6), 130.2 (Ar C-5), 136.7 (Ar C-1), 140.8 (β -olefinic C adjacent to enol), 159.5 (Ar C-3), 183.5 (enolic C); ESMS m/z 576 [M^{79}Br]⁺, 577 [$\text{M}^{79}\text{Br} + \text{H}$]⁺, 578 [$\text{M}^{79}\text{Br} + 2\text{H}$]⁺, 580 [M^{81}Br]⁺, 581 [$\text{M}^{81}\text{Br} + \text{H}$]⁺, 582, [$\text{M}^{81}\text{Br} + 2\text{H}$]⁺; Accurate mass found: m/z 576.0543, calculated for C₂₇H₃₀O₄⁷⁹Br₂ : 576.0511.

The compound **46b** was obtained in 21% yield under the conditions of method B.



Scheme 2.2

* Synthesised by method B, (scheme 2.3).

(1*E*,6*E*)-1,7-bis(4-(4-bromobutoxy)phenyl)hepta-1,6-diene-3,5-dione, **46c**, (66%) as a bright yellow solid, R_f 0.42 [petroleum ether : EtOAc, 3:1 v/v], m.p. 145.9-146.9 °C. IR (ν) 3433 (OH stretch), 3035 (aromatic C-H stretch), 2945 (aliphatic C-H stretch), 1628 (H-bonded >C=O stretch), 1600 (aromatic C=C stretch), 1510 (enol), 1420 (olefinic in plane bending vibration), 1257 (asymmetric C-O-C stretch), 1046 (symmetric C-O-C stretch), 837 cm⁻¹ (para di-substituted out of plane C-H stretch); ¹H NMR δ 1.92 - 2.14 (8H, m, -CH₂-CH₂-), 3.50 (4H, t, J = 6.4 Hz, -CH₂-Br), 4.04 (4H, t, J = 5.6 Hz, -O-CH₂-), 5.78 (1H, s, enolic -CH), 6.50 (2H, d, J = 15.5 Hz, Ar-CH=CH-CO-), 6.90 (4H d, J = 8.7 Hz, Ar H-3 and H-3'), 7.50 (4H, d, J = 8.7 Hz, Ar H-2 and H-2'), 7.62 (2H, d, J = 15.5 Hz, -CO-CH=CH-Ar); ¹³C NMR δ 28.1 (-O-CH₂-CH₂-), 29.7 (Br-CH₂-CH₂-), 33.6 (Br-CH₂-), 67.3 (-O-CH₂-), 101.6 (enolic methine C), 115.1 (Ar C-3, C-5), 122.1 (α-olefinic C adjacent to enol), 128.2 (Ar C-1), 130.0 (Ar C-2, C-6), 140.3 (β-olefinic C adjacent to enol), 160.8 (Ar C-4), 183.6 (enolic C); EIMS m/z 576 [M ⁷⁹Br]⁺ (3%), 578 [M ⁷⁹Br + 2H]⁺ (8%), 135, [C₄H₈ ⁷⁹Br]⁺ (100%), 137 [C₄H₈ ⁸¹Br]⁺ (98%); Accurate mass found: m/z 576.0535, calculated for C₂₇H₃₀O₄ ⁷⁹Br₂ : 576.0511.

The compound **46c** was obtained in 41% yield under the conditions of method B.

(1*E*,6*E*)-1,7-bis(4-(4-bromobutoxy)-3-methoxyphenyl)hepta-1,6-diene-3,5-dione, **46d**, (57%) was obtained as a dark yellow solid, between EtOAc and aqueous layers during work-up and no further purification was required; R_f 0.38 [petroleum ether : EtOAc, 2:1 v/v], m.p. 124.4-125.4 °C. IR (ν) 3548-3235 (OH enolic), 3003 (aromatic C-H stretch), 2955 and 2870 (aliphatic C-H stretch), 1620 (H-bonded >C=O), 1597 and 1581 (aromatic C=C stretch), 1508 (enol), 1422 cm⁻¹ (olefinic in plane bending

vibration); ^1H NMR δ 2.00 - 2.17 (8H, m, $-\text{CH}_2-\text{CH}_2-$), 3.51 (4H t, $J = 6.4$ Hz, $-\text{CH}_2-\text{Br}$), 3.92 (6H, s, $-\text{OCH}_3$), 4.10 (4H, t, $J = 5.9$ Hz, $-\text{O}-\text{CH}_2-$), 5.82 (1H, s, enolic $-\text{CH}$), 6.50 (2H, d, $J = 15.7$ Hz, $\text{Ar}-\text{CH}=\underline{\text{CH}}-\text{CO}-$), 6.87 (2H, d, $J = 8.2$ Hz, Ar H-5), 7.08 (2H, d, $J = 1.7$ Hz, Ar H-2), 7.13 (2H, dd, $J_{1,3} = 8.2$ and $J_{1,2} = 1.7$ Hz, Ar H-6), 7.61 (2H, d, $J = 15.7$ Hz, $-\text{CO}-\text{CH}=\underline{\text{CH}}-\text{Ar}$); ^{13}C NMR δ 28.0 ($-\text{O}-\text{CH}_2-\underline{\text{CH}}_2-$), 29.5 ($\text{Br}-\text{CH}_2-\underline{\text{CH}}_2-$), 33.6 ($\text{Br}-\text{CH}_2-$), 56.3 ($-\text{O}-\text{CH}_3$), 68.3 ($-\text{O}-\text{CH}_2-$), 101.5 (enolic methine C), 110.7 (Ar C-2), 113.0 (Ar C-5) 122.4 (α -olefinic C adjacent to enol), 123.0 (Ar C-6), 128.5 (Ar C-1), 140.6 (β -olefinic C adjacent to enol), 149.9 (Ar C-3), 150.7 (Ar C-4), 183.5 (enolic C); EIMS m/z 637 $[\text{M}+\text{H}]^+$ (18%), 619 $[\text{M}+\text{H} - \text{H}_2\text{O}]^+$ (31%), 324 $[\text{C}_{15}\text{H}_{18}\text{O}_3 \text{ }^{79}\text{Br} + \text{H}]^+$ (31%), 326 $[\text{C}_{15}\text{H}_{18}\text{O}_3 \text{ }^{81}\text{Br} + \text{H}]^+$ (29%), 324 $[\text{C}_{14}\text{H}_{16}\text{O}_3 \text{ }^{79}\text{Br}]^+$ (20%), 313 $[\text{C}_{14}\text{H}_{16}\text{O}_3 \text{ }^{81}\text{Br}]^+$ (18%), 135 $[\text{C}_4\text{H}_8 \text{ }^{79}\text{Br}]^+$ (100%), 137 $[\text{C}_4\text{H}_8 \text{ }^{81}\text{Br}]^+$ (99%); Accurate mass found: m/z 636.0714 (Br^{79}), calculated for $\text{C}_{29}\text{H}_{34}\text{O}_6 \text{ }^{79}\text{Br}_2$: 636.0722.

(1*E*,6*E*)-1,7-bis(3-methylthiophen-2-yl)-1,6-heptodiene-3,5-dione, **47b**, (51%) was obtained as a brown solid, purified by flash chromatography using [petroleum ether : EtOAc, 8:1 v/v] as eluent, R_f 0.44 [petroleum ether : EtOAc, 5:1 v/v], m.p. 114.9-115.6 °C. IR (ν) 3421 (OH stretch), 3068 (aromatic C-H stretch), 1606 (H-bonded $>\text{C}=\text{O}$), 1499 cm^{-1} (conjugated $\text{C}=\text{C}$); ^1H NMR δ 2.38 (6H, s, $-\text{CH}_3$), 5.73 (1H, s, enolic $-\text{CH}$), 6.35 (2H, d, $J = 15.5$ Hz, $\text{Ar}-\text{CH}=\underline{\text{CH}}-\text{CO}-$), 6.89 (2H, d, $J = 5.1$ Hz, Ar H-4), 7.28 (2H, d, $J = 5.1$ Hz, Ar H-5, overlapped with CDCl_3), 7.84 (2H, d, $J = 15.5$ Hz, $-\text{CO}-\text{CH}=\underline{\text{CH}}-\text{Ar}$); ^{13}C NMR δ 14.5 ($-\text{CH}_3$), 102.1 (enolic methine C), 122.5 (β -olefinic C adjacent to enol), 126.9 (α -olefinic C adjacent to enol), 127.4 (Ar C-2), 131.8 (Ar C-4), 135.0 (Ar C-5), 141.6 (Ar C-3), 183.1 (enolic C); (EIMS m/z 316

$[M]^+$ (54%), 205 $[C_{11}H_9O_2S]^+$ (17%), 165 $[C_9H_9OS]^+$ (11%), 151 $[C_8H_7OS]^+$ (100%), 123 $[C_7H_7S]^+$ (28%), 111 $[C_6H_7S]^+$ (65%); Accurate mass found: m/z 316.0600, calculated for $C_{17}H_{16}O_2S_2$: 316.0592.

(1*E*,6*E*)-1,7-bis(5-methylthiophen-2-yl)-1,6-heptadiene-3,5-dione, **47c**, (53%) was obtained as a brown solid, purified by flash chromatography using [petroleum ether : EtOAc, 8:1 v/v] as eluent, R_f 0.44 [petroleum ether : EtOAc, 5:1 v/v], m.p. 119.9-121.5 °C. IR (ν) 3448 (OH stretch), 3029 (aromatic C-H stretch), 1605 cm^{-1} (H-bonded $>C=O$). 1H NMR δ 2.51 (6H, s, -OCH₃), 5.70 (1H, s, enolic -CH), 6.27 (2H, d, J = 15.5 Hz, Ar-CH=CH- CO-), 6.72 (2H, d, J = 3.6 Hz, Ar H-4), 7.06 (2H, d, J = 3.6 Hz, Ar H-5), 7.68 (2H, d, J = 15.5 Hz, -CO-CH=CH-Ar); ^{13}C NMR δ 16.1 (-CH₃), 101.4 (enolic methine C), 120.7 (β-olefinic C adjacent to enol), 122.1 (α-olefinic C adjacent to enol), 127.0 (Ar C-4), 133.4 (Ar C-3), 138.9 (Ar C-2), 144.9 (Ar C-5), 183.0 (enolic C); EIMS m/z 316 $[M]^+$ (31%), 298 $[M - H_2O]^+$ (23%), 205 $[C_{11}H_9O_2S]^+$ (5%), 165 $[C_9H_9OS]^+$ (39%), 151 $[C_8H_7OS]^+$ (100%), 110 $[C_6H_6S]^+$ (3%); Accurate mass found: m/z 316.0592, calculated for $C_{17}H_{16}O_2S_2$: 316.0592.

(1*E*,6*E*)-1,7-bis(thiophen-3-yl)-1,6-heptadiene-3,5-dione, **47d**, (36%) was obtained as a yellow solid, purified from column chromatography using [petroleum ether : EtOAc, 6:1 v/v] as eluent, R_f 0.48 [petroleum ether : EtOAc, 5:1 v/v], m.p. 140.1-141.3 °C. IR (ν) 3435 (OH stretch), 3092 (aromatic C-H stretch), 1624 (H-bonded $>C=O$), 1584 (conjugated C=C), 1507 (enol), 1412 cm^{-1} (olefinic in plane bending vibration); 1H NMR δ 5.79 (1H, s, enolic -CH), 6.45 (2H, d, J = 15.5 Hz, Ar-CH=CH- CO-), 7.33 - 7.38 (4H, m, Ar H), 7.52 (2H, d, J = 2.6 Hz, Ar H-2), 7.66 (2H, d, J = 15.5 Hz, -CO-CH=CH-Ar); ^{13}C NMR δ 101.7 (enolic methine C), 124.2 (α-

olefinic C adjacent to enol), 125.2 (Ar C-5), 125.6 (Ar C-4), 126.9 (Ar C-2), 127.4 (Ar C-3), 134.3 (β -olefinic C adjacent to enol), 183.6 (enolic C); EIMS m/z 288 $[M]^+$ (60%), 270 $[M - H_2O]^+$ (8%), 192 $[C_{10}H_8O_2S]^+$ (4%), 179 $[C_9H_7O_2S]^+$ (5%), 151 $[C_8H_7OS]^+$ (21%), 137 $[C_7H_5OS]^+$ (100%), 109 $[C_6H_5S]^+$ (43%), 97 $[C_5H_4S]^+$ (21%); Accurate mass found: m/z 288.0277, calculated for $C_{15}H_{12}O_2S_2$: 288.0279.

Using method B, 23% product was obtained after purification by column chromatography using [petroleum ether : EtOAc, 6:1 v/v] as eluent. However some aldehyde peaks were also found in the 1H NMR of the product.

(*1E,6E*)-1,7-bis(furan-2-yl)hepta-1,6-diene-3,5-one, **48a**, (26%) was obtained as a dark brown solid m.p. 96-98.5 °C. IR (ν) 3448 (OH stretch), 3147 (aromatic C-H stretch), 2963 (aliphatic C-H stretch), 1627 cm^{-1} ($>C=O$); 1H NMR δ 5.76 (1H, s, enolic -CH), 6.55 (2H, d, $J = 15.5$ Hz, Ar-CH=CH- CO-), 6.64 (2H, s, Ar H-4'), 7.27 (2H s, H-3'), 7.42 (2H, d, $J = 16.0$ Hz, -CO-CH=CH-Ar), 7.50 (2H, s, H-5'), 15.90 (1H, broad s, enol OH); ^{13}C NMR δ 102.5 (enolic methine C), 112.8 (Ar C-4), 115.1 (Ar C-3), 122.1 (β -olefinic C adjacent to enol), 127.1 (α -olefinic C adjacent to enol), 145.0 (Ar C-5), 152.0 (Ar C-2), 183.0 (enolic C); EIMS m/z 256 $[M]^+$ (76%), 239 $[M-OH]$, (8.5%), 121 (100%, M-2furan rings); Accurate mass found: m/z 256.0707, calculated for $C_{15}H_{12}O_4$: 256.0737.

(*1E,6E*)-1,7-bis(3-methylfuran-2-yl)hepta-1,6-diene-3,5-dione, **48b**, (13%). IR (ν) 3322 (OH stretch), 1620 cm^{-1} ($>C=O$); 1H NMR δ 2.32 (6H, s, -CH₃) 5.68 (1H, s, enolic -CH), 6.70 (2H, s, Ar H-4'), 6.92 (2H, d, $J = 15.5$ Hz, Ar-CH=CH- CO-), 7.55 (2H, d, $J = 15.5$ Hz, -CO-CH=CH-Ar), 7.90 (2H, s, Ar H-5'), 15.30 (1H, broad s,

OH); EIMS m/z 284 [M^+]; Accurate mass found: m/z 284.1062, calculated for $C_{17}H_{16}O_4$: 284.1048.

(1*E*,6*E*)-1,7-bis(5-methylfuran-2-yl)hepta-1,6-diene-3,5-dione, **48c**, (63%), m.p.

137.2-138.4 °C. IR (ν) 3325 (OH stretch), 1623 cm^{-1} ($>C=O$); 1H NMR

δ 2.42 (6H, s, -CH₃) 5.71 (1H, s, enolic -CH), 6.11 (2H, s, Ar H-4'), 6.43 (2H, d, J =

15.5 Hz, Ar-CH=CH- CO-), 6.50 (2H, s, Ar H-3'), 7.32 (2H, d, J = 15.5 Hz, -CO-

CH=CH-Ar), 15.90 (1H, broad s, enol OH); ^{13}C NMR δ 14.2 (-CH₃), 102.2 (enolic

methine C), 109.4 (Ar C-4), 116.8 (Ar C-3), 120.5 (α -olefinic C adjacent to enol),

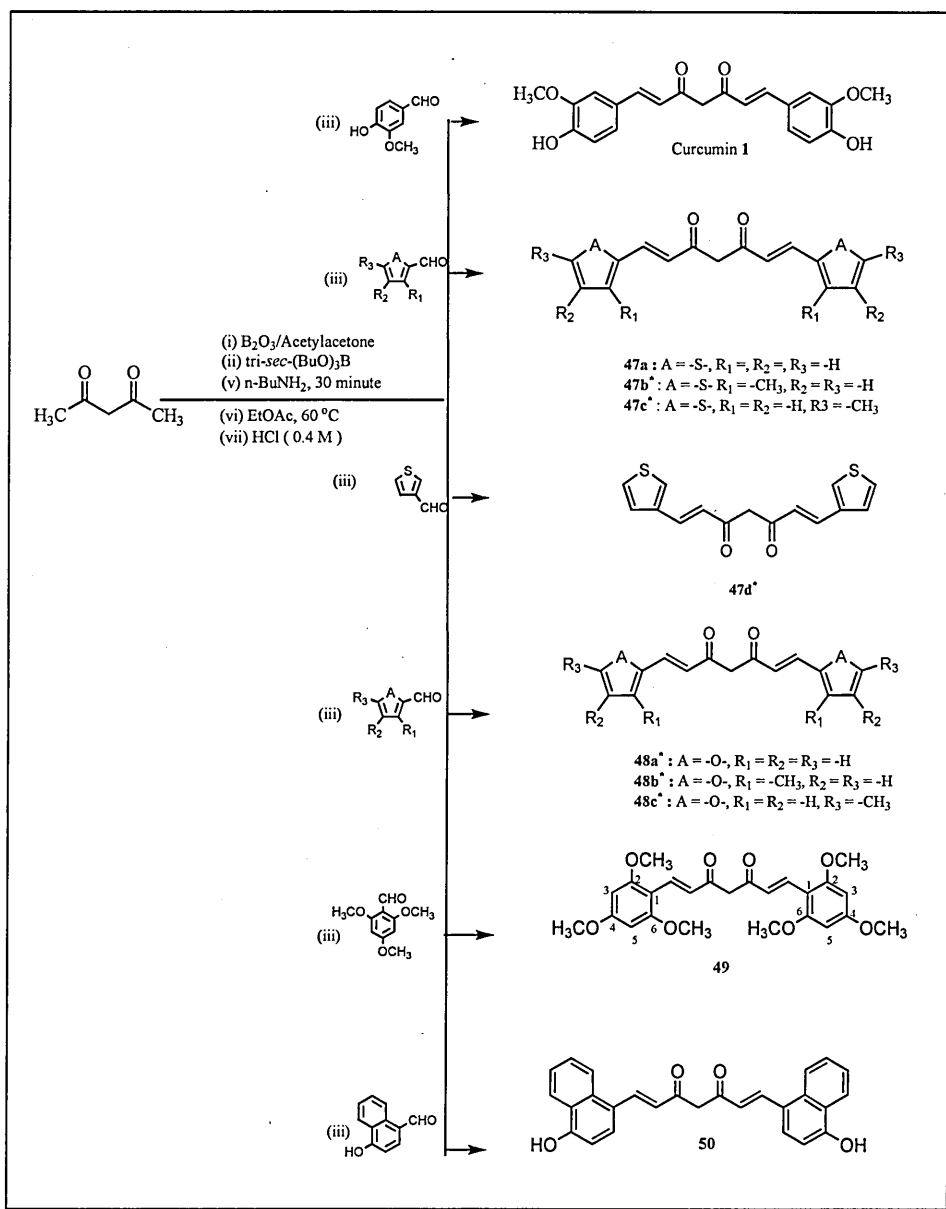
127.0 (β -olefinic C adjacent to enol), 150.7 (Ar C-2), 155.7 (Ar C-5), 183.1 (enolic

C); EIMS m/z 284 (32%) [M]⁺, 266 [$M-H_2O$] (5%), 202 [M -methylfuranyl] (2%),

135 [methylfuranyl-CH=CH-CO] (67%); Accurate mass found: m/z 284.1064,

calculated for $C_{17}H_{16}O_4$: 284.1048.

*Method B:*¹⁵³ In this procedure the synthesis of curcumin **1** and its derivatives **47a**, **49** and **50** was carried out by the *in situ* formation of acetyl-acetone-boron oxide complex **31**.



Scheme 2.3

* Synthesised by method A, (scheme 2.2).

Method
B:-

A typical procedure for making the curcuminoids shown in scheme 2.3 is illustrated by the formation of (1*E*,6*E*)-1,7-bis(4-hydroxy-3-methoxyphenyl)-1,6-heptadiene-3,5-dione, (curcumin, **1**). In a round bottom flask equipped with a drying tube and a dropping funnel, acetylacetone (0.5 gm, 0.005 mol) and boron-oxide (0.25 gm, 0.0035 mol) were mixed in EtOAc (5 ml) and stirred for 0.5 h at 40 °C followed by the addition of the corresponding aromatic aldehyde (0.01 mol) and tri-*sec*-butyl borate (2.3 gm, 0.01 mol) and stirred for additional 0.5 h. A solution of *n*-butylamine (0.5 ml) in EtOAc (5 ml) was added dropwise over a period of 30 minutes. After being stirred for further 4 h at 40 °C, the reaction mixture was allowed to stand overnight and then hydrolysed with HCl (0.4 M, 8 ml) and extracted with EtOAc (3 x 30 ml). The combined organic layers were washed with water, dried over MgSO₄, and then concentrated under vacuum. The residual crude product was subjected to flash silica column chromatography using [petroleum ether: EtOAc v/v] as eluent, to afford compound **1** in pure form, (33%, lit. 48%)¹⁵³ as orange solid, *R*_f 0.35 [petroleum ether : EtOAc, 1:1 v/v], m.p. 179-180 °C (lit. m.p. 178-180 °C).¹⁵⁴ IR (ν) 3501-3387 (OH stretch), 3015 (aromatic C-H stretch), 1627 (H-bonded >C=O), 1602 (conjugated C=C), 1510 (enol), 1428 cm⁻¹ (olefinic in plane bending vibration); ¹H NMR δ 3.95 (6H, s, -OCH₃), 5.80 (1H, s, enolic -CH), 6.48 (2H, d, *J* = 15.5 Hz, Ar-CH=CH-CO-), 6.93 (2H, d, *J* = 8.2 Hz, Ar H-5), 7.05 (2H, d, *J* = 1.5 Hz, Ar H-2), 7.12 (2H, dd, *J* = 8.2 and 1.5 Hz, Ar H-6), 7.59 (2H, d, *J* = 15.5 Hz, -CO-CH=CH-Ar); EIMS *m/z* 368 [M]⁺ (35%), 369 [M + H]⁺ (3%), 350 [M - H₂O]⁺ (59%), 177 [C₁₀H₉O₃]⁺ (100%), 191 [C₁₁H₁₁O₃]⁺ (24%), 137 [C₈H₉O₂]⁺ (32%), 232 [C₁₃H₁₂O₄]⁺ (9%); Accurate mass found: *m/z* 368.1256, calculated for C₂₁H₂₀O₆ : 368.1260.

(1*E*,6*E*)-1,7-bis(thiophen-2-yl)-1,6-heptadiene-3,5-dione, **47a**, (62%) obtained after the work-up as orange precipitates, R_f 0.44 [petroleum ether : EtOAc, 5:1 v/v], m.p. 183.5-184.7 °C. IR (ν) 3537 - 3412 (OH enolic), 3103 (aromatic C-H stretch), 1626 (H-bonded >C=O), 1569 (conjugated C=C), 1504 (enol), 1419 cm^{-1} (olefinic in plane bending vibration); ^1H NMR δ 5.75 (1H, s, enolic -CH), 6.42 (2H, d, J = 15.5 Hz, Ar-CH=CH-CO-), 7.07 (2H, t, J = 4.5 Hz, Ar H-4), 7.27 (2H, d, J = 4.5 Hz, Ar H-3, overlapped with CDCl_3), 7.39 (2H, d, J = 4.5 Hz, Ar H-5), 7.78 (2H, d, J = 15.5 Hz, -CO-CH=CH-Ar); ^{13}C NMR δ 102.0 (enolic methine C), 123.3 (β -olefinic C adjacent to enol), 128.3 (α -olefinic C adjacent to enol), 128.8 (Ar C-4), 131.1 (Ar C-3), 133.4 (Ar C-5), 140.8 (Ar C-2), 183.2 (enolic C); EIMS m/z 288 $[\text{M}]^+$ (48%), 270 $[\text{M} - \text{H}_2\text{O}]^+$ (21%), 192 $[\text{C}_{10}\text{H}_8\text{O}_2\text{S}]^+$ (8%), 179 $[\text{C}_9\text{H}_7\text{O}_2\text{S}]^+$ (6%), 151 $[\text{C}_8\text{H}_7\text{OS}]^+$ (31%), 137 $[\text{C}_7\text{H}_5\text{OS}]^+$ (100%), 109 $[\text{C}_6\text{H}_5\text{S}]^+$ (53%), 96 $[\text{C}_5\text{H}_4\text{S}]^+$ (3%); Accurate mass found: m/z 289.0351, calculated for $\text{C}_{15}\text{H}_{13}\text{O}_2\text{S}_2$: 289.0351.

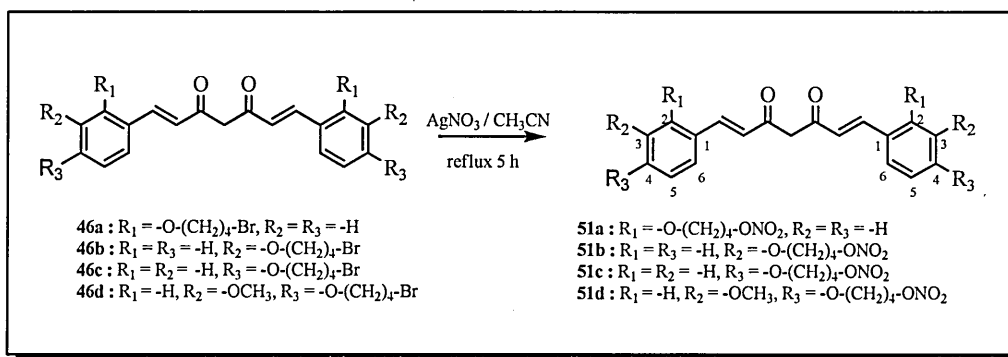
With method A, 23% yield of compound **47a** was obtained after purification by flash column chromatography using [petroleum ether: EtOAc, 6:1 v/v] as eluent.

(1*E*,6*E*)-1,7-bis(2,4,6-trimethoxyphenyl)hepta-1,6-diene-3,5-dione, **49**, (55%) obtained after the work-up as a red solid, R_f 0.46 [petroleum ether: EtOAc, 1:1 v/v], m.p. 193.4-193.6 °C. IR (ν) 3462 (OH stretch), 3001 (aromatic C-H stretch), 2937 and 2837 (aliphatic C-H stretch), 1600 (H-bonded >C=O), 1569 (conjugated C=C), 1504 (enol), 1414 cm^{-1} (olefinic in plane bending vibration). ^1H NMR (DMSO) δ 3.88 (18H, s, -OCH₃), 5.88 (1H, s, enolic -CH), 6.29 (4H, s, Ar H-3 and 5), 6.95 (2H, d, J = 16.0 Hz, Ar-CH=CH-CO-), 7.91 (2H, d, J = 16.0 Hz, -CO-CH=CH-Ar); ^{13}C NMR δ 55.8 (-OCH₃), 90.8 (Ar C-3, C-5), 101.8 (enolic methine C), 107.0 (Ar C-1),

124.8 (α -olefinic C adjacent to enol), 131.2 (β -olefinic C adjacent to enol), 161.5 (Ar C-2, C-6), 162.8 (Ar C-4), 185.0 (enolic C); ESMS m/z 457 $[M+H]^+$, 479 $[M+Na]^+$; Accurate mass found: m/z 456.1682, calculated for $C_{25}H_{28}O_8$: 456.1784.

(1*E*,6*E*)-1,7-bis(4-hydroxynaphthalen-1-yl)hepta-1,6-diene-3,5-dione, **50**, (25%) was purified as a blackish red solid, by flash chromatography using [petroleum ether : EtOAc, 1:1 v/v] as eluent, R_f 0.43 [petroleum ether : EtOAc, 1:1 v/v], m.p. 167.9-168.9 °C. IR (ν) 3135 (aromatic C-H stretch), 2744 (aliphatic C-H stretch), 1620 (H-bonded $>C=O$), 1567 (conjugated $C=C$), 1516 (enol); 1H NMR (DMSO) δ 6.34 (1H, s, enolic -CH), 6.89 (2H, d, $J = 15.5$ Hz, , Ar-CH=CH- CO-), 6.98 (2H, d, $J = 8.2$ Hz, Ar H-2), 7.51 – 7.73 (4H, m, Ar H-5, H-8), 7.97 (2H, d, $J = 8.2$ Hz, Ar H- 3), 8.25 (4H, t, $J = 8.9$ Hz, Ar H-6, H-7), 8.40 (2H, d, $J = 15.5$ Hz, CO-CH=CH-Ar); EIMS m/z 408 $[M]^+$ (100%), 409 $[M + H]^+$ (25%); Accurate mass found: m/z 408.1247, calculated for $C_{27}H_{20}O_4$: 408.1362.

2.1.5 Synthesis of butoxy nitrate curcuminoids **51a-d**



Scheme 2.4

General procedure

All of the desired butoxy nitrate curcuminoids **51a** to **d** (scheme 2.4) were synthesised by the following method which is illustrated by the formation of (*1E,6E*)-1,7-bis(2-(4-butoxy-nitrate)hepta-1,6-diene-3,5-dione, **51a**. In a one-neck round bottom flask, a mixture of silver nitrate (1.17 gm, 6.9 mmol) in acetonitrile (3 ml) was stirred for 30 minutes and then a solution of **46a**, (0.86 mmol) in acetonitrile (2 ml) was added. The reaction mixture was refluxed under stirring for 5 h at 80 °C. An aluminium sheet was wrapped round the flask to protect it from light and the mixture was allowed to stand overnight. Water (5 ml) was added and after filtration the mixture was extracted with EtOAc (2 x 30 ml). The organic layers were combined, dried over MgSO₄, filtered under gravity and the solvent was removed on the rotary evaporator to yield pure **51a**, (90%) as dark brown gum, *R*_f 0.43 [petroleum ether : EtOAc, 2:1 v/v], m.p. 136.0-136.8 °C. IR (ν) 3035 (aromatic C-H stretch), 2926 and 2878 (aliphatic C-H stretch), 1625 (conjugated >C=O stretch), 1596 and 1488 (aromatic C=C stretch), 1472 and 1280 (aliphatic NO₂ stretch), 1455 (CH₂ bending absorption), 1244 (asymmetric C-O-C stretch), 1049 (symmetric C-O-C stretch), 753 cm⁻¹ (*ortho* di-substituted out of plane C-H stretch); ¹H NMR δ 1.99 – 2.04 (8H, m, -CH₂-CH₂-), 4.10 (4H, t, J = 5.4 Hz, -O-CH₂-), 4.58 (4H, t, J = 5.9 Hz, -CH₂-ONO₂), 5.83 (1H, s, enolic -CH), 6.74 (2H, d, J = 16.0 Hz, Ar-CH=CH-CO-), 6.91 (2H, d, J = 8.0 Hz, Ar H-3), 6.99 (2H, t, J = 8.0 Hz, Ar H-5), 7.34 (2H, td, J = 8.0 and J = 1.7 Hz, Ar H-4), 7.58 (2H, dd, J = 8.0 and J = 1.7 Hz, Ar H-6), 7.97 (2H, d, J = 16.0 Hz, -CO-CH=CH-Ar); ¹³Carbon NMR δ 24.2 (-ONO₂-CH₂-CH₂-), 25.9 (-O-CH₂-CH₂-), 67.8 (-O-CH₂-), 73.1 (-CH₂-ONO₂), 102.1 (enolic methine C), 112.4

(Ar C-3), 121.3 (α -olefinic C adjacent to enol), 124.6 (Ar C-5), 125.2 (Ar C-1), 129.0 (Ar C-4), 131.5 (β -olefinic C adjacent to enol), 135.8 (Ar C-6), 157.7 (Ar C-2), 183.9 (enolic C); ESMS m/z 543 $[M + H]^+$, 332 $[C_{17}H_{18}O_6N]^+$; Accurate mass found: m/z 543.1964, calculated for $C_{27}H_{31}N_2O_{10}$: 543.1973.

(1*E*,6*E*)-1,7-bis(3-(4-butoxy-nitrate)hepta-1,6-diene-3,5-dione, **51b**, (58%) as a dark brown solid, R_f 0.46 [petroleum ether : EtOAc, 2:1 v/v], m.p. 133.9-134.9 °C. IR (ν) 3414 (OH stretch), 3020 (aromatic C-H stretch), 2929 and 2875 (aliphatic C-H stretch), 1638 (conjugated $>C=O$ stretch), 1596 and 1489 (aromatic C=C stretch), 1473 and 1279 (aliphatic NO_2 stretch), 1458 (CH_2 bending absorption), 1247 (asymmetric C-O-C stretch), 1041 cm^{-1} (symmetric C-O-C stretch); 1H NMR δ 1.95 (8H, t, $J = 2.8$ Hz, $-CH_2-CH_2-$), 4.04 (4H, t, $J = 5.1$ Hz, $-O-CH_2-$), 4.56 (4H, t, $J = 5.9$ Hz, $-CH_2-ONO_2$), 5.85 (1H, s, enolic $-CH$), 6.61 (2H, d, $J = 15.5$ Hz, Ar-CH=CH-CO-), 6.91 (2H, dd, $J = 7.7$ and 1.7 Hz, Ar H-4), 7.06 (2H, s, Ar H-2), 7.16 (2H, d, $J = 7.7$ Hz, Ar H-6), 7.31 (2H, t, $J = 7.7$ Hz, Ar H-5), 7.62 (2H, d, $J = 15.5$ Hz, $-CO-CH=CH-Ar$); ^{13}C NMR δ 24.2 ($-ONO_2-CH_2-CH_2-$), 25.9 ($-O-CH_2-CH_2-$), 67.3 ($-O-CH_2-$), 73.1 ($-CH_2-ONO_2$), 102.1 (enolic methine C), 113.9 (Ar C-2), 116.6 (Ar C-4), 121.3 (α -olefinic C adjacent to enol), 124.7 (Ar C-6), 130.3 (Ar C-5), 136.7 (Ar C-1), 140.7 (β -olefinic C adjacent to enol), 159.4 (Ar C-3), 183.5 (enolic C); ESMS m/z 543 $[M + H]^+$, 565 $[M + Na]^+$; Accurate mass found: m/z 543.1985, calculated for $C_{27}H_{31}N_2O_{10}$: 543.1973.

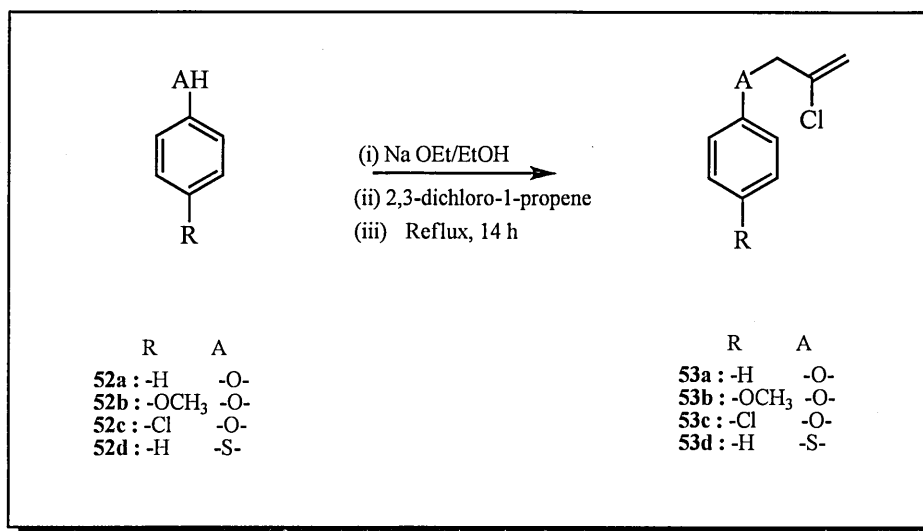
(1*E*,6*E*)-1,7-bis(4-(4-butoxy-nitrate)hepta-1,6-diene-3,5-dione, **51c**, (95%) golden yellow solid, R_f 0.35 [petroleum ether : EtOAc, 2:1 v/v], m.p. 112.6-113 °C. IR (ν) 3412 (OH stretch), 3040 (aromatic C-H stretch), 2936 (aliphatic C-H stretch), 1620

(conjugated $>C=O$ stretch), 1603 and 1511 (aromatic $C=C$ stretch), 1472 and 1287 (aliphatic NO_2 stretch), 1256 (asymmetric $C-O-C$ stretch), 1056 (symmetric $C-O-C$ stretch), 837 cm^{-1} (*para* di-substituted out of plane $C-H$ stretch); 1H NMR δ 1.95 (8H, m, $-CH_2-CH_2-$), 4.06 (4H, t, $J = 5.6\text{ Hz}$, $-O-CH_2-$), 4.56 (4H, t, $J = 5.3\text{ Hz}$, $-CH_2-ONO_2$), 5.79 (1H, s, enolic $-CH$), 6.51 (2H, d, $J = 15.5\text{ Hz}$, $Ar-CH=CH-CO-$), 6.90 (4H, d, $J = 8.8\text{ Hz}$, Ar H-3 and H-3'), 7.51 (4H, d, $J = 8.8\text{ Hz}$, Ar H-2 and H-2'), 7.63 (2H, d, $J = 15.5\text{ Hz}$, $-CO-CH=CH-Ar$); ^{13}C Carbon NMR δ 24.1 ($-ONO_2-CH_2-CH_2-$), 25.8 ($-O-CH_2-CH_2-$), 67.4 ($-O-CH_2-$), 73.1 ($-CH_2-ONO_2$), 101.6 (enolic methine C), 115.1 (Ar C-3, C-5), 122.1 (α -olefinic C adjacent to enol), 128.3 (Ar C-1), 130.0 (Ar C-2, C-6), 140.3 (β -olefinic C adjacent to enol), 160.7 (Ar C-4), 183.6 (enolic C); EIMS m/z 543 $[M + H]^+$, (42%); Accurate mass found: m/z 542.1938, calculated for $C_{27}H_{30}N_2O_{10}$: 542.1900.

(1*E*,6*E*)-1,7-bis(4-(4-butoxy-nitrate)-3-methoxyphenyl)hepta-1,6-diene-3,5-dione, **51d**, (92%) as an orange solid, R_f 0.43 [petroleum ether : EtOAc, 1:3 v/v], m.p. 101.6-102.6 °C. IR (ν) 3436 (OH stretch), 2954 (aromatic $C-H$ stretch), 2931 and 2873 (aliphatic $C-H$ stretch), 1621 (conjugated $>C=O$ stretch), 1458 (CH_2 bending absorption), 1512 (aromatic $C=C$ stretch), 1257 (asymmetric $C-O-C$ stretch), 1027 (symmetric $C-O-C$ stretch). 1H NMR δ 1.98 (8H, m, $-CH_2-CH_2-$), 3.91 (6H, s, $-O-CH_3$), 4.10 (4H, t, $J = 5.1\text{ Hz}$, $-O-CH_2-$), 4.58 (4H, t, $J = 5.9\text{ Hz}$, $-CH_2-ONO_2$), 5.83 (1H, s, enolic $-CH$), 6.50 (2H, d, $J = 15.5\text{ Hz}$, $Ar-CH=CH-CO-$), 6.87 (2H, d, $J = 8.2\text{ Hz}$, Ar H-5), 7.09 (2H, s, Ar H-2), 7.13 (2H, d, $J = 8.2\text{ Hz}$, Ar H-6), 7.61 (2H, d, $J = 15.5\text{ Hz}$, $-CO-CH=CH-Ar$); ^{13}C Carbon NMR δ 24.2 ($-ONO_2-CH_2-CH_2-$), 25.7 ($-O-CH_2-CH_2-$), 56.2 ($-OCH_3$), 68.5 ($-O-CH_2-$), 73.2 ($-CH_2-ONO_2$), 101.5 (enolic

methine C), 110.6 (Ar C-2), 113.1 (Ar C-5) 122.5 (α -olefinic C adjacent to enol), 122.9 (Ar C-6), 128.7 (Ar C-1), 140.6 (β -olefinic C adjacent to enol), 150.0 (Ar C-3), 150.5 (Ar C-4), 183.5 (enolic C); EIMS m/z 603 $[M]^+$ (38%), 604 $[M + H]^+$, (12%); Accurate mass found: m/z 603.2162, calculated for $C_{29}H_{35}N_2O_{10}$: 603.2184.

2.1.6 Synthesis of aromatic ethers **53a-c** and thioether **53d**¹⁵⁵



Scheme 2.5

General procedure

A typical procedure for making aromatic ethers and thioether shown in scheme 2.5 is illustrated by the formation of 2-(*-chloroallyloxy*)benzene, **53a**. To a dried 3-neck round bottom flask, fitted with double surface condenser, dropping funnel and a calcium chloride drying tube, dry EtOH (100 ml) was added. Freshly cut sodium metal (4.6 gm; 0.2 mol), pre-washed in toluene was added slowly to dry EtOH with gentle stirring under reflux, until all the sodium had reacted. The phenol **52a** (18.82

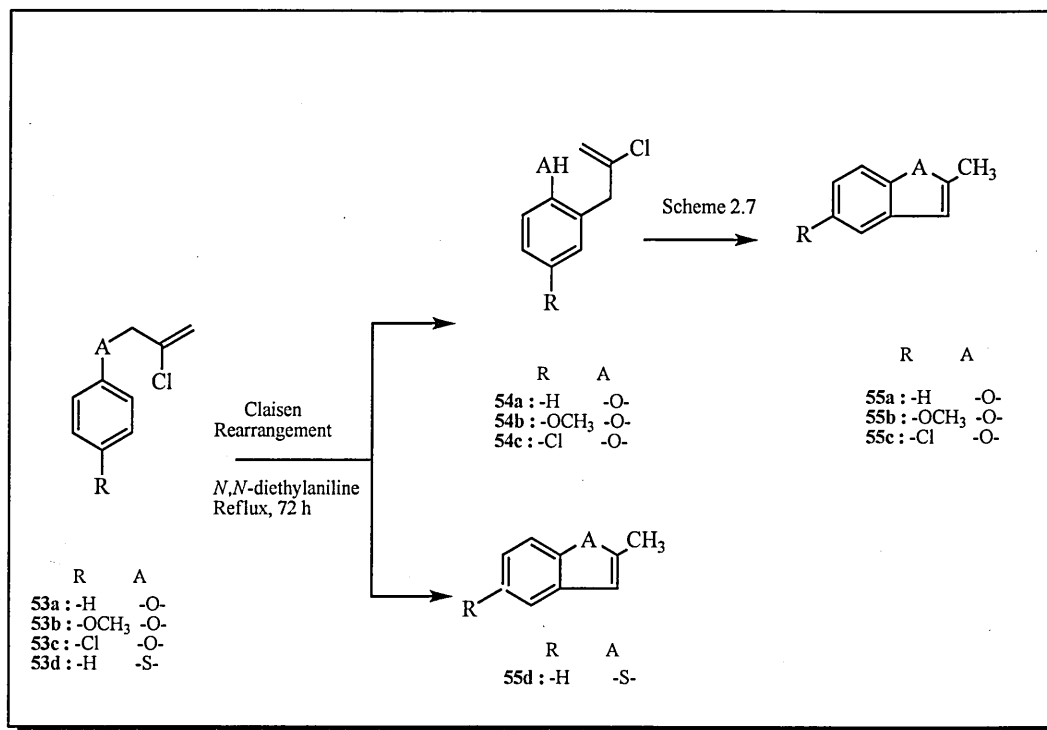
gm, 0.2 mol) was added and the reaction mixture was heated to 80 °C for 30 minutes. 2,3-Dichloropropene (23.96 gm; 0.2 mol) was added dropwise to the reaction mixture through the dropping funnel over a period of 35 minutes. The reaction mixture was refluxed for 14 h, after which it was allowed to settle and then filtered by suction filtration using a Buchner flask. The filtrate was concentrated on the rotary evaporator by removal of the excess EtOH. Water (100 ml) was added to the filtrate and extracted with EtOAc (2 x 90 ml). The combined organic extract was washed with NaOH solution (2M, 50 ml) and water. After drying over MgSO₄, the solution was filtered and the solvent was evaporated on the rotary evaporator to yield pure **53a**, (57%, lit. 68%).¹⁵⁵ IR (ν) 3039 (aromatic C-H stretch), 2925 and 2866 (aliphatic C-H stretch), 1642 and 1455 (aromatic C=C stretch), 1239 (asymmetric C-O-C stretch), 1050 (symmetric C-O-C stretch), 690 and 754 cm⁻¹ (mono substituted ring); ¹H NMR δ 4.60 (2H, t, J = 1.2 Hz, allylic protons), 5.45 (1H, q, J = 1.5 Hz, olefinic proton *trans* to -Cl), 5.57 (1H, q, J = 2.0 Hz, olefinic proton *cis* to -Cl), 6.91 - 7.03 (3H, m, Ar H-5 and H-6), 7.26 - 7.35 (2H, m, Ar H-4); EIMS m/z 168 [M ³⁵Cl]⁺ (1%), 133 [M - ³⁵Cl]⁺ (6 %).

1-(2-Chloroallyloxy)-4-methoxybenzene, **53b**, (63%, lit. 98%).¹⁵⁵ IR (ν) 3000-3045 (aromatic C-H stretch), 2933 and 2833 (aliphatic C-H stretch), 1639 (aromatic C=C stretch) 1620 (>C=C<), 824 cm⁻¹ (*para* disubstituted ring). ¹H NMR δ 3.78 (3H, s, -OCH₃), 4.53 (2H, s, allylic protons), 5.41 (1H, s, olefinic proton *trans* to -Cl), 5.55 (1H, s, olefinic proton *cis* to -Cl), 6.80 – 6.90 (4H, dd, AB system, Ar-H); EIMS m/z 198 [M ³⁵Cl]⁺, 200 [M ³⁷Cl]⁺.

1-Chloro-4-(2-chloroallyloxy)benzene, **53c**, (57%, lit. 67%).¹⁵⁵ IR (v) 3041 (aromatic C-H stretch), 2925 and 2868 (aliphatic C-H stretch), 1642 and 1454 (aromatic C=C stretch), 1241 (asymmetric C-O-C stretch), 1045 (symmetric C-O-C stretch), 824 cm⁻¹ (*para* disubstituted ring). ¹H NMR δ 4.56 (2H, t, J = 1.2 Hz, allylic protons), 5.45 (1H, q, J = 1.5 Hz, olefinic proton *trans* to -Cl), 5.54 (1H, q, J = 1.5 Hz, olefinic proton *cis* to -Cl), 6.86 (2H, d, J = 9.3 Hz, Ar H *ortho* to oxygen), 7.25 (2H, d, J = 8.7 Hz, Ar H *ortho* to Cl); EIMS m/z 206 [M ³⁷Cl]⁺ (7%), 204 [M³⁵Cl + 2]⁺ (38%), 202 [M ³⁵Cl]⁺ (63%), 167 [M - ³⁷Cl]⁺ (66%), 141 [C₇H₆O ³⁵Cl]⁺ (9%) 127 [C₆H₄O ³⁵Cl]⁺ (91%), 75 [C₃H₄ ³⁵Cl]⁺ (93%), 63 [C₂H₂ ³⁷Cl]⁺ (47%).

1-(2-Chlorothioallyloxy)benzene, **53d**, (76%, lit. 84%).¹⁵⁵ IR (v) 2918 (aliphatic C-H stretch), 1627 (aromatic C=C stretch); ¹H NMR δ 3.70 (2H, s, -CH₂S), 5.23 (1H, s, olefinic proton *trans* to -Cl), 5.28 (1H, s, olefinic proton *cis* to -Cl), 7.28-7.40 (5H, m, Ar-H) ; EIMS m/z 184 [M ³⁵Cl]⁺ (78%), 186 [M ³⁷Cl]⁺ (45%).

2.1.7 Synthesis of 2-(2-chloroallyl)phenols **54a-c** and 2-methylbenzo[*b*]thiophene **55d**¹⁵⁵



Scheme 2.6

General procedure

A typical procedure for the preparation of phenols **54a-c** and benzo[*b*]thiophene **55d** shown in scheme 2.6 is illustrated by the formation of 2-(2-chloroallyl)phenol **54a**. In a round bottom flask, 2-(2-chloroallyloxy)benzene **53a** (0.08 mol) was weighed and *N,N*-diethylaniline (0.4 mol) was added to it. A condenser was attached to the flask and the reaction mixture was refluxed under nitrogen for 72 h. The reaction mixture was then cooled and diluted with ether (300 ml). The phenol **54a** was extracted from the organic mixture, with aqueous 25% potassium hydroxide (3 x 100 ml). The aqueous phase was washed with ether (3 x 100 ml), neutralized with 10%

hydrochloric acid and extracted with ether (3 x 100 ml). The combined organic layer was dried over MgSO₄, concentrated in vacuo to afford pure **54a**, (66%, lit. 77%).¹⁵⁵ IR (ν) 3433 (OH-stretch), 3038 (aromatic C-H stretch), 2978 and 2912 (aliphatic C-H stretch), 1633 and 1455 (aromatic C=C stretch), 750 cm⁻¹ (*ortho* disubstituted ring); ¹H NMR δ 3.69 (2H, s, allylic protons), 5.07 (1H, br. s, -OH), 5.14 (1H, d, J= 1.5 Hz, olefinic proton *trans* to -Cl), 5.29 (1H, s, olefinic proton *cis* to -Cl), 6.80 - 7.27 (4H, m, Ar H-5 to 8); EIMS m/z 168 [M ³⁵Cl]⁺ (18%), 133 [M - ³⁵Cl]⁺ (95%), 105 [C₇H₅O]⁺ (100%).

2-(2-Chloroallyl)-4-methoxyphenol, **54b**, (34%, lit. 84%).¹⁵⁵ IR (ν) 3398 (OH-stretch), 2998, 2940, 2834 (aliphatic C-H stretch), 1705, 1635 cm⁻¹ (>C=C<); 750 cm⁻¹ (*ortho* disubstituted ring). ¹H NMR δ 3.76 (2H, s, -S-CH₂-), 4.64 (1H, s, OH), 5.13 (1H, s, olefinic proton *trans* to -Cl), 5.28 (1H, s, olefinic proton *cis* to -Cl), 6.70-6.80 (3H, m, Ar-H); EIMS m/z 198 [M ³⁵Cl]⁺ and 200 [M ³⁷Cl]⁺.

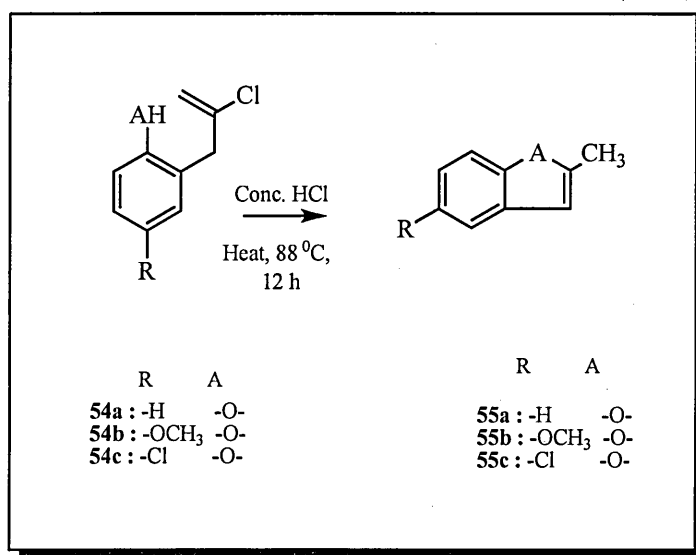
4-Chloro-2-(2-chloroallyl)phenol, **54c** was isolated from the ethereal reaction mixture after removal of *N,N*-diethylaniline with hydrochloric acid (2M, 2 x 200 ml). The ethereal solution was dried over MgSO₄, concentrated in vacuo and subjected to flash column chromatography using [petroleum ether : EtOAc, 15:1 v/v] as eluent, to afford pure **10c**, (66%, lit. 90%).¹⁵⁵ IR (ν) 3540-3397 (OH-stretch), 3397 (aromatic C-H stretch, overlapped with OH-stretch), 2925 (aliphatic C-H stretch), 1634 and 1421 cm⁻¹ (aromatic C=C stretch). ¹H NMR δ 3.64 (2H, s, allylic protons), 5.18 (1H, d, J= 1.5 Hz, olefinic proton *trans* to -Cl), 5.31 (2H, s, olefinic proton *cis* to -Cl and -OH), 6.74 (1H, d, J= 8.2 Hz, Ar H-6), 7.12 (1H, dd, J= 8.2 Hz and 2.5 Hz, Ar H-5),

7.18 (1H, d, $J = 2.5$ Hz, Ar H-4); EIMS m/z 202 $[M^{35}\text{Cl}]^+$ (28%), 204 $[M^{35}\text{Cl} + 2]^+$ (17%), 167 $[M - ^{35}\text{Cl}]^+$ (100%) 165 $[M - ^{37}\text{Cl}]^+$ (28%), 141 $[\text{C}_7\text{H}_6\text{O}^{35}\text{Cl}]^+$ (27%), 132 $[M - ^{35}\text{Cl}_2]^+$ (27%), 63 $[\text{C}_2\text{H}_2^{37}\text{Cl}]^+$ (21%).

2-Methylbenzo[b]thiophene, **55d**, (43%, lit. 75%)¹⁵⁵ R_f 0.42 [petroleum ether]. ^1H

NMR δ 2.34 (3H, s, -CH₃), 7.0–7.5 (5H, m, Ar-H); EIMS m/z 148 $[M]^+$ (25%).

2.1.8 Synthesis of 2-methylbenzofuran **55a-c**¹⁵⁵



Scheme 2.7

General procedure

A typical procedure for the preparation of **55a** and **55c** is illustrated by the formation of **55a**. A mixture of 2-(2-chloroallyl)phenol **54a** (0.029 mol) in concentrated hydrochloric acid (26 ml) was stirred for 12 h using an oil bath maintained at 88–89 °C. After that, the cooled two phase reaction mixture was diluted with water (85 ml), neutralized with 5% potassium hydroxide and extracted with ether (2 x 100 ml).

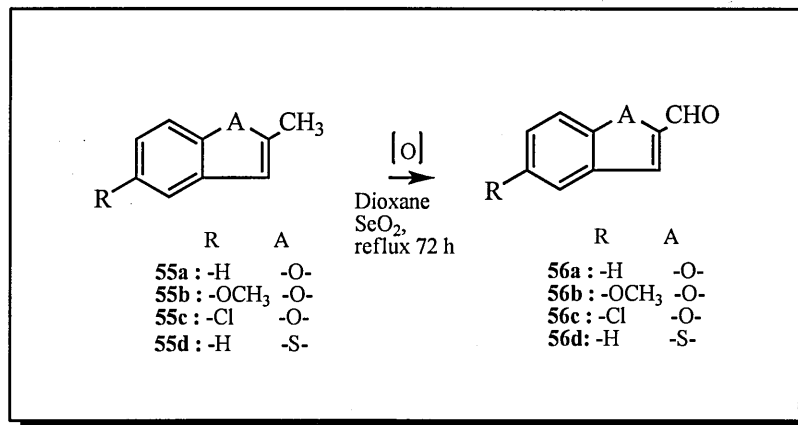
The combined ethereal solutions were dried over MgSO_4 and concentrated in vacuo to give a residue which was subjected to flash column chromatography using petroleum ether as eluent to yield *2-methylbenzofuran*, **55a**, (41%, lit. 56%).¹⁵⁵ IR (v) 3034 and 3056 (aromatic C-H stretch), 2952 (aliphatic C-H stretch), 1610 and 1439 cm^{-1} (aromatic C=C stretch); ^1H NMR δ 2.48 (3H, s, $-\text{CH}_3$), 6.38 (1H, d, $J = 1.0$ Hz, Ar H-1), 7.39 - 7.51 (4H, m, Ar H-2 to 5); EIMS m/z 131 $[\text{M}-\text{H}]^+$ (100%), 132 $[\text{M}]^+$ (79%).

5-Methoxy-2-methylbenzofuran, **55b**. In a round bottom flask, *2-(2-chloroallyl)-4-methoxyphenol* **54b** (0.029 mol) was stirred at room temperature for 24 h in trifluoroacetic acid (26 ml) and then diluted with ether (150 ml). The ethereal solution was washed with 5% aqueous potassium hydroxide (4 x 400 ml) and then with water (2 x 200 ml). After drying over MgSO_4 , it was filtered and concentrated on the rotary evaporator. The residue was subjected to flash column chromatography using petroleum ether as eluent, to afford **55b** (42%, lit. 29%).¹⁵⁵ ^1H NMR δ 2.42 (3H, s, $-\text{CH}_3$), 3.82 (3H, s, $-\text{OCH}_3$), 6.30 (1H, s, H-3), 6.82 (1H, s, H-6), 6.93 (1H, s, H-4), 7.25 (1H, s, H-7); EIMS m/z 162 $[\text{M}]^+$, 163 $[\text{M}+1]$ (100%).

5-Chloro-2-methylbenzofuran, **55c** was purified by flash column chromatography using petroleum ether as eluent, (63%, lit. 51%).¹⁵⁵ IR (v) 3114 (aromatic C-H stretch), 2921 and 2955 (aliphatic C-H stretch), 1600 and 1446 cm^{-1} (aromatic C=C stretch); ^1H NMR δ 2.46 (3H, d, $J = 1.0$ Hz, $-\text{CH}_3$), 6.33 (1H, t, $J = 1.0$ Hz, Ar H-1), 7.15 (1H, dd, $J = 8.7$ and 2.0 Hz, H-3), 7.31 (1H, d, $J = 8.7$ Hz, Ar H-4), 7.43 (1H, d,

$J = 2.0$ Hz, H-2); EIMS m/z 166 $[M]^+$ (100%), 165 $[M-H]^+$ (77%), 131 $[M - ^{35}Cl]^+$ (32%).

2.1.9 Synthesis of benzo[*b*]furan-2-carbaldehydes **56a-c** and benzo[*b*]thiophene-2-carbaldehyde **56d**¹⁵⁶



Scheme 2.8

A typical procedure for the preparation of benzo[*b*]furan-2-carbaldehydes **56a-c** and benzo[*b*]thiophene-2-carbaldehyde **56d** shown in scheme 2.8 is illustrated by the formation of aldehyde **56a**. To a three-neck round bottom flask fitted with a reflux condenser and a thermometer, dioxane (15 ml), selenium dioxide (1.11 gm, 0.01 mol) and water (0.5 ml) were placed and the reaction mixture was heated to 100 °C with constant stirring until all the solid had dissolved. A solution of compound **55a** (0.01 mol) in dioxane (1 ml) was added and the reaction was heated under reflux with stirring for 24 h. The hot solution was decanted from the black precipitate of elemental selenium using a fluted filter-paper and the dioxane was removed by distillation at atmospheric pressure. The crude product was dissolved in

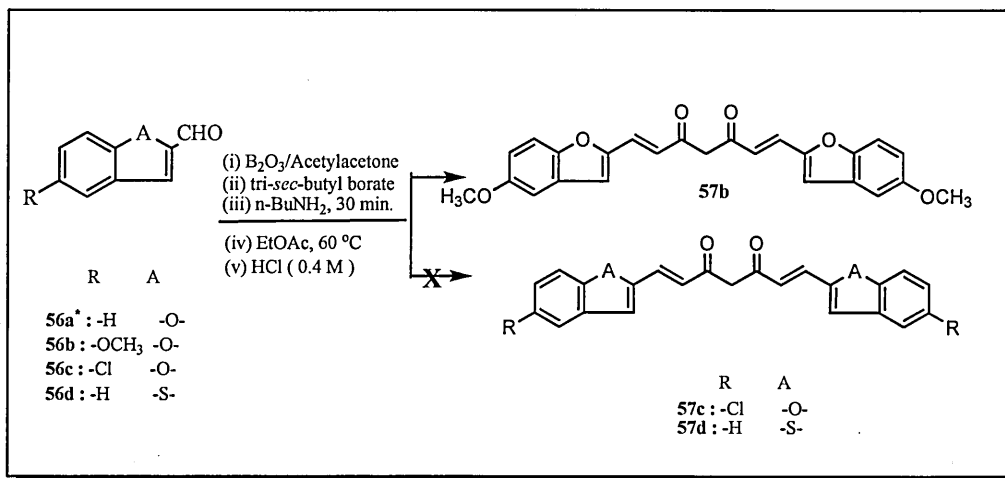
dichloromethane (50 ml) and washed with water (2 x 25 ml). The combined dichloromethane layer was dried over MgSO_4 and concentrated in vacuo to afford **56a**¹⁵⁷ (89%). ^1H NMR δ 7.23 (1H, td, $J = 7.2$ Hz, $J = 1.0$ Hz, Ar H-5), 7.41 (1H, td, $J = 7.2$ Hz, $J = 1.0$ Hz, Ar H-6), 7.41 (1H, s, Ar H-3), 7.49 (1H, d, $J = 7.2$ Hz, Ar H-7), 7.65 (1H, d, $J = 7.2$ Hz, Ar H-4), 9.76 (1H, s, -CHO); EIMS m/z 146 $[\text{M}]^+$ (100%), 145 $[\text{M}-\text{H}]^+$ (83%), 118 $[\text{M}-\text{CO}]^+$ (12%).

5-Methoxybenzofuran-2-carbaldehyde, **56b** (25%). IR (ν) 2835 (-CHO), 1680, 1636 cm^{-1} ($>\text{C}=\text{O}$); ^1H NMR δ 3.88 (3H, s, OCH_3), 7.13 (1H, s, H-3), 7.17 (1H, s, H-4), 7.45-7.53 (2H, m, H-5 and H-6), 9.85 (1H, s, -CHO); Accurate mass found: m/z 176.0456, calculated for $\text{C}_{10}\text{H}_8\text{O}_3$: 176.0473.

5-Chlorobenzofuran-2-carbaldehyde, **56c** (78%). IR (ν) 2845 (-CHO), 1685, 1634 cm^{-1} ($>\text{C}=\text{O}$); ^1H NMR δ 7.46 - 7.58 (3H, m, Ar H-2 to 4), 7.75 (1H, d, $J = 2.0$ Hz, Ar H-1), 9.89 (1H, s, -CHO); EIMS m/z 180 $[\text{M}]^+$ (100%), 179 $[\text{M}-\text{H}]^+$ (61%).

Benzo[b]thiophene-2-carbaldehyde **56d**¹⁵⁸ (20%). IR (ν) 1693, 1650 cm^{-1} ($>\text{C}=\text{O}$); ^1H NMR δ 7.2-7.7 (5H, m, Ar), 9.85 (1H, m, -CHO); Accurate mass found: m/z 146.0211, calculated for $\text{C}_9\text{H}_6\text{SO}$: 146.0190.

2.1.10 Synthesis of benzo[*b*]furan curcuminoid **57b** and attempted synthesis of **57c** and benzo[*b*]thiophene curcuminoid **57d**¹⁴⁴



Scheme 2.9

* Synthesis of curcuminoid from **56a** was not performed.

(1*E*,6*E*)-1,7-bis(5-methoxybenzofuran-2-yl)hepta-1,6-diene-3,5-dione, **57b**, (30%)

was prepared by the method described in section 2.1.4, method A, and was obtained as a yellow-orange solid. IR (ν) 3348 (OH stretch), 1667 cm⁻¹ (>C=O); ¹H NMR δ 3.85 (6H, s, -OCH₃), 5.70 (1H, s, enolic -CH), 6.58 (2H, d, *J* = 15.5 Hz, Ar-CH=CH-CO-), 6.94 (2H, dd, *J* = 3.2 and 7.8 Hz, Ar H-6'), 6.98 (2H, s, Ar H-3'), 7.02 (2H d, *J* = 3.2 Hz, Ar H-4'), 7.3 (2H, d, *J* = 7.8 Hz, Ar H-7'), 7.50 (2H, d, *J* = 15.5 Hz, -CO-CH=CH-Ar), 15.80 (1H, broad s, OH); EIMS *m/z* 416 [M⁺] (4%), 239 [M-OH] (8.5%), 121 (100%), [M-2furanyl rings]; Accurate mass found: *m/z* 416.1332, calculated for C₂₅H₂₀O₆ : 416.1259.

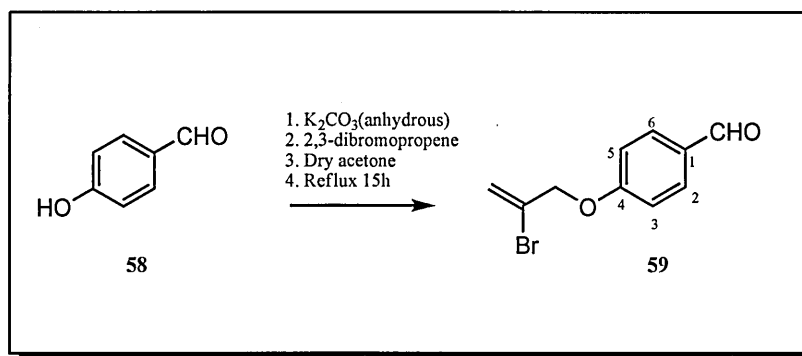
(1E,6E)-1,7-bis(5-chlorobenzofuran-2-yl)hepta-1,6-diene-3,5-dione, **57c**.

The TLC results did not show any formation of the desired curcumin and the reaction was abandoned after prolonged stirring.

(1E,6E)-1,7-bis(benzo[*b*]thiophen-2-yl)hepta-1,6-diene-3,5-dione, **57d**.

The bright yellow stain characteristic of curcumin formation was not observed on the TLC and this reaction was also discontinued after prolonged stirring under the usual reaction conditions.

2.1.11 Synthesis of 4-(2-bromoallyloxy)benzaldehyde **59**

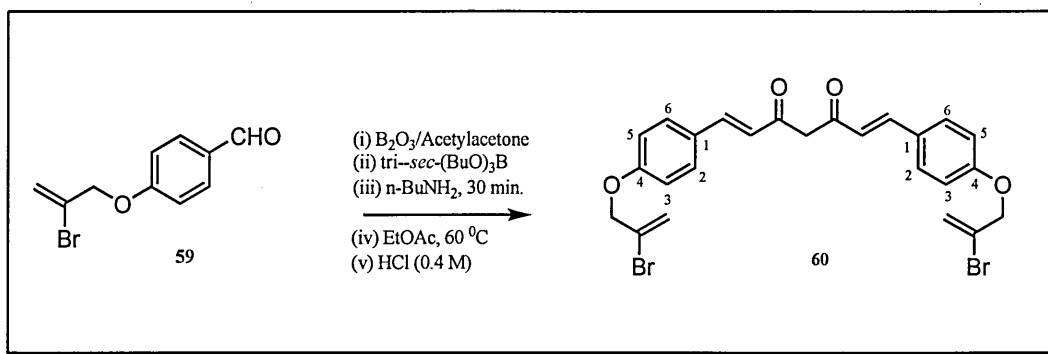


Scheme 2.10

To a 3-neck round bottom flask, fitted with double surface condenser, dropping funnel and a calcium chloride drying tube was added 4-hydroxybenzaldehyde **58** (24.43 gm, 0.2 mol) and dried acetone (150 ml). The reaction mixture was allowed to stir for 30 minutes till all the aldehyde dissolved. Potassium carbonate (33.16 gm, 0.23 mol) was then added and the reaction mixture was stirred for 30 minutes. 2,3-Dibromobutane (36 gm, 0.18 mol) was added slowly (over a period of 35 minutes) from a dropping funnel and the reaction mixture was refluxed for 15 h. After this period, the reaction mixture was allowed to settle and then filtered. To the mother

liquor was added water (100 ml) and the mixture was extracted with EtOAc (3 x 80 ml). The organic layers were combined, dried over MgSO₄ and concentrated on the rotary evaporator to give the crude product which was purified by flash column chromatography, using [petroleum ether : EtOAc, 5:1 v/v] as eluent, to afford **59**, (79%) as colourless oil which acquired magenta colouration upon keeping, *R_f* 0.42 [petroleum ether : EtOAc, 1:5 v/v]. IR (ν) 3468 (OH-stretch), 3105 and 3073 (aromatic C-H), 2925 (aliphatic C-H stretch), 2739 (aldehyde C-H stretch), 1600 and 1425 cm⁻¹ (aromatic C=C stretch); ¹H NMR δ 4.72 (2H, t, *J* = 1.0 Hz, allylic protons), 5.71 (1H, q, *J* = 1.0 Hz, olefinic proton *trans* to -Br), 5.99 (1H, q, *J* = 1.0 Hz, olefinic proton *cis* to -Br), 7.02 (2H, d, *J* = 8.8 Hz, Ar H-3 and H-3'), 7.84 (2H, d, *J* = 8.8 Hz, Ar H-2 and 2'), 9.89 (1H, s, -CHO); ¹³C NMR δ 71.9 (allylic -CH₂), 115.0 (Ar C-3, C-5), 118.3 (vinyl - CH₂), 126.3 (vinyl C), 130.9 (Ar C-1), 132.4 (Ar C-2, C-6), 162.9 (Ar C-4), 190.9 (-CHO); ESMS *m/z* 241 [M + H]⁺ for Br⁷⁹, 242 [M + 2H]⁺, 243 [M + H]⁺ for Br⁸¹.

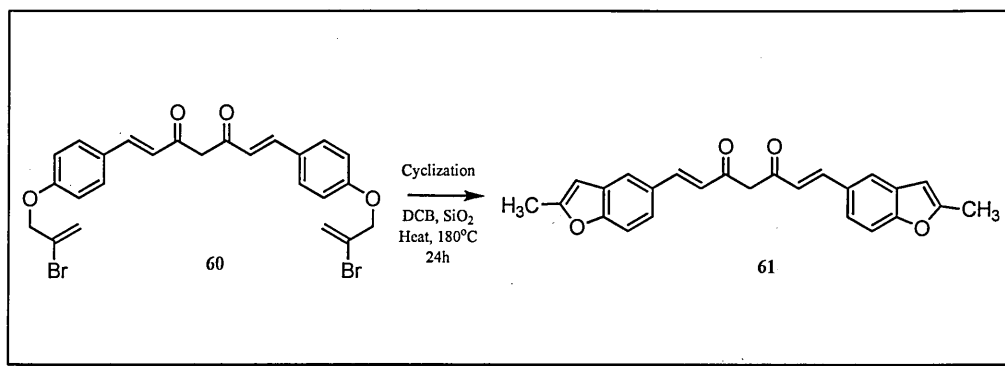
2.1.12 Synthesis of bromoallyloxy curcumin **60**¹⁴⁴



Scheme 2.11

(1*E*,6*E*)-1,7-bis(4-(2-bromoallyloxy)phenyl)hepta-1,6-diene-3,5-dione, **60**, (22%) was prepared by the method described in section 2.1.4, method A, and was obtained after the work-up as bright yellow precipitates, R_f 0.40 [petroleum ether: EtOAc, 5:1 v/v], m.p. 131.7-132.7 °C. IR (ν) 3440 (OH stretch), 3000 (aromatic C-H stretch), 1622 (H-bonded $>C=O$), 1600 and 1571 ($>C=C<$ stretch), 1249 cm^{-1} (C-O-C asymmetric stretch); ^1H NMR δ 4.69 (4H, s, allylic proton), 5.71 (2H, d, $J = 1.5$ Hz, olefinic proton *trans* to Br), 5.80 (1H, s, enolic -CH), 6.00 (2H, s, olefinic proton *cis* to Br), 6.52 (2H, d, $J = 16.0$ Hz, Ar-CH=CH-CO-), 6.94 (4H, d, $J = 8.2$ Hz, Ar H-2, H-2'), 7.52 (4H, d, $J = 8.2$ Hz, Ar H-3, H-3' AB system), 7.62 (2H, d, $J = 16.0$ Hz, -CO-CH=CH-Ar); ^{13}C NMR δ 71.9 (allyloxy-CH₂-), 101.7 (enolic methine C), 115.6 (Ar C-3, C-5), 118.3 (α -olefinic C adjacent to enol), 122.7 (vinylic -CH₂), 126.8 (Ar C-1), 129.0 (vinylic C), 130.0 (Ar C-2, C-6), 140.1 (β -olefinic C adjacent to enol), 183.5 (enolic C); Accurate mass found: m/z 544.9947, calculated for $\text{C}_{25}\text{H}_{23}\text{O}_4\text{Br}_2$: 544.9963.

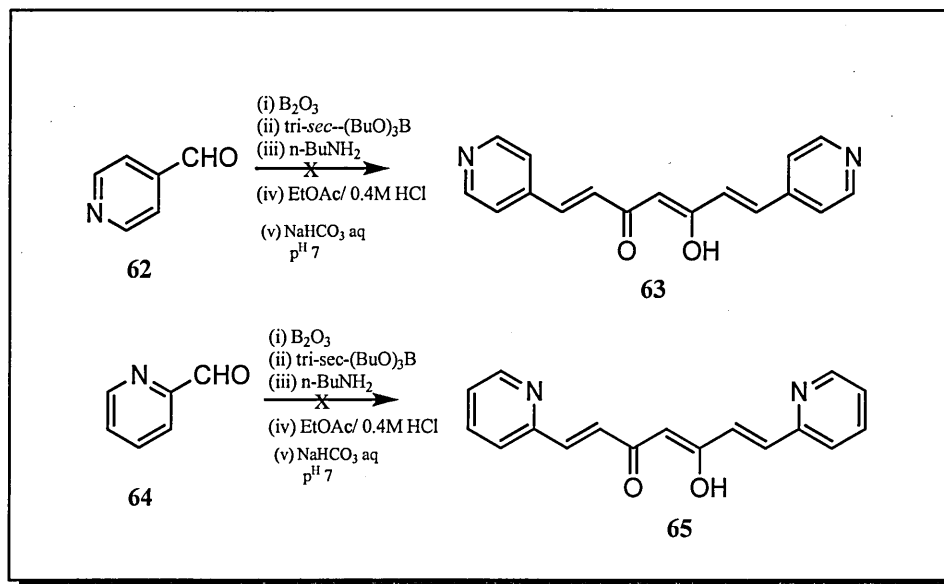
2.1.13 Synthesis of 2-methylbenzofuran-5-ylcurcumin **61**¹⁵⁹



Scheme 2.12

In a round bottom flask, fitted with a condenser, the solution of **60** (67.5 mg, 0.12 mmol) in 1,2-dichlorobenzene (DCB) (4mL) was heated for 20 minutes in a pre-heated (180 °C) oil-bath. Silica (30 mg) was also added to the reaction mixture and the reaction was refluxed under nitrogen for 24 h. The following day, the reaction mixture was filtered and the DCB was removed under reduced pressure (boiling point 149-150 °C/10mmHg) and the crude product was further purified by flash column chromatography using [petroleum ether : EtOAc, 8:1 v/v] as eluent, to afford **61**, (9%) as an orange gum. ^1H NMR δ 1.56 (6H, s, $-\text{CH}_3$), 5.70 (1H, s, enolic $-\text{CH}$), 6.00 (2H, s, Ar H-3), 6.52 (2H, d, $J = 15.5$ Hz, Ar-CH=CH-CO-), 6.94 (2H, d, $J = 8.5$ Hz, Ar H-7), 7.26 (overlapped with CDCl_3 , 2H, s, Ar H-4), 7.52 (2H, d, $J = 8.8$ Hz, Ar H-7), 7.62 (2H, d, $J = 15.5$ Hz, $-\text{CO}-\text{CH}=\text{CH}-\text{Ar}$).

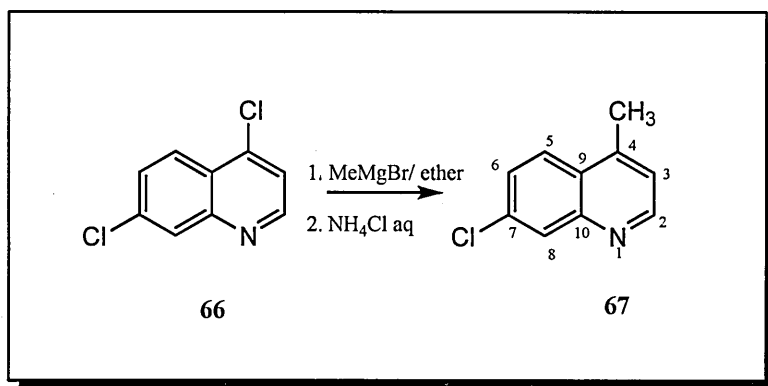
2.1.14 Attempted synthesis of pyridine curcuminoids **63** and **65**



Scheme 2.13

The attempted syntheses for making the curcuminoids **63** and **65** were carried out in the same manner via method A (section 2.1.4) as previously described for the aromatic curcumins except that at the end a solution of saturated sodium bicarbonate was added until the solution was neutral. The bicarbonate was necessary because the hydrochloric acid added in the work-up protonated the basic pyridine nitrogen making the curcuminoids soluble in water. The ^1H NMR did not show the formation of the desired products **63** and **65**.

2.1.15 Synthesis of 7-chloro-4-methylquinoline **67**

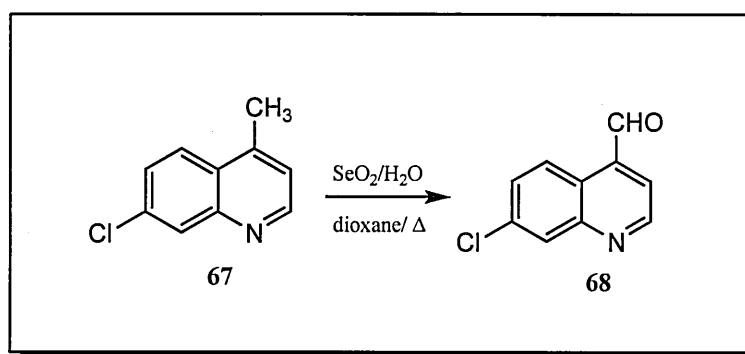


Scheme 2.14

To a solution of 4,7-dichloroquinoline **66** (20.0g, 101 mmol) in dry THF (50 ml) was added at room temperature a solution of methylmagnesium bromide (3.0M, 35 ml, 102 mmol) using a syringe and the reaction mixture under nitrogen was then refluxed under magnetic stirring for 2 h. The solvent was evaporated on the rotary evaporator and to the residue was added 10% NH_4Cl solution (150 ml). The mixture was extracted with EtOAc (2 x 100 ml) and the organic layer after drying over anhydrous MgSO_4 was filtered and evaporated to yield a bluish coloured residue which

eventually turned reddish. The crude product was purified by flash chromatography, to yield the desired product **67**¹⁶⁰ (64%) as a white solid, m.p. 57.3-58.4, R_f 0.3 [petroleum ether: EtOAc, 3:1v/v]. ^1H NMR δ 2.77 (3H, s, $-\text{CH}_3$), 7.35–7.45 (2H, m, H-3 and H-6), 7.68 (1H, d, $J = 10.5$ Hz, H-5), 8.07 (1H, d, $J = 4$ Hz, H-8), 8.75 (1H, d, $J = 5.3$ Hz, H-2); ^{13}C Carbon NMR δ 18.8 ($-\text{CH}_3$), 122.3 (Ar C-3), 125.2 (Ar C-5), 125.7 (Ar C-9), 127.4 (Ar C-6), 129.1 (Ar C-8), 135.2 (Ar C-7), 144.6 (Ar C-4), 148.7 (Ar C-10), 151.4 (Ar C-2); EIMS m/z 177 $[\text{M}^{35}\text{Cl}]^+$ (59%) and 179 $[\text{M}^{37}\text{Cl}]^+$ (25%); Accurate mass found: m/z 177.0381, calculated for $\text{C}_{10}\text{H}_8\text{NCl}$: 177.0345.

2.1.16 Oxidation of 7-chloro-4-methylquinoline **67** with selenium dioxide¹⁵⁶

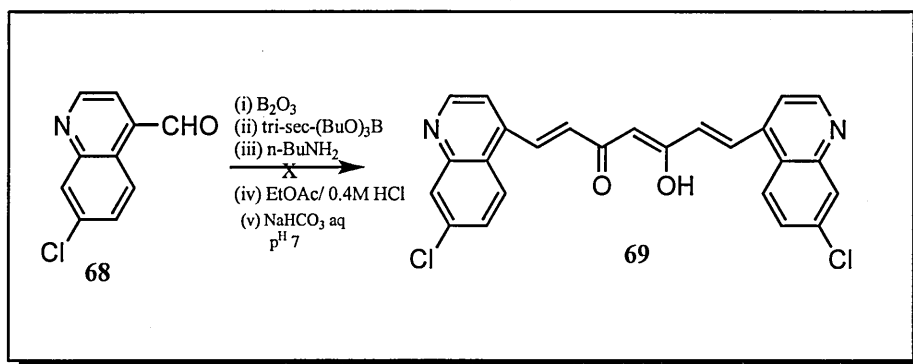


Scheme 2.15

Selenium dioxide (6.6 g, 59.4 mmol) was added to a stirred hot solution of compound **67** (10.0g, 56.3 mmol) in dioxane (55 ml) at 90 °C followed by water (2.5 ml) and the mixture was heated under reflux at 100-110 °C for 10 h. The cooled reaction mixture was filtered on a Buchner funnel to remove elemental selenium and after removing the solvent on the rotary evaporator the residue was chromatographed [petroleum ether : EtOAc, 1:1v/v] to yield pure 7-chloroquinoline-4-carbaldehyde, **68**, (58%) as a light brown solid m.p.100-103 °C. IR (ν) 2864, 2772 (H-CO) 1699 cm^{-1} ($\text{C}=\text{O}$); ^1H

NMR δ 7.68 (1H, dd, $J = 3.0$ and 10.8 Hz, H-6), 7.77 (1H, d, $J = 4.5$ Hz, H-3), 8.20 (1H, d, $J = 3$ Hz, H-8), 8.98 (1H, d, $J = 10.8$ Hz, H-5), 9.20 (1H, d, $J = 4.5$ Hz, H-2), 10.46 (1H, s, -CHO); EIMS m/z 191 (^{35}Cl) and 193 (^{37}Cl); Found: C, 62.48; H, 3.00; N, 7.15%. Calculated for $\text{C}_{10}\text{H}_6\text{ClNO}$: C, 62.68; H, 3.16; N, 7.31%.

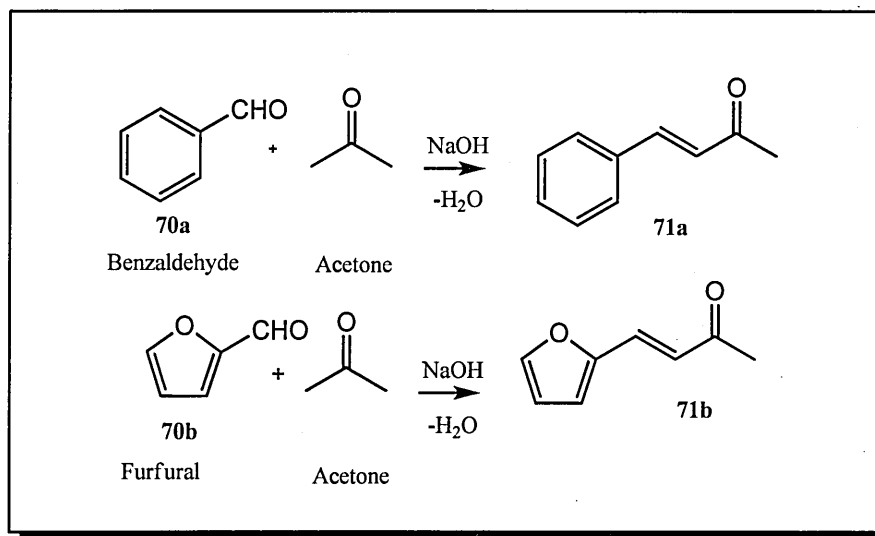
2.1.17 Attempted synthesis of quinoline curcuminoid **69**



Scheme 2.16

The attempted synthesis for making curcuminoid **69** was carried out in the same manner via method A (section 2.1.4) as previously described for the aromatic curcumins except that at the end a solution of saturated sodium bicarbonate was added until the solution was neutral. The bicarbonate was necessary because the hydrochloric acid added in the work-up protonated the basic pyridine nitrogen making the curcuminoids soluble in water. The ^1H NMR did not show the formation of the desired products **69**.

2.1.18 Synthesis of (*E*)-4-(phenylbut)-3-en-2-one **71a** and **71b**¹⁵⁶



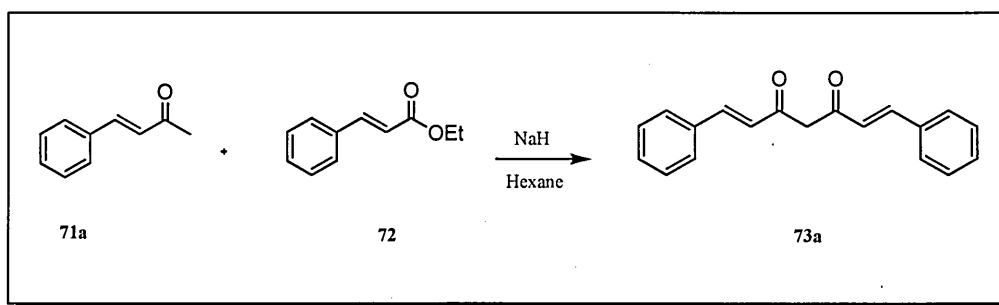
Scheme 2.17

To a stirred solution of pure benzaldehyde **70a** (8.50g, 0.08 mol) and pure distilled acetone (16 ml, 0.08 mol) in a 250 ml round bottomed flask was slowly added a solution of sodium hydroxide (10%, 10 ml) over a period of 10 minutes after which the reaction mixture was allowed to stir for 2 h. The mixture was acidified with 2M HCl producing two layers. The upper organic layer was removed, the lower aqueous layer was extracted with toluene (20 ml) and the combined organic layers were washed with water (20 ml) and then dried with anhydrous MgSO_4 . After filtration the toluene was evaporated on the rotary evaporator and the residue was distilled under reduced pressure (88-90 °C/0.3mmHg) to give benzylideneacetone **71a**, (36%) as colourless liquid which solidified (m.p. 42 °C) on keeping. IR (ν) 1680 cm^{-1} (C=O); ^1H NMR δ 2.40 (3H, s, CH_3), 6.58 (2H, d, $J = 16.0$ Hz, Ar-CH=CH-CO-), 7.30 –

7.50 (5H, m, Ph), 7.60 (2H, d, $J = 16.0$ Hz, $-\text{CO}-\text{CH}=\text{CH}-\text{Ar}$); EIMS m/z 146 (42%, M^+), 130 (86%), 103 (100%, $\text{Ph}-\text{CH}=\text{CH}$).

The compound (*E*)-4-(furan-2-yl)but-3-en-2-one, **71b** was similarly synthesised from furan-2-carbaldehyde and acetone (58% yield), b.p. (120-122 °C/7 mmHg). IR (ν) 1680 cm^{-1} (C=O); ^1H NMR δ 2.32 (3H, s, CH_3), 6.49 (1H, dd, $J = 3.6$ and $J = 1.6$ Hz, H-3), 6.61 (1H, d, $J = 16.0$ Hz, $\text{Ar}-\text{CH}=\text{CH}-\text{CO}-$), 6.67 (1H, d, $J = 3.6$ Hz, H-4), 7.28 (1H, d, $J = 16.0$ Hz, $-\text{CO}-\text{CH}=\text{CH}-\text{Ar}$), 7.50 (1H, d, $J = 1.6$ Hz, H-5); EIMS m/z 136 (46%, M^+).

2.1.19 Condensation reaction of (*E*)-4-(phenylbut)-3-en-2-one, **71a** with ethyl cinnamate **72**

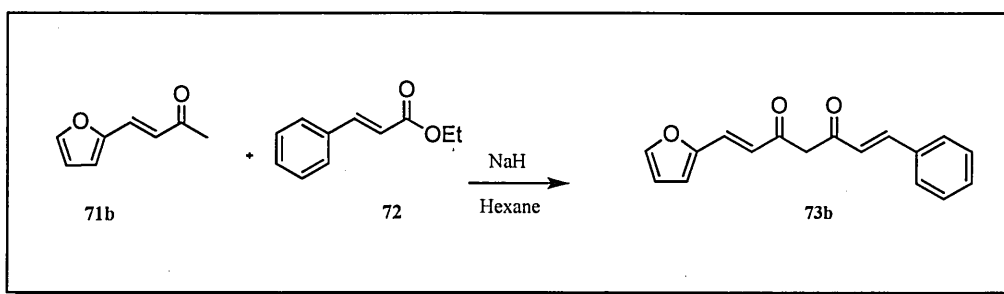


Scheme 2.18

To a stirred and refluxing suspension of sodium hydride (60% in oil, 1.20g, 30 mmol) in dry cyclohexane (35 ml) was added dropwise a solution of benzylideneacetone **71a** (4g, 27.4 mmol) and ethyl cinnamate **72** (9.65g, 54.8 mmol) in dry cyclohexane (10 ml) over 15 minutes. After the exothermic reaction was over the reaction mixture was refluxed for further 15 minutes. After cooling to room temperature the mixture was slowly acidified with aqueous acetic acid (20% v/v solution, 20 ml) and ice water (20

ml) added. The organic phase was evaporated and the aqueous layer was extracted with ether (2 x 30 ml). The combined organic extracts were washed with water (30 ml) and the organic phase after drying over dry MgSO_4 was evaporated on the rotary evaporator to yield a yellowish oil which eventually crystallize on scratching in petroleum ether to yield (56%) a cream coloured solid; TLC [petroleum ether : EtOAc, 5:1 v/v] showed streak. IR (ν) 3348 (broad, OH), 3059, 3027, 2925, 1710 ($\text{C}=\text{O}$), 1601 cm^{-1} ($>\text{C}=\text{C}<$); $^1\text{H NMR}$ δ 6.0 – 8.0 (m, complex); EIMS m/z 313 (5%), 149 (13%), 148 (68%), 147 (100%), 103 (57%).

2.1.20 Condensation reaction of (*E*)-4-(furan-2-yl)but-3-en-2-one **71b** with ethyl cinnamate **72**



Scheme 2.19

The reaction was carried out in an identical manner to that described above for benzylideneacetone **71a** to yield a yellowish-orange coloured oil which on trituration in petroleum ether yielded (58%) a yellowish coloured solid, TLC [petroleum ether : EtOAc, 4:1 v/v] showed streak. IR (ν) 3439 (weak, OH), 3117, 2993, 2950, 1716 ($\text{C}=\text{O}$), $1671, 1637\text{ cm}^{-1}$; $^1\text{H NMR}$ δ 6-8 (complex mixture); EIMS m/z 760 (5%), 720 (5%), 643 (14%), 625 (14%), 525 (23%), 507 (31%), 464 (23%), 396 (10%), 389

(45%), 346 (47%), 279 (42%), 266 (30%), 254 (58%), 211 (48%), 173 (77%), 147 (100%).

2.1.21 Synthesis of hydroxylpropyl- γ -cyclodextrin (HP- γ -CD) complexes of thiophene curcuminoids **47a-d/HP- γ -CD**.¹⁶¹

The HP- γ -CD inclusion complexes of thiophene curcuminoids were prepared via slightly modified method of Tang et al.¹⁶¹ Respective curcuminoid (34 mmol) was dissolved in a minimum amount of MeOH at 60 °C and then added dropwise into the aqueous solution of HP- γ -CD at 60 °C, with vigorous stirring. The mixture was refluxed with vigorous stirring at 70 °C for 4 h. Refluxing was stopped and the reaction mixture was heated at 70 °C to remove MeOH. After this, stirring was continued for 8 h, at room temperature and then the reaction mixture was stored at 4 °C to facilitate crystallization. However, no crystallization was observed therefore the aqueous solution was frozen to -80 °C and then freeze-dried.

Part B

Pharmacology section

2.2 Materials

2.2.1 Chemicals

The parent drug curcumin **1** and all its analogues **47a-d** and **51a-d** tested for the purpose of pharmacological studies, undertaken in this thesis, were synthesised as described in part A of this chapter. Cell culture media, RPMI-1640 (with NaHCO₃, without L-glutamine), minimum essential medium eagle (MEM) (with Earle's salts and NaHCO₃, without L-glutamine), MEM non-essential amino acid solution (100x, cell culture tested), trypan blue solution (0.4%, cell culture tested), dimethylsulfoxide (DMSO, cell culture tested) were purchased from Sigma-Aldrich (Irvine, Ayrshire, UK). Lipopolysaccharide (LPS) *Escherichia coli* O127:B8 (cell culture tested), albumin bovine serum fraction V, approx. 99%, protease-free and essentially γ -globulin free, L-methionine sulfoximine (MS), tween 20, tris-buffered saline were obtained from Sigma-Aldrich (St. Louis, MO, USA). Dulbecco's phosphate buffer saline (DPBS, 10x, without CaCl₂ and MgCl₂), foetal bovine serum (FBS), L-glutamine 200 mM (100x), 0.5% trypsin-EDTA (1x), penicillin-streptomycin were purchased from Gibco-Invitrogen (Paisley, UK). Sodium azide was obtained from Fisher-Scientific (Leicestershire, UK). CellTiter 96 AQueous one solution cell proliferation assay and Griess reagent were obtained from Promega corporation (Madison, USA). DuoSet ELISA kits for antibodies against human IL-1 β /IL-1F2 (catalogue number DY201), human TNF- α /TNFSF1A (catalogue number DY210),

human CXCL-8/IL-8 (catalogue number DY208), substrate solution (catalogue number DY999) were purchased from R&D Systems Europe Ltd. (Abingdon, UK).

2.2.2 Cell lines

Human monocytic leukemia (THP-1) cell line and human caucasian colon adenocarcinoma (CACO-2) cell lines were obtained as frozen cells from European collection of cell cultures (ECACC) (Salisbury, Wiltshire, UK).

2.3 Methods

2.3.1 Preparation of drug treatments

For all cytotoxicity (MTS) assays, nitric oxide (Griess reagent) assay and enzyme-linked immunosorbent (ELISA) assays, the stock solutions (33 mM) of all the drugs were prepared in DMSO (100%). A dilution of 10, 50 and 100 μ M was then performed in appropriate media. The final concentration of vehicle or solvent (DMSO) in test solution of the drugs was 0.3% (v/v). Stimulant, lipopolysaccharide, LPS (10 μ g/ml) was prepared from the stock solution of 1mg/ml in test media. 4 mM solution of L-methionine sulfoximine (MS) was prepared in the test media with or without LPS.

For the determination of cytotoxic effects of drugs **47a-d** complexed with hydroxypropyl- γ -cyclodextrin (HP- γ -CD), a 100 mM stock solution was prepared using DMSO (100%). The drug/ HP- γ -CD complex (1:2 molar ratio) was diluted to 10, 50 and 100 μ M (relative to the drug concentration).¹⁶²

2.3.2 Cell culture (general procedures)

All cell culture techniques i.e. thawing, passaging, plating as well as respective drug treatments applied to the cells and cytotoxicity (MTS) assays were performed under sterile conditions using a laminar flow cabinet (Heraeus). For all experiments, samples were prepared in test media, i.e. for THP-1 cells (serum-free RPMI) and for CACO-2 cells (serum-free MEM, section 2.3.9.1.).¹⁶³ Supplemented media and test media was pre-warmed to 37 °C before adding to the cells. All incubations (unless otherwise stated in the protocol) were carried out in a humidified incubator maintained at 37 °C with 5% (v/v) CO₂ and 95% air. Experiments were performed in duplicate wells of the 96-well plates and were repeated at least four times unless otherwise stated in the figure legend.

2.3.3 THP-1 cell culture

Frozen THP-1 cells were grown in suspension. Briefly, the frozen ampoule was left at room temperature for 1 minute and then immediately immersed into a water-bath maintained at 37 °C for 1-2 minutes until fully thawed. Contents of the ampoule were transferred to a 15 ml centrifuge tube. Pre-warmed RPMI media (4 ml) supplemented with L-glutamine (2 mM), penicillin (100 U/ml), streptomycin (100 µg/ml) and heat-inactivated FBS (10%) (allowed to thaw at room temperature and then incubated for 30 minutes in a water-bath heated to 56 °C) was added slowly and cells were gently re-suspended and centrifuged at 208.5 x g at 20 °C for 5 minutes. Supernatant was removed and the cell pellet was re-suspended in pre-warmed fresh RPMI media (3 ml) and cells were transferred to 75cm² flasks (NUNC, Roskilde, Denmark) already

containing pre-warmed supplemented RPMI media (15 ml). The cells were incubated until a confluency of 85-95% was achieved. Cells were routinely passaged every week.

2.3.4 Trypan-blue exclusion test

Trypan blue is a dye that is routinely used to determine the number of viable cells in cell suspension. The assay works on the principle that the cells having an intact cell membrane (viable cells) do not take up (or exclude) the dye whereas cells lacking the intact cell membrane (dead cells) take up the dye and are stained blue.¹⁶⁴

Cultured THP-1 cells were centrifuged (as above). Supernatant was removed and cells were re-suspended in pre-warmed test media (3 ml). 20 μ L of this cell suspension was aseptically removed and transferred into a sterile plastic vial and 20 μ L of trypan blue solution (0.4%) was added to it and mixed gently. After 2 minutes, 10 μ L of trypan blue-cell mixture was introduced to the haemocytometer chamber¹⁶⁴ (Neubauer, Marienfeld, Germany), and stained and unstained cells were counted. The calculated percentage of unstained (viable) cells was found to be 98-99% in all experiments.

2.3.5 Plating THP-1 cells

Once the cells reached the confluency of 85-90%, they were passaged, centrifuged and the supernatant was discarded. The cell pellet was re-suspended in test media (3 ml). Cell viability was assessed by performing trypan blue exclusion test and cell counting was performed using a hemocytometer. For all experiments, cells between

passage number 10-30 were used and were plated in flat-bottom, 96-well plate (NUNC, Roskilde, Denmark) at a density of 5×10^4 cells/200 μ L of media/well.

2.3.6 Application of drug treatments to THP-1 cells and collection of supernatants

2.3.6.1 *For the measurement of MTS assay, Griess reagent assay and ELISAs (IL-1 β and TNF- α)*

Immediately after plating, treatments were applied to THP-1 cells. Control wells of the 96-well plates were treated either with media alone or with vehicle and/or the stimulant, LPS. Subsequent treatment with curcumin **1** and drugs **47a-d** or **51a-d** at 10, 50 and 100 μ M with or without LPS was applied to the sample wells in separate experiments. For MTS assays, an additional triplicate set of control wells (without cells) containing the same volumes of the test media and CellTiter 96 AQueous one solution reagent, as used in the sample wells, was also prepared to correct the non-specific background absorbance at 490 nm. Plates were incubated for 24 h.

After 24 h incubation of cells with the respective treatments, supernatants were collected for the measurement of nitric oxide by Griess reagent or for the analysis of secreted cytokines by ELISA. The supernatants were transferred to Eppendorf tubes (1 ml) and centrifuged at 15,700 x g for 15 minutes. After centrifugation, supernatants were carefully transferred (without disturbing the pellet) to clean Eppendorf tubes (1 ml) and were stored at -80 °C until assayed.

For the measurement of MTS using the drugs **47a-d** complexed with hydroxypropyl- γ -cyclodextrin, the procedure described above was followed except, the cells were exposed to HP- γ -CD alone or drug/ HP- γ -CD complex along with the appropriate controls i.e. cells with or without DMSO. At the end of the incubation, MTS assay following the procedure described in (section 2.4.3) was performed.

2.3.7 CACO-2 cell culture

CACO-2 cells were thawed and grown as a monolayer as described in (section 2.3.3) except that the cell culture media used was MEM, supplemented with non essential amino acid solution (NEAA) (1%), L-glutamine (2 mM), heat-inactivated FBS (10%). Media was changed every third day. Cells were passaged (as described below) every tenth day when they reached the confluency of 85-95%. Cells between passage number 25-40 were used.

2.3.8 Passaging and plating CACO-2 cells

Media was removed and the cell monolayer was washed twice with DPBS (5 ml). Trypsin/EDTA solution (5 ml) was added to the cells and the flask was incubated for 5 minutes (until all the cells detached). Pre-warmed supplemented media (8 ml) was quickly added to the trypsinized cells and the cells were suspended and centrifuged for 8 minutes. Supernatant was removed and the cell pellet was re-suspended in supplemented media (3 ml) and the cell count was performed using a haemocytometer. Cells at a density of 5×10^4 cells/200 μ L of media/well were seeded in a flat-bottom, 96-well plate (NUNC, Roskilde, Denmark) and the plate was

incubated for 48 h. After 48 h incubation, cells were found to be 80-90% confluent, and were washed with PBS and the respective treatments were applied as described below.

2.3.9 Application of treatments to CACO-2 cells

2.3.9.1 Measurement of cell viability using MTS assay

CACO-2 cells were treated with the respective treatments according to the method adapted from Huang et al¹⁶³ Briefly, all the control and experimental wells were treated with un-supplemented MEM (MEM without FBS, glutamine and non-essential amino acid) (100 μ L/well), except for the control wells containing test media with L-methionine sulfoximine (MS) (4 mM) and incubated for 24 h. At the end of the first incubation control and experimental wells were treated with un-supplemented MEM \pm LPS or drugs **1**, **47a-d** at 10, 50 and 100 μ M (100 μ L/well) and incubated for additional 24 h. Control wells of MS (4 mM) were also treated with additional 4 mM MS (100 μ L/well). At the end of incubation cells were subjected to the MTS assay (section 2.4.3).

2.3.9.2 ELISA for CXCL-8

For the determination of CXCL-8 in cell supernatants using ELISA, cells were treated with un-supplemented media (100 μ L/well) with or without L-methioninesulfoximine (MS, 4 mM) and were incubated for 24 h. After 24 h incubation, cells were exposed to drugs **1**, **47a-d** at three concentrations i.e. 10, 50 and 100 μ M with or without LPS and MS (4 mM) and were incubated for further

24 h. At the end of incubation supernatants were collected following the method described in (section 2.3.6.1).

2.4 Cytotoxicity assay

2.4.1 MTS assay

In these experiments, the CellTiter 96 AQueous one solution cell proliferation assay, a colorimetric assay which is also a well established substitute for the previously used MTT assay¹⁶⁵ for the determination of the cell viability *in vitro*, was used, to examine the effects of the synthesised curcumin and curcuminoids on cell viability.

2.4.2 Principle of the assay

The CellTiter 96 AQueous one solution reagent consists of Owen's reagent i.e. tetrazolium, inner salt, MTS **74** (figure 2.1)¹⁶⁶ and an electron coupling reagent (phenazine ethosulfate; PES). The MTS tetrazolium compound **74** is bio-reduced by metabolically active cells into a coloured and soluble formazan product **75** (figure 2.1)¹⁶⁶, by the reduction of NADPH or NADH¹⁶⁷ produced by the dehydrogenase enzymes. The quantity of the formazan **75** thus produced is directly proportional to the number of viable cells in the culture and can be measured as absorbance at 490 nm.¹⁶⁶

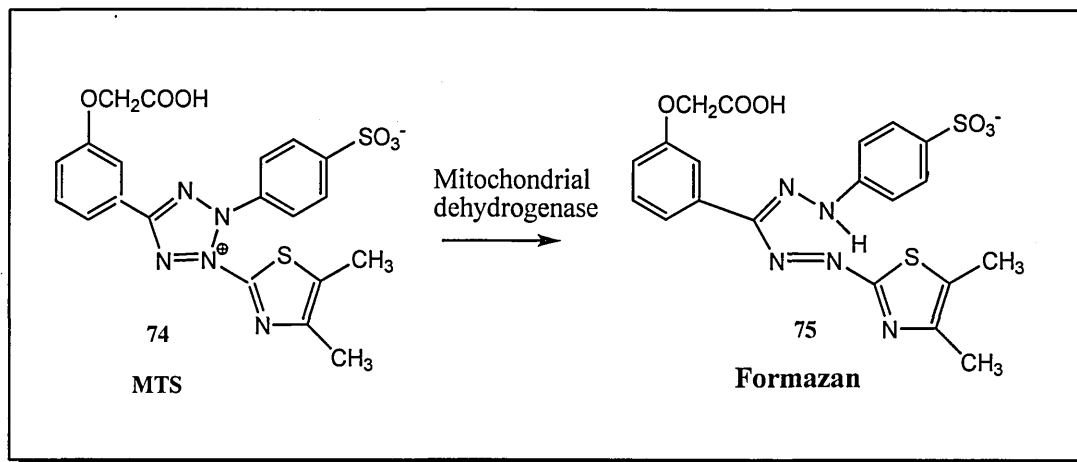


Figure 2.1: Structures of MTS tetrazolium salt **74** and its formazan product **75**.¹⁶⁶

The MTS tetrazolium salt **74** is reduced to a coloured formazan **75** product that can be read at 492 nm. The reduction takes place by the action of the mitochondrial dehydrogenase enzyme.¹⁶⁸

2.4.3 Assay protocol

After 24 h incubation with the respective treatments, the CellTiter 96 AQueous one solution reagent was added to the experimental plates following the manufacture's protocol. Briefly, the CellTiter 96 AQueous one solution reagent was thawed (in a water-bath maintained at 37 °C) and 40 µL was added quickly into each well of the 96-well plates containing the controls as well as samples in 200 µL of the test media. Plates were incubated for 4 h. At the end of the incubation a change in the colour of the media was observed from light yellow to dark brown, indicative of the presence of viable cells. Absorbance was recorded at 490 nm using a 96-well plate reader.

2.5 Nitric oxide production assay

2.5.1 The Griess reagent assay

Since the inorganic free radical gaseous molecule nitric oxide (NO) has been reported to be involved in various physiological as well pathological conditions, the detection of its level using reliable, reproducible and sensitive analytical techniques is essential.¹⁶⁹ The measurement of nitrite in biological samples by Griess reagent is a simple spectrophotometric method that indirectly quantifies NO levels by estimating its stable end product (nitrite anion) which is formed as a result of nitric oxide oxidation.¹⁷⁰

2.5.2 Principle of the assay

The use of colorimetric detection with Griess reagent entails the formation of a chromophore **78** (diazonium product) from the diazotization of sulphanilamide **76** (SAA) by acidic nitrite followed by coupling with bicyclic amines such as *N*-1-(naphthyl)ethylenediamine **77** (NED) as shown in figure 2.2:

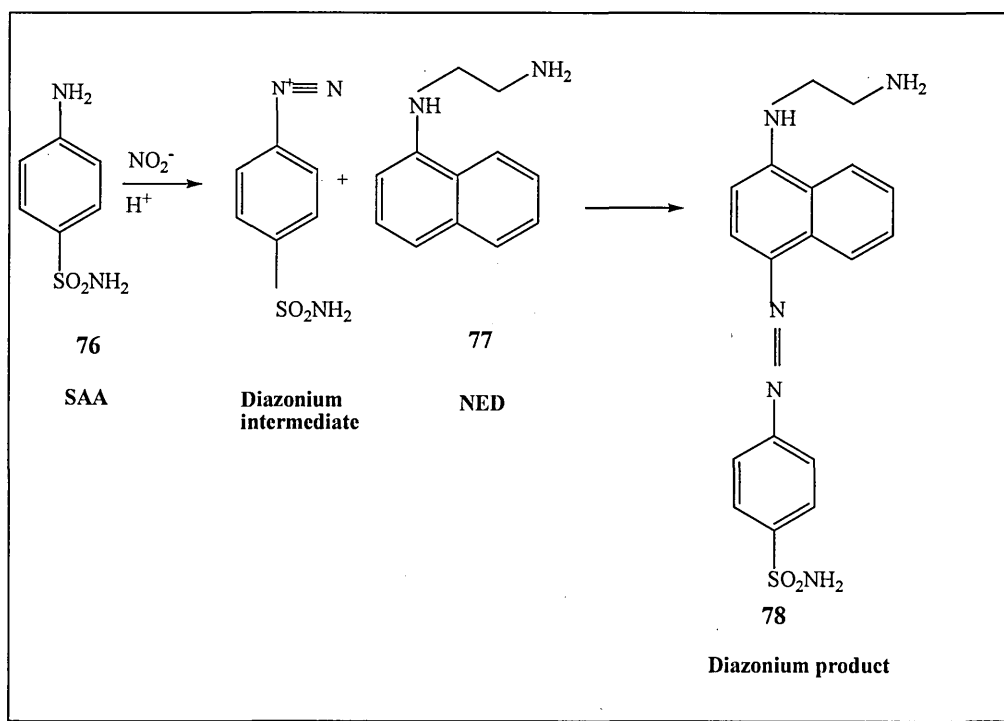


Figure 2.2 : Chemical reaction involved in the measurement of nitrite (NO_2^-) using the Griess reagent system.¹⁶⁹

In acidic media, nitrite reacts with the diazotizing reagent sulphanilamide **76** (SAA, an arylamine) to form the diazonium intermediate, which reacts with a coupling reagent *N*-1-(naphthyl)ethylenediamine **77** (NED) to form the corresponding azo dye **78**.¹⁷¹

2.5.3 Assay protocol

2.5.3.1 Preparation of nitrite standard curve

For each experiment, a separate nitrite standard reference curve was prepared using the same matrix as used for the experimental samples. Briefly, a 100 μ M of nitrite solution (1 ml) was prepared by diluting the provided 0.1 M sodium nitrite standard in the matrix. Immediately 6 serial two fold dilutions (100, 50, 25, 12.5, 6.25, 3.13, 1.56 and 0 μ M) were performed and 50 μ L/well was added in triplicate wells of 96-well plate to generate the nitrite standard curve.

2.5.3.2 Griess reaction

The assay was run according to the manufacturer's (Promega) protocol.

Frozen samples were thawed and allowed to equilibrate at room temperature along with sulphanilamide **76** (SAA) and *N*-1-(naphthyl)ethylenediamine **77** (NED) solutions for 15-30 minutes, prior to use. Experimental samples (50 μ L/well) were added to duplicate wells of a 96-well plate. Using a multi-channel pipettor, SAA **76** solution (50 μ L) was dispensed to all experimental samples and to the wells containing the dilution series for the nitrite standard reference curve. The plate was incubated for 5-10 minutes at room temperature protected from light. Using a multi-channel pipettor, NED **77** solution (50 μ L) was subsequently added to all wells. Incubation was performed for further 5-10 minutes at room temperature protected from light. A magenta colour started to appear immediately. Absorbance was measured at 570 nm using a plate reader (Wallac Victor 2 multi-label plate reader).

2.6 Enzyme-linked immunosorbant assay (ELISA)

Immunoassays using antibodies or their derivatives are commonly used as a powerful tool both in the fields of diagnosis and research.¹⁷² The capacity of an antibody to recognize its corresponding antigen¹⁷³ (in biological samples), makes these immunoassays highly selective as well as sensitive.¹⁷³ Among different immunoassays, ELISAs in general, have become a standard method for analyzing large numbers of serum samples for cytokines and other proteins, and sandwich ELISAs in particular, are a widely used method for the quantitative detection of specific proteins.¹⁷⁴ Various advantages including, selective antibody-antigen reactions, the use of excess capture antibody and enzyme-antibody conjugate and the chemical amplification with enzyme-conjugates that allows the detection of very low concentrations of analytes, all contribute towards the superiority of sandwich ELISA carried out in polystyrene microtitre plates in terms of sensitivity, specificity and kinetics, over other types of heterogeneous solid-phase immunoassays.¹⁷⁵

2.6.1 Sandwich ELISA, principle of the assay

The traditional sandwich-type or two-site antigen capture ELISA utilises the formation of complexes or sandwiches consisting of an antigen and two monoclonal antibodies (mAbs) i.e. capture and detector antibodies directed against different epitopes of an antigenic molecule, hence recognizing two separate epitopes of the same antigen. The capture antibody is coupled to a solid phase (polystyrene microtitre plates) while the detection antibody is coupled to an enzyme.¹⁷⁶ Substrate is added which reacts with the enzyme producing a colour change, the intensity of which is

directly proportional to the concentration of antigen in incubation mixture¹⁷⁶ allowing its spectrophotometric detection and quantification (figure 2.3). Standard proteins of known concentrations are incorporated into the assay to allow quantification of specific proteins to be determined.

2.6.2 Assay protocol

All capture, detection antibodies and cytokine standards provided for IL-1 β , TNF- α and CXCL-8 were reconstituted according to the manufacturer's (R&D Systems) protocol and stored at -80°C until used.

2.6.2.1 ELISA plate preparation for the detection of IL-1 β or TNF- α in cell supernatants of THP-1 cells

ELISA flat-bottom 96-well plates (catalogue number DY990) and ELISA plate sealers (catalogue number DY992) were purchased from R&D Systems, (Abingdon, UK). Separate plates were prepared according to the manufacturer's protocol for the detection of IL-1 β and TNF- α . Briefly, capture antibodies, mouse anti-human IL-1 β or mouse anti-human TNF- α were diluted to a working concentration of 4.0 μ g/ml in PBS (without carrier proteins). An ELISA flat-bottom 96-well plate was immediately coated with 100 μ L/well of the diluted capture antibody, sealed and incubated overnight at room temperature. Next day, each well of the 96-well micro plate was aspirated and washed six times with wash buffer (WB) (0.05% Tween 20 in PBS). After the last wash, the plate was dried by blotting against clean paper towel, blocked by adding 300 μ L/well of reagent diluent (RD) (1% bovine serum albumin in PBS) and incubated at room temperature for 1h. The plate was aspirated, washed and dried as described above.

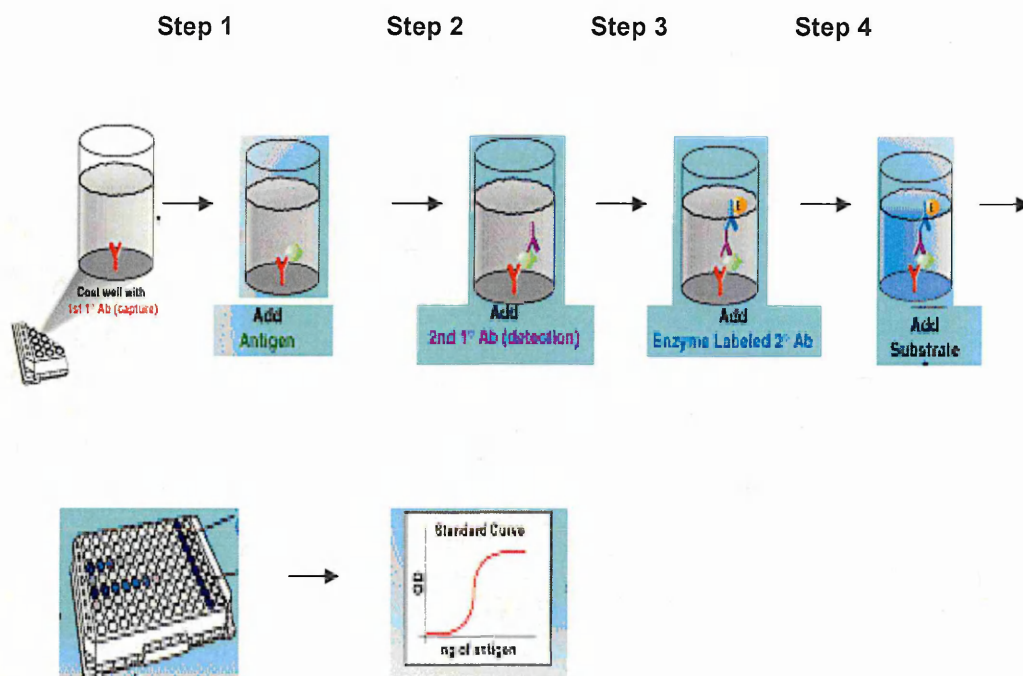


Figure 2.3 : Diagram showing different stages involved in sandwich ELISA.¹⁷⁷

A 96-well microtitre plate is coated with capture antibody (1st antibody) and the target protein or antigen is added. Detection antibody (2nd antibody) is added followed by the addition of enzyme, horseradish peroxidase (HRP)-linked antibody. Substrate solution containing colorimetric substrate, 3,3',5,5'-tetramethylbenzidine (TMB) and hydrogen peroxide (H₂O₂) is added. TMB reacts with H₂O₂ in the presence of HRP enzyme to produce a water-soluble, blue coloured by-product the intensity of which is proportional to the amount of HRP activity, which in turn is related to the levels of target analyte in the experimental sample. Upon acidification with sulphuric-acid (stop solution) the colour changes from blue to yellow, enabling accurate measurement of the intensity at 450nm using a plate-reader.¹⁷⁸

2.6.2.2 Preparation of standard curve

For all experiments a separate standard curve was obtained. Briefly, the reconstituted standards 100 ng/ml of recombinant human IL-1 β or 290 ng/ml of recombinant human TNF- α were thawed. For IL-1 β a seven point standard curve using a highest standard of 250 pg/ml with 2-fold serial dilutions (250, 125, 62.5, 31.2, 15.6, 7.8 and 0 pg/ml) in RD, and for TNF- α a seven point standard curve using a highest standard of 1000 pg/ml with 2-fold serial dilutions (1000, 500, 250, 125, 62.5, 31.25, 0 pg/ml) in RD was prepared. All triplicate readings at 570 nm for each standard were subtracted from the triplicate readings at 450 nm. The corrected absorbance values were averaged and the average zero standard optical density was subtracted.

2.6.2.3 Assay procedure

100 μ L of cell supernatant samples or standards in RD was added per well and the plate was sealed and incubated at room temperature for 2 h. After 2 h incubation, the plate was washed (as above). Detection antibody (biotinylated goat anti-human IL-1 β or biotinylated goat anti-human TNF- α) was diluted to the working concentrations of 300 ng/ml and 250 ng/ml respectively, in RD and 100 μ L/well was added to the plate. The plate was sealed and incubated for 2 h at room temperature. The aspiration/wash step was repeated, followed by the addition of 100 μ L/well of streptavidin-horse radish peroxidase (HRP), diluted to the working concentration of 1:200 in RD and the plate was incubated for 20 minutes at room temperature, protected from light. The plate was washed. Substrate solution (1:1 mixture of colour reagent A (H₂O₂) and colour reagent B (tetramethylbenzidine, TMB) was added 100 μ L/well, and the plate

was incubated for 20 minutes at room temperature, protected from light. 50 μ L/well of the stop solution (2 N H_2SO_4) was added with gentle tapping. The optical density of the plate was read at 450 and 570 nm using a micro plate reader (Wallac Victor 2 multi-label plate reader).

2.6.2.4 ELISA plate preparation for the detection of CXCL-8 in CACO-2 cell supernatants

Capture antibody, mouse anti-human IL-8 was diluted to a working concentration of 4.0 μ g/ml in PBS (without carrier proteins). A 96-well micro plate was immediately coated with 100 μ L/well of the diluted capture antibody, sealed and incubated overnight at room temperature. Next day, each well of the 96-well micro plate was aspirated and washed six times with wash buffer (WB) (0.05% Tween[®] 20 in PBS). After the last wash the plate was dried by blotting against clean paper towel, blocked by adding 300 μ L/well of block buffer (BB) (1% bovine serum albumin in PBS with 0.05% NaN_3) and incubated at room temperature for 1h. Plate was aspirated, washed and dried (as described previously).

2.6.2.5 Preparation of standard curve

For all experiments a separate standard curve was obtained. Briefly, the reconstituted standard 140 ng/ml of recombinant human IL-8 was thawed. A seven point standard curve using a highest standard of 2000 pg/ml with 2-fold serial dilutions (2000, 1000, 500, 250, 125, 62.5, 0 pg/ml) in RD was prepared. All triplicate readings at 570 nm for each standard were subtracted from the triplicate readings at 450 nm. The

corrected absorbance values were averaged and the average zero standard optical density was subtracted.

2.6.2.6 Assay procedure

The assay procedure followed was the same as described in section 2.6.2.3. except that the RD was consisted of 0.1% BSA, 0.05% Tween[®] 20 in tris-buffered saline (20 mM Trizma base, 150 mM NaCl, p^H 7.2) and the detection antibody (biotinylated goat anti-human IL-8) was diluted to the working concentrations of 20 ng/ml in RD.

2.7 Data manipulation and statistical analysis

For all individual MTS experiments, the mean 490 nm absorbance from the "no cell" control wells was subtracted from all other absorbance values to yield corrected absorbance values. All corrected absorbance values from separate experiments were averaged and data was plotted as mean \pm S.E.M. (standard error of the mean). In Griess reagent assays the mean absorbance values of each experimental sample were used to determine the concentrations (μ M) using the standard curves. All concentrations (μ M) from three separate experiments were averaged and plotted as mean \pm S.E.M. For all ELISA assays, the 570 nm absorbance values for the control and sample wells were subtracted from the corresponding 490 nm absorbance values to get the corrected absorbance. The corrected duplicate readings for each control and sample wells were averaged and the average zero standard optical density was subtracted from it. Concentrations (pg/100 ml) were obtained using the standard reference curves.

Shapiro-Wilk W test for non-normality followed by Kruskal-Wallis : Conover-Inman post-hoc test was used to determine significance. P value < 0.05 was considered as significant.

CHAPTER 3

RESULTS AND DISCUSSION

Part A

Chemistry Section

3.1 Results and discussion

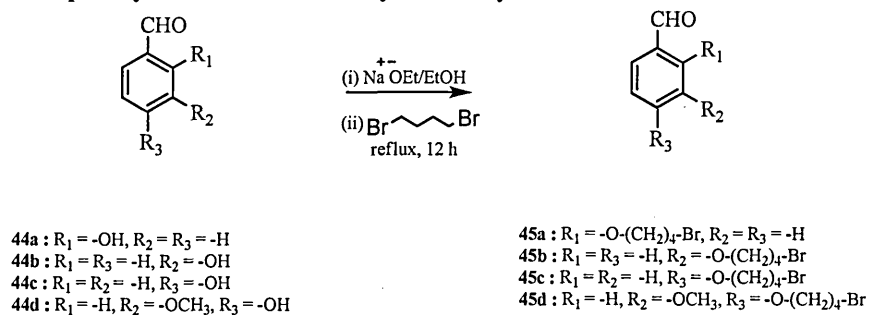
3.1.1 Synthesis of nitric oxide donating curcuminoids **51a-d** and curcumin **1**

Aim : Based on the considerable number of studies, it is generally accepted that nitric oxide donating-derivatives of non-steroidal anti-inflammatory drugs (NO-NSAIDs) have enhanced anti-inflammatory activity and possess lesser side-effects over that of the parent NSAIDs.^{179,180} However a major limitation of the current array of NO-NSAIDs is that the NO is rapidly released and relatively small quantities are produced in the systemic circulation. Thus it is possible to postulate that the nitric oxide donating curcuminoids **51a-d** could represent an advance in the application of NO derivatization by enabling prolonged production of NO to be achieved *in vivo*.

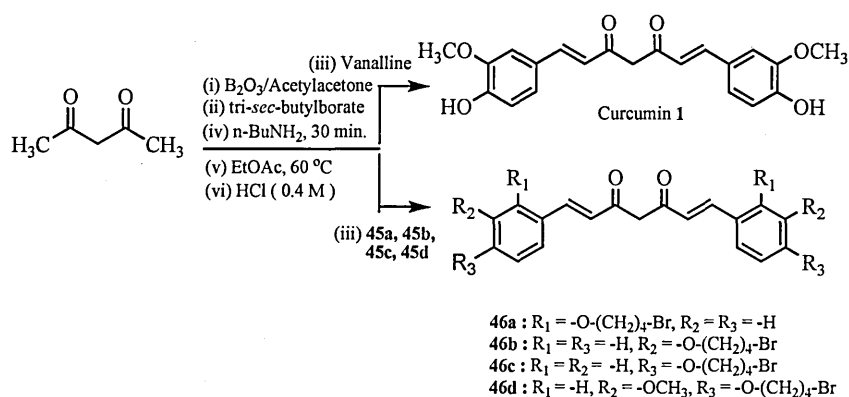
It is important to note that the nitric oxide donating curcuminoids **51a-d** synthesised in this thesis are phenolic ethers of NO as compared with the carboxylate esters of conventional NO-NSAIDs.

The overall strategy for the synthesis of nitric oxide donating curcuminoids **51a-d** is shown in figure 3.1. This synthesis consisted of three steps of which the first step involved the formation of bromobutoxybenzaldehydes **45a-d** (scheme 2.1, chapter 2). The starting materials for the synthesis of these compounds were 2-hydroxybenzaldehyde **44a**, 3-hydroxybenzaldehyde **44b**, 4-hydroxybenzaldehyde **44c** and vanillin **44d** respectively, which were chosen because these were commercially available and cheap.

Step 1 : Synthesis of bromobutoxybenzaldehydes 45a - d



Step 2 : Synthesis of curcumin 1 and bromobutoxy curcuminoids 46a - d



Step 3 : Synthesis of butoxynitrate curcuminoids 51a - d

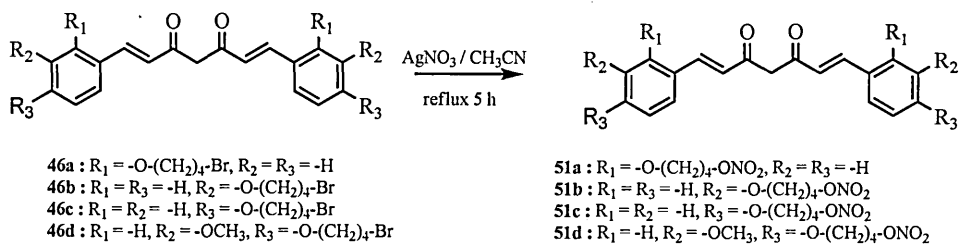


Figure 3.1: Synthesis of nitricoxide donating curcuminoids **51a-d** and curcumin **1**.

The bromobutoxybenzaldehydes **45a-d** were prepared by the Williamson ether synthesis, reaction of which involved the sodium salts of hydroxybenzaldehyde, **44a-d**, with 3 molar equivalents of 1,4-dibromobutane in ethanol. The structures of bromobutoxybenzaldehydes **45a-d** were determined on the basis of their spectrometric analysis using ^1H NMR, MS and IR spectroscopies.

The characteristic features in the ^1H NMR spectra of the compound **45a-d** were the resonances of the two methylene group in the alkyl chain adjacent to oxygen and bromine. The methylene adjacent to oxygen resonated at δ 4.4 as triplet and the methylene attached to the bromine appeared as a triplet at δ 3.5. The characteristic peak for the aldehyde proton was also observed as a singlet at about δ 10.5. The EIMS spectrum gave the correct molecular ion peaks at m/z 256 and 258 corresponding to the presence of two isotopes of bromine i.e. ^{79}Br and ^{81}Br .

The infrared spectra of compounds **45a-d** showed a characteristic aldehyde hydrogen stretch ($-\text{CHO}$) at about 2759cm^{-1} . Although the aldehyde group in the aromatic ring reduces the nucleophilicities of corresponding phenolic groups in their salt form, the yields of the products **45b** and **45c** were quite high (79% and 81% respectively). The 2-hydroxybenzaldehyde **44a** gave product **45a** in only 58% yield whilst vanillin **44d** reacted poorly to give **45d** in 50% yield.

The resonance stabilized canonical forms of the phenoxides of **44a-c** are shown in figure 3.2. The negative charge on the oxygen in the phenoxides of **44a** and **44c** is quite adequately delocalised on the aromatic ring and the aldehyde group and possibly accounts for the relatively low yield of the alkylated product **45a**. The alkylation of **44c** to give **45c** in high yield (81%) is surprising because one expects the similar mesomeric effects operating in the phenoxide anion derived from **44c**.

In the *meta*-hydroxybenzaldehyde **44b**, the mesomeric effects are only confined to the aromatic ring and relatively high yield of 79% obtained for the alkylated product **45b** is less surprising.

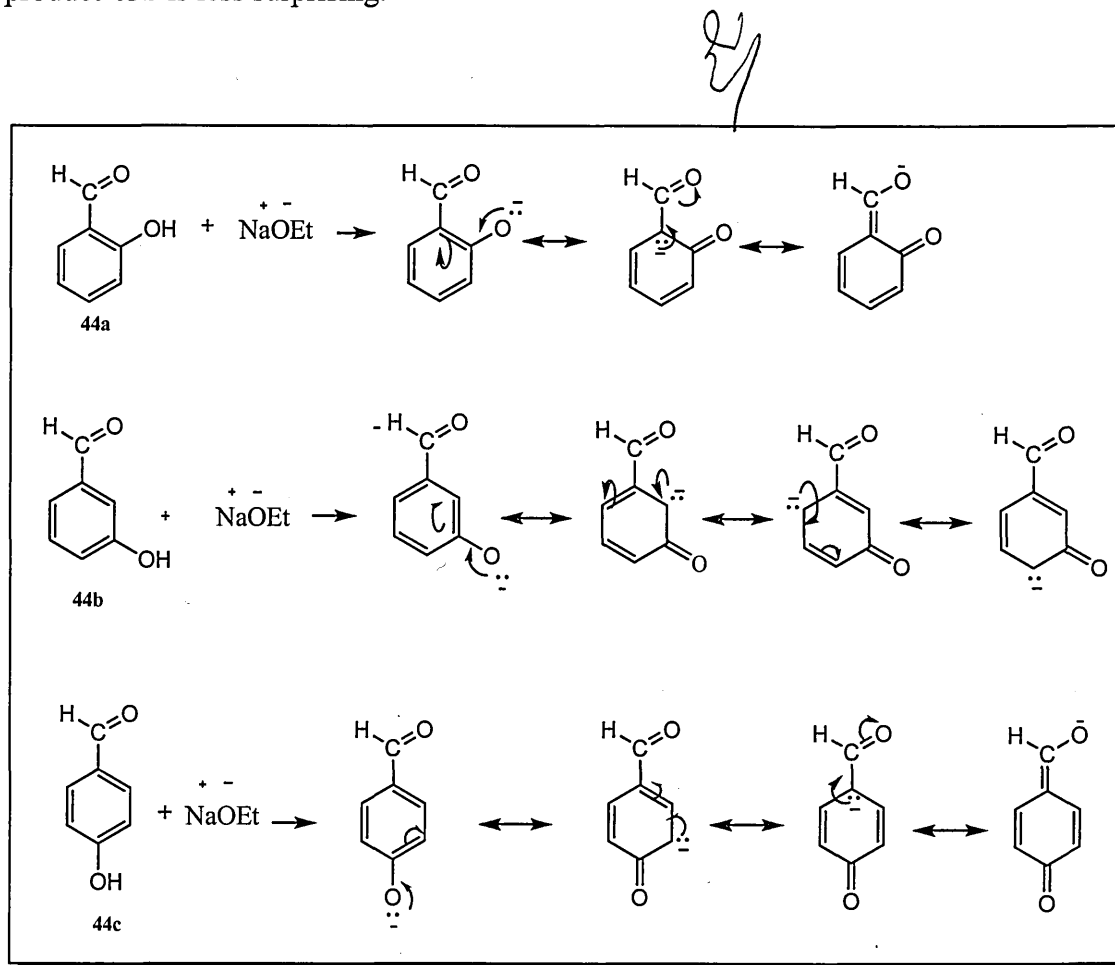


Figure 3.2 : Resonance stabilised canonical forms of phenoxides of 2-hydroxybenzaldehyde **44a**, 3-hydroxybenzaldehyde **44b** and 4-hydroxybenzaldehyde **44c**.

The synthesis of curcuminoids shown in schemes 2.2 and 2.3 (chapter 2) was carried out via two reported pathways, that differ only in technique, however the reaction mechanism is the same¹¹³ in both methods. In method A, (section 2.1.4, chapter 2) the acetylacetone-boron oxide complex **31** was prepared separately in order to avoid the moisture that is produced during the course of the acetylacetone-boron oxide complex **31** formation. However, in various curcuminoid syntheses reported in the literature the acetylacetone-boron oxide complex **31** is prepared *in situ*¹⁵³ (method B, section 2.1.4, chapter 2) and we have also used this strategy to get better yields. The trialkylborate is also believed to facilitate the formation of curcuminoids. Although, Pabon's¹⁴⁴ method of curcumin synthesis has the benefits of simple and easy handling, moderate temperature conditions, its major draw back is the low yields of the products obtained. During the course of this study both methods for the preparations of some curcuminoids were tried including, **46a-c** and **47a** and **47d**, and our results have shown that in all of the cases method A resulted in better yields in comparison with method B with the exception of **47a** which resulted in a better yield using method B.

Describing the structure of curcumin **1** in solution form, using the NMR techniques including DEPT, HMQC, HMBC and COSY, Payton et al¹⁸¹ have shown that curcumin **1** in solvents like CDCl₃, DMSO or mixtures of DMSO-*d*₆ in water and in buffers (p^H 3 to 9), exists in keto-enol tautomers as shown in figure 3.3b and all of our ¹H NMR results also confirm this with the enolic H found at about δ 5.8.

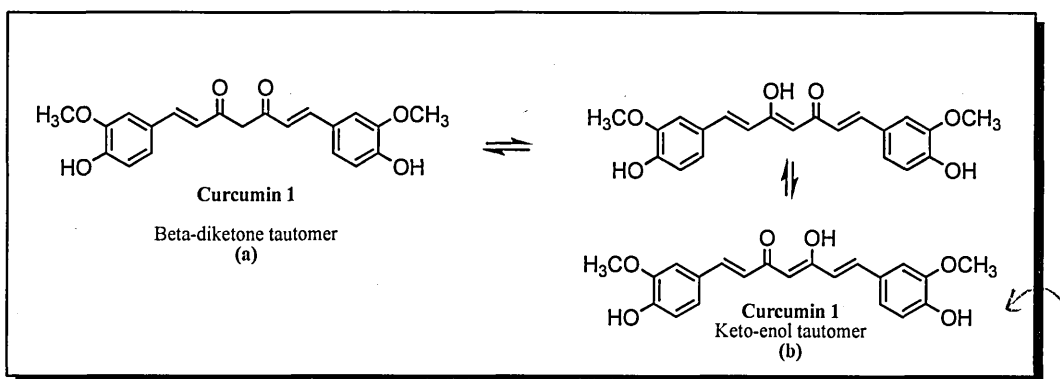


Figure 3.3 : Equilibrating keto-enol tautomers of curcumin 1.¹⁸¹

Compound **46a**, with method A (section 2.1.4) was obtained in 34% yield where as with method B (section 2.1.4) the yield was 21%. The ^1H NMR spectrum of **46a** showed three distinguishing features characteristic of curcumin structure; the peak at δ 5.8 that appears as a singlet for the enolic methine proton, the peak at δ 6.7 for the α -olefinic proton adjacent to the carbonyl group and the third peak due to the deshielded β -olefinic proton at about δ 7.9. The α,β -unsaturated protons in all the curcuminoids appear as two doublets with a J value of 16.0 Hz, which suggests that the double bonds are of *E* or trans configuration. The peak patterns shown by the aromatic protons H-3 (as doublet) and H-6 (as double doublet) confirmed the ortho substituted aromatic ring in compound **46a**. The presence of bromobutoxy side chain was evident from the multiplet found in the region δ 1.9-2.2 that corresponded to two central- CH_2 - groups of the butyl chain whilst the two triplets at δ 3.5 and δ 4.1 corresponded to the $-\text{CH}_2\text{Br}$ and $-\text{OCH}_2$ respectively. The EIMS spectrum also confirmed the presence of the molecular ion peaks at m/z 576 and 580 suggesting the presence of ^{79}Br and ^{81}Br .


Compounds **46b-d** showed similar spectroscopic characteristics and were characterised likewise from their ^1H NMR and mass spectra.

The third step in the synthesis of target compounds, butoxynitrate curcuminoids **51a-d** (figure 3.1) involved nitration of bromobutoxy curcuminoids **46a-d**. This was conveniently achieved by $\text{S}_{\text{N}}2$ reaction of the corresponding bromobutoxy curcuminoid **46a-d** with silver nitrate in acetonitrile on heating and resulted in moderate to good yields of the desired nitric oxide donating curcuminoids **51a-d**. The infrared spectra of all the butoxynitrates **51a-d** showed characteristic absorption for the $-\text{NO}_2$ group at 1472 and 1280 cm^{-1} . The salient features of the proton magnetic resonance spectra of **51a-d** were the disappearance of the triplet at about δ 3.5 associated with the $-\text{CH}_2\text{Br}$ group and appearance of a new triplet integrating to two protons at δ 4.1 due to $-\text{CH}_2\text{ONO}_2$ group being relatively more deshielded than the ethereal methylene counterpart at the other end of the butyl chain. The remaining features of the ^1H NMR spectra were similar to the NMR spectra of the precursors **46a-d**. The ESMS produced molecular ions for which m/z 543 was accurately measured thus confirming the identity of the target molecules thus synthesised.

The synthesis of the lead compound, curcumin **1**, figure 3.1, was carried out using method B (section 2.1.4, chapter 2). Curcumin **1** was obtained as an orange solid in 33% yield and its structure was confirmed spectroscopically. Thus the ^1H NMR spectrum of **1** showed the characteristic resonance of the enolic methine moiety at δ 5.8, the α -olefinic proton attached to the carbon bearing the carbonyl group at δ 6.4 and the β -olefinic proton attached to the carbon bearing the aromatic ring at δ 7.5. The singlet peak for the protons of the two methoxy groups appeared at δ 3.9.

In the EIMS spectrum the peak at m/z 368 corresponded to the molecular ion peak. The IR spectrum as a thin film showed an absorption at $3501\text{-}3387\text{cm}^{-1}$ for the enolic-OH group and a strong absorption for the carbonyl group at 1627cm^{-1} . The peaks at 1602 cm^{-1} corresponded to $>\text{C}=\text{C}<$.

3.1.2 Synthesis of aromatic heterocyclic curcuminoids 47a-d and 48a-c


Aim : After the successful synthesis of nitric oxide donating curcuminoids **51a-d**, it was then decided to synthesise the heterocyclic curcuminoids in the hope of obtaining enhanced anti-inflammatory activities normally associated with the curcumin class of compounds and decided to investigate the synthesis of furan and thiophene derived curcuminoids figure 3.4.

For these classes of compounds many starting aldehydes were commercially available. The curcuminoids were prepared from the parent heterocyclic aldehydes such as thiophene-2-carbaldehyde or furan-2-carbaldehyde as illustrated in figure 3.4. The reactions, after the usual work-up, produced the expected curcuminoids **47a** and **48a** which were purified by flash chromatography and spectroscopically characterised.

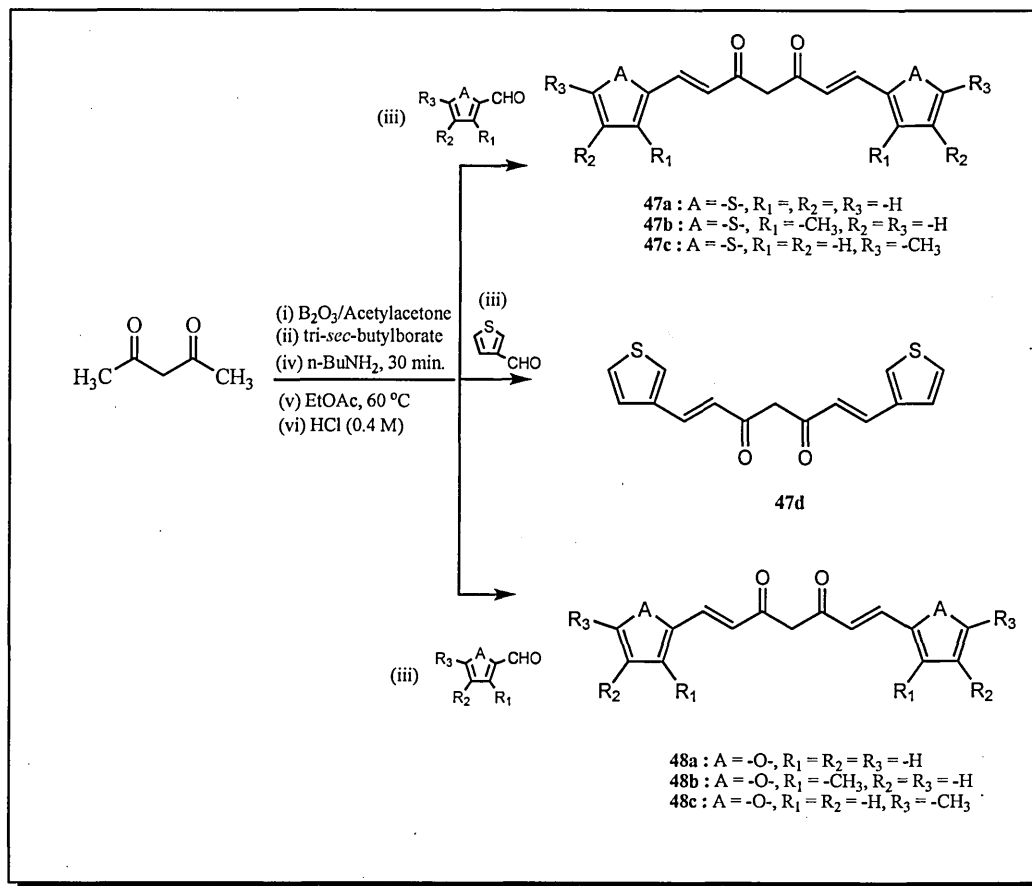


Figure 3.4 : Synthesis of thiophene curcuminoids **47a-d** and furan curcuminoids **48a-c**.

The thiophene curcuminoid **47a** was obtained as orange precipitates using method B (section 2.1.4, chapter 2) in 62% yield, where as with method A (section 2.1.4, chapter 2) the yield was only 23%. The ^1H NMR spectrum of **47a** also showed the typical signals of curcumin structure, at δ 5.7 as a singlet for the enolic methine proton, the peak at δ 6.4 for the α -olefinic proton attached to the carbon bearing the carbonyl moiety, where as the third peak was located in the further down field region of δ 7.7 for the β -olefinic proton. Both of these protons appear as a doublet with a J value of 15.5 Hz, which suggests that the double bonds are found in *E* configuration. The EIMS spectrum showed the presence of molecular ion peak at m/z 288. In the IR spectrum, the OH stretch was found at $3537\text{-}3412\text{ cm}^{-1}$, the aromatic C-H stretch appeared at 3103 cm^{-1} and the hydrogen bonded carbonyl

showed a peak at 1626 cm^{-1} . The peaks at 1569 cm^{-1} for conjugated $>\text{C}=\text{C}<$ and 1504 cm^{-1} for the enol were also present.

The furan curcuminoid **48a** was obtained as a dark brown solid with method A (section 2.1.4, chapter 2) in 26% yield and showed similar spectroscopic characteristics.

Having achieved success with the thiophene and furan curcuminoids **47a** and **48a** it was then decided to use this strategy for making some analogues of these compounds and which are displayed in figure 3.4. All of the curcuminoids **47a-d** and **48a-c** were successfully made, albeit in low to moderate yields, and after purification by flash chromatography the products were characterized spectroscopically. Molecular ions were produced for all the analogues and the accurate masses were determined.

The main structural features found in the ^1H NMR spectra of **47b-d** include the peak at δ 5.7 as a singlet for the enolic methine proton, the peak at δ 6.3 for the α -olefinic proton adjacent to the carbonyl group, where as the third peak located in the further down field region of δ 7.8 was due to the presence of deshielded β -olefinic proton. Both of these protons appeared as a doublet with a J value of 15.5 Hz, which suggests that the double bonds are found in *E* configuration. The EIMS spectrum showed the presence of molecular ion peak at m/z 316. In the IR spectrum, as the OH stretch was found in the region of 3421 cm^{-1} , the aromatic

C-H stretch appeared at 3068 cm^{-1} and the hydrogen bonded carbonyl showed a peak at 1606 cm^{-1} . The peak at 1499 cm^{-1} for the conjugated $>\text{C}=\text{C}<$ was also present.

The compounds **48b-c** were prepared by method A (section 2.1.4, chapter 2). The characteristic features of the ^1H NMR spectra were the presence of peak at δ 5.6 as a singlet for the enolic methine proton, the peak at δ 6.9 for the α -olefinic proton attached to the carbon bearing the carbonyl group, where as the third peak at δ 7.5 indicated the presence of deshielded β -olefinic proton. Both of these protons appeared as a doublet with a J value of 15.5 which confirms that the double bonds are found in *E* configuration. The singlet peak at δ 2.3 for two methyl protons was also present. The EIMS spectrum showed the presence of molecular ion peak at 284. In the IR spectrum, the OH stretch appeared at 3322 cm^{-1} , the aromatic C-H stretch hydrogen bonded carbonyl showed a peak at 1620 cm^{-1} .

3.1.3 Synthesis of fused-ring aromatic heterocyclic curcuminoids **57b-d** and **61**

Aim : In medicinal chemistry it is a well recognized strategy to extend rings by ring fusion and in this context we decided to synthesise the benzo[*b*]furan and benzo[*b*]thiophene curcuminoids. The benzo[*b*]furan and benzo[*b*]thiophene ring systems occur in natural products¹⁸² and would therefore make good candidates for anti-inflammatory studies. Benzothiophene derivatives have previously been recognised as potential anticancer agents.¹⁸³

The strategy adopted for the synthesis of benzo[*b*]furan **57b** and **57c** and benzo[*b*]thiophene **57d** curcuminoids is displayed in figure 3.5.

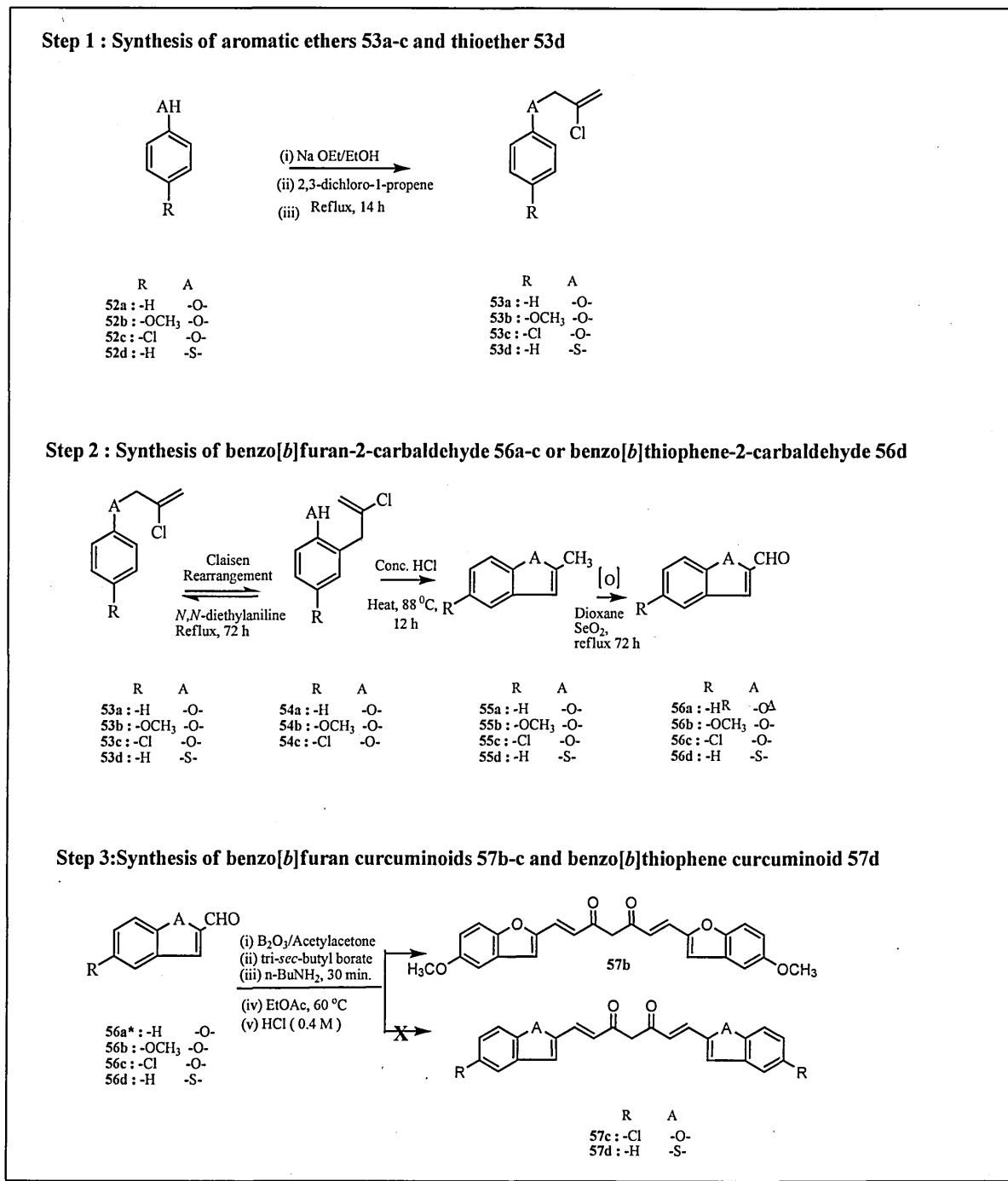


Figure 3.5 : Synthesis of benzo[*b*]furan curcuminoids **57b-c** or benzo[*b*]thiophene curcuminoid **57d** (1st strategy).

* Synthesis of curcuminoid from **56a** not performed.

The required aldehydes **56a-d** were synthesised in four chemical steps from the corresponding 4-substituted phenols/thiophenols **52a-d**. Alkylation of the phenols/thiophenols with 2,3-dichloropropene produced the corresponding ethers/thioethers **53a-d** which were then rearranged by the Claisen rearrangement reaction. The Claisen rearrangement¹⁸⁴ is a highly stereoselective [3,3]-sigmatropic reaction of allyl vinyl ethers **79** or allyl aryl ethers **80** to yield γ,δ -unsaturated carbonyl compounds **81** or *O*-allyl substituted phenols **82**, respectively as shown in figure 3.6.

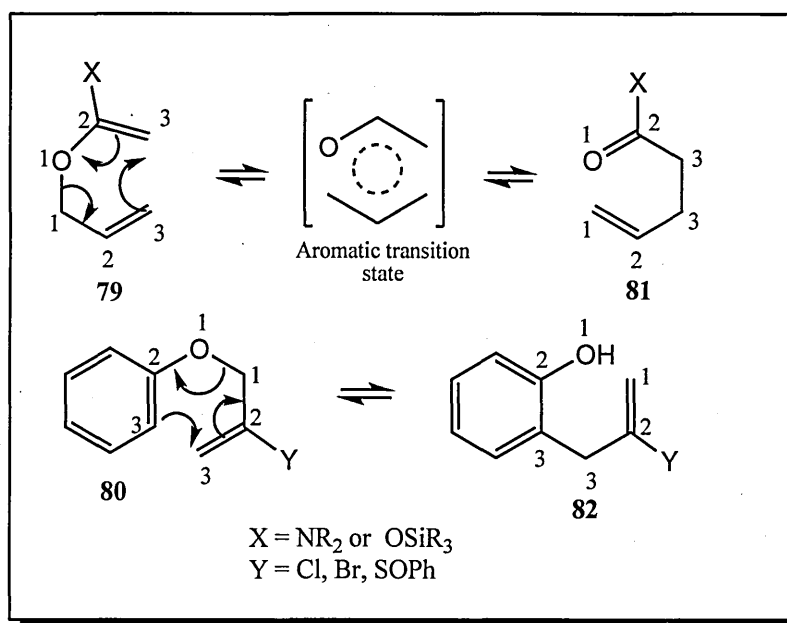


Figure 3.6 : Mechanism of Claisen rearrangement.

The reaction has enjoyed widespread use in organic synthesis for constructing new carbon-carbon bonds. When X = NR₂, the reaction is referred to as the Eschenmoser-Claisen rearrangement.¹⁸⁵ When X = OR, the reaction is referred to

as the Johnson-Claisen rearrangement.¹⁸⁶ When X = OSiR₃ or OLi, the reaction is referred to as the Ireland-Claisen rearrangement.¹⁸⁷ A reaction in which Y = Cl has been reported to yield 2-methylbenzo[*b*]furans and 2-methylbenzo[*b*]thiophenes.¹⁵⁵

The phenolic ethers **53a-c** underwent [3,3] sigmatropic rearrangement in refluxing N,N-dimethylaniline after 24-48 h to give the Claisen products **54a-c** in 34-66% purified yields (lit. 77-90 % yields).¹⁵⁵

On the other hand the thiophenol ether **53d** on refluxing in N,N-dimethylaniline for 24 h yielded the benzo[*b*]thiophene **55d** directly in 43% yield. Due to the increased nucleophilicity of the benzenethiol the presumed Claisen rearrangement product underwent cyclisation to yield the benzo[*b*]thiophene **55d** without being isolated. The IR spectra of **54a-c** showed a broad absorption at about 3433 to 3540 cm⁻¹ whilst their ¹H NMR spectra showed an upfield shift for the allylic protons from about δ 4.6 in the phenolic ethers **53a-c** to about δ 3.6 in the alkenyl products **54a-c**. Cyclisation of the phenolic compounds was achieved under acid catalysed conditions to give the corresponding benzo[*b*]furans **55a-c** in 42-63% yield after purification by flash chromatography. Benzylic methylene groups and methyl groups on aromatic rings are reactive centres that can be oxidized under mild conditions using selenium dioxide to ketones and aldehydes respectively.¹⁵⁶ Thus the 2-methylbenzo[*b*]furans **55a-c** underwent oxidation at the methyl group with a mixture of selenium dioxide and water in refluxing dioxane to produce the aldehydes **56a-c** in 25-89% yields after purification by flash chromatography. The aldehydes were characterized from their *R_f* which were lower (0.2) compared with

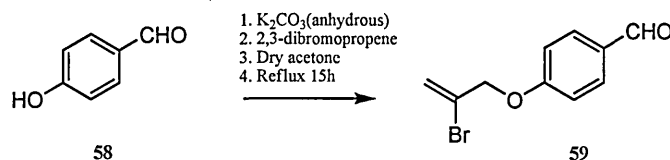
the corresponding methyl precursors **55a-c** (R_f 0.7) in the same solvent system [petroleum.ether : EtOAc, 5:1 v/v] and IR spectra which showed a characteristic -CHO stretch at about 2835 cm^{-1} and carbonyl absorption at about 1680 cm^{-1} . The ^1H NMR spectra for the aldehydes displayed a low field signal for the aldehyde proton at about δ 9.7 and a deshielding effect for the H-3 proton from about δ 6.3 in the 2-methyl benzo[*b*]furans **55a-c** to δ 7.2. The mass spectra of the aldehydes **56a-c** produced molecular ions of correct value and high intensity. The 2-methylbenzo[*b*]thiophene **55d** was oxidized in a similar way to yield the aldehyde product **56d** which was fully characterized.

The next task was to convert the aldehydes **56b-d** into the curcuminoids **57b-d**. In making the curcumins the usual protocol of method A(section 2.1.4, chapter 2) was followed but the reaction did not produce the usual intense colouration nor a stain upon examination by TLC. Examination of the isolated products of these reactions by ^1H NMR spectroscopy showed the absence of any curcuminoid **57c** and **57d** formation. However, the reaction of aldehyde **56b** produced curcumin **57b** in low yield (30%) after purification by flash chromatography. The IR spectrum showed the typical enolic OH group absorption at around 3348 cm^{-1} and a $>\text{C}=\text{O}$ absorption at 1667 cm^{-1} whilst its ^1H NMR spectrum showed the characteristic enone α and β protons at δ 6.5 and δ 7.5 respectively. A correct molecular ion of m/z 416 was also found in the mass spectrum of **57b**. Although one curcumin was obtained namely from the methoxyaldehyde **56b**, the results on the whole from these set of experiments were very disappointing since we had shown that the furan and thiophene derived curcuminoids were possible and this

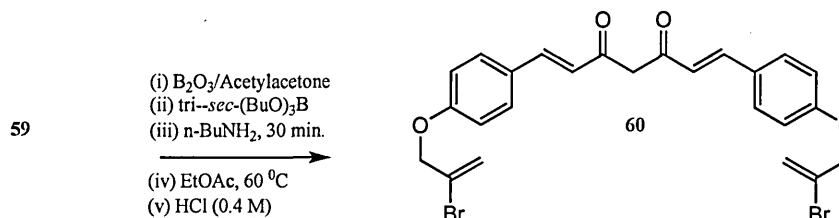
failure of the reactions to produce the expected curcuminoids **57c** and **57d** could not be understood.

We next decided to synthesise the alternate benzo[*b*]furan curcuminoid **61** as shown in figure 3.7. In this strategy the starting aldehyde **58** was alkylated with 2,3-dibromo propene in dry acetone using anhydrous potassium carbonate as base to give the expected bromoallyloxy benzaldehyde **59** in 79% yield. The IR spectrum of **59** showed the absence of OH absorption at around 3468 cm^{-1} and the mass spectrum gave molecular ion peak at m/z 241 (Br^{79}). The ^1H NMR spectrum showed an AB system for the aromatic ring as two doublets at δ 7.0 and δ 7.8 and a singlet for the allylic protons at δ 4.7. The aldehyde **59** reacted with acetylacetone-boric acid complex **31** under the usual conditions (method A section 2.1.4) to yield the desired curcumin **60** in 22% yield after purification by flash chromatography.

Step 1 : Synthesis of bromoallyloxy benzaldehyde 59



Step 2 : Synthesis of bromoallyloxy curcumin 60



Step 3 : Synthesis of 2-methylbenzofuran curcumin 61

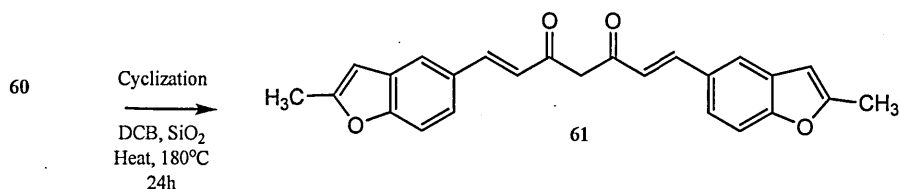


Figure 3.7 : Synthesis of benzo[*b*]furan curcuminoid **61** (2nd strategy).

The formation of the curcumin **60** was confirmed by TLC analysis which showed it as a yellowish stain, R_f 0.3 [petroleum ether : $EtOAc$, 4:1 v/v] and by spectroscopic analysis. For example the mass spectrum of **60** showed two molecular ions at m/z 544 (Br^{79}) and m/z 548 (Br^{81}) and the 1H NMR spectrum showed the typical trans protons of the enone system as two doublets ($J = 16.0$ Hz) resonating at δ 6.5 and δ 7.62. When compound **60** was heated under reflux in 1,2-dichlorobenzene with a catalytic amount of silica for 24 h, it underwent [3,3] sigmatropic rearrangement reaction to produce curcumin **61** in a low yield (9%).

The compound was spectroscopically characterised. Its ^1H NMR spectrum showed well defined peaks. Noticeable features in the proton magnetic spectrum of **61** were the resonances of the H-4 proton of the enolic system at δ 5.7 as a singlet, the benzofuran H-3' proton as singlet at δ 6.0, the two α and β protons of the enone system at δ 6.5 and δ 7.6 as doublets ($J = 15.8$ Hz) indicative of trans configuration of the double bonds.

3.1.4 Attempted synthesis of pyridine and quinoline curcuminoids **63, **65** and **69****

Aim : It was next decided to synthesise some nitrogen containing heterocyclic curcuminoids and we chose to make pyridine and quinoline derivatives for two reasons. Firstly, pyridine and the related quinoline ring systems occur widely in natural products such as for example nicotine and quinine the anti-malarial compounds. Secondly, for curcumin synthesis by the so-called Pabon's method¹⁴⁴ the basic starting material required is an aldehyde and the three aldehydes of pyridine namely pyridine-2-carboxaldehyde, pyridine-3-carboxaldehyde and pyridine-4-carboxaldehyde are all commercially available. Literature search had revealed that some pyridine curcuminoids had previously been synthesised.¹⁸⁸ Hence it was decided to make the curcuminoids **63**, **65** and **69** shown below in figure 3.8.

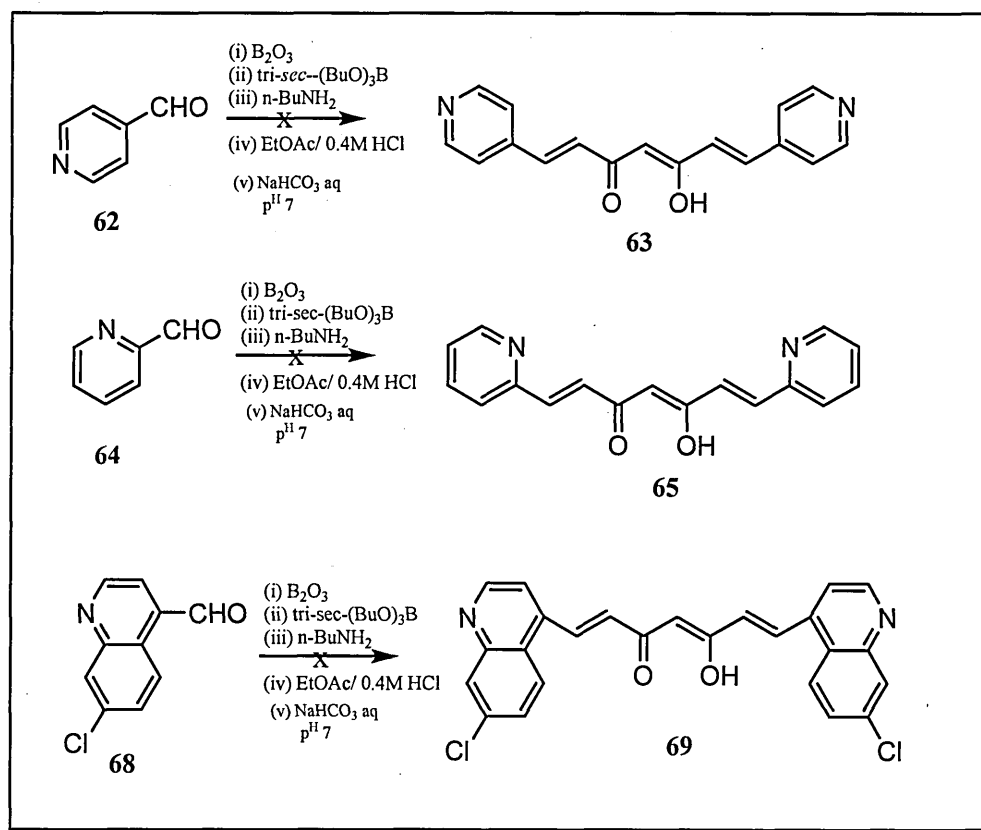


Figure 3.8 : Attempted synthesis of pyridine curcuminoids **63** and **65** and quinoline curcuminoid **69**.

Surprisingly, the slightly brown coloured solid product that was isolated showed none of the characteristic doublets of the curcumin enone system in the aromatic region 6.5-8.0 ppm. Normally, the curcumin compounds have an intense colour of some description and that was also absent in compounds **63** and **65**. It was next decided to synthesise the curcumin **69** from the starting aldehyde **68** which was made from 4,7-dichloroquinoline by nucleophilic substitution reaction with methyl magnesium bromide to give the alkylated product **67** and subsequent oxidation of **67** with selenium dioxide to yield **68** as shown in figure 3.9.

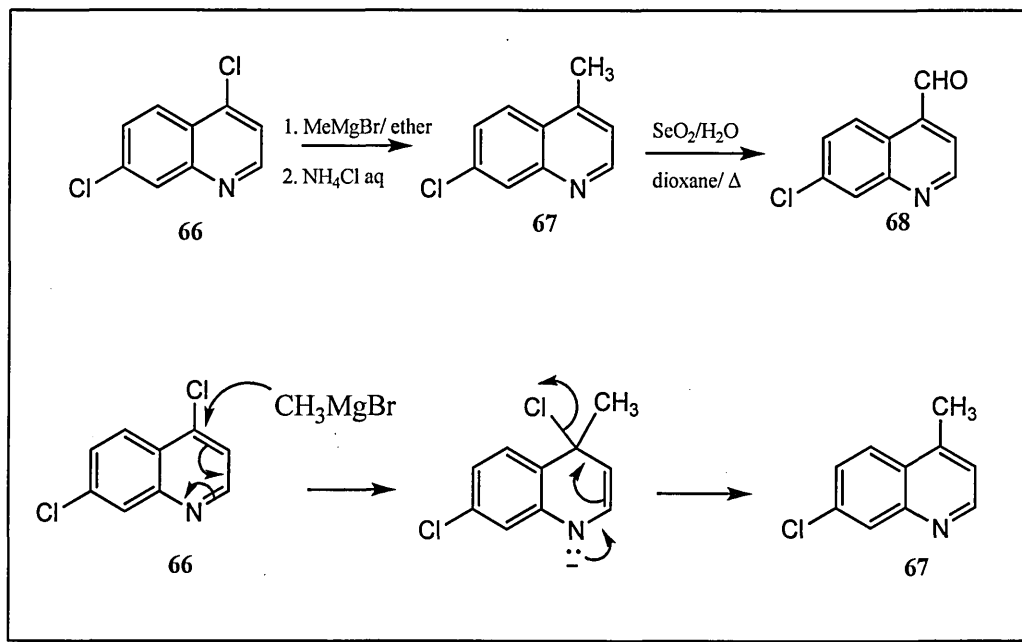


Figure 3.9 : Synthesis of 7-chloroquinoline-4-carboxyaldehyde **68**.

The colour of the starting aldehyde was light brown and the product from the reaction of **68** with boric acid/borate complex after work up was intense dark brown which was a healthy sign. However, inspection of the ¹H NMR spectrum of the dark brown solid revealed once again that it was not the anticipated curcuminoid **69** due to the lack of the characteristic enone doublets.

It was envisaged that perhaps the nitrogen atom of the pyridine ring was complexing with the electron deficient boron atom of the tri-*sec*-butyl borate and boric acid complex and the synthesis of the curcuminoids **63** and **65** were repeated using a molar excess of the boric acid/borate complex. The experiments had the same outcome and hence the compounds **63** and **65** could not be obtained. These results were perplexing and it appeared that the synthesis of the nitrogen derived

150
1 or 2

curcuminoids **63**, **65** and **69** could not be established despite literature report¹⁸⁸ suggesting otherwise for pyridine curcuminoid.

3.1.5 Attempted syntheses in search of new synthetic protocol for curcumin formation

Aim : In the light of failures of some of the reactions and very low yields for the obtainable product curcuminoids it was decided to search for new methods for making curcumins. Retrosynthetically, it was envisaged that by employing the Claisen condensation reaction it should be possible to construct curcumins as shown in figure 3.10a.

The retrosynthetic rationale suggests that the Claisen-Schmidt condensation¹⁸⁹ reaction can be used to construct the curcumin skeleton. Thus, benzylideneacetone **71a** or furfurylidene **71b** obtainable by the Claisen-Schmidt condensation of acetone with benzaldehyde can be reacted with ethyl cinnamate **72** in the presence of a strong base such as sodium hydride or potassium t-butoxide in a suitable non-protic solvent to give the curcumin **73a** (figure 3.10b). The mechanism involved in this reaction is shown in figure 3.10c. The biggest advantage of this method would be that its success would enable non-symmetrical curcuminoids to be synthesised. To test the validity of this new synthetic strategy benzylideneacetone **71a**¹⁹⁰ and furfurylidene-acetone¹⁹¹ **71b** were first synthesised by established procedures in the literature using the Claisen-Schmidt reaction¹⁵⁶ as shown in scheme 2.17 (chapter 2).

Conclusions

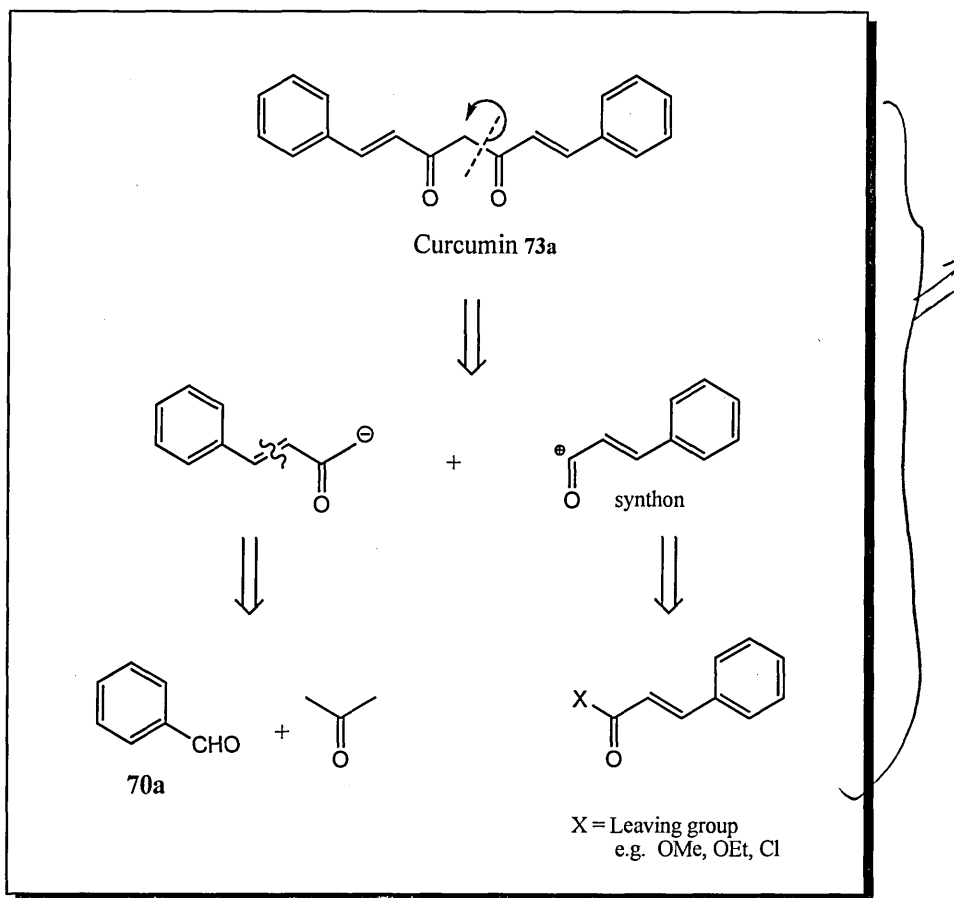


Figure 3.10a : Retrosynthetic analysis of curcumin.

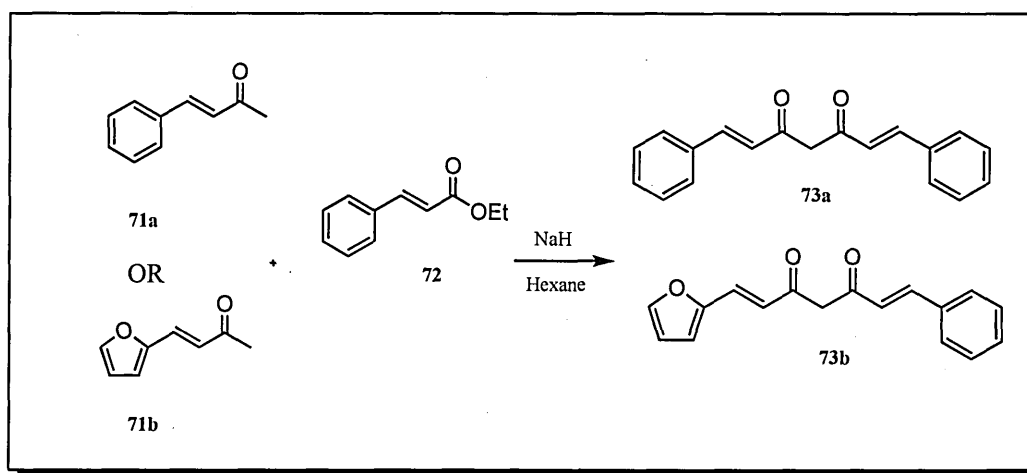


Figure 3.10b : New synthesis of curcumin based on retrosynthetic analysis.

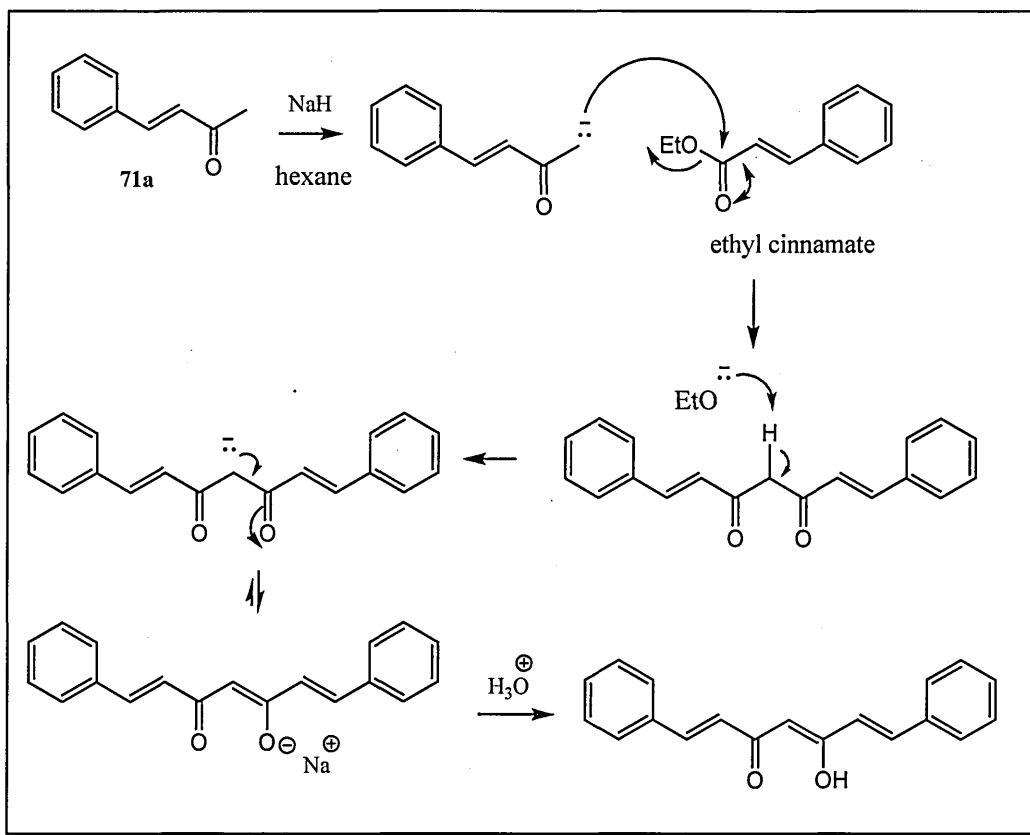


Figure 3.10c : Mechanism involved in the new synthetic pathway of curcumin formation.

The Claisen condensation¹⁹² (acetoacetic ester condensation) is a base-catalyzed condensation of an ester containing an α -hydrogen atom with a molecule of the same ester or a different one to give β -keto esters as shown in figure 3.11.

The synthetic procedure for the Claisen condensation of the arylidene-acetones **71a** and **71b** with ethyl cinnamate **72** was adopted from the similar procedure reported for the formation of dibenzoylmethane from acetophenone and ethyl benzoate in hexane using sodium hydride as the base.¹⁹³ Thus when a solution of **71b** with a molar excess of ethyl cinnamate **72** in dry hexane was slowly added to a refluxing stirred suspension of sodium hydride (50% excess) in dry hexane a yellowish brown solid started to precipitate. After acidification and aqueous work-up the mixture yielded a yellowish-brown solid as the reaction product which was spectroscopically analysed. The TLC [petroleum ether : EtOAc, 9:1v/v] showed the product had different R_f to the R_f of the starting furfurylidene-acetone **71b** but the product appeared as a streak indicating impurities. The IR spectrum of **73b** showed a very strong absorption at 1716 cm^{-1} and minor peaks at 1671 and 1637 cm^{-1} . The ^1H NMR spectrum of product **73b** showed some minor evidence for curcuminoid formation as the typical doublets associated with the α,β -unsaturated enone protons was present amongst many complicated peaks in the aromatic region. The electron impact mass spectrum of the product showed one peak corresponding to m/z 265 (28%, M-1). However, there were many other peaks of which two interesting peaks were m/z 396 (10%) and m/z 525 (24%, M-1) possibly corresponding to the structures **83** and **84** shown in (figure 3.12).

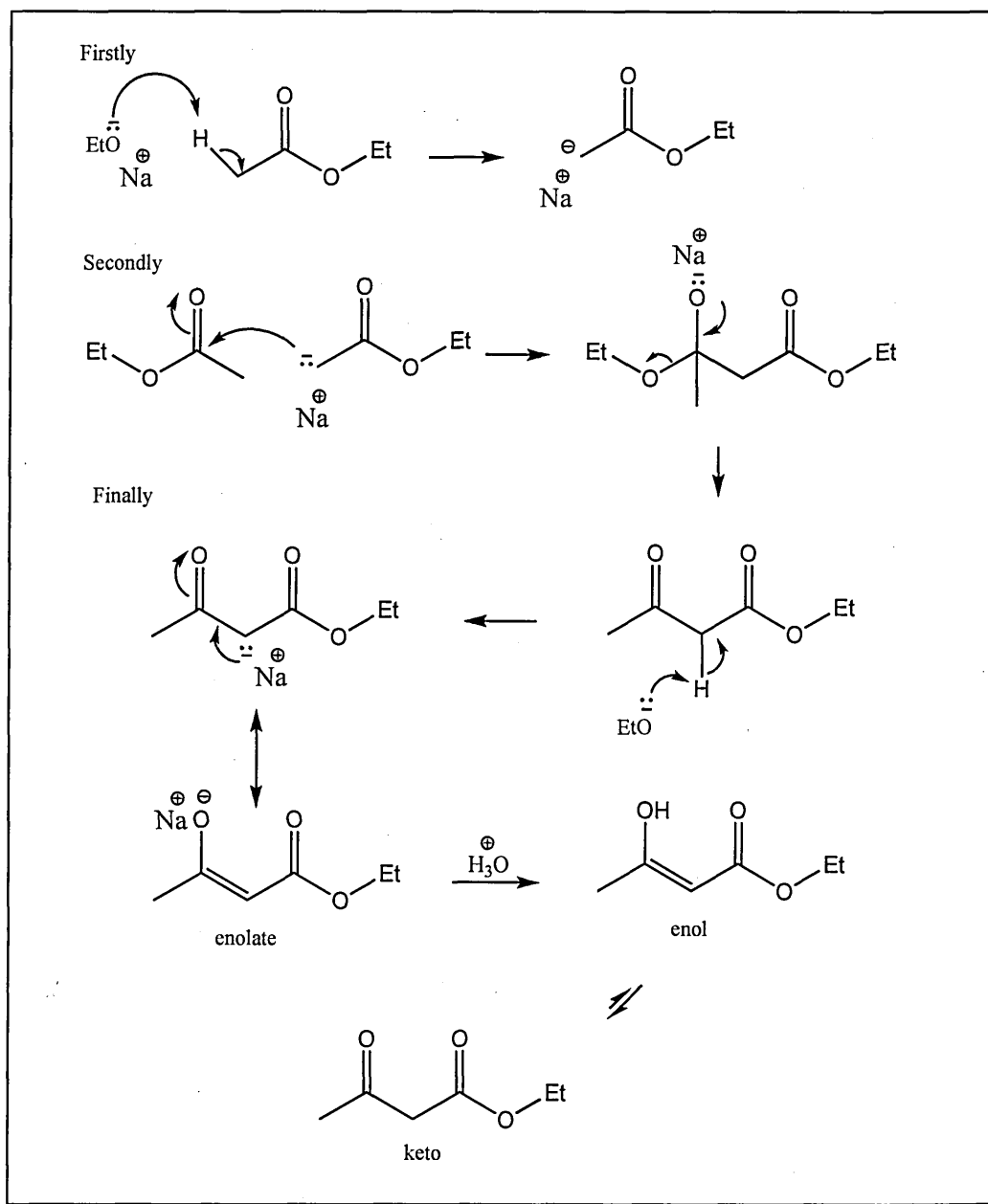


Figure 3.11 : The mechanism of acetoacetic ester condensation reaction.

The reaction of benzylidene-acetone **71a** with ethyl cinnamate **72** under similar conditions produced creamy coloured solid which on TLC was a mixture of products and inspection by ^1H NMR spectroscopy showed a complicated picture with some evidence for the curcuminoid **73a** as the typical doublets associated with the α,β -unsaturated enone protons were slightly evident. This was supported by the EI mass spectrum of crude product **73a** which showed many peaks of which one peak corresponded to the required molecular structure **73a** of m/z 275 (19%, M-1).

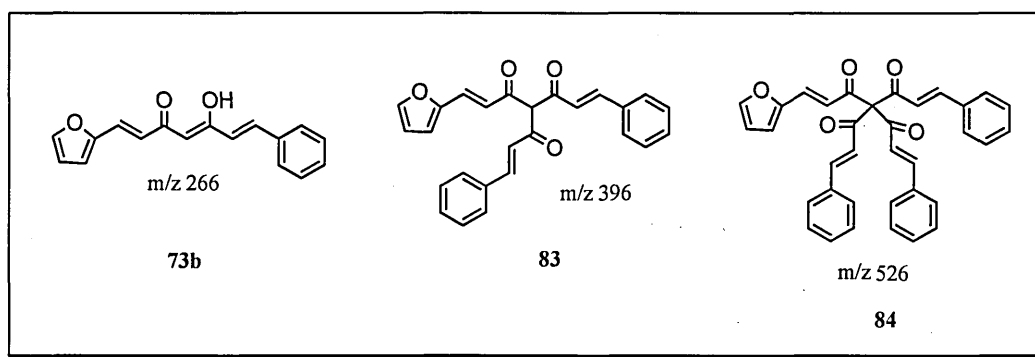


Figure 3.12 : Postulated structures of the compounds found in EIMS spectrum of Claisen condensation reaction of furfurylidene-acetone and ethyl cinnamate.

There was some evidence for the formation of curcuminoids by the Claisen condensation reaction. In future, it may be possible to investigate newer reaction conditions and may be other reagent such as TiCl_4 ¹⁹⁴ that could be used to bring about the success of this Aldol type reaction in a better and more cleaner way as shown in figure 3.13.

194

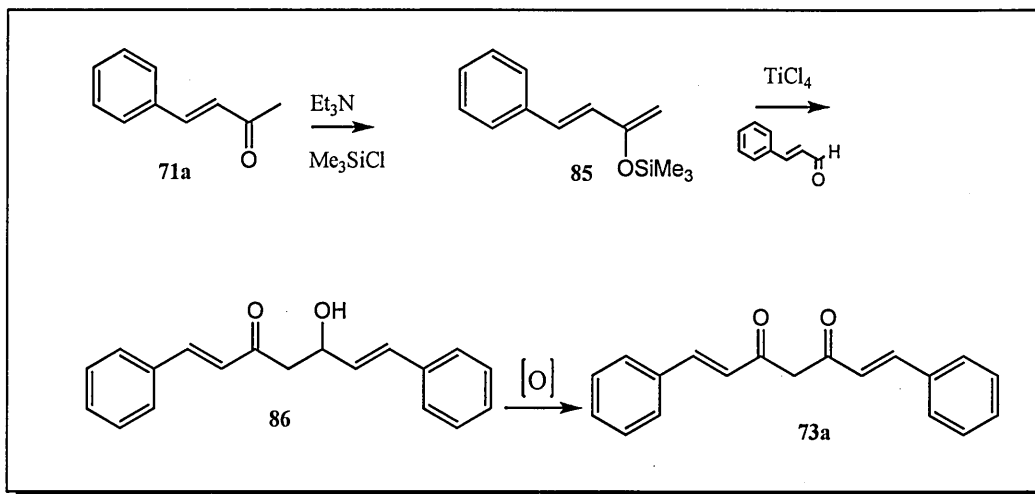


Figure 3.13 : Postulated use of TiCl_4 in Aldol type reaction for curcumin synthesis.

Part B

Pharmacology Section

3.2 Results

3.2.1 Effects of drugs on cell viability (The MTS assay)

Along with all the drug samples at 10, 50 and 100 μM concentrations, each experimental design was consisted of four controls i.e. cells alone or untreated cells, the solvent DMSO and the stimulants LPS and or MS to validate the results. In all experiments two comparisons were made. In the first comparison (shown by*) all drugs were compared to the DMSO (0.3% v/v) control, and in the second comparison, the drugs were compared to the curcumin **1** control (shown by *).

3.2.1.1 Effects of curcumin 1, and nitric oxide donating curcuminoids 51a-d on the viability of THP-1 cells

Using the MTS reduction method, the cytotoxic effects of curcumin **1** and its nitroxybutyl derivatives **51a-d** were studied (figure 3.14). THP-1 cells were treated as described in section 2.3.6.1. Compared to the cells alone control, the DMSO (0.3% v/v) did not show any cytotoxic effects whereas LPS also did not significantly affect the cell viability. Except curcumin **1** (which was cytotoxic at 50 and 100 μM), all drugs increased the cell proliferation in concentration dependent manner compared to the DMSO control (shown by *). At the concentration of 10 μM , all drugs including curcumin **1**, non-significantly increased the cell proliferation. At 50 μM and 100 μM all drugs significantly increased the cell viability, except **51c** where the effect appeared to be non-significant at 50 μM , however was significant at 100 μM .

When compared with curcumin **1**, (shown by *), all drugs at 10 μ M were as non-toxic as curcumin **1**, whereas at 50 and 100 μ M the synthetic nitric oxide donating analogues **51a-d** were significantly non-toxic to the cells compared to the curcumin **1** control.

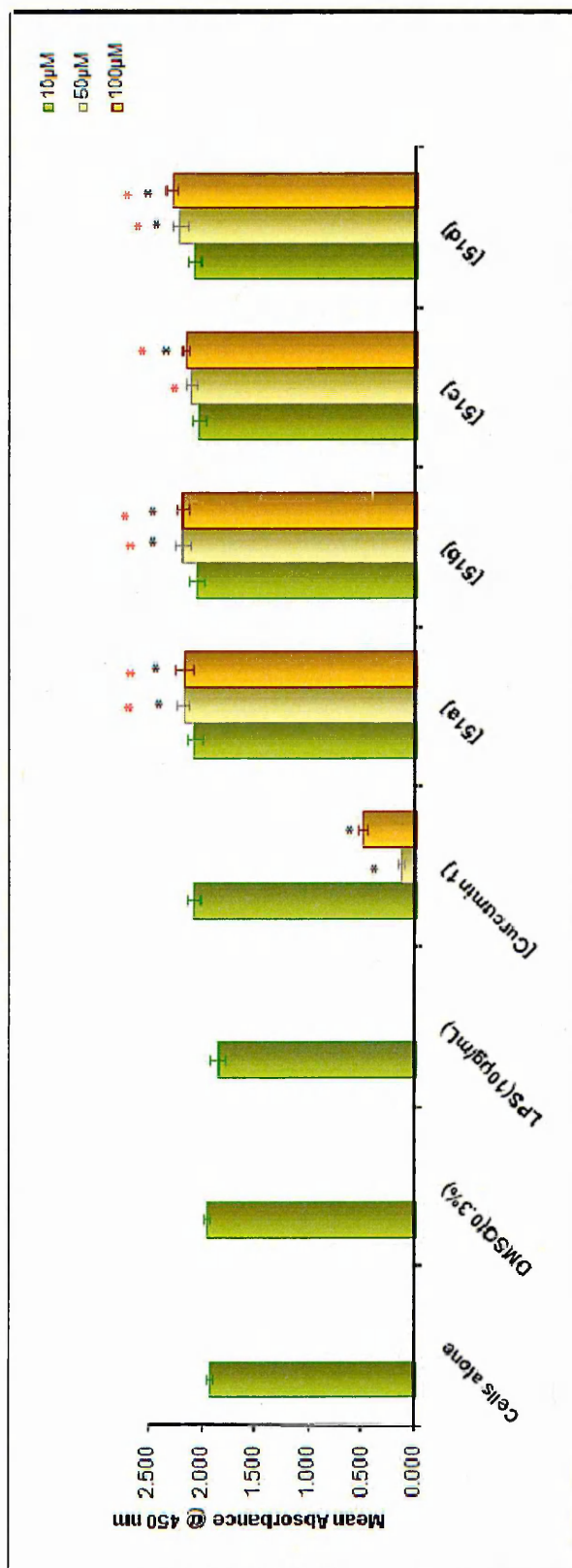


Figure 3.14: Results of the MTS assay showing the effects of synthesised curcumin **1** and nitric oxide donating curcuminoids **51a-d** on the viability of THP-1 cells. THP-1 cells were incubated in the absence or presence of the corresponding drugs at three different concentrations i.e. 10, 50 and 100 µM for 24h along with the appropriate controls. Absorbance corresponded to the number of viable cells. Results are expressed as mean \pm SEM of four separate experiments (n=8). Shapiro-Wilk W test for non-normality followed by Kruskal-Wallis: Conover-Inman post-hoc test was used to determine significance. P value < 0.05 was considered as significant. * denotes the comparison of the drugs vs. vehicle (DMSO) control. * denotes the comparison of the drugs vs. curcumin **1** control.

3.2.1.2 Effects of curcumin 1 and thiophene curcuminoids 47a-d on the viability of THP-1 cells

Figure 3.15 shows the effects of curcumin 1 and its thiophene analogues **47a-d** on the viability of THP-1 cells using the MTS assay. Treatment was applied to the cells as described in section 2.3.6.1. The controls DMSO and LPS did not have any cytotoxic effects at the concentrations used and showed the same viability as the cells alone control. Compared with DMSO control (shown by *), the parent drug curcumin 1, thiophene curcuminoids **47b** and **47c** significantly decreased the cellular viability in concentration dependent manner. Drug **47a** was non-cytotoxic at all the three concentrations studied i.e. (10, 50 and 100 μ M), whereas, **47d** was cytotoxic at 100 μ M only. All drugs including curcumin 1 were non-toxic at 10 μ M.

In comparison with parent drug curcumin 1 (shown by *), drugs **47a** and **47d** were as non-cytotoxic as curcumin at 10 μ M, whereas **47b** and **47c**, were more cytotoxic than curcumin. At 50 and 100 μ M all drugs were significantly non-cytotoxic than curcumin 1 except **47c** at 100 μ M.

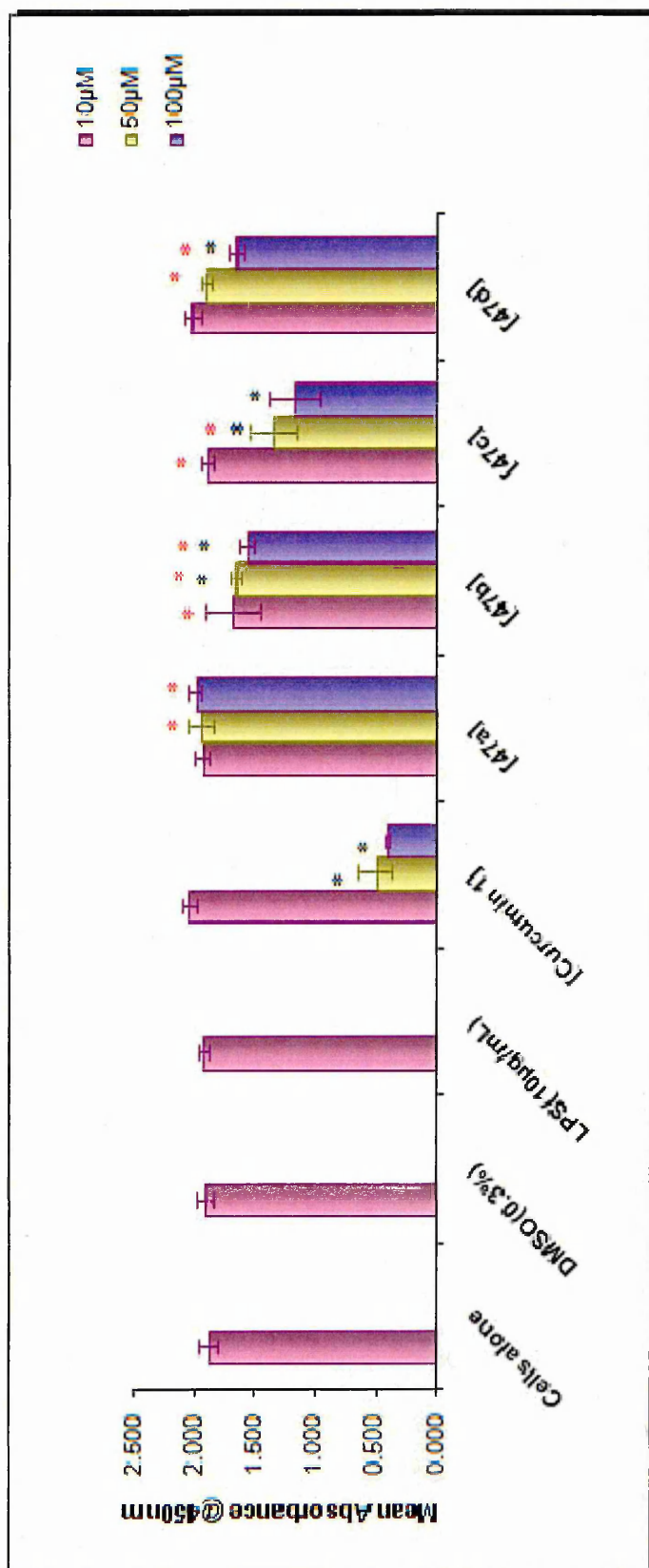


Figure 3.15: Results of the MTS assay showing the effects of synthesised curcumin **1** and thiophene curcuminoids **47a-d** on the viability of THP-1 cells. THP-1 cells were incubated in the absence or presence of the corresponding drugs at three different concentrations i.e. 10, 50 and 100µM for 24h along with the appropriate controls. Absorbance corresponded to the number of viable cells. Results are expressed as mean \pm SEM of four separate experiments (n=8). Shapiro-Wilk W test for non-normality followed by Kruskal-Wallis : Conover-Inman post-hoc test was used to determine significance. P value < 0.05 was considered as significant. * denotes the comparison of the drugs vs. vehicle (DMSO) control. * denotes the comparison of the drugs vs. curcumin **1** control.

3.2.1.3 Effects of drugs curcumin 1 and thiophene curcuminoids 47a-d on the viability of CACO-2 cells

Cytotoxic effects of the synthesised curcumin 1 and its thiophene analogues **47a-d** were studied in CACO-2 cells using the MTS assay. CACO-2 cells were treated as described in section 2.3.9.1. As shown in figure 3.16 the DMSO and the LPS controls did not show any cytotoxic effects compared to the cell alone control, however, L-methionine sulfoximine (MS) significantly reduced the cell viability. In comparison to the DMSO control (shown by *), curcumin 1, drugs **47c** and **42d** decreased the cell viability in concentration dependent manner. At the concentration of 10µM all drugs did not show any cytotoxic effects. At 50µM, no cytotoxic effects were observed with **47b** and **47d**, however, curcumin 1, **47a** and **47c** showed a significant decrease in cell viability. At 100µM, curcumin 1 and **47c** significantly reduced the cell viability.

When compared to the curcumin 1 control (shown by *), at 10 µM concentration all drugs appeared to be as non-toxic to CACO-2 cells as curcumin 1 itself, however, at 50 µM all drugs showed non-significant cytotoxic effects similar to curcumin 1. All drugs were less cytotoxic than curcumin 1 at 100µM except **47c** where the effect was non-significant.

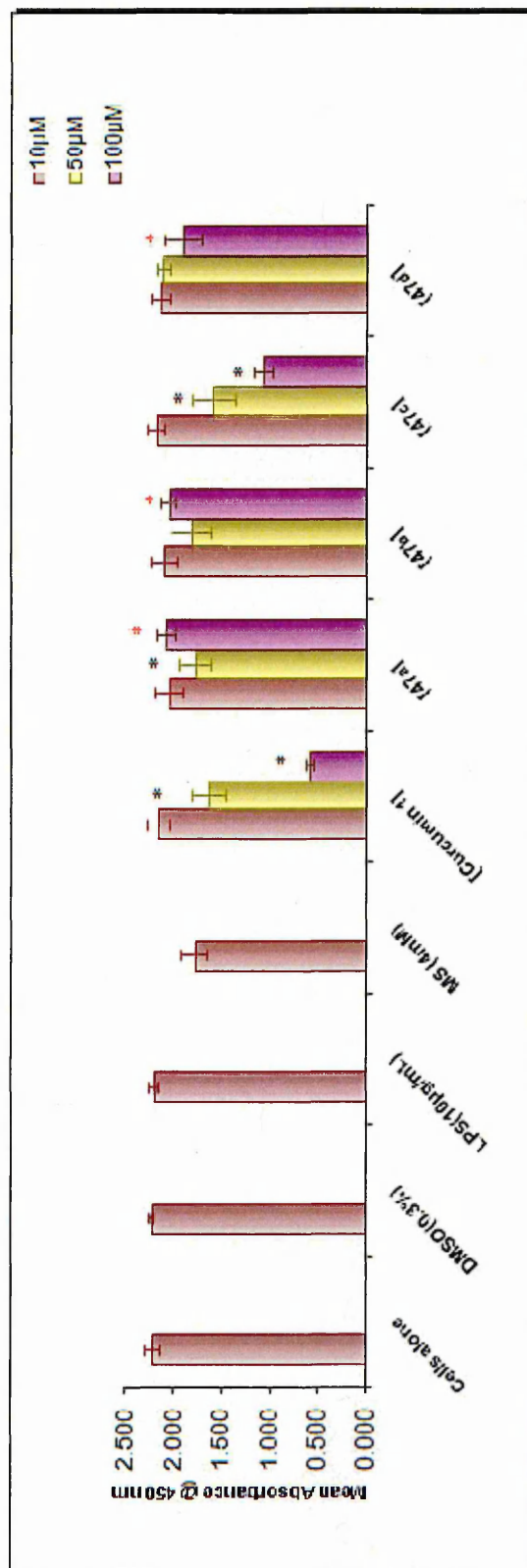


Figure 3.16: Results of the MTS assay showing the effects of synthesised curcumin **1** and thiophene curcuminoids **47a-d** on the viability of CACO-2 cells. CACO-2 cells were incubated in the absence or presence of the corresponding drugs at three different concentrations i.e. 10, 50 and 100µM for 24h along with the appropriate controls. Absorbance corresponded to the number of viable cells. Results are expressed as mean \pm SEM of four separate experiments (n=8). Shapiro-Wilk W test for non-normality followed by Kruskal-Wallis; Conover-Inman post-hoc test was used to determine significance. P value < 0.05 was considered as significant. * denotes the comparison of the drugs vs. vehicle (DMSO) control. * denotes the comparison of the drugs vs. curcumin **1** control.

3.2.1.4 Effects of hydroxypropyl- γ -cyclodextrin (HP- γ -CD) and 47a-d/ HP- γ -CD on the viability of THP-1 cells

Figure 3.17 shows the viability of THP-1 cells treated with free hydroxypropyl- γ -cyclodextrin (HP- γ -CD) and the drug/HP- γ -CD (section 2.3.6.1.). The viability was assessed using the MTS assay. All of the drugs/HP- γ -CD complexes were less cytotoxic than the free HP- γ -CD, and increased the cell viability in concentration dependent manner.

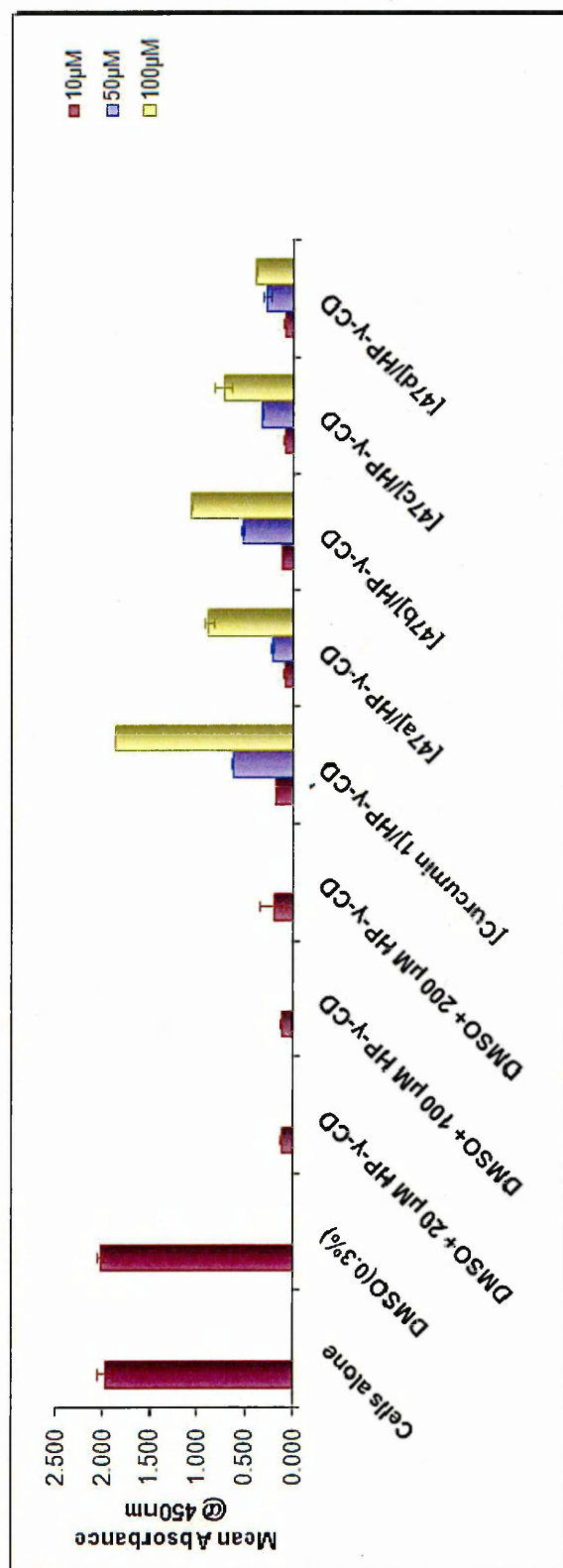


Figure 3.17: Results of the MTS assay showing the effects of synthesised curcumin **1** and thiophene curcuminoids **47a-d** complexed with HP-γ-CD on the viability of THP-1 cells. THP-1 cells were incubated in the absence or presence of the corresponding drugs at three different concentrations i.e. 10, 50 and 100 μM for 24h along with the appropriate controls. Absorbance corresponded to the number of viable cells. Results are expressed as mean ± SEM of two separate experiments (n=2).

3.2.2 The nitric oxide (NO) production assay (Griess reagent system)

3.2.2.1 Standard curve for nitric oxide (NO)

Standard curves for the estimation of nitrite (NO_2^-) was obtained by diluting the sodium nitrite standard in sample matrix to the concentration range of 0 to 100 μM according to the procedure described in section 2.5.3.1.

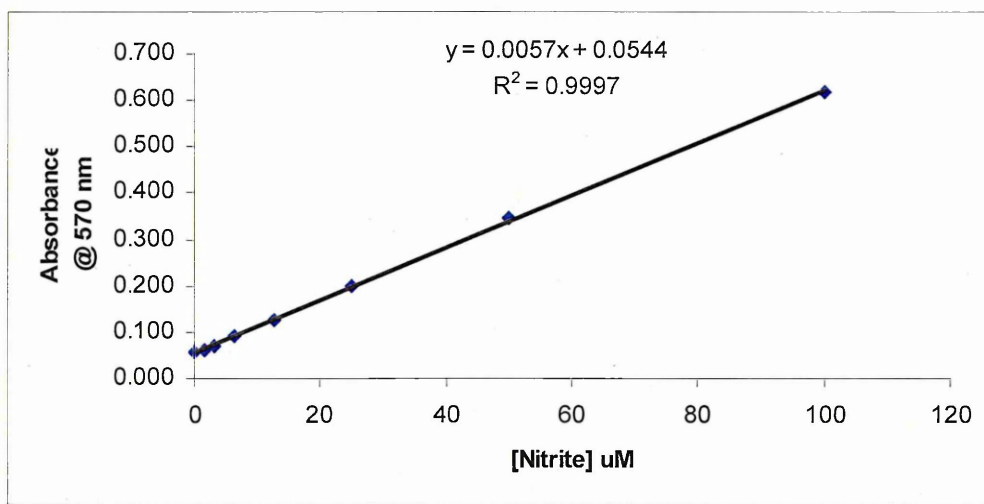


Figure 3.18: A typical nitrite standard curve using nitrite standard.

Nitrite standard curves were generated by plotting the mean absorbance value of each concentration of the sodium nitrite standard as a function of Y-axis with nitrite concentration as a function of X-axis. The equation shown on the graph was used to calculate the unknown concentrations of NO in experimental samples or the controls.

3.2.2.2 Measurement of nitrite concentration in the cell supernatants of THP-1 cells treated with curcumin 1 and nitric oxide donating curcuminoids 51a-d

Cell supernatants collected from the THP-1 cells treated according to the method described in section 2.3.6.1 were used. Figure 3.19a, shows a non-significant decrease in nitrite production with the DMSO control (0.3% v/v) compared to the cells alone control. Compared to the DMSO control (shown by *) a concentration dependent increase in the production of nitrite was observed with drugs **51a** and **51d** at all the three concentrations i.e. 10, 50 and 100 μ M, however the effect was significant at 50 and 100 μ M. Curcumin **1**, and drug **51c** at 10, 50 and 100 μ M concentration non-significantly affect the nitrite production. A significant increase in the nitrite production was observed with drug **51b** at 10 and 100 μ M concentrations, however, at 50 μ M a non-significant effect on nitrite production was observed.

In comparison with curcumin **1** (shown by *), at 10 μ M, only drug **51b** at 10 μ M showed a significant increase in nitrite production.

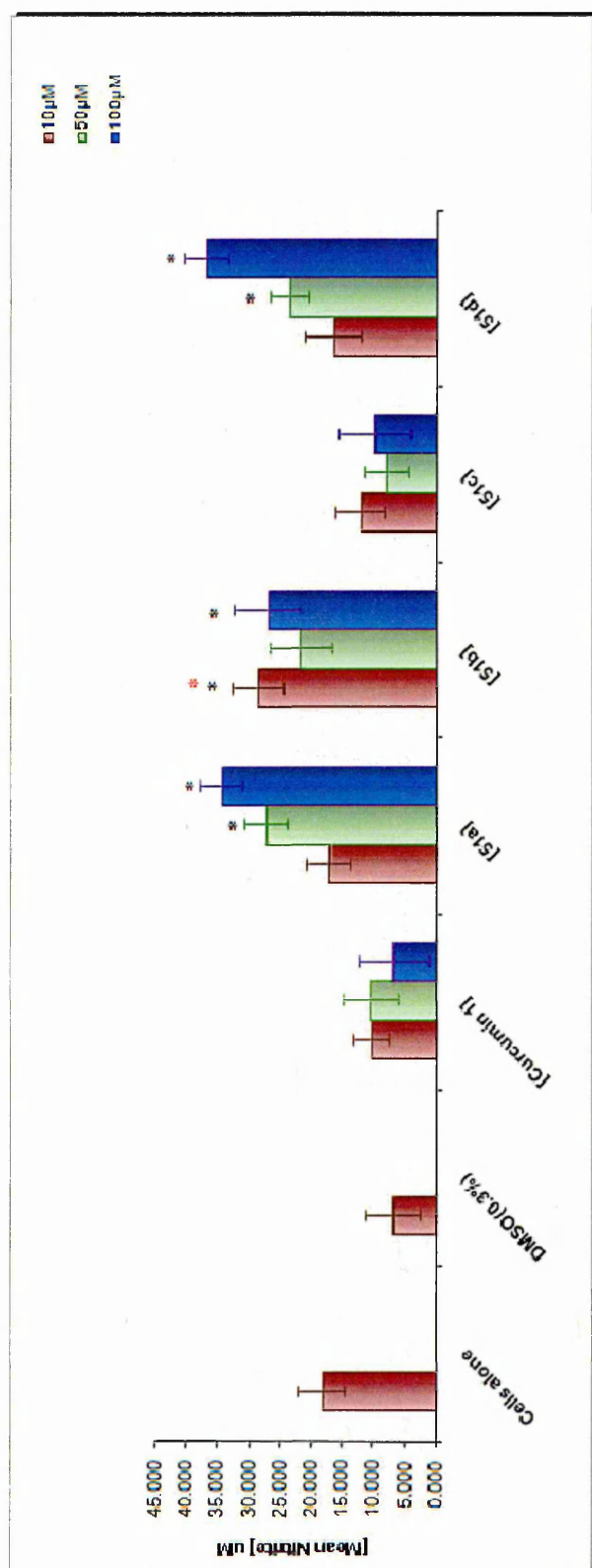


Figure 3.19a: Results of the Griess reagent assay showing the effects of synthesised curcumin **1** and nitric oxide donating curcuminoids **51a-d** on the production of nitric oxide in THP-1 cells. THP-1 cells were incubated in the absence or presence of the corresponding drugs alone at three different concentrations i.e. 10, 50 and 100 μ M for 24h along with the appropriate controls. Results are expressed as mean \pm SEM of three separate experiments ($n=6$). Shapiro-Wilk W test for non-normality followed by Kruskal-Wallis: Conover-Inman post-hoc test was used to determine significance. P value < 0.05 was considered as significant. * denotes the comparison of the drugs vs. DMSO control. * denotes the comparison of the drugs vs. curcumin **1** control.

3.2.2.3 Measurement of nitrite concentration in the cell supernatants of THP-1 cells treated with curcumin 1 and nitric oxide donating curcuminoids 51a-d stimulated with LPS

Figure 3.19b shows the effects of the synthesised curcumin **1** and its nitric oxide donating derivatives **51a-d** on nitric oxide (NO) production in the presence of LPS. THP-1 cells were stimulated according to the method described in section 2.3.6.1 and the cell supernatants were tested. In comparison to the cells alone control, DMSO + LPS control significantly reduced the nitrite production, whereas a non-significant effect in nitrite production was observed with the LPS control. When compared with the DMSO + LPS control (shown by *) a concentration dependent increase in nitrite production was observed with **51a**, at 50 and 100 μ M however with **51b** the effect was equally significant at all the three concentrations studied. On the other hand, with **51c** the effect was only found to be significant at 100 μ M and with **51d** a significant increase in nitrite production was observed at 50 and 100 μ M. In comparison with curcumin **1** control (shown by *), only drug **51b** showed a significant effect at 10 μ M.

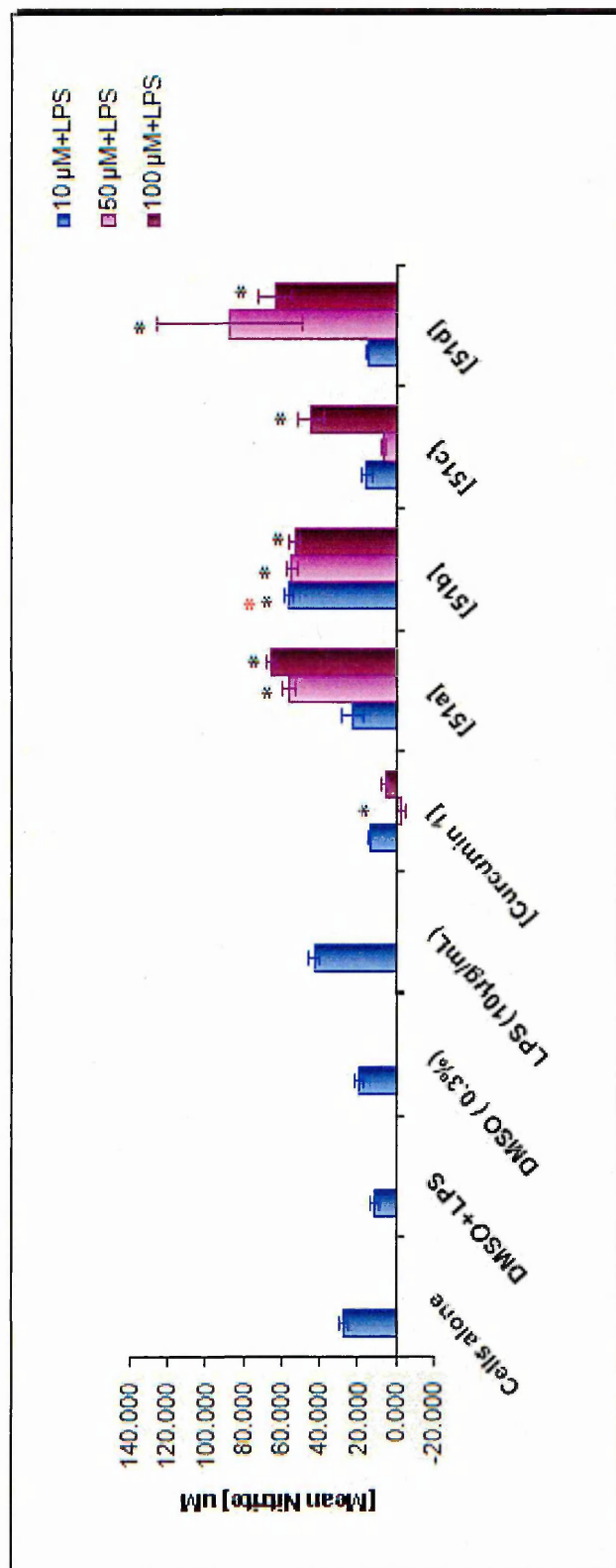


Figure 3.19b: Results of the Griess reagent assay showing the effects of synthesised curcumin **1** and nitric oxide donating curcuminoids **51a-d** on the production of nitric oxide in THP-1 cells. THP-1 cells were incubated in the absence or presence of the corresponding drugs \pm LPS at three different concentrations i.e. 10, 50 and 100 μ M for 24h along with the appropriate controls. Results are expressed as mean \pm SEM of three separate experiments (n=6). Shapiro-Wilk W test for non-normality followed by Kruskal-Wallis; Conover-Inman post-hoc test was used to determine significance. P value < 0.05 was considered as significant. * denotes the comparison of the drugs vs. DMSO+LPS control. * denotes the comparison of the drugs vs. curcumin **1** control.

3.2.3 Enzyme-linked immunosorbent assay (ELISA)

3.2.3.1 Standard curve for IL-1 β

A typical standard curve, figure 3.20 for the estimation of IL-1 β in the cell supernatants of THP-1 cells, using the standard recombinant human IL-1 β was obtained according to the procedure described in section 2.6.2.2. The IL-1 β concentration limit was 0-250 pg/mL, however, all experimental samples (except LPS stimulated control) all showed concentration below 62.5 pg/mL and fall within the linear limit of 80 pg/mL the standard curve shown below has been plotted at the limit of 80 pg/mL. The points at 125 and 250 pg/mL have not been shown as at these points the saturation with the capture antibody was observed.

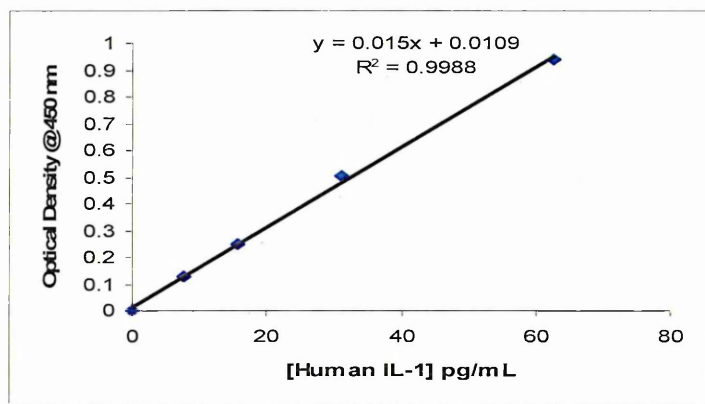


Figure 3.20 : A typical standard curve used for the quantification of IL-1 β in cell supernatants of THP-1 cells.

Standard curves were generated by plotting the corrected average optical density of each concentration of the IL-1 β standard as a function of Y-axis with IL-1 β concentration as a function of X-axis.

3.2.3.2 Effects of curcumin 1 and thiophene curcuminoids 47a-d on the production of IL-1 β in cell supernatants of THP-1 cells

As shown in figure 3.21, the controls i.e. cells alone and the DMSO (0.3% v/v), as well as all experimental samples i.e. the drugs (alone) did not have any detectable IL-1 β in cell supernatants. A significant increase in the production of IL-1 β was observed with the LPS control compared to the cells alone control and DMSO did not affect this IL-1 β production as shown by DMSO + LPS control.

In LPS stimulated cells, compared with DMSO + LPS control, curcumin **1** significantly reduced the production of IL-1 β at its non-cytotoxic concentration of 10 μ M, however no detectable IL-1 β production was obtained at 50 and 100 μ M, which could be due to the cytotoxic effects of **1** at these concentrations. On the other hand drugs **47a** at all the three concentrations studied i.e. 10, 50 and 100 μ M reduced the IL-1 β production in concentration dependent manner however the effect was significant at 50 and 100 μ M. Drug **47d**, was effective in reducing the IL-1 β production in concentration dependent manner, at its non-cytotoxic concentrations of 10 and 50 μ M, whereas, at 100 μ M the effect could be due to the reduced cell viability. Drugs **47b** and **47c** at their non-cytotoxic concentration of 10 μ M also reduced the IL-1 β production.

In comparison with curcumin **1** control at, 10 μ M all drugs at 10 μ M were as effective as curcumin **1**, however the effect was non-significant.

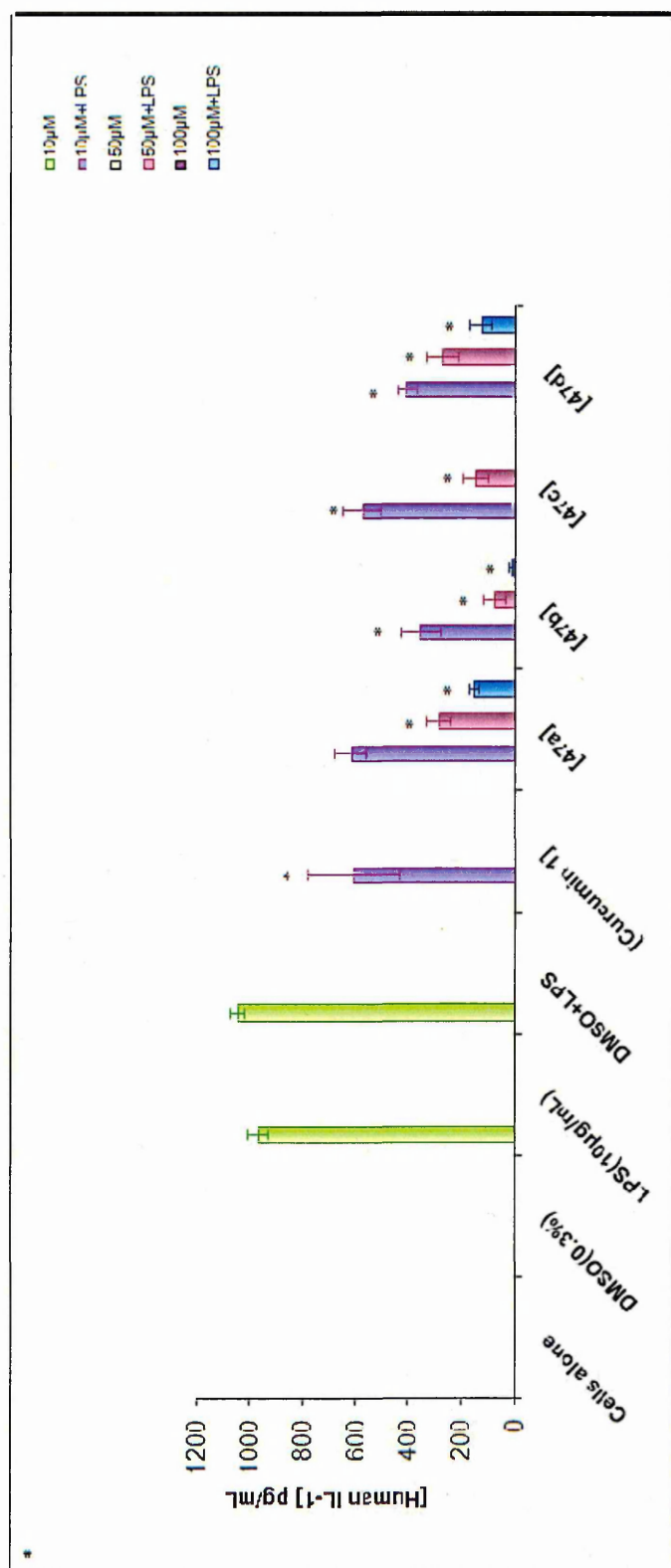


Figure 3.21: Results of the ELISA assay showing the effects of synthesised curcumin **1** and thiophene curcuminoids **47a-d** on the production of IL-1 in THP-1 cells. THP-1 cells were incubated in the absence or presence of the corresponding drugs at three different concentrations i.e. 10, 50 and 100 µM ± LPS for 24h along with the appropriate controls. Results are expressed as mean ± SEM of four separate experiments (n=8). Shapiro-Wilk W test for non-normality followed by Kruskal-Wallis: Conover-Inman post-hoc test was used to determine significance. P value < 0.05 was considered as significant. * denotes the comparison of the drugs vs. DMSO + LPS control.

3.2.3.3 Standard curve for TNF- α

A typical standard curve for the estimation of TNF- α in the cell supernatants of THP-1 cells, using the standard recombinant human TNF- α is shown in figure 3.22. The standard curves were obtained according to the procedure described in section 2.6.2.2. The TNF- α concentration limit was 0-1000 pg/mL, however, all experimental samples (except LPS stimulated control) showed concentration below 250 pg/mL and fall within the linear limit of 300 pg/mL. The standard curves were plotted at the limit of 300 pg/mL. The points at 500 and 1000 pg/mL have not been shown as at these points the saturation with the capture antibody was observed.

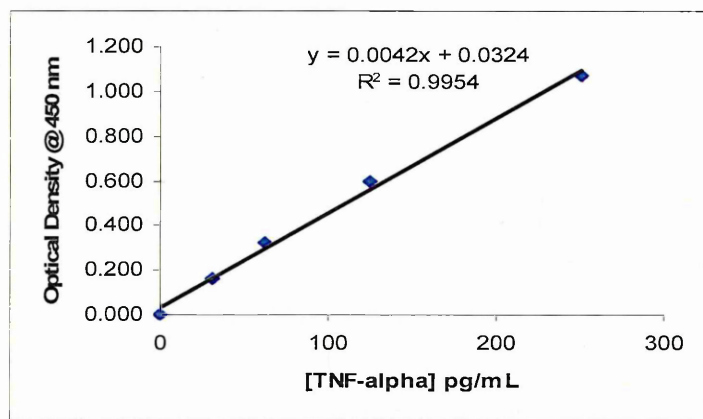


Figure 3.22 : A typical standard curves used for the quantification of TNF- α in cell supernatants of THP-1 cells.

Standard curves were generated by plotting the corrected average optical density of each concentration of the TNF- α standard as a function of Y-axis with TNF- α concentration as a function of X-axis.

3.2.3.4 Effects of curcumin 1 and thiophene curcuminoids 47a-d on the production of TNF- α in cell supernatants of THP-1 cells

Figure 3.23 shows the effects of the drugs curcumin **1** and thiophene curcuminoids **47a-d** on the production of TNF- α in THP-1 treated as described in section 2.3.6.1. The controls i.e. cells alone and the DMSO (0.3% v/v), as well as all experimental samples i.e. the drugs (alone) did not produce any detectable TNF- α . A significant (5000 pg/ml) increase in the production of TNF- α was observed with the DMSO + LPS control compared to the cells alone control. All experimental samples i.e. drugs in the presence of LPS did not significantly reduce the production of TNF- α compared with the DMSO + LPS control (shown by *), except **47c** which at 100 μ M concentration significantly reduced the TNF- α production, however this effect was due to the reduced cell viability and not due to the drug's own effect. When compared with the curcumin **1** control, at 10 μ M, all drugs increased the TNF- α production, however the effect was non-significant.

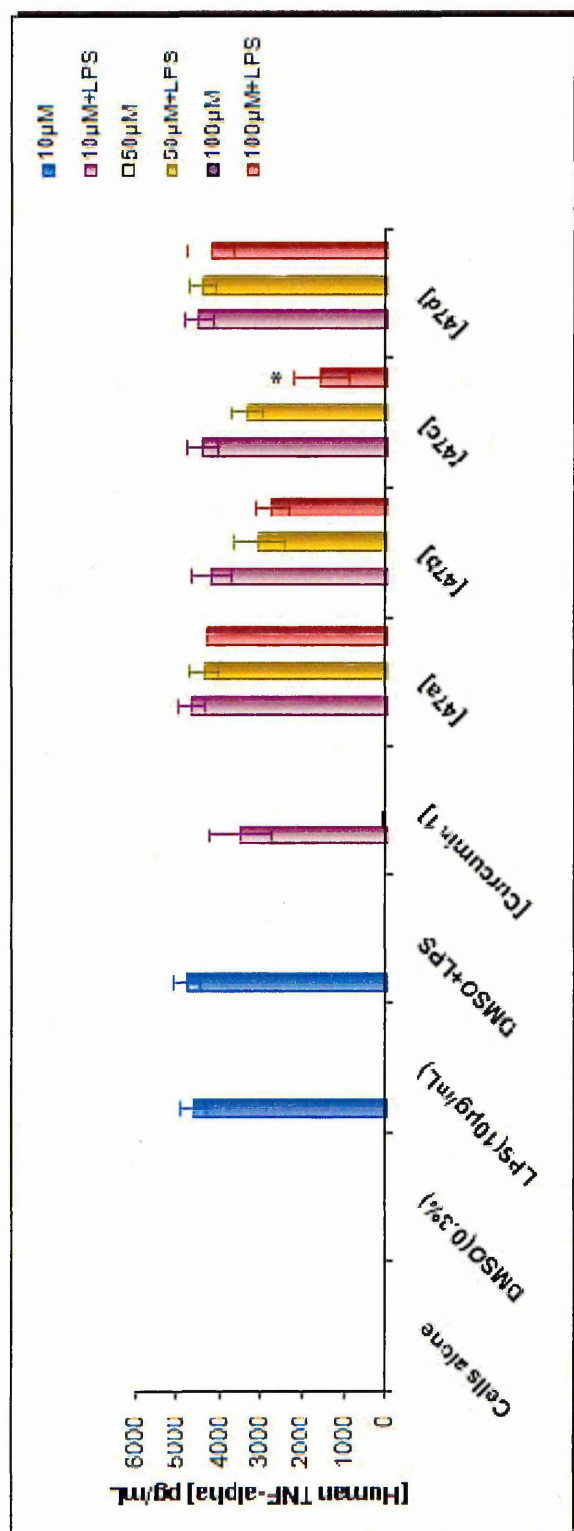


Figure 3.23: Results of the ELISA assay showing the effects of synthesised curcumin **1** and thiophene curcuminoids **47a-d** on the production of TNF- α in THP-1 cells. THP-1 cells were incubated in the absence or presence of the corresponding drugs at three different concentrations i.e. 10, 50 and 100 μ M \pm LPS for 24h along with the appropriate controls. Results are expressed as mean \pm SEM of three separate experiments ($n=6$). Shapiro-Wilk W test for non-normality followed by Kruskal-Wallis; Conover-Inman post-hoc test was used to determine significance. P value < 0.05 was considered as significant. * denotes the comparison of the drugs vs. DMSO + LPS control.

3.2.3.5 Standard curve for CXCL-8

A typical standard curve, figure 3.24 for the estimation of CXCL-8 in cell supernatants of CACO-2 cells using the standard recombinant human IL-8 or CXCL-8 was obtained according to the procedure described in section 2.6.2.5.

The full concentration range of the standard curve for CXCL-8 estimation was 0-2000 pg/mL, however at the range of 500 to 2000 pg/mL the saturation with the capture antibody was observed. Since all experimental samples as well as controls showed concentration below 2000 pg/mL, and fall within the linear limit of 150 pg/mL the standard curve (figure 3.24) has been plotted at the limit of 250 pg/mL and been used for the determination of the concentrations in the experimental samples.

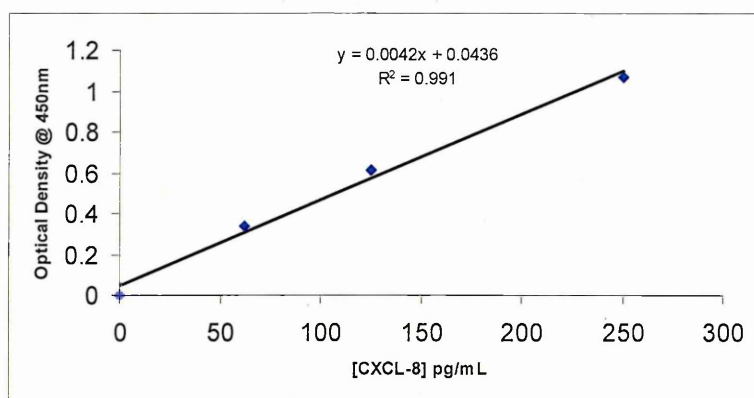


Figure 3.24: Typical standard curves used for the quantification of CXCL-8 in cell supernatants of CACO-2 cells.

Standard curves were generated by plotting the corrected average optical density of each concentration of the CXCL-8 standard as a function of Y-axis with CXCL-8 concentration as a function of X-axis.

3.2.3.6 Effects of drugs curcumin 1 and thiophene curcuminoids 47a-d on the production of CXCL-8 in cell supernatants of CACO-2 cells

The effects of the parent drug, curcumin **1**, and its thiophene curcuminoids **47a-d** on the production of CXCL-8 in the cell supernatants of CACO-2 cells are shown in figure 3.25. CACO-2 cells were treated as described in section 2.3.9.2. The controls i.e. cells alone and the DMSO (0.3% v/v) as well as the experimental samples i.e. drugs alone did not show detectable CXCL-8 in cell supernatants. A significant increase in the production of CXCL-8 was observed with DMSO+LPS+MS control compared to the LPS control.

In drug+MS+LPS stimulated cells, compared to the DMSO+LPS+MS (shown by *), curcumin **1** at its non-cytotoxic concentration of 10 μ M did not inhibit the production of CXCL-8 and the thiophene curcuminoids **47a-d** (10 μ M) also did not significantly affect the CXCL-8 production. At 50 μ M, drugs **47b** and **47d** significantly reduced the CXCL-8 production whereas at 100 μ M drugs **47a**, **47b** and **47d** significantly reduced the CXCL-8 production. The reduction in CXCL-8 production by curcumin **1** and **47c** at 50 and 100 μ M could be the result of the reduced cell viability.

In comparison to curcumin **1** (shown by *) at its non-cytotoxic concentration of 10 μ M, only drug **47c** (10 μ M) significantly reduced the CXCL-8 production.

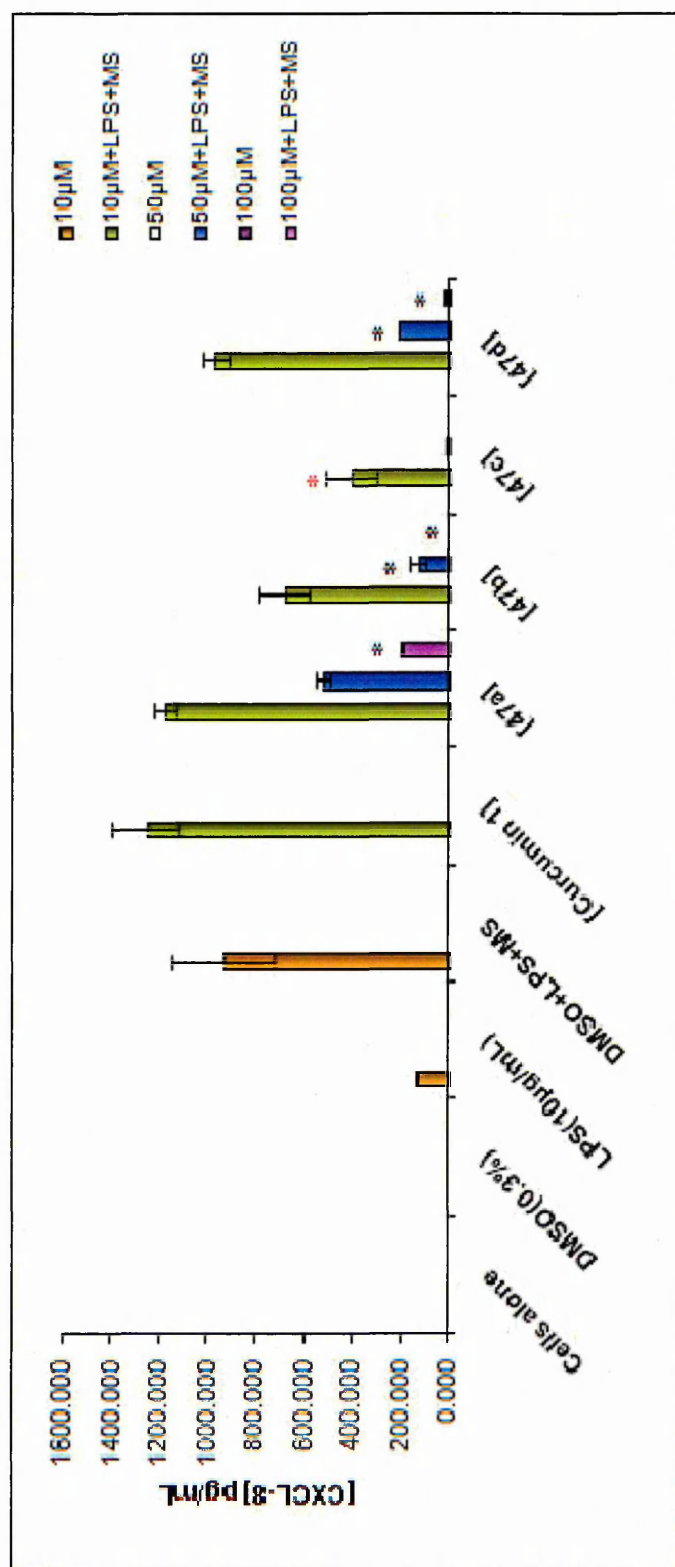


Figure 3.25: Results of the ELISA assay showing the effects of synthesised curcumin **1** and thiophene curcuminoids **47a-d** on the production of CXCL-8 in CACO-2 cells. CACO-2 cells were incubated in the absence or presence of the corresponding drugs at three different concentrations i.e. 10, 50 and 100 µM ± LPS and MS for 24h along with the appropriate controls. Results are expressed as mean ± SEM of two separate experiments (n=4). Shapiro-Wilk W test for non-normality followed by Kruskal-Wallis : Conover-Inman post-hoc test was used to determine significance. P value < 0.05 was considered as significant. * denotes the comparison of the drugs vs. DMSO + LPS + MS control. * denotes the comparison of the drugs vs. curcumin **1** control.

3.3 Discussion

Overall strategy

In the present study, two different cancer cell lines, the human monocytic leukaemia, THP-1 cells and the human caucasian colon adenocarcinoma-2, CACO-2 cells were used to evaluate :

- The cytotoxicity of synthesised curcumin **1**, its thiophene derivatives **47a-d** and nitric oxide donating derivatives **51a-d**.
- Their effects on the production of nitric oxide and pro-inflammatory cytokines (IL-1 β , TNF- α and CXCL-8), to assess whether these compounds possess anti-inflammatory properties.
- The cytotoxic effects of thiophene derivatives **47a-d** complexed with HP- γ -CD were also assessed using the THP-1 cells.

THP-1 monocytic cell line (figure 3.26a) was selected as an *in vitro* model which has been previously reported to be responsible for the production of pro-inflammatory cytokines (IL-1, TNF- α)¹⁹⁵ and nitric oxide NO¹⁹⁶, whereas CACO-2 cells (figure 3.26b) were used as a model cell-line, previously reported to be responsible for the production of pro-inflammatory cytokine CXCL-8.¹⁴¹ Also, CACO-2 cells is a well-established model to study the absorption and related mechanisms of the drugs¹⁹⁷ allowing oral administration. Since commercially available curcumin consists of a mixture of naturally occurring curcuminoids¹⁹⁸ with curcumin **1** as a main constituent; pure curcumin **1** was synthesised from vaniline.

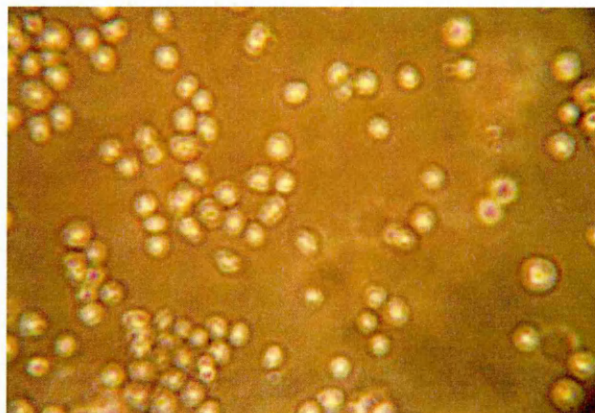


Figure 3.26a : The human monocytic leukaemia, THP-1 cells.

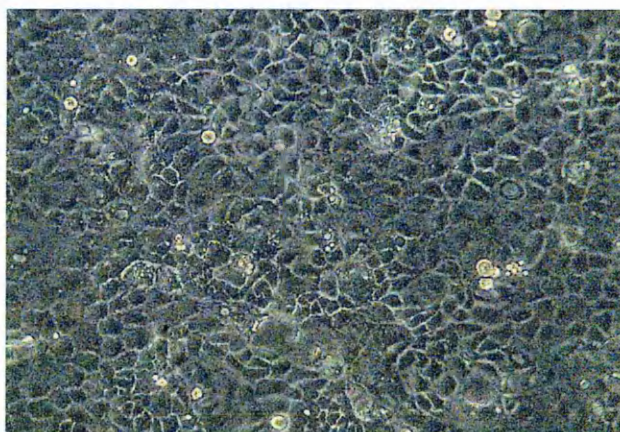


Figure 3.26b : The human caucasian colon adenocarcinoma-2, CACO-2 cells.

3.3.1 Cytotoxic effects

The aims of the cytotoxicity or viability (MTS) assays were:

- To determine cytotoxic effects of curcumin **1**, its nitric oxide donating derivatives **51a-d**, thiophene derivatives **47a-d** and HP- γ -CD complexed thiophene derivatives **47a-d** in order to ensure that the pharmacological effects exhibited by these drugs on the production of the reactive oxygen species, nitric oxide NO, pro-inflammatory cytokines (IL-1 β , TNF- α), chemokine (CXCL-8) were not due to reduced cell viability.
- To determine, whether the synthesised curcuminoids are more cytotoxic than the lead compound, curcumin **1** or not.

3.3.2 The Griess reagent assay or the ELISA

After evaluating the cytotoxic effects of the drugs, the reactive oxygen species nitric oxide NO released by the nitric oxide donating curcuminoids **51a-d** was measured using the Griess reagent assay. ELISA assays were undertaken to evaluate the effects of the synthesised thiophene curcuminoids **47a-d** on the production of pro-inflammatory cytokines, IL-1 β , TNF- α and CXCL-8. All experiments were aimed to evaluate:

- The effects of the drugs alone (without the stimulant LPS) on the production of nitric oxide NO or the respective cytokine (IL-1 β , TNF- α and CXCL-8) to

ensure that the drugs do not produce the NO or the cytokines being investigated.

- The effects of the drugs in cells stimulated with LPS. Cells were stimulated with LPS to mimic an inflammatory situation.

3.3.2.1 Cytotoxic and nitric oxide donating effects of curcumin 1 and nitric oxide donating curcuminoids 51a-d in THP-1 cells

The nitric oxide donating curcuminoids **51a-d** were synthesised by adding a nitroxybutyl moiety, which is covalently attached to the lead compound curcumin **1**. At first, cytotoxic effects of curcumin **1** and the nitric oxide donating curcuminoids alone were assessed compared with the DMSO control (as shown by *), and our findings shown in figure 3.14 clearly demonstrated that all the nitric oxide donating curcuminoids **51a-d** increased the cell viability or resulted in cell proliferation in concentration-dependent manner, and are non-toxic to THP-1 cells. Based on these findings the nitric oxide donating curcuminoids were next compared with curcumin **1** (shown by *) and it appeared from this comparison that at 10 μ M, all drugs were as non-toxic as curcumin **1** whereas at 50 and 100 μ M, the nitric oxide donating drugs were significantly more non-toxic than curcumin **1**.

From the structure-activity relationships, it appears that the replacement of both the phenolic hydrogens of curcumin **1** with the nitroxybutyl ether moiety, is in fact responsible for the enhanced non-cytotoxic property of these drugs. On the other hand, the presence of the methoxy group (-OCH₃) at the *meta* positions of the phenyl

rings (as in found in drug **1** and **51d** does not seem to be crucial, regarding the cytotoxic effects as it is evident that drugs **51a-c** (which do not possess any -OCH₃ groups) were as non-cytotoxic as **51d** even at 50 and 100μM. Furthermore, change in the position of the nitroxybutyl moiety (as shown in the structures of the drugs **51a-c**) also did not have any effect on cell viability.

In summary, our results show that all of the nitroxybutyl curcuminoids are non-toxic to THP-1 cells and are less cytotoxic than curcumin **1** at 10, 50 and 100μM concentrations and therefore can serve as potential nitric oxide donating NSAIDs in future.

Curcumin **1** possesses anti-proliferative activities against various tumor cells *in vitro* and has been reported to be a potent inhibitor of tumor initiation *in vivo*.¹⁹⁹ Curcumin **1** exerts its chemopreventive effects and inhibit tumor promotion via suppressing a number of key elements in cellular signal transduction pathways, predominantly, phosphorylation catalyzed by protein kinases, c-Jun/AP-1 activation and prostaglandin biosynthesis at a concentration range of 10 to 100μM.¹⁹⁹ *In vitro*, the main mechanism by which curcumin **1** blocks or suppresses the proliferation of a wide variety of cancer cells including leukaemia, colon carcinoma, breast carcinoma and other tumor cell types, is through the induction of apoptosis.¹³⁰ When compared with the DMSO control (shown as *), our findings are in complete agreement with the previous studies^{200,201,202} showing that the treatment of THP-1 cells for 24 h with curcumin **1** decreases the cell viability in concentration dependent manner. Figure

3.27 shows the effects of curcumin 1 on signal transduction pathways involved in apoptosis and cellular proliferation.

Describing the mechanism and signalling pathways involved in curcumin 1 induced cytotoxicity in THP-1 cells, Cheng et al²⁰² have recently shown that, in THP-1 cells, the curcumin 1 induced cytotoxic effects are mediated through apoptosis (programmed cell death) in a concentration and time dependent manner. Using flow cytometry (FCM) and mouse anti-human fluorescein isothiocyanate (FITC)-conjugated CD95 monoclonal antibody, the authors of the study have detected a 3-fold increase in the levels of cell surface protein Fas. Western blot analysis indicated that active caspase-8 and caspase-9 expression of myelocytic leukaemia cell lines increased after treatment with 25µM curcumin 1 for 24 h. These results indicated that curcumin 1 induced Fas expression in myelocytic leukaemia cells followed by intracellular Fas-associated death domain (FADD) clustering and its structure change, which linked with death effect domain (DED) of caspase-8 and initiated the caspase-9 cascade reaction, thereby confirming the role of the death receptor and mitochondria in curcumin induced apoptosis in myelocytic leukaemia cell line or THP-1 cells. Generally, *in vitro* in leukaemia cells, e.g. T-cell leukaemia cell lines, curcumin 1 has been shown to suppress the growth in a dose-dependent manner via various signalling mechanisms. Studying the mechanism of inhibition of cell proliferation by curcumin 1, Hussain et al²⁰⁰ investigated the effect of curcumin 1 on the activation of apoptotic pathway at the concentration range of 10, 20, 40 and 80µM for 24 h using four T-cell acute lymphoblastic leukaemia (T-ALL) malignant cells including CEM, HSB2,

Jurkat and Molt-4. The anti-proliferative effects of curcumin 1 were determined using the MTT assay, whereas, the TUNEL assay and assay for cytochrome c release were performed to measure apoptosis. The authors of the study have demonstrated that curcumin 1 causes a concentration dependent suppression of cell proliferation via suppressing the constitutively activated targets of P13'-kinase proteins (AKT, FOXO and GSK3) through de-phosphorylation or inactivation. Curcumin inhibits 1 the AKT phosphorylation at Ser473 and Thr308 amino acids, accompanied with the release of cytochrome c from mitochondria into the cytoplasm, suggesting a link between mitochondria and curcumin 1 induced cell growth inhibition of T cells. Curcumin 1 induced release of cytochrome c leads to the activation of the downstream caspases-9 and caspases-3 and the down-regulation of survival proteins including caspase-inhibitor of apoptosis protein (cIAP1), X-linked inhibitor of apoptosis protein (XIAP) and survivin that result in the cell death. Another mechanism involved in curcumin 1 induced cell growth has been proposed by Rajasingh et al²⁰¹, who have demonstrated that treatment with curcumin 1 induced a dose dependent decrease in the Janus family of kinase (JAK) and signal transducer and activator of transcription (STAT) phosphorylation, resulting in the induction of growth-arrest and apoptosis in T- cell leukaemias. Using the MTT assay, the authors of the study have shown that in human T cell lymphotropic/leukaemia virus type 1 (HTLV-1) transformed leukaemia cell lines MT-2, Hut-102 and SLB-1, curcumin 1 at the concentration range of 0, 1, 5 and 10µg/mL inhibits the growth in a concentration dependent manner. In order to confirm that curcumin 1 mediated cytotoxicity occurs through apoptosis, Rajasingh et al²⁰¹, have demonstrated that in agarose gel electrophoresis and in TUNEL assay, a

dose-dependent increase in DNA fragmentation following treatment with curcumin 1 for 48 h occurs. Using the immunoprecipitation method they have further shown that curcumin 1 blocks the constitutive phosphorylation of JAK3, TYK2, STAT3 and STAT5A growth signaling proteins within 30 minutes in a dose dependent manner. In MT-2 and HuT-102 cell lines, curcumin 1 at 10µg/mL significantly reduced the phosphorylation of STAT5A protein, which was completely inhibited after treatment with 25µg/mL. In contrast to this, in SLB-1 cells a partial inhibition of STAT5A was observed. Treatment with curcumin 1 also resulted in a dose-dependent decrease in the constitutive phosphorylation of STAT3 in MT-2 and SLB-1 cells. While at 5 and 10µg/mL curcumin 1 resulted in partial inhibition, treatment with 25µg/mL curcumin 1 completely inhibited STAT3 phosphorylation. Similarly, in the case of TYK2 proteins, a partial inhibition was observed at 10µg/mL curcumin 1 which completely disappeared after treatment with 25µg/mL, however, with JAK3 proteins; curcumin 1 induced partial inhibition of the phosphorylation at 10µg/mL, which completely disappeared after treatment with 25µg/mL for 30 minutes in MT-2 and SLB-1 cells, whereas, the HuT-102 cells expressed no detectable level of JAK3 phosphoproteins. These data suggest the role of JAK-STAT pathway as an effective target in the treatment of T cell leukaemia.

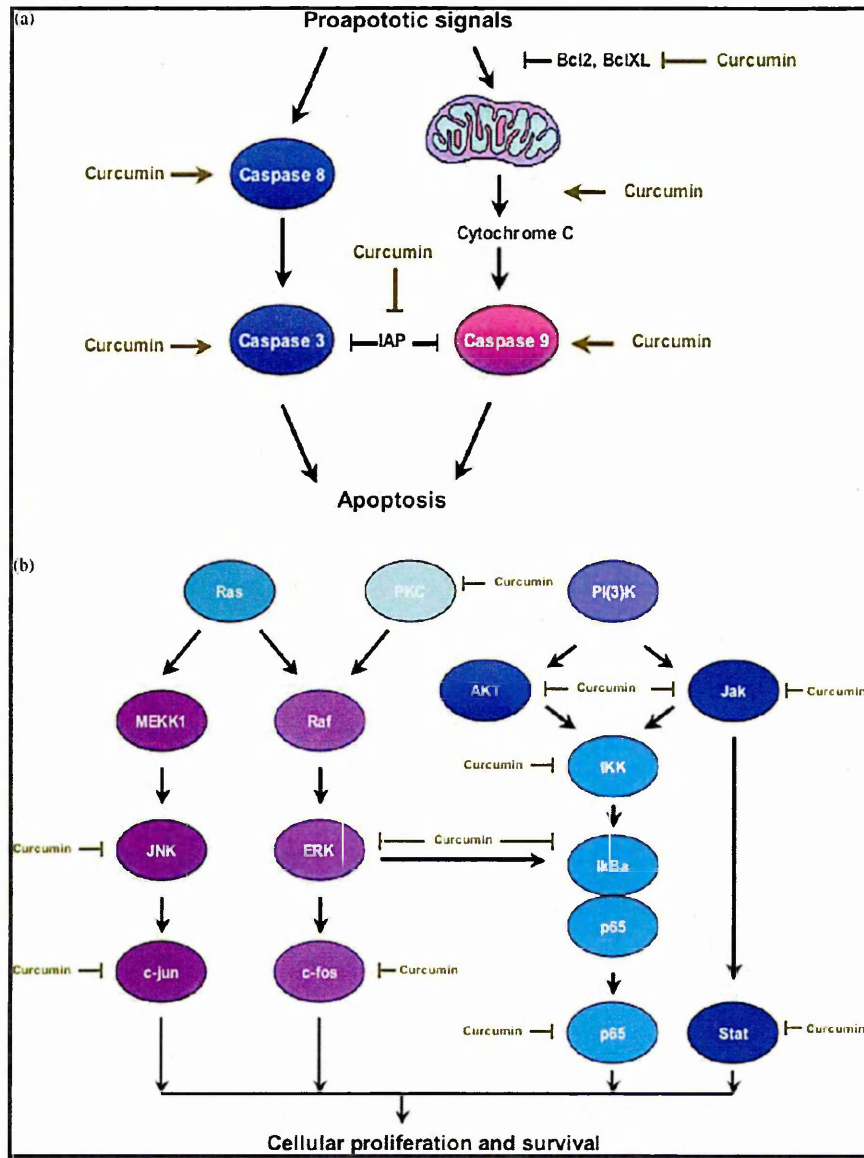


Figure 3.27: Signal transduction pathways affected by curcumin 1 treatment leading (a) to controlled cell death or (b) to cellular proliferation and survival.²⁰³

Nitric oxide NO exhibits a dual effect on cell viability; as various studies have shown that it can be cytotoxic as well as cytoprotective.²⁰⁴ Based on our findings, the cytoprotective effects of NO are the main focus of this discussion.

NO-donating aspirin (**9**, figure 1.8A) is chosen as an example to help understand the possible mechanism that could be involved in the cytoprotective effects of these nitroxy butyl curcuminoids **51a-d**. The intracellular donation of NO followed by the regulation of respiratory chain, coupled with an inhibition of the activation on pro-apoptotic caspases²⁰⁵ and the prevention of the opening of the permeation transition pore of the cell membrane to inhibit cytochrome *c* release⁸⁸ are the various events that have been reported to explain the cytoprotective effects of **9**. Using a mitochondria-dependent model of apoptosis in human umbilical endothelial cells (HUVEC), Fiorucci et al⁸⁸ have demonstrated that **9** modulates cell respiration and mitochondrial function and protects cells against death caused by staurosporine **25** (an apoptotic agent, figure 1.12) by modulating intracellular mediators associated in the apoptotic cascade (figure 3.29). They first confirmed that **9** generates NO and results in hyperpolarization of the mitochondrial membrane potential ($\Delta\psi_m$). A time and concentration-dependent intracellular formation of NO was recorded in cells treated with **9** at 1-500 μ M or 10-100 μ M using the confocal microscope and DAF-DA **87** (figure 3.28). The highest concentrations of NO generated were observed in specific sub-cellular compartments localized near the plasma membrane. These results were further validated by the findings that no significant increase in DAF-DA **87** related fluorescence was observed in cells exposed to aspirin. Flow cytometry was used to

measure the hyperpolarization of the mitochondrial membrane potential ($\Delta\psi_m$). In the absence of apoptogenic stimuli, a concentration-dependent hyperpolarization was observed, however, exposure of the HUVEC cells to staurosporine **25** resulted in time and concentration-dependent decrease in cell viability which was due to the mitochondrial damaged and resulted in the early collapse of the $\Delta\psi_m$ whereas, addition of **9** protected the mitochondrial depolarization caused by staurosporine **25**, as significant hyperpolarization was observed when staurosporine **25** treated cells were exposed to **9** (500 μ M). The hyperpolarization caused by **9** was due to the NO-releasing moiety of the molecule, as no hyperpolarization was observed with aspirin at 500 μ M. The translocation of cytochrome *c* from the mitochondrial inner space to the cytosol (the intrinsic pathway of apoptotic progression) with staurosporine **25**, was also inhibited by **9** and not by aspirin. Exposure of staurosporine **25** treated cells to **9** (1-500 μ M) for up to 8 h also inhibited the caspase-8 and 9 activity in concentration-dependent manner. Collectively these findings suggest that **9** penetrates into the endothelial cell membrane, releases NO and dynamically regulates mitochondrial function that result in protection against cell injury.⁸⁸

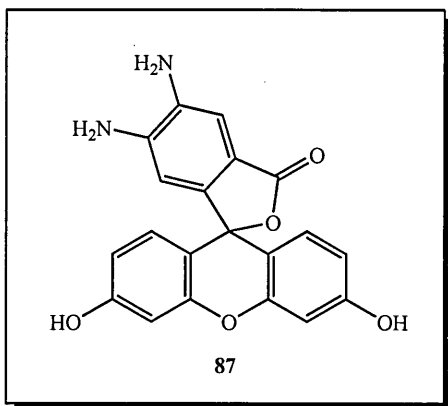


Figure 3.28 : Chemical structure of DAF-DA **87** (diamino difluorescein diacetate).²¹⁸

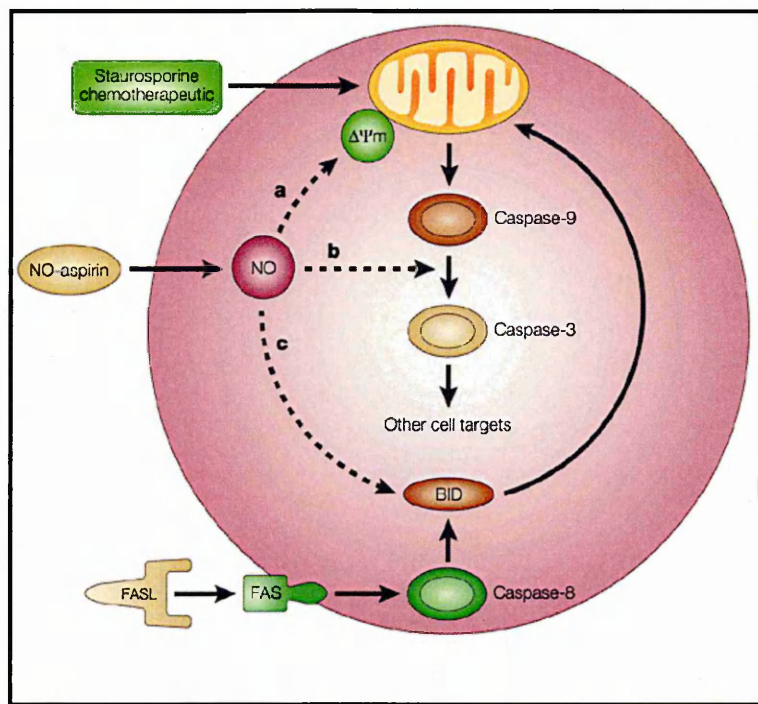


Figure 3.29 : Anti-apoptotic effects of NO-aspirin 9.⁸⁶

NO-aspirin 9 inhibits death-factor-induced apoptosis (intrinsic pathway), and apoptosis caused by agents (staurosporine, chemotherapeutics) that directly damage the mitochondrion (extrinsic pathways). NO-aspirin 9 inhibits apoptosis by acting at different points in the apoptotic pathway. (a) NO-aspirin 9 increases the mitochondrial membrane potential ($\Delta\Psi_m$). (b,c) NO-aspirin 9 directly inhibits caspase activity by causing *S*-nitrosylation of cysteine residues in the catalytic core of these enzymes. Crosslinking of cell-surface death receptors by FAS ligand (FASL) or TNF- α activates caspase-8. NO-aspirin 9 inhibits caspase-8 (through *S*-nitrosylation), thereby preventing the cleavage of pro-BID. BID is a pro-apoptotic member of the BCL2 family that, once activated, causes mitochondrial membrane depolarization.

After the evaluation of the cytotoxic effects of the drugs **51a-d**, the measurement of their nitrite production was assessed. For this purpose, firstly, the effects of the drugs alone were evaluated in the cell supernatants of THP-1 cells not stimulated with LPS. Results presented in figure 3.19a, show that all of the nitric oxide donating derivatives of curcumin enhanced the nitric oxide production except drug **51c**. **51a** and **51d** enhanced the production of NO in concentration dependant manner whereas **51b** showed a significant effect at 10 and 100 μ M. These results were consistent with the cytotoxicity results and the effects exhibited by the drugs were solely their own effects and were not due to the cell viability. In comparison with curcumin **1** at its non-cytotoxic concentration of 10 μ M, only drug **51b** showed a significant increase in nitrite production.

The release of the nitric oxide from these nitric oxide donating drugs **51a-d** was further confirmed in the cells stimulated with LPS. Here also, the effects were similar as the effects of the drugs **51a** and **51d** in non-stimulated cells, however drug **51b** equally produced NO at 10, 50 and 100 μ M and **51c** was effective at 100 μ M only.

From the structure activity relationship studies, it is appropriate to conclude that the replacement of the phenolic hydrogen of the curcumin **1** with nitroxybutyl ether moiety, significantly lowers the cytotoxic effects and results in an enhanced nitric oxide releasing activity.

3.3.2.2 Effects of curcumin 1 and the thiophene curcuminoids 47a-d on the viability and IL-1 β production in THP-1 cells

Using the MTS assay, the cytotoxic effects of the synthesised curcumin **1** and its thiophene analogues **47a-d** were studied (figure 3.15). The thiophene analogues of curcumin **47a-d** were synthesised by replacing both the phenyl rings of the lead compound **1** with aromatic sulphur containing heterocycles, the thiophene or substituted thiophene rings. The cytotoxicity studies reveal that curcumin **1** was non-toxic to THP-1 cells only at 10 μ M concentration, however, drug **47a** was non-toxic to the cells at all the three concentrations studied i.e. 10, 50 and 100 μ M, similarly, drug **47d** was non-toxic at 10 and 50 μ M. On the other hand, drugs **47b** and **47c** were appeared to be non-toxic at 10 μ M only.

Regarding the structure-activity relationships, very important conclusions can be drawn from these studies. As shown in figure 3.15 it can be concluded that the replacement of both of the phenyl rings of the curcumin **1** with that of thiophene rings resulted in lesser cytotoxic effects. Among all the four thiophene curcuminoids, however drugs **47b** and **47c** which are the methyl substituted derivatives of **47a** at 3 or 5 positions respectively, show significant ($P < 0.05$) cytotoxic effects in concentration-dependent manner, rendering the methyl group being responsible for the cytotoxic effects. On the other hand, **47d**, which is a positional isomer of **47a**, also appeared to be less cytotoxic than **47b** and **47c**, which further confirms that there is a possibility of methyl group to be involved in the induction of cytotoxic effects associated with these derivatives. In comparison with the curcumin **1** shown by *, only thiophene curcuminoids **47a** and **47d** at 10 μ M, were as non-cytotoxic as curcumin **1**. On the other hand, the methyl substituted thiophenes curcuminoids **47b**

and **47c** at 10 μ M appeared more cytotoxic than curcumin **1** therefore their role as anti-inflammatory drugs needs further evaluation using non-cancerous cell lines. Since **47b** and **47c** at their lowest concentration (10 μ M) are more toxic than curcumin **1**, these can serve as potential anticancer drugs.

Thus although the mechanism of cell death was not investigated in this study, in the view of the findings described above, we can hypothesize that apoptosis could be the main mechanism involved in the thiophene induced cytotoxic effects in THP-1 cells.

After the confirmation of the cytotoxic effects of the drugs, their effects on the production of pro-inflammatory cytokine IL-1 β were evaluated using the ELISA assay.

IL-1 β , a pro-inflammatory cytokine, is one of the cytokines involved in various inflammatory processes, and has been reported to exhibit its inflammatory effects through its ability to induce the expression of genes associated with inflammatory and autoimmune diseases, and, elevated IL-1 β levels have been reported during intestinal inflammation in mammals, which suggest an important role of this cytokine in inflammatory diseases associated with the gastrointestinal tract.¹³⁷ The beneficial role of curcumin **1** in prevention of inflammatory bowel disease (IBD) is well documented and various studies have shown that it attenuates experimental colitis in rats²⁰⁶ and murine²⁰⁷ models of IBD. Furthermore, curcumin **1** has also been reported to reduce the LPS stimulated production of IL-1 in human peripheral blood monocytes and alveolar macrophages in concentration and time dependent manner.¹⁰⁰ Based on these

findings, we investigated the role of synthesised curcumin **1** and its thiophene analogues **47a-d** on IL-1 β production in THP-1 cells. The results presented in figure 3.21 provide evidence that curcumin **1** at 10 μ M, **47a** and **47d** significantly decreased the IL-1 β production in concentration dependent manner in THP-1 cells stimulated with LPS. On the other hand in the case of drugs **47b** and **47c** the decreased effect of IL-1 β production exhibited at 10 μ M was also significant. In comparison with curcumin, at 10 μ M all drugs were as potent as curcumin **1**.

In summary, these results were in complete accord with the cytotoxicity results, and hence it can be concluded that these effects are not due to the reduced cell viability.

The thiophene curcuminoids **47a** from 10 to 100 μ M and **47d** at 10 to 50 μ M range appeared to be potential candidates with enhanced activity and low cytotoxicity for future anti-inflammatory drugs that inhibit IL-1 β production in THP-1 leukaemia cells.

Recently, Hsu et al²⁰⁸ have demonstrated that curcumin **1** mediated down regulation of LPS-induced IL-1 and IL-6 expression in THP-1 monocytic cells occurs through a mechanism that involves the induction of heme-oxygenase-1 enzyme (HO-1).

Studying the mechanism of suppressive effect of curcumin **1** on LPS-induced IL-1, IL-6 and TNF- α in THP-1 monocytes, Hsu et al²⁰⁸ have shown that stimulation of THP-1 cells with LPS for 24 h resulted in a significant increase in IL-1, IL-6 and TNF production. They then confirmed that pre-incubation of human THP-1 monocytes with curcumin **1** (10 μ M) inhibited LPS-induced IL-1, IL-6 and TNF

production suggesting that curcumin 1 inhibits the production of these pro-inflammatory cytokines in THP-1 cells. The authors of the study have further assessed the potential role of HO-1 involved in the inhibition of LPS-induced cytokine production, using an inhibitor of HO-1, the tin protoporphyrin (SnPP), as well as an inducer of HO-1 enzyme, the cobalt protoporphyrin (CoPP). Pre-incubation of THP-1 cells with SnPP reversed the inhibitory effects of curcumin 1 on IL-1 and IL-6 production only and not on TNF. Similarly, pre-incubation of cells with CoPP could not reverse the inhibitory effect of curcumin 1 on IL-1 and IL-6 secretion suggesting that HO-1 is involved in curcumin 1 mediated down regulation of IL-1 and IL-6 production within THP-1 monocytes. In order to confirm the role of HO-1 in curcumin 1 mediated suppression of LPS stimulated IL-1 and IL-6 in THP-1 cells, Hsu et al²⁰⁸ have also studied the gene expression of HO-1, using small interfering RNA (siRNA) and pcDNA3.1 vector. The curcumin 1 induced HO-1 expression was reduced by transfection of cells with siRNA specifically targeting HO-1, however the HO-1 expression in curcumin 1 stimulated cells was not reduced by transfecting the cells with negative control of siRNA. Transfection of cells with HO-1 siRNA and not the negative control of siRNA reversed the inhibition of curcumin 1 on cytokine secretion from LPS stimulated cells. The over-expression of HO-1 within THP-1 cells resulted in a decrease in LPS-induced secretion compared to the case for pcDNA3.1. The involvement of various signalling pathways that are responsible for the regulation of curcumin 1 induced HO-1 expression, i.e. pα, P13-Kinase, PKCα, PKCδ/ERK1/2 and H₂O₂ has been proposed in figure 3.30.

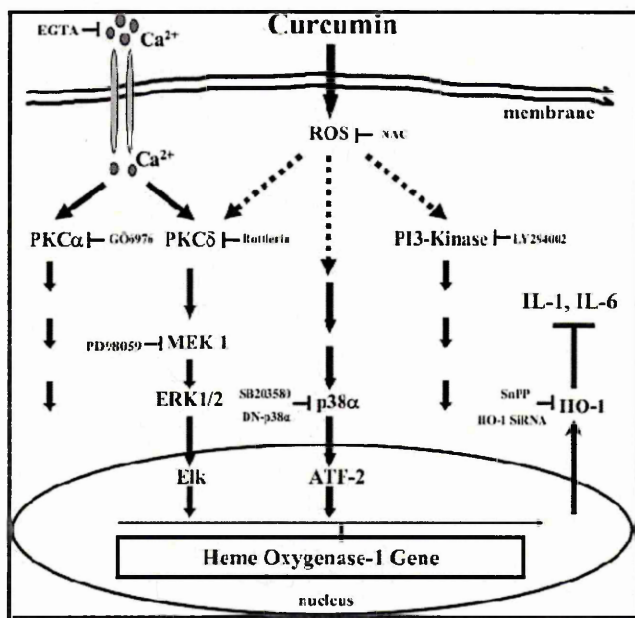


Figure 3.30 : Proposed signalling pathway related to curcumin 1 induced HO-1 gene expression within THP-1 monocytes.²⁰⁸

3.3.2.3 Effects of curcumin 1 and the thiophene curcuminoids 47a-d on the viability and production of TNF- α in THP-1 cells

The cytotoxic effects of curcumin **1** and drugs **47a-d**, using the MTS assay, are shown in figure 3.15. Thus, after the evaluation of the cytotoxic effects of the drugs, their effects on the production of pro-inflammatory cytokine TNF- α were studied using the ELISA assay.

Tumour necrosis factor- α (TNF- α) is a potent pro-inflammatory cytokine that is primarily produced by monocytes and macrophages and is implicated in a variety of chronic inflammatory diseases such as rheumatoid arthritis (RA), inflammatory bowel disease, psoriasis and Crohn's disease.²⁰⁹ The reports on the effects of curcumin **1** induced TNF- α inhibition in THP-1 cells are scarce.

TNF- α exhibits its inflammatory effects via the major transcription factor, nuclear factor- κ B (NF- κ B). Binding of TNF- α to its receptors leads to the activation of nuclear factor- κ B (NF- κ B).²¹⁰ Activation of NF- κ B by pro-inflammatory stimuli or cytokines such as TNF- α , leads to the expression of genes that induce and maintain inflammation²¹¹, and due to the fact that increased nuclear translocation of NF- κ B has been reported in a wide range of disease states including endotoxin-induced sepsis, malignancy and chronic inflammatory disorders such as rheumatoid arthritis, asthma, ulcerative colitis²¹² the search for pharmacological inhibitors that block NF- κ B induced transcription is ongoing. Under normal conditions, NF- κ B resides in its inactive form in the cytoplasm as a heterotrimer consisting of p50, p65 and I κ B α .

subunits, however upon activation, I κ B α subunit undergoes phosphorylation and ubiquitination-dependent degradation by the 26S proteasome, thus exposing nuclear localization signals on the p50-p65 heterodimer, resulting in nuclear translocation and binding to a specific consensus sequence in the DNA which in turn activates gene expression and ultimately results in gene transcription.²¹³ Curcumin **1** has been reported to inhibit LPS-induced production of TNF- α in human monocytic macrophage cell line Mono Mac 6.²¹⁴

As shown in figure 3.23, during the course of these experiments, in order to evaluate the effects of the drugs alone, the cells were treated with the drugs only in the absence of LPS. Thiophene curcuminoids **47a-d** as well as curcumin **1** alone did not produce any TNF- α at all the three concentration studies i.e. 10, 50 and 100 μ M. However, treatment of LPS stimulated cells with curcumin **1** for 24 h showed a concentration-dependent decrease in TNF- α production, however the effects appeared to be significant only at 50 and 100 μ M which might be due to the cytotoxic effects of curcumin **1** at these concentrations (figure 3.15). Furthermore, the thiophene curcuminoids **47a-d** at their non-cytotoxic concentrations (figure 3.15) did not inhibit TNF- α production in LPS stimulated cells.

In conclusion, our results demonstrate that substitution of both the phenyl rings of the lead compound curcumin **1**, either with thiophene rings as in the case of **47a** and **47d** or with the methyl-substituted thiophenes **47b** and **47c** did not result in inhibition of LPS induced TNF- α production in THP-1 leukaemia cell lines, however their effects as anti-inflammatory drugs needs further investigation using non-cancerous cell lines.

3.3.2.4 Effects of curcumin 1 and the thiophene curcuminoids 47a-d on the viability and production of CXCL-8 in CACO-2 cells

The aim of the present study, was to evaluate the cytotoxic effects and to study the effects of the drugs **47a-d** and the parent drug curcumin **1** on the production of pro-inflammatory cytokine CXCL-8 using the human colon adenocarcinoma cell line CACO-2 cells. As mentioned earlier, CACO-2 cells were chosen because of their well established role as an *in vitro* model used to determine the transport characteristics and cytotoxic effects of drugs, and to design formulation strategies for membrane permeability enhancement.²¹⁵ The advantage associated with the use of CACO-2 cells over other gastrointestinal cell lines, is that these cells show a spontaneous differentiation pathway in long term culture conditions and express several morphological and biochemical characteristics of small intestinal enterocytes.²¹⁶ The pro-inflammatory cytokine CXCL-8, has been reported to play crucial roles in various pathological conditions such as chronic inflammation and cancer as well as acts as a key mediator in neutrophil mediated acute inflammation due to its potent action on neutrophils.¹⁴⁰ The low incidence of colon cancer in Asian countries could be related to low meat intake, but may also be attributed to the regular use of turmeric in the diet of these regions.²¹⁷

In evaluating the cytotoxic effects of the drugs alone, using MTS assay, our results shown in (figure 3.16), have revealed that curcumin **1** and the thiophene derivative **47c** reduced the cell viability in concentration dependent manner. Curcumin **1** and all its synthesised thiophene derivatives **47a-d** appeared to be non-cytotoxic at 10 μ M

concentration. At 50 μ M concentration, drugs **47b** and **47d** were non-toxic. On the other hand, at 100 μ M, curcumin **1** and **47c** were cytotoxic. In comparison to curcumin **1** at 10 μ M, all of the synthesised derivatives were as non-toxic as curcumin **1**, however, at 50 μ M all drugs showed non-significant cytotoxic effects similar to curcumin **1**. At 100 μ M, concentration, a significant increase in cell viability was observed with drugs **47a**, **47b** and **47d**.

After determining the cytotoxic effects of the drugs, their effects on the production of CXCL-8 were evaluated. L-methionine sulfoximine (MS) in conjunction with LPS, was used based on the findings of Huang et al.¹⁶³ al who have demonstrated that in CACO-2 cells the largest amount of CXCL-8 was secreted by cells in the presence of MS with no glutamine in the medium. As shown in figure (3.25), a 9 fold increase in the production of CXCL-8 was observed in the cells treated with MS along with LPS compared with the cells treated with LPS alone, thus confirming the findings of Huang et al.¹⁶³

Curcumin **1** at its non-cytotoxic concentration of 10 μ M, did not inhibit the production of CXCL-8, however, **47a** at 100 μ M and **47b** and **47d** at 50 and 100 μ M showed significant decrease in CXCL-8 production. In comparison to curcumin **1** at 10 μ M only drug **47c** significantly reduced CXCL-8 production.

Since curcumin **1** was cytotoxic to cells at 50 and 100 μ M concentration, the non-detectable levels of CXCL-8 at these concentration of curcumin **1** are due to the reduced cell viability. Based on these cytotoxic effects of curcumin **1**, it was not

appropriate to further compare the effects of thiophene derivatives **47a-d** at 50 and 100 μ M with curcumin **1**.

From the structure-activity relationship, these studies show that the replacement of both of the phenyl rings of curcumin **1** with (un)substituted thiophene rings reduces the cytotoxic effects of curcumin **1**, however, the effect of this finding on the production of CXCL-8 needs further evaluation.

CHAPTER 4

CONCLUSION

Various inflammatory diseases like rheumatoid arthritis provide drug discoverers with a tremendous challenge as these diseases are currently being treated with relatively old drugs such as non-steroidal anti-inflammatory drugs (NSAIDs), corticosteroids and methotrexate which have limited efficacy and / or inadequate safety profile.²¹⁹ Also, the long-term use of NSAIDs, is associated with serious gastrointestinal complications.²²⁰ Based on the previous findings describing the beneficial role of curcumin **1** in inflammation as well as its protective effects on gastrointestinal tract, the overall aim of the project presented in this thesis was to develop new curcuminoids that would have better efficacy and lower side effects than the conventional NSAIDs. The overall strategy of the project was to synthesise and characterise the following three types of curcumin derivatives (chosen based on their well established protective effects on gastrointestinal tract or as an anti-inflammatory agent), and to test the effects of these curcuminoids on the production of nitric oxide, pro-inflammatory cytokines IL-1 β , TNF- α and CXCL-8 using two cancer cell lines i.e. THP-1 cells and CACO-2 cells.

The curcuminoids of interest were:

- Nitric oxide donating curcuminoids
- Thiophene and furan derived curcuminoids
- Benzofuran and benzothiophene curcuminoids

In total we have successfully synthesised 15 curcuminoids as well as the lead compound curcumin **1** and spectroscopically characterised them, however the yields obtained were not very brilliant.

The nitric oxide donating curcuminoids **51a-d** were synthesised in three steps. In the first step bromobutoxybenzaldehydes **45a-d** were prepared by the Williamson ether synthesis and were next subjected to curcumin synthesis using Pabon's method to obtain bromobutoxy curcuminoids **46a-d**. In the third step, the nitration of compounds **46a-d** was performed to yield the desired nitric oxide curcuminoids **51a-d**. Using the MTS assay the cytotoxic effects of the synthesised nitric oxide curcuminoids were determined and two comparisons were made. First the drugs were compared with the vehicle (DMSO 0.3 v/v) control and then with the lead compound curcumin. Our results show that nitroxybutyl curcuminoids are non-toxic to THP-1 cells and are less cytotoxic than curcumin at 10, 50 and 100 μ M concentrations and all of them except **51c** (in unstimulated THP-1 cells) enhanced the production of nitric oxide in LPS stimulated or unstimulated cells therefore can serve as potential nitric oxide donating NSAIDs in future.

Synthesis of aromatic heterocyclic curcuminoids **47a-d** and **48a-c** was also performed and reaction resulted in moderate yield. The cytotoxic effects of the thiophene curcuminoids **47a-d** were determined using the MTS assay and then their effects on the production of IL-1, TNF- α and CXCL-8 were evaluated using human leukaemia cell line THP-1 cells and human colon cancer cells respectively.

The thiophene curcuminoids **47a** was non-cytotoxic to THP-1 cells at 10, 50 and 100 μ M and **47d** appeared to be non-cytotoxic at 10 and 50 μ M, whereas, **47b** and **47c** were non-cytotoxic at 10 μ M only. When compared with curcumin **1**, at 10 μ M, **47a** and **47d** were as non-cytotoxic as curcumin, however, **47b** and **47c** were more

toxic than curcumin. In CACO-2 cells, **47b** and **47d** appeared to be non-toxic at 10 to 100 μM , whereas, **47a** was non-toxic at 10 and 100 μM and **47c** was non-cytotoxic at 10 μM only.

These results clearly indicate that the introduction of a nitroxybutyl moiety to curcumin and the replacement of both of the phenyl rings of the curcumin with unsubstituted thiophenes reduces the cytotoxic effect of the parent curcumin **1**, whereas, methyl substituted thiophene increase the cytotoxic effects. In THP-1 cells, drugs **47a-d** significantly decreased the IL-1- β production at their non-cytotoxic concentrations, whereas, did not decrease the TNF- α production. For the effects on CXCL-8 in CACO-2 cells, **47a** at 100 μM and **47b** and **47d** at 50 and 100 μM showed significant decrease in CXCL-8 production. In comparison to curcumin **1** at 10 μM only drug **47c** significantly reduced CXCL-8 production.

The synthesis of fused-ring aromatic heterocyclic curcuminoids **57b** and **61** was carried out via two different routes however both the methods resulted in poor yields. On the other hand in case of nitrogen derived curcuminoids **63**, **65** and **69** no product was obtained at all. New method for the synthesis of curcuminoids using Claisen condensation reaction was tried but complete evidence of curcumin formation was not achieved, hence a new strategy for the formation of curcumin based on Claisen and Heck type reaction is being proposed.

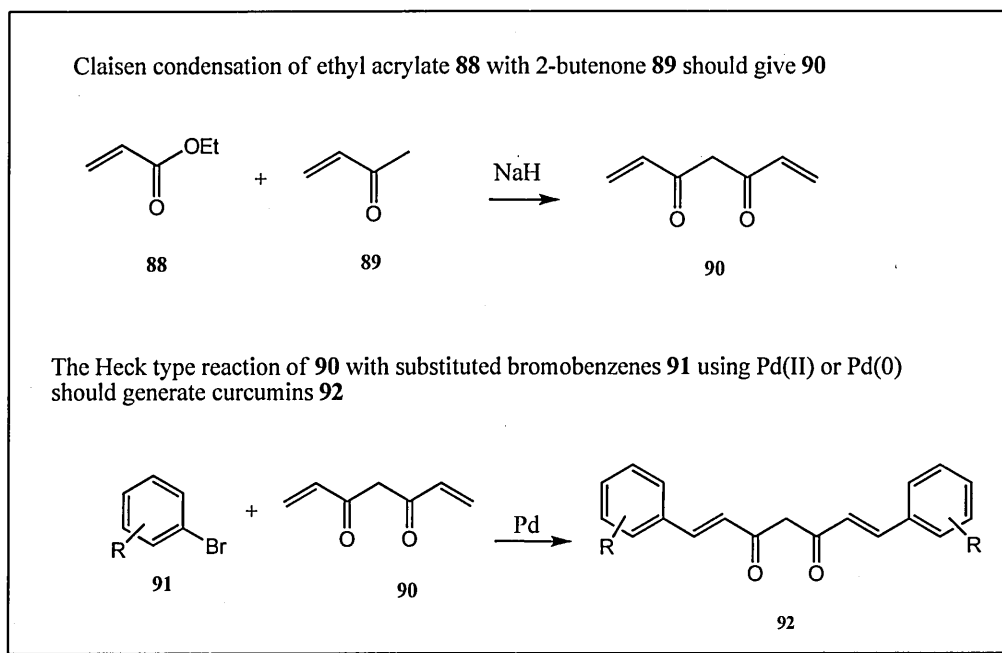
CHAPTER 5
FUTURE WORK

Part A : Chemistry

As evident from our results as well as those reported by others, that, the major drawback of Pabon's method¹⁴⁴ of curcumin synthesis is that it often results in low yields. Therefore, in future it would be worthwhile finding a new method for curcumin synthesis that can give better yields.

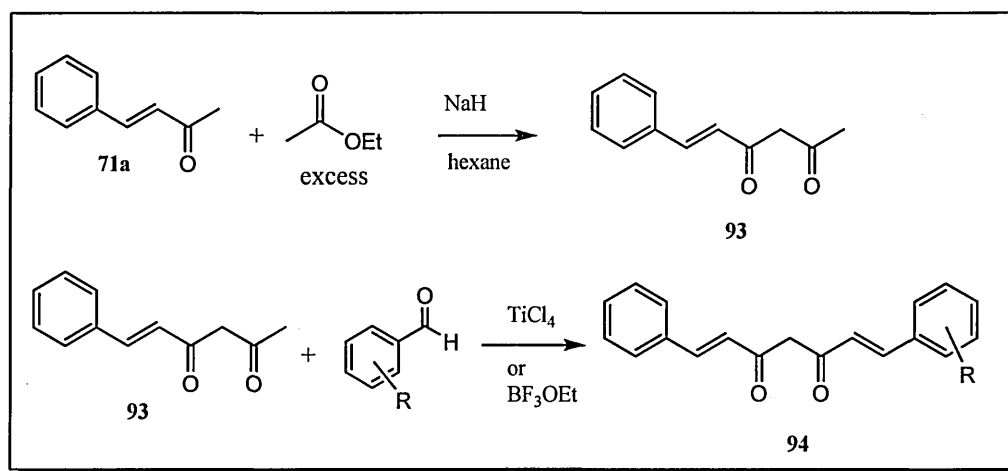
Thus, the following two synthetic strategies depicted in schemes 5.1 and 5.2 could be used in search of better synthetic method for curcumin preparation.

The proposed synthesis of curcumin formation outlined in scheme 5.1 involves two known reactions i.e. the Claisen condensation reaction and the Heck-type reaction.²²¹ However, the success of this strategy relies on the formation of the key precursor **90** for the double Heck type reaction to occur to give curcumin derivative **92**.



Scheme 5.1 : New proposed strategy for curcumin synthesis using Heck-type reaction.

In scheme 5.2 the product **93** obtained by the reaction of benzylideneacetone **71a** could be reacted with a variety of aldehydes to synthesise unsymmetrical curcumin derivatives **94**. Also, it would be interesting to try the same strategy in conjunction with Pabon's method too, for the synthesis of unsymmetrical curcumins.



Scheme 5.2 : New proposed strategy for curcumin synthesis

Part B : Pharmacology

Nitric oxide donating curcuminoids 51a-d :

- Based on the findings generated from this study that nitric oxide donating curcuminoids **51a-d** possess non-cytotoxic effects as well as are non-cytotoxic in comparison with the parent compound curcumin **1**, in human leukaemia monocytic cell line THP-1 cells at the concentration range of 10 to 100 μ M, it would be interesting to evaluate their cytotoxic effects in non-cancerous cells lines.
- We have shown that these nitric oxide donating curcuminoids enhance the nitric oxide production in THP-1 cells in the presence of LPS (an inducer of NO), this could be further confirmed using various inhibitors of nitric oxide.
- It would also be worth while, looking at the effects of nitric oxide donating curcuminoids **51a-d** on the production of pro-inflammatory cytokines in THP-1/CACO-2 cells as it can be postulated that the NO derivatives could be more potent inhibitors of cytokine production, especially IL-1 β and TNF- α , since it is known that these cytokines are negatively regulated by NO.

Thiophene derived curcuminoids 47a-d

- The thiophene derived curcuminoids **47a** and **47d** appeared to be the potential candidates as future non-steroidal anti-inflammatory drugs, as these are non-cytotoxic to THP-1 cells as well as to CACO-2 cells, therefore, it can be postulated to evaluate their effects in non-cancerous cells lines.

- The pharmacological studies conducted in this thesis have also revealed that thiophene curcuminoids **47a** and **47d** inhibit the production of pro-inflammatory cytokine IL-1 β and CXCL-8 in concentration dependent manner, therefore, it is suggested to further evaluate their effects on the production of IL-1 β using chondrocytes as a model of arthritic diseases.

REFERENCES

1. WYSS-CORAY, T. and MUCKE, L. (2002). Inflammation in neurodegenerative disease-A double-edged sword. *Neuron*, **35**, 419-432.
2. SEBBAN, H. and COURTOIS, G. (2006). NF- κ B and inflammation in genetic disease. *Biochemical Pharmacology*, **72**, 1153-1160.
3. LAWRENCE, T. (2007). Inflammation and cancer: A failure of resolution? *Trends in Pharmacological Sciences*, **28**, 162-165.
4. CIRINO, G., FIORUCCI, S. and SESSA, W. C. (2003). Endothelial nitric-oxide synthase: The cinderella of inflammation? *Trends in Pharmacological Sciences*, **24**, 91-95.
5. BOCHNER, B. S. (2000). Road signs guiding leukocytes along the inflammation superhighway. *The Journal of Allergy and Clinical Immunology*, **106**, 817-828.
6. BABICH, J. W. and FISCHMAN, A. J. (1999). Targeted imaging of infection. *Advanced Drug Delivery Reviews*, **37**, 237-252.
7. CORTAN, R. S., KUMAR, V., ROBBINS, S. L. (1994). *Pathological Basis of Diseases*, Saunders company, Philadelphia, 51-92.
8. <http://www.octc.kctcs.edu/GCaplan/anat2/notes/Image449.gif>
9. KAMINSKA, B. (2005). MAPK signalling pathways as molecular targets for anti-inflammatory therapy- From molecular mechanisms to therapeutic benefits. *Biochimica et Biophysica Acta (BBA) - Proteins & Proteomics*, **1754**, 253-262.
10. FUNK, C. D. (2001). Prostaglandins and leukotrienes: Advances in eicosanoid biology. *Science*, **294**, 1871-1875.
11. <http://nic.sav.sk/logos/books/scientific/node25.html>
12. ZHANG, M., THURMOND, R. L. and DUNFORD, P. J. (2007). The histamine H4 receptor: A novel modulator of inflammatory and immune disorders. *Pharmacology & Therapeutics*, **113**, 594-606.
13. BUCHNER, E. (1993). Histamine is a major mechanosensory neurotransmitter candidate in drosophila melanogaster. *Cell and Tissue Research*, **273**, 119-125.
14. RAMOS-JIMÉNEZ, J., SORIA-JASSO, L., LOPEZ-COLOMBO, A., REYES-ESPARZA, J., CAMACHO, J. and ARIAS-MONTANO, J. (2007). Histamine augments β 2-adrenoceptor-induced cyclic AMP accumulation in human prostate cancer cells DU-145 independently of known histamine receptors. *Biochemical Pharmacology*, **73**, 814-823.

15. HASALA, H., GIEMBYCZ, M. A., JANKA-JUNTILA, M., MOILANEN, E. and KANKAANRANTA, H. (2008). Histamine reverses IL-5-afforded human eosinophil survival by inducing apoptosis: Pharmacological evidence for a novel mechanism of action of histamine. *Pulmonary Pharmacology & Therapeutics*, **21**, 222-233.
16. FALUS, A. and MERETY, K. (1992). Histamine: An early messenger in inflammatory and immune responses. *Immunology Today*, **13**, 154-156.
17. TRIGGIANI, M., PETRAROLI, A., LOFFREDO, S., FRATTINI, A., GRANATA, F., MORABITO, P., STAIANO, R. I., SECONDO, A., ANNUNZIATO, L. and GIANNI-MARONE, G. (2007). Differentiation of monocytes into macrophages induces the upregulation of histamine H₁ receptor. *Journal of Allergy and Clinical Immunology*, **119**, 472-481.
18. AKDIS, C. A. and SIMONS, F. E. R. (2006). Histamine receptors are hot in immunopharmacology. *European Journal of Pharmacology*, **533**, 69-76.
19. SMALL, R. C. (2005). Histamine and antihistamines. *Anaesthesia & Intensive Care Medicine*, **6**, 250-252.
20. SHOJI, N., YOSHIDA, A., YU, Z., ENDO, Y. and SASANO, T. (2006). Lipopolysaccharide stimulates histamine-forming enzyme (histidine decarboxylase) activity in murine dental pulp and gingiva. *Archives of Oral Biology*, **51**, 856-860.
21. LEON-PONTE, M., AHERN, G. P., O'CONNELL, P. J. (2007). Serotonin provides an accessory signal to enhance T-cell activation by signalling through the 5-HT₇ receptor. *Blood*, **109**, 3139-3146.
22. BARNES, P. J. (2001). Histamine and serotonin. *Pulmonary Pharmacology and Therapeutics*, **14**, 329-339.
23. VON-MENTZER, B., MURATA, Y., AHLSTEDT, I., LINDSTROM, E. and MARTINEZ, V. (2007). Functional CRF receptors in BON cells stimulate serotonin release. *Biochemical Pharmacology*, **73**, 805-813.
24. HERBERT, M. K. and SCHMIDT, R. F. (1992). Activation of normal and inflamed fine articular afferent units by serotonin. *Pain*, **50**, 79-88.
25. WALTHER, D. J. and BADER, M. (2003). A unique central tryptophan hydroxylase isoform. *Biochemical Pharmacology*, **66**, 1673-1680.
26. WALKER, K., PERKINS, M. and DRAY, A. (1995). Kinins and kinin receptors in the nervous system. *Neurochemistry International*, **26**, 1-16.

27. TAKANO, M., HORIE, M., YAYAMA, K. and OKAMOTO, H. (2003). Lipopolysaccharide injection into the cerebral ventricle evokes kininogen induction in the rat brain. *Brain Research*, **978**, 72-82.
28. BHOOLA, K. D. (1996). Translocation of the neutrophil kinin moiety and changes in the regulation of kinin receptors in inflammation. *Immunopharmacology*, **33**, 247-256.
29. GROENEVELD, T. W. L., RAMWADHDOEBÉ, T. H., TROUW, L. A., HAM, D. L. D., BORDEN, V. D., DRIJFHOUT, J. W., HIEMSTRA, P. S., DAHA, M. R. and ROOS, A. (2007). Human neutrophil peptide-1 inhibits both the classical and the lectin pathway of complement activation. *Molecular Immunology*, **44**, 3608-3614.
30. SHERWOOD, E. R. and TOLIVER-KINSKY. (2004). Mechanisms of the inflammatory response. *Best Practice & Research Clinical Anaesthesiology*, **18**, 385-405.
31. MOLLNES, T. E. and FOSSE, E. (1994). The complement system in trauma-related and ischemic tissue damage: A brief review. *Shock*, **2**, 301-310.
32. KRISHNAN, V., XU, Y., MACON, K., VOLANAKIS, J. E. and NARAYANA, S.V.L. (2007). The crystal structure of C2a, the catalytic fragment of classical pathway C3 and C5 convertase of human complement. *Journal of Molecular Biology*, **367**, 224-233.
33. JANSSEN, B. J. C. and GROS, P. (2007). Structural insights into the central complement component C3. *Molecular Immunology*, **44**, 3-10.
34. SIM, R. B., TSIFTSOGLU, S. A. (2004). Proteases of the complement system. *Biochemical Society Transaction*, **32**, 21-27.
35. DEGN, S. E., THIEL, S. and JENSENIUS, J. C. (2007). New perspectives on mannan-binding lectin-mediated complement activation. *Immunobiology*, **212**, 301-311.
36. http://www.new-science-press.com/info/illustration_files/nsp-immunity-3-3-3_11.jpg
37. TROUW, L. A., SEELLEN, M. A., DUIJS, J. M. G. J., WAGNER, S., LOOS, M., BAJEMA, I. M., KOOTEN C.V., ROOS, A. and DAHA, M. R. (2005). Activation of the lectin pathway in murine lupus nephritis. *Molecular Immunology*, **12**, 731-740.
38. BOOS, L., SZALAI, A. J. and BARNUM, S. R. (2005). C3a expressed in the central nervous system protects against LPS-induced shock. *Neuroscience Letters*, **387**, 68-71.

39. BONIFATI, D. M. and KISHORE, U. (2007). Role of complement in neurodegeneration and neuroinflammation. *Molecular Immunology*, **44**, 999-1010.
40. McGEER, E. G., KLEGERIS, A. and McGEER, P. L. (2005). Inflammation, the complement system and the diseases of aging. *Neurobiology of Aging*, **26**, 94-97.
41. ZIPFEL, P. F., HEINEN, S., JÓZSI, M. and SKERKA, C. (2006). Complement and diseases: Defective alternative pathway control results in kidney and eye diseases. *Molecular Immunology*, **43**, 97-106.
42. FEGHALI, C. A. and WRIGHT, T. M. (1997). Cytokines in acute and chronic inflammation. *Frontiers in Bioscience*, **2**, d12-d26.
43. MOREL, J. and BERENBAUM. (2004). Signal transduction pathways: New targets for treating rheumatoid arthritis. *Joint Bone Spine*, **71**, 503-510.
44. KIM, K-M., KWON, Y-G., CHUNG, H-T., YUN, Y-G., PAE, H-O., HAN, J-A., HA, K-S., KIM, T-W. and KIM, Y-M. (2003). Methanol extract of *Cordyceps prunosa* inhibits in vitro and in vivo inflammatory mediators by suppressing NF- κ B activation. *Toxicology and Applied Pharmacology*, **190**, 1-8.
45. RAINSFORD, K. D. (2000). Anti-inflammatory and anti-rheumatic drugs. CRC Press, **1**, 22-87.
46. SOUZA, P. P. C., FUKADA, S. Y., CUNHA, F. Q., COSTA, C. A. S. and COSTA-NETO, C. M. (2007). Regulation of angiotensin II receptors levels during rat induced pulpitis. *Regulatory Peptides*, **140**, 27-31.
47. SPORER, K. R. B., BURTON, J. L., EARLEY, B. and CROWE, M. A. (2007). Transportation stress in young bulls alters expression of neutrophil genes important for the regulation of apoptosis, tissue remodelling, margination, and anti-bacterial function. *Veterinary Immunology and Immunopathology*, **118**, 19-29.
48. SECCO, D. D., PARON, J. A., DeOLIVEIRA, S. H. P., FERREIRA, S. H., SILVA, J. S. and CUNHA, F. Q. (2004). Neutrophil migration in inflammation: Nitric-oxide inhibits rolling, adhesion and induces apoptosis. *Nitric Oxide*, **9**, 153-164.
49. LEY, K. (1996). Molecular mechanisms of leukocyte recruitment in the inflammatory process. *Cardiovascular Research*, **32**, 733-742.
50. HUSSAIN, M. A., MERCHANT, S. N., MOMBASAWALA, L. S. and PUNIYANI, R. R. (2004). A decrease in effective diameter of rat mesenteric venules due to leukocyte margination after a bolus injection of pentoxifylline-

digital image analysis of an intravital microscopic observation. *Microvascular Research*, **67**, 237-244.

51. POWNER, D. J., PETTITT, T. R., ANDERSON, R., NASH, G. B. and WAKELAM, M. J. O. (2007). Stable adhesion and migration of human neutrophils requires phospholipase D-mediated activation of the integrin CD11b/CD18. *Molecular Immunology*, **44**, 3211-3221.
52. CARVALHO, D. and SAVAGE, C. (1997). Cytokines, adhesion molecules, anti-endothelial cell auto-antibodies and vascular disease. *Cardiovascular Pathology*, **6**, 61-78.
53. <http://www.bio.davidson.edu/courses/immunology/Students/spring2006/Latting/home%20copy.html>
54. SPRINGER, T. A. (1995). Traffic signals on endothelium for lymphocyte recirculation and leukocyte emigration. *Annual Review Physiology*, **5**, 827-872.
55. WONG, D., PRAMEYA, R. and DOROVINI-ZIS, K. (2007). Adhesion and migration of polymorphonuclear leukocytes across human brain microvessel endothelial cells are differentially regulated by endothelial molecules and modulate monolayer permeability. *Journal of Neuroimmunology*, **184**, 136-148.
56. GRANGER, D. N. and KUBES, P. (1994). The microcirculation and inflammation: Modulation of leukocyte-endothelial cell adhesion. *Journal of Leukocyte Biology*, **55**, 662-674.
57. GAVIRO-GOMEZ, M. V., GONZALEZ-ALVARO, I., DOMINGUEZ-JIMENEZ, C., PESCHON, J., BLACK, R. A., SANCHEZ-MADRID, F. and DIAZ-GONZALEZ, F. (2002). Structure-function relationship and role of tumor necrosis factor- α -converting enzyme in the down-regulation of L-selectin by non-steroidal anti-inflammatory drugs. *Journal of Biological Chemistry*, **277**, 38212-38211.
58. SKUPSKY, R., McCANN, C., NOSSAL, R. and LOSER, W. (2007). Bias in the gradient-sensing response of chemotactic cells. *Journal of Theoretical Biology*, **247**, 242-258.
59. HADJOUTA, N., YIN, X., KNECHTA, D. A. and LYNESA, M. A. (2007). Automated real-time measurements of leukocyte chemotaxis. *Journal Immunological Methods*, **320**, 70-80.
60. DOWNEY, G. P. (1994). Mechanisms of leukocyte motility and chemotaxis. *Current Opinion in Immunology*, **6**, 113-124.

61. ZEN, K., REAVES, T. A., SOTO, I., LIU, Y. (2006). Response to genistein: Assaying the activation status and chemotaxis efficacy of isolated neutrophils. *Journal of Immunological Methods*, **309**, 86-98.
62. WITKO-SARSAT, V., RIEU, P., DESCAMPS-LATSCHA, B., LESAVRE, P. and HALBWACHS-MECARELLI, L. (2000). Biology of disease: Neutrophils: Molecules, functions and pathophysiological aspects. *Laboratory Investigation*, **80**, 617-653.
63. LAWRENCE, T., GILROY, D. W., COLVILLE-NASH, P. R. and WILLOUGHBY, D. A. (2001). Possible new role for NF- κ B in the resolution of inflammation. *Nature Medicine*, **7**, 1291-1297.
64. GENTILI, A. (2007). LC-MS methods for analyzing anti-inflammatory drugs in animal food products. *Trends in Analytical Chemistry*, **26**, 595-608.
65. CRONSTEIN, B. N. and WEISSMANN, G. (1995). Targets for anti-inflammatory drugs. *Annual Review of Pharmacology and Toxicology*, **35**, 449-462.
66. LEE, D. M. and WEINBLATT, M. E. (2001). Rheumatoid arthritis. *Lancet*, **358**, 903-911.
67. VAN-RIEL, P. L. C. M., HAAGSMA, C. J. and FURST, D. E. (1999). Pharmacotherapeutic combination strategies with disease-modifying antirheumatic drugs in established rheumatoid arthritis. *Bailliere's Clinical Rheumatology*, **13**, 689-700.
68. GARDNER, G. C. (2005). Inflammatory arthritis in the era of the biologics. *Clinical and Applied Immunology Reviews*, **5**, 19-44.
69. REILLY, P. A., COSH, J. A. and MADDISON, P. J., RASKER, J. J. and SILMAN, A. J. (1990). Mortality and survival in rheumatoid arthritis. A 25 year perspective study of 100 patients. *Annals of the Rheumatic Diseases*, **49**, 363-369.
70. MANNIK, M. (1992). Rheumatoid factors in the pathogenesis of rheumatoid arthritis. *Journal of Rheumatology Supplement*, **32**, 46-49.
71. NAGY, G., CLARK, J. M., BUZAS, E. I., GORMAN, C. L. and COPE, A. P. (2007). Nitric oxide, chronic inflammation and autoimmunity. *Immunology Letters*, **111**, 1-5.
72. CHANNON, K. M. (2006). The endothelium and the pathogenesis of atherosclerosis. *Pathology and Prevention of Atherosclerosis*, **34**, 173-177.
73. ONGINI, E. and BOLLA, M. (2006). Nitric oxide based nonsteroidal anti-inflammatory agents. *Drug Discovery Today: Therapeutic Strategies*, **3**, 395-400.

74. SPIEGEL, A., HUNDLEY, T. R., CHEN, J., GAO, J., OUYANG, N., LIU, X., GO, M. F., TSIOLIAS, G. J., KASHFI, K., RIGAS, B. (2005). NO-donating aspirin inhibits both the expression and catalytic activity of inducible nitric oxide synthase in HT-29 human colon cancer cells. *Biochemical Pharmacology*, **70**, 993-100.
75. JANSSON, E. A., PETERSSON, J., REINDERS, C., SOBKO, T., BJORNE, H., PHILLIPSON, M., WEITZBERG, E., HOLM, L. and LUNDBERG, J. O. (2007). Protection from nonsteroidal anti-inflammatory drug (NSAID) induced gastric ulcers by dietary nitrate. *Free Radical Biology and Medicine*, **42**, 510-518.
76. WALLACE, J. L. and MILLER, M. J. S. (2000). Nitric oxide in mucosal defence: A little goes a long way. *Gastroenterology*, **119**, 512-520.
77. WANG, P. G., CAI, T. B. and TANIGUCHI, N. (2005). *Nitric Oxide Donors*, Wiley-Vch Verlag GmbH & Co. KGaA, Weinheim, 3-4.
78. JANERO, D. R. (2000). Nitric oxide related pharmaceuticals: Contemporary approaches to therapeutic NO modulation. *Free Radical Biology and Medicine*, **28**, 1495-1506.
79. FIALKOW, L., WANG, Y. and DOWNEY, G. P. (2007). Reactive oxygen and nitrogen species as signaling molecules regulating neutrophil function. *Free Radical Biology and Medicine*, **42**, 153-164.
80. COSEN-BINKER, L. I., BINKER, M. G., COSEN, R., NEGRI, G. and TISCORNIA, O. (2006). Influence of nitric oxide donating nonsteroidal anti-inflammatory drugs on the evolution of acute pancreatitis. *Shock*, **25**, 190-203.
81. RIGAS, B., KASHFI, K. (2004). Nitric-oxide donating NSAIDs as agents for cancer prevention. *Trends in Molecular Medicine*, **10**, 324-330.
82. PAUL-CLARK, M. J., ROVIEZZO, F., FLOWER, R. J., CIRINO, G., SOLDATO, P. D. (2003). Glucocorticoid receptor nitration leads to enhanced anti-inflammatory effects of novel steroid ligands. *The Journal of Immunology*, **171**, 3245-3252.
83. CORAZZI, T., LEONE, M., MAUCCI, R., CORAZZI, L. and GRESELE, P. (2005). Direct and irreversible inhibition of cyclooxygenase-1 by nitroaspirin (NCX 4016). *The Journal of Pharmacology and Experimental Therapeutics*, **315**, 1331-1337.
84. FIORUCCI, S., DISTURTTI, E., AJUEBOR, M. N., MENCARELLI, A., MANNUCCI, R., PALAZZETTI, B., SOLDATO, P. D., MORELLI, A. and WALLACE, J. L. (2001). NO-mesalamine protects colonic epithelial cells against

- apoptotic damage induced by pro-inflammatory cytokines. *American Journal of Physiology-Gastrointestinal and Liver Physiology*, **281**, G654-G665.
85. ZAYED, M. A., NOUR-EL-DIEN, F. A., MOHAMED, G. G. and EL-GAMEL, N. E. A. (2007). FTIR, magnetic, mass spectral, XRD and thermal studies of metal chelates of tenoxicams. *Journal of Molecular Structure*, **841**, 41-50.
 86. WALLACE, J. L., IGNARRO, L. J., and FIORUCCI, S. (2002). Potential cardioprotective actions of NO-releasing aspirin. *Nature Reviews Drug Discovery*, **1**, 375-382.
 87. CARINI, M., ALDINI, G., ORIOLI, M. and FACINO, R. M. (2002). In vitro metabolism of a nitroderivative of acetylsalicylic acid (NCX4016) by rat liver: LC and LC-MS studies. *Journal of Pharmaceutical and Biomedical Analysis*, **29**, 1061-1071.
 88. FIORUCCI, S., MENCARELLI, A., MANNUCCI, R., DISTRUTTI, E., MORELLI, A., SOLDATO, P. S. and MONCADA, S. (2002). NCX-4016, a nitric-oxide releasing aspirin protects endothelial cells against apoptosis by modulating mitochondrial function. *The Federation of American Societies for Experimental Biology*, **16**, 1645-1647.
 89. LI, J., BILLIAR, T. R., TALANIAN, R. V. and KIM, Y. M. (1997). Nitric-oxide reversibly inhibits seven members of the caspase family via S-nitrosylation. *Biochemical and Biophysical Research Communications*, **240**, 419-424.
 90. BELTRÁN, B., MATHUR, A., DUVHEN, M. R., ERUSALIMSKY, J. D. and MONCADA, S. (2000). The effect of nitric-oxide on cell respiration: A key to understanding its role in cell survival or death. *Proceedings of the National Academy of Sciences*, **97**, 14602-14607.
 91. DICULESCU, V. C., BARBOSA, R. M. and BRETT, A. M. O. (2005). *In situ* sensing of DNA damage by a nitric oxide releasing compound. *Analytical Letters*, **38**, 2525-2540.
 92. LI, H. and FORSTERMANN, U. (2000). Structure-activity relationship of staurosporine analogues in regulating expression of endothelial nitric oxide synthase gene. *Molecular Pharmacology*, **57**, 427-435.
 93. SMILEY, S. T., REERS, M., MOTTOLA-HARTSHORN, C., LIN, M., CHEN, A., SMITH, T. W., STEELE, G. D. and CHEN, L. B. (1991). Intracellular heterogeneity in mitochondrial membrane potentials revealed by a J-aggregate-forming lipophilic cation JC-1. *Proceedings of the National Academy of Sciences*, **88**, 3671-3675.

94. SALOMON, A. R., ZHANG, Y., SETO, H. and KHOSLA, C. (2001). Structure-activity relationships within a family of selective cytotoxic macrolide natural products. *Organic Letters*, **3**, 57-59.
95. SHINDO, M., SUGIOKA, T., UMABA, Y. and SHISHIDO, K. (2004). Total synthesis of (+)-bongkrelic acid. *Tetrahedron Letters*, **45**, 8863-8866.
96. BELTRÁN, B., QUINTERO, M., GARCIA-ZARAGOZA, E., O'CONNOR, E. and ESPLUGUES, J. V. (2002). Inhibition of mitochondrial respiration by endogenous nitric- oxide: A critical step in Fas signaling. *Proceedings of the National Academy of Sciences*, **99**, 8892-8897.
97. BUXTON, I. L. O., CHEEK, D. J., ECKMAN, D., WESTFALL, D. P., SANDERS, K. M. and KEEF, K. D. (1993). N^G -nitro L-arginine methyl ester and other alkyl esters of arginine are muscarinic receptor antagonists. *Circulation Research*, **72**, 387-395.
98. TIERAONA, L. D. (2006). A reason to season: The therapeutic benefits of spices and culinary herbs. *Explore: The Journal of Science and Healing*, **2**, 446-449.
99. HOUGHTON, P. J. (1995). The role of plants in traditional medicine and current therapy. *Journal of Alternative and Complementary Medicine*, **1**, 131-143.
100. JAGETIA, G. C. and AGGARWAL, B. B. (2007). Spicing-up of the immune system by curcumin. *Journal of Clinical Immunology*, **27**, 19-35.
101. LEUNG, A. Y. and FOSTER, S. (1996). *Encyclopedia of Common Natural Ingredients Used in Food, Drugs and Cosmetics*, New York: Wiley, Ed. 2nd, 499-501.
102. SCARTEZZINI, P. and SPERONI, E. (2000). Review on some plants of Indian traditional medicine with antioxidant activity. *Journal of Ethnopharmacology*, **71**, 23-43.
103. AHMAD, S., ANUNTIYO, J., MALEMUD, C. J. and HAQQI, T. M. (2005). Biological basis for the use of botanicals in osteoarthritis and rheumatoid arthritis: A review. *Evidence-Based Complementary and Alternative Medicine*, **2**, 301-308.
104. CHAINANI-Wu, N. (2003). Safety and anti-inflammatory activity of curcumin: A component of turmeric (*curcuma longa*). *Journal of Alternative and Complementary Medicine*, **9**, 161-168.
105. NADKARNI, K. M. (1976). *Indian Materia Medica*, Bombay: Popular Prakashan, **1**, 414-418.
106. JAIN, S. K. and DEFILLIPS, R. A. (1991). *Medicinal Plants of India*, **2**, 615.

107. CHANG, H-M. and BUT, P. P-H. (1986). *Pharmacology and Applications of Chinese Materia Medica*, Philadelphia, PA. World Scientific, **2**, 936-939.
108. PARANJPE, P. (2001). *Indian medicinal plants forgotten healers - A guide to ayurvedic herbal medicine with identity, habitat, botany, phytochemistry, ayurvedic properties, formulations and clinical usage*. Chaukhamba Sanskrit Pratishthan, 94-96.
109. <http://www.doctorsview.info/wp-content/uploads/2009/06/Curcumin.jpg>
110. ROBINSON, T. P., HUBBARD, R. B., EHLERS, T. J., ARBSIER, J. L., GOLDSMITH, D. J. and BOWEN, J. P. (2005). Synthesis and biological evaluation of aromatic enones related to curcumin. *Bioorganic and Medicinal Chemistry*, **13**, 4007-4013.
111. ANAND, P., THOMAS, S. G., KUNNUMAKKARA, A. B., SUNDARAM, C., HARIKUMAR, K. B., SUNG, B., THARAKAN, S. T., MISRA, K., PRIYADARSINI, I. K., RAJASEKHARAN, K. N. and AGGARWAL, B. B. (2008). Biological activities of curcumin and its analogues (congeners) made by man and mother nature. *Biochemical Pharmacology*, **76**, 1590-1611.
112. NURFINA, A. N., REKSOHADIPRODJO, M. S., TIMMERMAN, H., JENIE, U. A., SUGIYANTO, D. and GOOT, H. V. D. (1997). Synthesis of some symmetrical curcumin derivatives and their anti-inflammatory activity. *European Journal of Medicinal Chemistry*, **32**, 321-328.
113. HANDLER, N., JAEGER, W., PUSCHACHER, H., LEISSER, K. and ERKER, T. (2007). Synthesis of novel curcumin analogues and their evaluation as selective cyclooxygenase-1 (COX-1) inhibitors. *Chemical & Pharmaceutical Bulletin*, **55**, 64-71.
114. GARG, S. N., BANSAL, R. P., GUPTA, M. M., KUMAR, S. (1999). Variation in the rhizome essential oil and curcumin contents and oil quality in the land races of turmeric curcuma longa of north Indian plains. *Flavour and Fragrance Journal*, **14**, 315-318.
115. HAN, X., SHEN, T. and LOU, H. (2007). Dietary polyphenols and their biological significance. *International Journal of Molecular Sciences*, **8**, 950-988.
116. CAMACHO-BARQUERO, L., VILLEGAS, I., SÁNCHEZ-CALVO, J. M., TALERO, E., SÁNCHEZ-FIDALGO, S., MOTILVA, V. and ALARCÓN DE LA LASTRA, C. (2007). Curcumin, a curcuma longa constituent, acts on MAPK p38 pathway modulating COX-2 and iNOS expression in chronic experimental colitis. *International Immunopharmacology*, **7**, 333-342.

117. NONN, L., DUONG, D. and PEEHL, D. M. (2007). Chemopreventive anti-inflammatory activities of curcumin and other phytochemicals mediated by MAP kinase phosphatase-5 in prostate cells. *Carcinogenesis*, **28**, 1188-1196.
118. KIM, H. Y., PARK, E. J., JOE, E-H. and JOU, I. (2003). Curcumin suppresses janus kinase-stat inflammatory signaling through activation of Src homology 2 domain-containing tyrosine phosphatase 2 in brain microglia. *Journal of Immunology*, **171**, 6072-6079.
119. APPIAH-OPONG, R., COMMANDEUR, J. N. M., VUGT-LUSSENBURG, B. V. and VERMEULEN, N. P. E. (2007). Inhibition of human recombinant cytochrome P450s by curcumin and curcumin decomposition products. *Toxicology*, **235**, 83-91.
120. ZHENG, J. and RAMIREZ, V. D. (2000). Inhibition of mitochondrial proton FOF1-ATPase/ATP synthase by polyphenolic phytochemicals. *British Journal of Pharmacology*, **130**, 1115-1123.
121. NISHINAKA, T., ICHIJO, Y., ITO, M., KIMURA, M., KATSUYAMA, M., IWATA, K., MIURA, T., TERADA, T. and YABE-NISHIMURA, C. (2007). Curcumin activates human glutathione S-transferase P1 expression through antioxidant response element. *Toxicology Letters*, **170**, 238-247.
122. SHEN, S-Q., ZHANG, Y., XIANG, J-J. and XIONG, C-L. (2007). Protective effect of curcumin against liver warm ischemia/reperfusion injury in rat model is associated with regulation of heat shock protein and antioxidant enzymes. *World Journal of Gastroenterology*, **13**, 1953-1961.
123. YOUN, H. S., SAITOH, S. I., MIYAKE, K. and HWANG, D. H. (2006). Inhibition of homodimerization of Toll-like receptor 4 by curcumin. *Biochemical Pharmacology*, **72**, 62-69.
124. PAN, M-H., LIN-SHIAU, S-Y. and LIN, J-K. (2000). Comparative studies on the suppression of nitric oxide synthase by curcumin and its hydrogenated metabolites through down-regulation of I κ B kinase and NF κ B activation in macrophages. *Biochemical Pharmacology*, **60**, 1665-1676.
125. BHARTI, A. C., DONATO, N. and AGGARWAL, B. B. (2003). Curcumin (diferuloylmethane) inhibits constitutive and IL-6-inducible stat3 phosphorylation in human multiple myeloma cells. *The Journal of Immunology*, **171**, 3863-3871.
126. KLUTH, D., BANNING, A., PAUR, I., BLOMHOFF, R. and BRIGELIUS-FLOHÉ, R. (2007). Modulation of pregnane X receptor and electrophile

responsive element-mediated gene expression by dietary polyphenolic compounds. *Free Radical Biology and Medicine*, **42**,315-325.

127. KOWLURU, R. A. and KANWAR, M. (2007). Effects of curcumin on retinal oxidative stress and inflammation in diabetes. *Nutrition & Metabolism*, **4**, 1-8.
128. KUNNUMAKKARA, A. B., GUHA, S., KRISHNAN, S., DIAGARADJANE, P., GELOVANI, J. and AGGARWAL B. B. (2007). Curcumin potentiates antitumor activity of gemcitabine in an orthotopic model of pancreatic cancer through suppression of proliferation, angiogenesis, and inhibition of nuclear factor-kb-regulated gene products. *Cancer Research*, **67**, 3853-3861.
129. COLLETT, G. P. and CAMPBELL, F. C. (2004). Curcumin induces c-jun N-terminal kinase dependent apoptosis in HCT116 human colon cancer cells. *Carcinogenesis*, **25**, 2183-2189.
130. ANTO, R. J., MUKHOPADHYAY, A., DENNING, K. and AGGARWAL, B. B. (2002). Curcumin (diferuloylmethane) induces apoptosis through activation of caspase-8, BID cleavage and cytochrome c release: Its suppression by ectopic expression of Bcl-2 and Bcl-xL. *Carcinogenesis*, **23**, 143-150.
131. AOKI, H., TAKADA, Y., KONDO, S., SAWAYA, R., AGGARWAL, B. B. and KONDO, Y. (2007). Evidence that curcumin suppresses the growth of malignant gliomas in vitro and in vivo through induction of autophagy: Role of Akt and extracellular signal-regulated kinase signaling pathways. *Molecular Pharmacology*, **72**, 29-39.
132. GARCIA-ALLOZA, M., BORRELLI, L. A., ROZKALNE, A., HYMAN, B. T., BACSKAI, B. J. (2007). Curcumin labels amyloid pathology in vivo, disrupts existing plaques, and partially restores distorted neurites in an Alzheimer mouse model. *Journal of Neurochemistry*, **102**, 1095-1104.
133. LIN, C-L. and LIN, J-K. (2008). Curcumin: A potential cancer chemopreventive agent through suppressing NF- κ B signalling. *Journal of Cancer Molecules*, **4**, 11-16.
134. RENARD, P. and RAES, M. (1999). The pro-inflammatory transcription factor NF- κ B: A potential target for novel therapeutic strategies. *Cell Biology and Toxicology*, **15**, 341-344.
135. SHAKIBAEI, M., JOHN, T., SCHULZE-TANZIL, G., LEHMANN, I., and MOBASHERI A. (2007). Suppression of NF- κ B activation by curcumin leads to inhibition of expression of cyclo-oxygenase-2 and matrix metalloproteinase-9 in human articular chondrocytes: Implications for the treatment of osteoarthritis. *Biochemical Pharmacology*, **73**, 1434-1445.

136. REYES-GORDILLO, K., SEGOVIA, J., SHIBAYAMA, M., VERGARA, P., MORENO, M. G., and MURIEL, P. (2007). Curcumin protects against acute liver damage in the rat by inhibiting NF- κ B, pro-inflammatory cytokines production and oxidative stress. *Biochimica et Biophysica Acta*, **1770**, 989-996.
137. DUQUE, J., DIAZ-MUNOZ, M. D., FRESNO, M., and INIGUEZ, M. A. (2006). Up-regulation of cyclooxygenase-2 by interleukin-1 β in colon carcinoma cells. *Cellular Signalling*, **18**, 1262-1269.
138. JURRMANN, N., BRIGELIUS-FLOHE, R. and BOL, G-F. (2005). Curcumin blocks interleukin-1 (IL-1) signalling by inhibiting the recruitment of the IL-1 receptor-associated kinase IRAK in murine thymoma EL-4 cells. *Journal of Nutrition*, **135**, 1859-1864.
139. MENON, V. P. and SUDHEER, A. R. (2007). *The Molecular Targets and Therapeutic Uses of Curcumin in Health and Disease*, Springer, **112**.
140. MUKAIDA, N. (2003). Pathophysiological roles of interleukin-8/CXCL-8 in pulmonary diseases. *American Journal of Physiology-Lung Cellular and Molecular Physiology*, **284**, L566-L577.
141. STURM, A., BAUMGART, D. C., D'HEUREUSE, J. H., HOTZ, A., WIEDENMANN, B. and DIGNASS, A. U. (2005). CXCL8 modulates human intestinal epithelial cells through a CXCR1 dependent pathway. *Cytokine*, **29**, 42-48.
142. GAUTAM, S. C., GAO, X. and DULCHAVSKY, S. (2007). Immunomodulation by curcumin. *Advances in Experimental Medicine*, **595**, 321-341.
143. LIANG, G., SHAO, L., WANG, Y., ZHAO, C., CHU, Y., XIAO, J., ZHAO, Y., LI, X. and YANG, S. (2009). Exploration and synthesis of curcumin analogues with improved structural stability both in vitro and in vivo as cytotoxic agents. *Bioorganic & Medicinal Chemistry*, **17**, 2623-2631.
144. PABON, H. J. J. (1964). Synthesis of curcumin and related compounds. *Recueil Des Travaux Chimiques Des Pays Bas*, **83**, 379-386.
145. LIN, L., SHI, Q., NYARKO, A. K., BASTOW, K. F., WU, C-Y., SU, C- Y., SHIH, C. C-Y. and LEE, K-H. (2006). Antitumor agents 250. Design and synthesis of new curcumin analogues as potential anti-prostate cancer agents. *Journal of Medicinal Chemistry*, **49**, 3963-3972.
146. MESTRES, R. (2004). A green look at the aldol reaction. *Green Chemistry*, **6**, 583-603.

147. CHIROLI, V., BENEDINI, F., ONGINI, E., and SOLDATO, P. D. (2003). Nitric-oxide donating nonsteroidal anti-inflammatory drugs: The case of nitroderivatives of aspirin. *European Journal of Medicinal Chemistry*, **38**, 441-446.
148. THOMSON, R. H. (1985). *The Chemistry of Natural Products*. Chapman and Hall, 124-125.
149. IDDON, B. (1970). Recent advances in the chemistry of benzo[b]thiophenes. *Advances in Heterocyclic Chemistry*, Academic Press, **II**, 177-381.
150. CAGNIANT, P. and CAGNIANT, D. (1975). Recent advances in the chemistry of benzo[b]furan and its derivatives. Part I: Occurrence and synthesis. *Advances in Heterocyclic Chemistry*, Academic Press, 337-482.
151. MOLVI, K. I., VASU, K. K., YERANDE, S. G., SUDARSANAM, V. and HAQUE, N. (2007). Syntheses of new tetrasubstituted thiophenes as novel anti-inflammatory agents. *European Journal of Medicinal Chemistry*, **42**, 1049-1058.
152. WILLIAMS, E. J., HAQUE, S., BANKS, C., JHONSON, P., SARSFIELD, P. and SHERON, N. (2000). Distribution of the interleukin-8 receptors, CXCR 1 and CXCR-2 in inflamed gut. *Journal of Pathology*, **192**, 533-539.
153. DENG, S-L., CHEN, W-F., ZHOU B., YANG, L. and LIU, Z-L. (2006). Protective effects of curcumin and its analogues against free radical-induced oxidative haemolysis of human red blood cells. *Food Chemistry*, **98**, 112-119.
154. VENKATESWARLU, S., RAMACHANDRA, M. S. and SUBBARAJU, G. V. (2005). Synthesis and biological evaluation of polyhydroxycurcuminoids. *Bioorganic & Medicinal Chemistry*, **13**, 6374-6380.
155. ANDERSON, W. K., LAVOIEE., J. and BOTTARO, J. C. (1976). Use of 2,3-dichlorobut-2-ene as synthons for heterocyclic compounds: Synthesis of 2-methylbenzo[b]furans, 2-methylbenzo[b]thiophenes and 4-methyl-2H-chromen. *Journal of Chemical Society Perkin Transactions I Organic and Bioorganic Chemistry*, 1-4.
156. VOGEL, A. (1979). *Textbook of Practical Organic Chemistry*, 4th edition, Longman, 440-441.
157. PAN, F. and WIESE, G. A. (2006). The synthesis and anti-fungal studies of some benzofuran compounds. *Journal of the American Pharmaceutical Association*, **49**, 259-264.

158. SHIRLEY, D. A. and DANZIG, M. J. (1952). The synthesis of 2-thianaphthaldehyde and some of its derivatives. *Journal American Chemical Society*, **74**, 2935-2936.
159. KHAN, M. A. (1991). The Claisen rearrangement of 2-phenylsulfinyl-2-propenyl phenyl ethers - A new route to functionalized phenols and methylbenzofurans. *Bulletin of Chemical Society of Japan*, **64**, 3682-3686.
160. RANU, B. C., HAJRA, A., DEY, S. S. and JANA, U. (2003). Efficient microwave-assisted synthesis of quinolines and dihydroquinolines under solvent-free conditions. *Tetrahedron*, **59**, 813-819.
161. TANG, B., WANG, H-Y. and ZHANG G-Y. (2002). Study on the supramolecular interaction of curcumin and β -cyclodextrin by spectrophotometry and its analytical application. *Journal of Agricultural and Food Chemistry*, **50**, 1355-1361.
162. CORREA, D. H. A., MELO, P. S., DE CARVALHO, C. A. A., DE AZEVEDO, M. B. M., DURAN, N. and HAUN, M. (2005). Dehydrocrotonin and its β -cyclodextrin complex: Cytotoxicity in V79 fibroblasts and rat cultured hepatocytes. *European Journal of Pharmacology*, **510**, 17-24.
163. HUANG, Y., LI, N., LIBONI, K. and NEU, J. (2003). Glutamine decreases lipopolysaccharide-induced IL-8 production in caco-2 cells through a non-NF- κ B p50 mechanism. *Cytokine*, **22**, 77-83.
164. http://www.hyclone.com/media/protocol/viability_assay.htm
165. HONTZEAS, N., HAFER, K. and SCHIESTL, R. H. (2007). Development of a microtiter plate version of the yeast DEL assay amenable to high-throughput toxicity screening of chemical libraries. *Mutation Research/Genetic Toxicology and Environmental Mutagenesis*, **634**, 228-234.
166. CellTiter 96[®] Aqueous one solution cell proliferation assay, *Technical Bulletin*, products G3580, G3581, G3582, Promega, 1-2.
167. DEBNAM, P. M. and SHEARER, G. (1997). Colorimetric assay for substrates of NADP⁺ dependent dehydrogenases based on reduction of a tetrazolium dye to its soluble formazan. *Analytical Biochemistry*, **250**, 253-255.
168. O'TOOLE, S. A., SHEPPARD, B. L., MCGUINNES, E. P. J., GLEESON, N. C., YONEDA, M. and BONNAR J. (2003). The MTS assay as an indicator of chemosensitivity/resistance in malignant gynaecological tumours. *Cancer Detection and Prevention*. **27**, 47-54.

169. MIRANDA, K. M., ESPEY, M. G. and WINK, D. A. (2001). A rapid, simple spectrophotometric method for simultaneous detection of nitrate and nitrite. *Nitric Oxide*, **5**, 62-71.
170. SASTRY, K. V. H., MOUDGAL, R. P., MOHAN, J., TYAGI, J. S. and RAO, G. S. (2002). Spectrophotometric determination of serum nitrite and nitrate by copper - cadmium alloy. *Analytical Biochemistry*, **306**, 79-82.
171. MOODY, A. J. and SHAW, F. L. (2006). Re-evaluation of the Griess reaction: How much of a problem is interference by nicotinamide nucleotides? *Analytical Biochemistry*, **356**, 154-156.
172. SUZUKI, C., UEDA, H., TSUMOTO, K., MAHONEY, W. C., KUMAGAI, I. and NAGAMUNE, T. (1999). Open sandwich ELISA with VH-/VL-alkaline phosphatase fusion proteins. *Journal of Immunological Methods*, **224**, 171-184.
173. DAI, Z., CHEN, J., YAN, F. and JU, H. (2005). Electrochemical sensor for immunoassay of carcinoembryonic antigen based on thionine monolayer modified gold electrode. *Cancer Detection and Prevention*, **29**, 233-240.
174. HENNIG, C., RINK, L., FAGIN, U., JABS, W. J. and KIRCHNER H. (2000). The influence of naturally occurring heterophilic anti-immunoglobulin antibodies on direct measurement of serum proteins using sandwich ELISAs. *Journal of Immunological Methods*, **235**, 71-80.
175. ETESHOLA, E. and LECKBAND, D. (2001). Development and characterization of an ELISA assay in PDMS microfluidic channels. *Sensors & Actuators B: Chemical*, **72**, 129-133.
176. NIKULINA, V. A., KIZMI, E. A., MASSINO, Y. S., SEGAL, O. L., SMIRNOVA, M. B., AVILOV, V. V., SAPRIGIN, D. B., SMOTROV, S. P., TICHITCHENKO, V. A., KOLYASKINA, G., I. and DMITRIEV, A. D. (2000). Synergistic effects in antigen capture ELISA using three monoclonal antibodies directed at different epitopes of the same antigen. *Clinica Chimica Acta*, **299**, 25-44.
177. http://www.millipore.com/drugdiscovery/dd3/elisa_kits
178. <http://www.piercenet.com/products/browse.cfm?fldID=08020402>
179. DHAWAN, V., SCHWALB, D. J., SHUMWAY, M. J., WARREN, M. C., WEXLER, R. S., ZEMTSEVA, I. S., ZIFCAK, B. M. and JANERO, D. R. (2005). Selective nitros(yl)ation induced in vivo by a nitric-oxide donating cyclooxygenase-2 inhibitor: A nobonomic analysis. *Free Radical Biology & Medicine*, **39**, 1191-1207.

180. RANATUNGE, R. R., AUGUSTYNIAK, M., BANDARAGE, U. K., COCHRAN, E. D., EARLE, R. A., ELLIS, J. L., GARVEY, D. S., JANERO, D. R., LETTS, L. G., MARTINO, A. M., MURTY, M. G., RICHARDSON, S. K., SCHROEDER, J. D., SHUMWAY, M. J., TAM, S. W., TROCHA, A. M. and YOUNG, D. V. (2004). Synthesis and selective cyclooxygenase-2 inhibitory activity of a series of novel nitric-oxide donor containing pyrazoles. *Journal of Medicinal Chemistry*, **47**, 2180-2193.
181. PAYTON, F., SANDUSKY, P. and ALWORTH, W. L. (2007). NMR study of the solution structure of curcumin. *Journal of Natural Products*, **70**, 143-146.
182. YUE, D., YAO, T. and LAROCK, R. C. (2005). Synthesis of 2,3-disubstituted benzo[b]furans by the palladium-catalyzed coupling of o-iodoanisoles and terminal alkynes, followed by electrophilic cyclization. *The Journal of Organic Chemistry*, **70**, 10292-10296.
183. SARAF, S., EDUN, M. and KHAN, M. A. (1985). Potential anticancer agents: Pharmacologically active benzo[b]thiophene derivatives. *Heterocycles (sendai)*, **23**, 1173-1180.
184. YOON, T. P., DONG, V. M. and MACMILLAN, D. W. C. (1999). Development of a new Lewis acid-catalyzed Claisen rearrangement. *Journal American Chemical Society*, **121**, 9726-9727.
185. COATES, B., MONTGOMERY, D. and STEVENSON, P. J. (1991). Efficient synthesis of 3-substituted lactams using Meerwein Eschenmoser Claisen [3,3] sigmatropic rearrangements. *Tetrahedron Letters*, **32**, 4199-4202.
186. BASAVAIAH, D. and PANDIARAJU, S. (1995). The Johnson-Claisen rearrangement of 3-hydroxy-2-methylenealkanenitriles: Stereoselective synthesis of functionalized trisubstituted alkenes. *Tetrahedron Letters*, **36**, 757-758.
187. HATTORI, K. and YAMAMOTO, H. (1994). Highly selective enolization method for heteroatom substituted esters; its application to the Ireland ester enolate Claisen rearrangement. *Tetrahedron*, **50**, 3099-3112.
188. ANTO, R. J., KUTTAN, G., BABU, D. K. V., RAJASEKHARAN, K. N., and KUTTAN, R. (1998). Anti-inflammatory activity of natural and synthetic curcuminoids. *Pharmacy and Pharmacology Communication*, **4**, 103-106.
189. FINE, S. A. and PULASKI, P. D. (1973). Re-examination of the Claisen-Schmidt condensation of phenylacetone with aromatic aldehydes. *The Journal of Organic Chemistry*, **38**, 1747-1749.

190. PITTMAN, J. R. C. U. and LIANG, Y. F. (1980). Sequential catalytic condensation-hydrogenation of ketones. *The Journal of Organic Chemistry*, **45**, 5048-5052.
191. VOGEL, A. (1979). *Textbook of Practical Organic Chemistry*, 4th edition, Longman, 795.
192. BARTMESS, J. E., HAYS, R. L. and CALDWELL, G. (1981). The addition of carbanions to the carbonyl group in the gas phase. *Journal American Chemical Society*, **103**, 1338-1344.
193. TIETZE, L. F. (1989). *Reactions and Syntheses*, University Science Books, Oxford University Press, 181.
194. HARRISON, C. R. (1987). Transient titanium enolate aldol condensations. *Tetrahedron Letters*, **28**, 4135-4138.
195. KHOA, N. D., MONTESINOS, M. C., REISS, A., B., DELANO, D., AWADALLAH, N. and CRONSTEIN, N. B. (2001). Inflammatory cytokines regulate function and expression of adenosine A_{2A} receptors in human monocytic THP-1 cells 1. *The Journal of Immunology*, **167**, 4026-4032.
196. FUKUDA, K., HIBIYA, Y., MUTOH, M., OHNO, Y., YMASHITA, K., AKAO, S. and FUJIWARA, H. (2000). Inhibition by parthenolide of phorbol-ester induced transcriptional activation of inducible nitric-oxide synthase gene in a human monocyte cell line THP-1. *Biochemical Pharmacology*, **60**, 595-600.
197. HOU, X-L., TAKAHASHI, K., KINOSHITA, N., QIU, F. and TANAKA, K. (2007). Possible inhibitory mechanism of curcuma drugs on CYP3A4 in 1 α ,25 dihydroxyvitamin D₃ treated caco-2 cells. *International Journal of Pharmaceutics*, **337**, 169-177.
198. PÉRET-ALMEIDA, L., CHERUBINO, A. P. F., ALVES, R. J., DUFOSSE, L. and GLORIA, M. B. A. (2005). Separation and determination of the physico-chemical characteristics of curcumin, demethoxycurcumin and bisdemethoxycurcumin. *Food Research International*, **38**, 1039-1044.
199. WOO, J. H., KIM, Y-H., CHOI, Y-J., KIM, D-G., LEE, K-S., BAE, J. H., MIN, D. S., CHANG, J-S., JEONG, Y-J., LEE, Y-H., PARK, J-W. and KWON, T-K. (2003). Molecular mechanisms of curcumin-induced cytotoxicity: Induction of apoptosis through generation of reactive oxygen species, down-regulation of Bcl-XL and IAP, the release of cytochrome c and inhibition of Akt. *Carcinogenesis*, **24**, 1199-1208.

200. HUSSAIN, A. R., AL-RASHEED, M., MANOGARAN, P. S., AL-HUSSEIN, K. A., PLATANIAS, L. C., AL-KURAYA, K. and UDDIN, S. (2006). Curcumin induces apoptosis via inhibition of PI3'-kinase/AKT pathway in acute T cell leukemias. *Apoptosis*, **11**, 245-254.
201. RAJASINGH, J., RAIKWAR, H. P., MUTHIAN, G., JOHNSON, C. and BRIGHT, J. J. (2006). Curcumin induces growth-arrest and apoptosis in association with the inhibition of constitutively active JAK-STAT pathway in T cell leukemia. *Biochemical and Biophysical Research Communications*, **340**, 359-368.
202. CHENG, F., YU, Q., ZENG Q., LIU, Q. and XUE, K. (2008). Study on the mechanism of apoptosis of myelocytic leukemia cell lines induced by curcumin. *The Chinese-German Journal of Clinical Oncology*, **7**, 111-114.
203. DUVOIX, A., BLASIUS, R., DELHALLE, S., SCHNEKENBURGER, M., MORCEAU, F., HENRY, E., DICATO, M. and DIEDERICH, M. (2005). Chemopreventive and therapeutic effects of curcumin. *Cancer Letters*, **223**, 181-190.
204. RIEDER, J., JAHNKE, R., SCHLOESSER, M., SEIBEL, M., CZECHOWSKI, M., MARTH, C. and HOFFMANN, G. (2001). Nitric-oxide dependent apoptosis in ovarian carcinoma cell lines. *Gynecologic Oncology*, **82**, 172-176.
205. BOLLA, M., MOMI, S. and GRESELE, P. (2006). Nitric oxide-donating aspirin (NCX- 4016): An overview of its pharmacological properties and clinical perspectives. *European Journal of Clinical Pharmacology*, **62**, 145-154.
206. UKIL, A., MAITY, S., KARMAKAR, S., DATTA, N., VEDASIROMONI, J. R. and DAS, P. K. (2003). Curcumin, the major component of food flavour turmeric, reduces mucosal injury in trinitrobenzene sulphonic-acid induced colitis. *British Journal of Pharmacology*, **139**, 209-218.
207. SALH, B., ASSI, K., TEMPLEMAN, V., PARHAR, K., OWEN, D., GOMEZ-MUNOZ, A. and JACOBSON, K. (2003). Curcumin attenuates DNB-induced murine colitis. *American Journal of Physiology-Gastrointestinal and Liver Physiology*, **285**, G235-243.
208. HSU, H-Y., CHU, L-C., HUA, K-F., and CHAO, L-K. (2008). Heme oxygenase-1 mediates the anti-inflammatory effect of curcumin within LPS-stimulated human monocytes. *Journal of Cellular Physiology*, **215**, 603-612.
209. GILMORE, J. L., KING, B. W., ASAKAWA, N., HARRISON, K., TEBBEN, A., SHEPPECK II, J. E., LIU, R-Q., COVINGTON, M. and DUAN, J. J-W. (2007). Synthesis and structure-activity relationship of a novel, non-hydroxamate

Series of TNF- α converting enzyme inhibitors. *Bioorganic & Medicinal Chemistry Letters*, **17**, 4678-4682.

210. RANGAMANI, P. and SIROVICH, L. (2007). Survival and apoptotic pathways initiated by TNF- α : Modeling and predictions. *Biotechnology and Bioengineering*, **97**, 1216-1229.
211. LOEWE, R., HOLNTHONER, W., GROGER, M., PILLINGER, M., GRUBER, F., MECHTCHERIAKOVA, D., HOFER, E., WOLFF, K., and PETZELBAUER, P. (2002). Dimethylfumarate inhibits TNF-induced nuclear entry of NF- κ B/p65 in human endothelial cells. *The Journal of Immunology*, **168**, 4781-4787.
212. WHITE, B., SCHMIDT, M., MURPHY, C., LIVINGSTONE, W., O'TOOLE, D., LAWLER, M., O'NEILL, L., KELLEHER, D., SCHWARZ, H. P. and SMITH, O. P. (2000). Activated protein C inhibits lipopolysaccharide-induced nuclear translocation of nuclear factor-kappa B (NF- κ B) and tumour necrosis factor-alpha (TNF- α) production in the THP-1 monocytic cell line. *British Journal of Haematology*, **110**, 130-134.
213. BHARTI, A. C., DONATO, N., SINGH, S. and AGGARWAL, B. B. (2003). Curcumin (diferuloylmethane) down-regulates the constitutive activation of nuclear factor- κ B and I κ B α kinase in human multiple myeloma cells, leading to suppression of proliferation and induction of apoptosis. *Blood*, **101**, 1053-1062.
214. CHAN, M. M. Y. (1995). Inhibition of tumor necrosis factor by curcumin, a phytochemical. *Biochemical Pharmacology*, **49**, 1551-1556.
215. SHAH, R. B., PALAMAKULA, A. and KHAN, M. A. (2004). Cytotoxicity evaluation of enzyme inhibitors and absorption enhancers in caco-2 cells for oral delivery of salmon calcitonin. *Journal of Pharmaceutical Sciences*, **93**, 1070-1082.
216. SAMBUY, Y., DE-ANGELIS, I., RANALDI, G., SCARINO, M. L., STAMMATI, M. A. and ZUCCO, F. (2005). The caco-2 cell line as a model of the intestinal barrier: Influence of cell and culture-related factors on caco-2 cell functional characteristic. *Cell Biology and Toxicology*, **21**, 1-26.
217. NAGANUMA, M., SARUWATARI, A., OKAMURA, S. and TAMURA, H. (2006). Turmeric and curcumin modulate the conjugation of 1-naphthol in caco-2 cells. *Biochemical Pharmacology Bulletin*, **29**, 1476-1479.
218. LEIKERT, J. F., RATHIEL, T. R., MULLER, C., VOLLMAR, A. M., and DIRSCH, V. M. (2001). Reliable in vitro measurement of nitric oxide released from endothelial cells using low concentrations of the fluorescent probe 4,5-diaminofluorescein. *Federation of European Biochemical Societies*, **506**, 131-134.

219. LEWIS, A. J. and MANNING, A. M. (1999). New targets for anti-inflammatory drugs. *Current Opinion in Chemical Biology*, **3**, 489-494.
220. TOMISATO, W., TSUTSUMI, S., HOSHINNO, T., HWANG, H-J., MIO, M., TSUCHIYA, T., MIZUSHIMA, T. (2004). Role of direct cytotoxic effects of NSAIDs in the induction of gastric lesions. *Biochemical Pharmacology*, **67**, 575-585.
221. HECK, R. F. and NOLLEY, J. P. (1972). Palladium-catalyzed vinylic hydrogen substitution reactions with aryl, benzyl, and styryl halides. *Journal of Organic Chemistry*, **37** (14), 2320-2322.